THE

LONDON, EDINBURGH, AND DUBLIN

PHILOSOPHICAL MAGAZINE

AND

JOURNAL OF SCIENCE.

[SEVENTH SERIES.]

JULY 1932.

I. *Some Aspects of the Valve Bridge with a Description of a New Compensated Valve-Voltmeter.* By A. S. McFarlane, *M.A., B.Sc., M.B., Ch.B.**

THE application of a thermionic valve-bridge circuit to the measurement of small currents and voltages appears to have been first described in the literature by Brentano [1], although Wold [2] has a prior patent specification of a similar idea. During the last few years a great many additions to the skeleton bridge circuit have been suggested with the idea of achieving a greater degree of zero stability. Brentano [3], [4] used separate filament resistances so as to compensate for fluctuations in the L.T. supply voltage by applying fixed fractions of this voltage to the two filaments. Wynn-Williams [5], [6] extended this scheme and simplified it by the introduction of a special filament potentiometer. Although he discussed the problem of H.T. voltage compensation and suggested the use of a large capacity H.T. battery from which the L.T. supply might also be drawn, he does not appear to have made any actual attempt to achieve simultaneous H.T. and L.T. compensation. Brentano [3] and Eglin [7], [8] have both pointed out that H.T. compensation can be achieved by finding a critical ratio for the two resistances which occupy two of the arms of the bridge, and the latter author has suggested that this procedure may also

* Communicated by Prof. E. Taylor Jones, D.Sc., F.Inst.P.

be used to achieve immunity from grid-battery effects, provided valves with closely identical amplification factors are available. He does not appear to have found this compensation procedure very satisfactory in practice, however. Razek and Mulder[9],[10],[11],[12] have devoted much time to the problem and give a general mathematical statement of the relationship which must hold for universal compensation against all battery voltage fluctuations. They describe a compensated bridge amplifier in which the plate and grid voltages are derived from a common battery, and in which complete compensation is achieved, although somewhat laboriously, using a series of xylol-alcohol grid resistances. Their scheme seems to offer a number of advantages in the accurate measurement of extremely minute photoelectric and ionization currents.

We have been concerned with a slightly different aspect of the valve-bridge compensation problem, viz., the production of a robust thermionic voltmeter which will measure accurately to tenths of a millivolt and the zero of which will be unaffected by gross changes in the supply voltages—changes which would result, for instance, from the indiscriminate use in a laboratory of batteries of doubtful voltage. In so far as the principle evolved does not appear to have been described before and may, in addition, easily lend itself to the stabilization of more delicate amplifiers, it has been thought fit to make a full communication on it here.

Theoretical Considerations.

High-tension compensation.

In the bridge circuit in fig. 1, the following general relationships hold:—

$$I_1 = i_1 - i, \quad . \quad . \quad . \quad . \quad . \quad . \quad . \quad . \quad (1)$$

$$I_2 = i_2 + i, \quad . \quad . \quad . \quad . \quad . \quad . \quad . \quad . \quad (2)$$

where I_1, I_2 are the anode currents of valves (1) and (2), i_1 and i_2 are the currents flowing in the resistances R_1 and R_2, respectively, and i is the current passing through the galvanometer.

Also,

$$V_{a_1} = E - R_1 i_1, \quad . \quad . \quad . \quad . \quad . \quad . \quad . \quad (3)$$

$$V_{a_2} = E - R_2 i_2, \quad . \quad . \quad . \quad . \quad . \quad . \quad . \quad (4)$$

where V_{a_1}, V_{a_2} are the respective anode voltages, and E is the H.T. battery voltage.

And

$$I_1 = \alpha_1\left(V_{g_1} + \frac{V_{a_1}}{\mu_1} + \epsilon_1\right)^2, \quad \ldots \quad (5)$$

$$I_2 = \alpha_2\left(V_{g_2} + \frac{V_{a_2}}{\mu_2} + \epsilon_2\right)^2, \quad \ldots \quad (6)$$

where α_1, α_2 are filament emission constants,

μ_1, μ_2 are the voltage amplification factors of the valves,

V_{g_1}, V_{g_2} are the grid voltages,

and ϵ_1, ϵ_2 are additional valve constants. The general relationship represented by equations (5) and (6) is empirical and is due to Van der Bijl[13], who has shown it

Fig. 1.

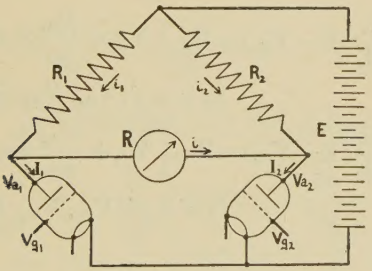

Simple bridge circuit.

to hold with a high degree of accuracy for all cases except where the valve is under consideration as a detector.

If R is the internal resistance of the galvanometer,

$$i = \frac{V_{a_1} - V_{a_2}}{R}, \quad \text{and, from (3),} \quad i_1 = \frac{E - V_{a_1}}{R_1}.$$

Substituting the above values for I_1, i, and i_1 in equation (1), we have

$$\alpha_1\left[V_{g_1} + \frac{V_{a_1}}{\mu_1} + \epsilon_1\right]^2 = \frac{E - V_{a_1}}{R_1} - \frac{V_{a_1} - V_{a_2}}{R},$$

i. e.,

$$V_{a_2} = V_{a_1} - \frac{R}{R_1}(E - V_{a_1}) + R\alpha_1\left[V_{g_1} + \frac{V_{a_1}}{\mu_1} + \epsilon_1\right]^2, \quad (7)$$

and, similarly,

$$\alpha_2\left[V_{g_2}+\frac{V_{a_2}}{\mu_2}+\epsilon_2\right]^2=\frac{E-V_{a_2}}{R_2}+\frac{V_{a_1}-V_{a_2}}{R},$$

i. e.,

$$V_{a_1}=V_{a_2}-\frac{R}{R_2}(E-V_{a_2})+R\alpha_2\left[V_{g_2}+\frac{V_{a_2}}{\mu_2}+\epsilon_2\right]^2, \quad (8)$$

A general consideration of equations (7) and (8) shows that, unless the valve constants are identical and $R_1=R_2$, it is impossible to obtain an expression for $(V_{a_1}-V_{a_2})$ which does not involve E. This bears out the experimental finding that the galvanometer current at any instant is dependent on E. To find how i varies with E we proceed as follows:—

Assume the grid voltages and R_1, R_2, and R constant. Equations (7) and (8) become functions of the three variables, V_{a_1}, V_{a_2}, and E, and may be represented thus:

$$V_{a_2}-V_{a_1}+\frac{R}{R_1}(E-V_{a_1})-R\alpha_1\left[V_{g_1}+\frac{V_{a_1}}{\mu_1}+\epsilon_1\right]^2 = u=f(V_{a_1}, V_{a_2}, E)=0, \quad (9)$$

$$V_{a_1}-V_{a_2}+\frac{R}{R_2}(E-V_{a_2})-R\alpha_2\left[V_{g_2}+\frac{V_{a_2}}{\mu_2}+\epsilon_2\right]^2 = u'=f'(V_{a_1}, V_{a_2}, E)=0. \quad (10)$$

From (9),

$$\frac{\partial u}{\partial(V_{a_2})}=1,$$

$$\frac{\partial u}{\partial(V_{a_1})}=-1-\frac{R}{R_1}-2R\alpha_1\left[V_{g_1}+\frac{V_{a_1}}{\mu_1}+\epsilon_1\right]\times\frac{1}{\mu_1},$$

and $$\frac{\partial u}{\partial E}=\frac{R}{R_1};$$

$$\therefore \frac{du}{dE}=(1)\cdot\frac{d(V_{a_2})}{dE}+\left[-1-\frac{R}{R_1}-\frac{2R\alpha_1}{\mu_1}\left(V_{g_1}+\frac{V_{a_1}}{\mu_1}+\epsilon_1\right)\right]\cdot\frac{d(V_{a_1})}{dE}+\frac{R}{R_1}=0,$$

i. e.,

$$\frac{d(V_{a_2})}{dE}=\left(1+\frac{R}{R_1}+2RD_1\right)\cdot\frac{d(V_{a_1})}{dE}-\frac{R}{R_1}, \quad (11)$$

where

$$D_1=\frac{\alpha_1}{\mu_1}\left(V_{g_1}+\frac{V_{a_1}}{\mu_1}+\epsilon_1\right).$$

Similarly, from (10),

$$\frac{\partial u'}{\partial(\mathrm{V}_{a_1})} = 1,$$

$$\frac{\partial u'}{\partial(\mathrm{V}_{a_2})} = -1 - \frac{\mathrm{R}}{\mathrm{R}_2} - \frac{2\mathrm{R}\alpha_2}{\mu_2}\left(\mathrm{V}_{g_2} + \frac{\mathrm{V}_{a_2}}{\mu_2} + \epsilon_2\right),$$

and $$\frac{\partial u'}{\partial \mathrm{E}} = \frac{\mathrm{R}}{\mathrm{R}_2}.$$

$$\therefore \frac{du'}{d\mathrm{E}} = (1) \cdot \frac{d(\mathrm{V}_{a_1})}{d\mathrm{E}} + \left[-1 - \frac{\mathrm{R}}{\mathrm{R}_2} - \frac{2\mathrm{R}\alpha_2}{\mu_2}\left(\mathrm{V}_{g_2} + \frac{\mathrm{V}_{a_2}}{\mu_2} + \epsilon_2\right)\right] \cdot \frac{d(\mathrm{V}_{a_2})}{d\mathrm{E}} + \frac{\mathrm{R}}{\mathrm{R}_2} = 0.$$

i. e., $$\frac{d(\mathrm{V}_{a_1})}{d\mathrm{E}} = \left(1 + \frac{\mathrm{R}}{\mathrm{R}_2} + 2\mathrm{R}\mathrm{D}_2\right) \cdot \frac{d(\mathrm{V}_{a_2})}{d\mathrm{E}} - \frac{\mathrm{R}}{\mathrm{R}_2}, \quad . \quad (12)$$

where $$\mathrm{D}_2 = \frac{\alpha_2}{\mu_2}\left(\mathrm{V}_{g_2} + \frac{\mathrm{V}_{a_2}}{\mu_2} + \epsilon_2\right).$$

Eliminating $\frac{d(\mathrm{V}_{a_1})}{d\mathrm{E}}$ between (11) and (12)—

$$\frac{d(\mathrm{V}_{a_2})}{d\mathrm{E}} = \frac{\left(1 + \frac{\mathrm{R}}{\mathrm{R}_1} + 2\mathrm{R}\mathrm{D}_1\right)\left(-\frac{\mathrm{R}}{\mathrm{R}_2}\right) - \frac{\mathrm{R}}{\mathrm{R}_1}}{1 - \left(1 + \frac{\mathrm{R}}{\mathrm{R}_1} + 2\mathrm{R}\mathrm{D}_1\right)\left(1 + \frac{\mathrm{R}}{\mathrm{R}_2} + 2\mathrm{R}\mathrm{D}_2\right)},$$

and, similarly,

$$\frac{d(\mathrm{V}_{a_1})}{d\mathrm{E}} = \frac{\left(1 + \frac{\mathrm{R}}{\mathrm{R}_2} + 2\mathrm{R}\mathrm{D}_2\right)\left(-\frac{\mathrm{R}}{\mathrm{R}_1}\right) - \frac{\mathrm{R}}{\mathrm{R}_2}}{1 - \left(1 + \frac{\mathrm{R}}{\mathrm{R}_2} + 2\mathrm{R}\mathrm{D}_2\right)\left(1 + \frac{\mathrm{R}}{\mathrm{R}_1} + 2\mathrm{R}\mathrm{D}_1\right)}.$$

The function which interests us particularly is

$$\frac{di}{d\mathrm{E}} \quad \text{or} \quad \frac{1}{\mathrm{R}} \cdot \frac{d(\mathrm{V}_{a_1} - \mathrm{V}_{a_2})}{d\mathrm{E}} \quad \text{or} \quad \frac{1}{\mathrm{R}}\left[\frac{d(\mathrm{V}_{a_1})}{d\mathrm{E}} - \frac{d(\mathrm{V}_{a_2})}{d\mathrm{E}}\right],$$

which is equal to

$$\frac{1}{\mathrm{R}}\left\{\frac{\frac{\mathrm{R}}{\mathrm{R}_2}\left(1 + \frac{\mathrm{R}}{\mathrm{R}_1} + 2\mathrm{R}\mathrm{D}_1\right) - \frac{\mathrm{R}}{\mathrm{R}_1}\left(1 + \frac{\mathrm{R}}{\mathrm{R}_2} + 2\mathrm{R}\mathrm{D}_2\right) + \frac{\mathrm{R}}{\mathrm{R}_1} - \frac{\mathrm{R}}{\mathrm{R}_2}}{1 - \left(1 + \frac{\mathrm{R}}{\mathrm{R}_2} + 2\mathrm{R}\mathrm{D}_2\right)\left(1 + \frac{\mathrm{R}}{\mathrm{R}_1} + 2\mathrm{R}\mathrm{D}_1\right)}\right\},$$

$$i.\,e.,\quad \frac{di}{dE} = \frac{2R\left(\frac{D_1}{R_2} - \frac{D_2}{R_1}\right)}{1 - \left(1 + \frac{R}{R_2} + 2RD_2\right)\left(1 + \frac{R}{R_1} + 2RD_1\right)}$$

and this is equal to zero if $R_1D_1 = R_2D_2$, or $R = 0$, which is inadmissible. If, now, we consider the special case of the bridge at balance,

$$i = 0, \quad i_1 = I_1 \quad \text{and} \quad i_2 = I_2.$$

Therefore, from (3),

$$V_{a_1} = E - R_1I_1 = E - R_1\alpha_1\left(V_{g_1} + \frac{V_{a_1}}{\mu_1} + \epsilon_1\right)^2.$$

The roots of this quadratic equation in V_{a_1} are

$$V_{a_1} = -(\epsilon_1 + V_{g_1}).\mu_1 - \frac{\mu_1}{2R_1\alpha_1}\left[1 \pm \sqrt{1 + \frac{4R_1\alpha_1}{\mu_1}\left(V_{g_1} + \frac{E}{\mu_1} + \epsilon_1\right)}\right],$$

and, therefore,

$$R_1D_1 = \frac{R_1\alpha_1}{\mu_1}\left\{-\frac{\mu_1}{2R_1\alpha_1}\left[1 \pm \sqrt{1 + \frac{4R_1\alpha_1}{\mu_1}\left(V_{g_1} + \frac{E}{\mu_1} + \epsilon_1\right)}\right]\right\}$$

$$= -\frac{I}{2} \pm \frac{1}{2}\sqrt{1 + \frac{4R_1\alpha_1}{\mu_1}\left(V_{g_1} + \frac{E}{\mu_1} + \epsilon_1\right)},$$

and, by symmetry,

$$R_2D_2 = -\frac{1}{2} \pm \frac{1}{2}\sqrt{1 + \frac{4R_2\alpha_2}{\mu_2}\left(V_{g_2} + \frac{E}{\mu_2} + \epsilon_2\right)}.$$

Equating the two—

$$\frac{R_1\alpha_1}{\mu_1}\left(V_{g_1} + \frac{E}{\mu_1} + \epsilon_1\right) = \frac{R_2\alpha_2}{\mu_2}\left(V_{g_2} + \frac{E}{\mu_2} + \epsilon_2\right) \quad . \quad (13)$$

—which is the general condition that the bridge should be balanced, and that the galvanometer zero should simultaneously be uninfluenced by small changes in the H.T. voltage.

The following experimental results show this equation to hold with a degree of accuracy which is very satisfactory in view of the empirical nature of Van der Bijl's equation, the validity of which is assumed in the proof. Bridge circuits with the components shown in Table I. were constructed

and, in each case, balance was achieved under circumstances in which the galvanometer zero was not appreciably dependent on the H.T. voltage. To achieve this, various values were given to one variable—usually one or other grid voltage or filament emission constant (which was altered by varying the filament voltage) and the bridge balanced by suitably altering the values of R_1 and R_2. At each point of balance the galvanometer deflexion induced by a drop of 20 volts in

TABLE I.

All valves used were Mullard PMIHL valves.

	Expt. 1.	Expt. 2.	Expt. 3.	Expt. 4.
R_1 (ohms)	9618	10440	10070	12060
R_2 (ohms)	9069	8371	9727	9677
$a_1 \times 10^4$	4·287	4·340	4·363	3·568
$a_2 \times 10^4$	4·602	4·213	4·696	3·748
μ_1	33·32	33·32	29·23	33·05
μ_2	33·05	29·23	29·73	29·73
ϵ_1 (volts)	−·207	−·169	−·314	−·026
ϵ_2 (volts)	−·276	−·251	−·246	−·020
V_{g_1} (volts)	−·975	−·831	−·922	−·688
V_{g_2} (volts)	−·944	−·973	−·960	−·873
E (volts)	110	110	92	110
A. $\frac{R_1 a_1}{\mu_1}\left(V_{g_1}+\frac{E}{\mu_1}+\epsilon_1\right)$ ...	·264	·314	·287	·342
B. $\frac{R_2 a_2}{\mu_2}\left(V_{g_2}+\frac{E}{\mu_2}+\epsilon_2\right)$ ...	·268	·308	·290	·344

E was measured. Two or three adjustments and measurements sufficed to show the direction in which the variable should be altered so as to diminish the effect of a change in E, and a few further adjustments enabled a point to be found at which a change of 20 volts in E produced a galvanometer-zero change of not more than ·1 microamp. At this point R_1, R_2, V_{g_1}, V_{g_2}, and E were measured directly. μ_1 and μ_2 were determined by finding the slope of the grid-volts, anode-volts curve for constant anode current. Since this graph is accurately a straight line, two points only are

required to determine μ. The author found more accurate values for ϵ_1 and ϵ_2 than are obtained by the procedure recommended by Van der Bijl, viz., the determination of the greatest anode voltage which produces no measurable anode current for a constant value of grid bias, to result from the following procedure. The anode current for two values of anode voltage, V_a and $V_{a'}$, is measured, keeping V_g constant. If the currents found are I and I', then, according to equation (5),

$$I = \alpha\left(V_g + \frac{V_a}{\mu} + \epsilon\right)^2 \quad . \quad . \quad . \quad . \quad . \quad (14)$$

and

$$I' = \alpha\left(V_g + \frac{V_{a'}}{\mu} + \epsilon\right)^2, \quad . \quad . \quad . \quad . \quad (15)$$

from which,

$$I\left(V_g + \frac{V_{a'}}{\mu} + \epsilon\right)^2 = I'\left(V_g + \frac{V_a}{\mu} + \epsilon\right)^2,$$

which is then solved for ϵ Substitution of ϵ in (14) or (15) gives α. In this way, ϵ_1, ϵ_2, α_1, and α_2 were determined.

Lines A and B of Table I. show the extent of agreement, in the four experiments performed, between the two sides of equation (13). The practical conclusion from the foregoing is that in any balanced-bridge circuit using triode valves of the 10,000 to 20,000-ohm class, the galvanometer zero will not be altered by more than ·1 microamp. by a change of 20 volts in the H.T. supply, if

$$\frac{R_1\alpha_1}{\mu_1}\left(V_{g_1} + \frac{E}{\mu_1} + \epsilon_1\right) = \frac{R_2\alpha_2}{\mu_2}\left(V_{g_2} + \frac{E}{\mu_2} + \epsilon_2\right).$$

Since the above relationship was deduced, and experimentally verified, the author's attention has been drawn to a comprehensive paper by Nottingham [14], dealing with the general theoretical relationships of the valve-bridge circuit. He arrives at the following two equations, which must hold simultaneously for H.T. compensation and zero current in the galvanometer, viz.,

$$\mu_1 V_{g_1} + E_{o_1} = \mu_2 V_{g_2} + E_{o_2}$$

and

$$R_1 Z_2 = R_2 Z_1,$$

where E_{o_1}, E_{o_2} are constants, and Z_1, Z_2 are the plate impedances of valves (1) and (2). The equations do not appear to be so useful as equation (13), but it has to be

acknowledged that they lead to the same general conclusion, viz , that it is possible to achieve balance and H.T. compensation by a number of independent circuit adjustments.

Low-tension Compensation.

The author has verified that Wynn-Williams's potentiometric system confers a high degree of immunity from zero-drift due to L.T. fluctuations. It possesses a certain disadvantage in practice, however, in that, unless one has been particularly fortunate in the choice of matched valves,

Fig. 2.

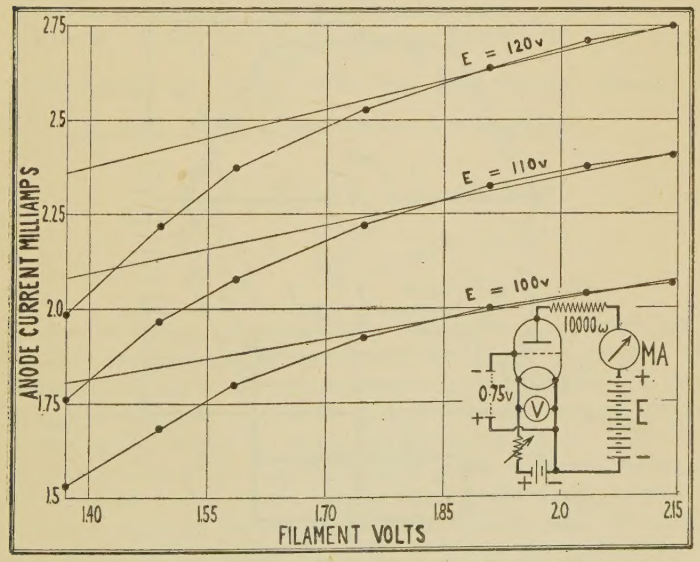

Filament emission characteristic curves for Mazda HL 210 valve.

it may be necessary to operate the filaments at a voltage considerably removed from that recommended by the makers, and also with differences of as much as ·2 volt in the potential applied to the two filaments, a state of affairs which results in zero-drift of a different type and due, in the author's experience, to unequal thermal conduction from the two filaments. Furthermore, as Wynn-Williams himself has shown, it is not possible to effect simultaneous H.T. and L.T. compensation by meaus of a filament-circuit adjustment alone.

Fig. 2 shows curves obtained by recording the anode current for varying filament voltages applied to a Mazda

HL 210 valve at three selected values of E (see circuit inset). The type of curve is general for any triode in circuit with an anode resistance of value, approximately that of the impedance of the valve itself. It will be seen that to the right of a certain point, viz., where the space-charge begins to have effect, the curves approximate to parallel straight lines, making an angle of θ with the filament-voltage axis. Assuming an accurate straight-line relationship for this part of the curve, a change of $d\mathrm{E}_1$ in the filament voltage will produce a change of $d\mathrm{E}_1 \tan\theta$, in the anode current, for all values of E.

Fig. 3.

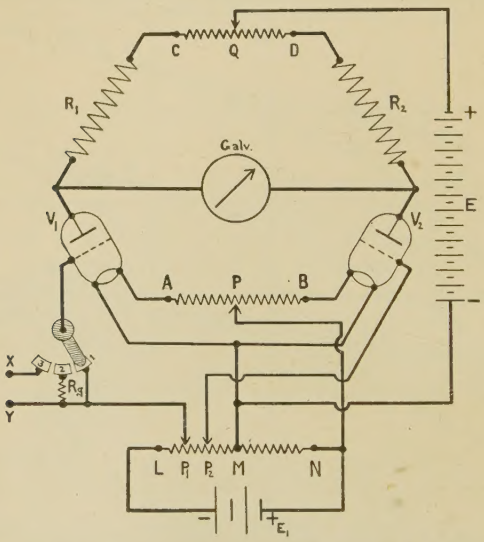

Circuit of compensated valve amplifier.

Now, if the angle which the straight portion of the grid-volts, anode-current curve of the same valve makes with the grid-voltage axis be ϕ, a change of $d\mathrm{E}_1$ in the grid voltage will produce a change of $d\mathrm{E}_1 \tan\phi$ in the anode current, and again this holds for all values of E. Therefore, if, by any artificial means, a change in the filament voltage of $d\mathrm{E}_1$ is always accompanied by a change in the grid voltage of $d\mathrm{E}_1'$, and

$$d\mathrm{E}_1 \tan\theta = d\mathrm{E}_1' \tan\phi,$$

there will result no change in the anode current. A consideration of fig. 3 will show how this can be effected.

A single 4-volt battery, E_1, is used both for heating the filaments and for giving the grids a small negative bias (less than 2 volts). M is so chosen on the potentiometer, LMN, that, approximately, 1·85 volts is applied to both filaments when P is fixed at the mid-point of AB.

$$\text{Considering valve 1, its grid voltage} = \frac{P_1M}{R_f} . E_1$$

$$\text{and its filament voltage} = \frac{K}{R_f} . E_1,$$

where R_f is the total resistance in series with E_1, and the factor K is determined by the resistances of MN, the two filaments, and AB. The exact relationship need not concern us here. If the voltage E_1 changes by dE_1, the grid voltage will change by $-\frac{P_1M}{R_f} . dE_1$, and the filament voltage by $\frac{K}{R_f} . dE_1$, and, if the anode current is unchanged,

$$\frac{P_1M}{R_f} . dE_1 \tan\phi = \frac{K}{R_f} . dE_1 \tan\theta$$

or

$$\frac{P_1M}{K} = \frac{\tan\theta}{\tan\phi},$$

a state of affairs which is easily realizable in practice, since P_1M is variable and K, $\tan\theta$, and $\tan\phi$ are constant. The linearity of the relationship between grid voltage and a small range of filament voltage for constant anode current may be tested quite simply by using the circuit of fig. 1. The valve filaments and grids are all supplied from different batteries. With valve 1 at constant filament and grid voltage, valve 2 is given a series of values of filament voltage and the corresponding grid voltage required to bring the galvanometer back to zero is measured. The results obtained by such a test on a pair of Mazda HL 210 valves are shown in fig. 4. Filament voltages lower than 1·55 were not used in the test, since it is only above this voltage that the space-charge influence becomes fully felt in a Mazda HL 210 valve under the conditions specified. The choice of a 2-volt valve of low filament consumption is dictated by the fact that this class of valve has a much smaller delay in the filament heating after closing the L.T. circuit than most others, and, in a compensation device of this kind, it is obviously undesirable that the filament effect should lag behind the grid effect to an appreciable extent, although it is obviously impossible to eliminate this altogether. The linearity of this graph

lends substantial support to the assumption made in the theory.

It is clearly a simple matter to choose positions for both P_1 and P_2 (fig. 3), such that a small change in E_1 will induce no change in the anode current of either valve and, therefore, will not affect the galvanometer zero. Such a system was, indeed, used with satisfactory results by the author in earlier experiments but has since been modified in an important respect. The disadvantages of this compensation method, as it stands, are two-fold. Firstly, the valves must be biased at a certain grid voltage which is predetermined by the $\tan\theta : \tan\phi$ ratio of the valve, and, for certain applications of such a voltmeter, it is desirable to be able to choose

Fig 4.

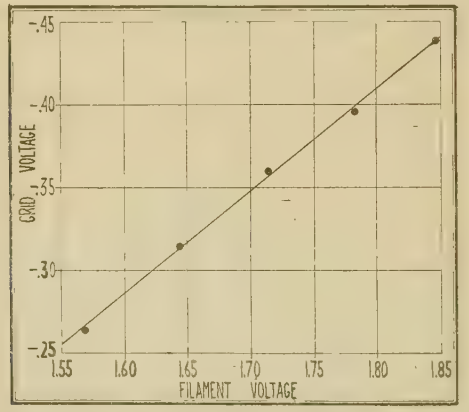

Grid-voltage, filament-voltage curve for constant anode current.

a particular value of standing grid voltage at which to operate. For instance, in using the instrument to measure the e.m.f. of electrochemical cells such as are used in ionic-concentration determinations, it is desirable to bias the valve at the lowest point on the straight portion of the grid-volts, anode-current characteristic so that there is available the maximum range of positive grid-voltage change before the valve begins to pass appreciable grid-current. Also, not all valves have $\tan\theta : \tan\phi$ ratios which are less than unity, and this is necessary if both grid and filament voltages are to be derived from the same 4-volt battery In this connexion it may be mentioned that valves of the 10,000 to 20,000-ohm class with mutual conductivities greater than one will generally be found to satisfy this condition. Secondly, where, as in this

case, the aim is to achieve simultaneous H.T. and L.T. compensation, it has been found that maintaining both valves in a state of constant anode current raises practical difficulties in the way of establishing compensation. It will now be shown that such a state is not absolutely necessary.

For any positions of P_1 and P_2 on LM, the following holds. A change of dE_1 in E_1 will cause a change in the anode current of valve 1 of

$$\frac{P_1M}{R_f} . dE_1 \tan \phi_1 - \frac{K_1}{R_f} . dE_1 \tan \theta_1,$$

and in the anode current of valve 2 of

$$\frac{P_2M}{R_f} . dE_1 \tan \phi_2 - \frac{K_2}{R_f} . dE_1 \tan \theta_2.$$

If this change is to result in an undisturbed galvanometer zero,

$$R_1 . \frac{dE_1}{R_f} [P_1M \tan \phi_1 - K_1 \tan \theta_1]$$

$$= R_2 . \frac{dE_1}{R_f} [P_2M \tan \phi_2 - K_2 \tan \theta_2],$$

i. e., $$P_1M \tan \phi_1 = \frac{R_2}{R_1} [P_2M \tan \phi_2 - K_2 \tan \theta_2] + K_1 \tan \theta_1.$$

The fact that this relationship between P_1M and P_2M is a first degree one establishes that for any position of P_1 there is a corresponding position for P_2, and *vice versa*, for which L.T. compensation holds. Experiment shows that such a compensation scheme is capable of reducing the galvanometer deflexion caused by a change of ·3 volt in E_1 to less than ·2 microamp.

In considering the problem of simultaneous H.T. and L.T. compensation it is clear from the foregoing that, since both depend on a number of independent variables, there are a large number of possible specified circuits which achieve dual compensation. The problem is to find the simplest experimental technique which will enable the rapid construction of one such compensated bridge arrangement using two given valves. Using the scheme now to be described, it is possible to do this with no knowledge of the valve constants and without having to measure any circuit voltages.

The circuit of fig. 3 is used and the compensation adjustment is made by means of the two potentiometers AB and CD, and the variable grid-bias leads P_1 and P_2. The earlier

technique used by the author for arriving at a state of dual compensation was rendered laborious by the fact that immediately one attempts H.T. compensation on a circuit already L.T. compensated the necessary alterations have an H.T. decompensating effect, and *vice versa*. Only by a laborious process of trial and error and the use of the $\tan\theta : \tan\phi$ ratios of the valves was success possible. Later, the purely empirical observation was recorded that an alteration to P_1 or P_2 could be made with almost negligible H.T. decompensating effect provided the bridge was restored to balance by shifting P and not Q, as was previously the custom in restoring balance. In absence of more definite knowledge relating filament voltage to the emission constant α, the author has not been able to offer a rational explanation of this and must merely state it as an experimental fact—and one which is of the greatest help in facilitating the compensation operation described below.

Description of Compensated Valve Voltmeter.

The valves used are two Mullard PMIHL valves matched in a general way, *i. e.*, with no attempt at obtaining identity in respect of one particular valve constant. New valves are run for 50 hours before use. R_1 and R_2 are Ferranti 10,000-ohm fixed non-inductive resistances. CD is a 400-ohm potentiometer with Vernier control giving steps of 1 ohm. AB is 8 inches of bare No. 30 S.W.G. eureka wire with P as a sliding clip on it. LM has a resistance of 7 ohms and is bared in one part where it carries the two sliding clips P_1 and P_2. MN has a resistance of 22·5 ohms. The switch K incorporates a 1-megohm grid leak (R_g) in such a way that in switching-in the voltage to be measured, which is applied across XY, the grid of valve 1 is never left free, when an injurious current might be induced in the galvanometer. Most of these circuit details may be modified in accordance with the principles given—and should be—to suit the circumstances in which the instrument is to be used. With the possible exception of potentiometer CD, which must have reliable low-resistance contacts, no special or costly parts need be used in the construction of the instrument.

The compensation adjustment is performed as follows. P_1 and P_2 are both given positions on LM such that the valve grids are biased at voltages in the region of which it is desired to operate valve 1. P is placed to the left side of the mid-point of AB and the bridge is balanced by moving Q.

Should the range of CD be insufficient to enable balance, P_2 may be moved to another position which allows of Q bringing the galvanometer to zero. The galvanometer deflexion induced by a drop of 20 volts in E is now measured. A new position is then found for P on AB and the bridge again balanced by means of Q. The extent of H.T. decompensation is again measured, and P is now moved along AB in whichever direction results in a diminution in the extent of H.T. decompensation. In this way, positions are ultimately found for P and Q such that the bridge is balanced and also compensated against H.T. change. At this point a drop of ·3 volt in E_1 is induced by inserting a resistance temporarily in series with E_1 and LMN. The resulting galvanometer deflexion is usually large (200–300 microamps) The position of P_2 is altered a little and balance restored by moving P. On no account must it be restored by means of Q, which is kept fixed during all L.T. compensation adjustments. As already stated, moving both P_2 and P in such a way that bridge-balance is always maintained, produces but slight H.T. decompensation. Now measure again the extent of L.T. decompensation. If it is less than before, move P_2 further in the same direction ; if it is more, move P_2 in the opposite direction. A point will ultimately be found at which ·3 volt drop in E_1 produces not more than ·2 microamp. galvanometer current. With P_2 now fixed, re-examine the H.T. compensation. It will usually be found that about 1 microamp. decomposition (for 20 volts H.T. change) has been introduced by the L.T. compensation operations. Re-establish the H.T. decompensation limit (·1 microamp.) by adjustments of P and Q in the manner described. Finally, readjust the L.T. compensation by means of P_2 and P ; it will require but slight movement of P_2 and P to do this and the system is now balanced, so that changes of 20 volts in E and ·3 volt in E_1 do not cause a deflexion in the galvanometer of more than ·2 microamp. The whole operation need not take longer than half an hour. P_1 throughout remains in the position given to it originally, so that valve 1 always has a grid bias of the operator's own choosing. If, in the final position of P this clip is almost at one end of AB, it is advisable that the compensation operation be undertaken again, this time starting with P to the right of the mid-point of AB. By this means the author has never failed to obtain final compensation with P somewhere in the centre portion of AB, and, as already pointed out, it is highly desirable that the filaments be given voltages as nearly equal as possible.

As thus adjusted the stability of the zero is remarkable. Within five to ten minutes of closing the L.T. and H.T. circuit the galvanometer pointer will be found to be within ·25 microamp. of the zero of the previous day. Such minute fluctuations as exist from day to day, and presumably due to valve changes, are eliminated by means of the Vernier control on CD. The initial compensation adjustment need not be repeated for months, with the instrument in daily use, and it is advisable to substitute soldered connexions for the clips P, P_1, and P_2.

Fig. 5.

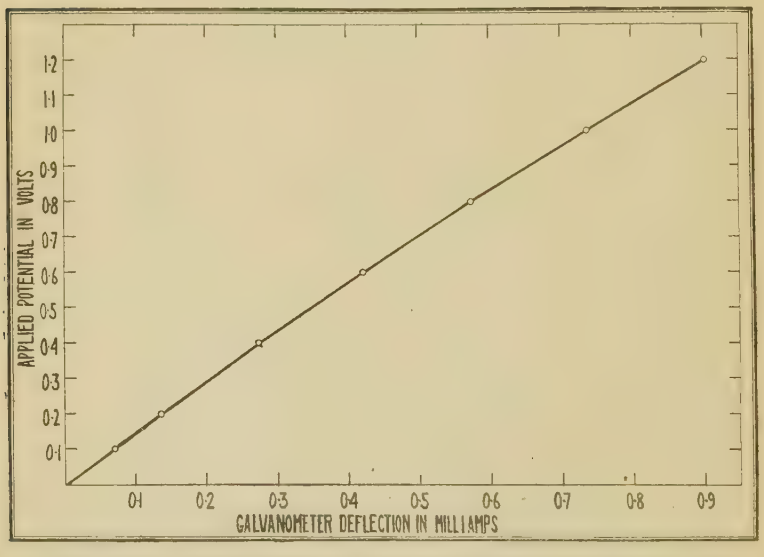

Curve showing galvanometer deflexion against voltage introduced into the grid-circuit of one valve of the bridge amplifier.

With E (fig. 3) equal to 120 volts and giving valve 1 a standing grid bias of $-1{\cdot}2$ volt, the curve shown in fig. 5 was obtained, showing the current induced in the galvonometer by various voltages applied at XY. It will be seen that the linearity of the relationship is not absolute, so that, for accurate work, it is necessary to calibrate the voltmeter over the whole of its scale. For rough work—to within 3 per cent.—a straight-line relationship may be assumed, and the calibration then consists merely in applying a standard voltage, most conveniently from a Weston cell, at XY. The grid-circuit current in valve 1 is approximately

10^{-9} amp. until a grid voltage of $-\cdot 1$ volt is reached. For grid voltages more positive than this, grid current increases rapidly and is equal to 40 microamps. at a grid voltage of $+1$.

The instrument was particularly designed for rapid and accurate measurements of electrochemical potentials. Standard cells may be left connected to it for long periods with negligible polarization effects. It has also been demonstrated that with optimum values of E and R_1 and R_2, the instrument may be used to measure small A.C. voltages with a rectification efficiency equal to that of the best Moullin voltmeter of its class.

Summary.

(1) The general theoretical relationships which hold in a Wheatstone Bridge system, two of the arms of which consist of triode valves, are considered and an expression is deduced, and experimentally verified, for the condition that the bridge may be simultaneously balanced and compensated against fluctuations in the H.T. supply.

(2) The theory of a new device, whereby the filament and grid voltages are derived from the 4-volt battery in such a way that minor changes in voltage of this battery have no significant effect on the bridge zero, is given.

(3) There is described a robust practical form of valve-voltmeter, compensated against changes of 20 volts in the H.T. supply and ·3 volt in the common grid, L.T. supply, and a simple empirical procedure is given for adjusting the compensation device.

The author wishes to express his indebtedness to Dr. L. R. Woodhouse Price for much careful work in the preparation of the circuit diagrams.

References.

(1) J. Brentano, 'Nature,' cviii. p. 532 (1921).
(2) P. I. Wold, U.S. Patent, No. 1, 232, 879 (1916–1917).
(3) J. Brentano, Phil. Mag. vii. p. 685 (1929).
(4) J. Brentano, *Zs. f. Phys.* liv. p. 571 (1929).
(5) C. E. Wynn-Williams, Proc. Camb. Phil. Soc. xxiii. p. 811 (1927).
(6) C. E. Wynn-Williams, Phil. Mag. vi. p. 324 (1928).
(7) J. M. Eglin, Phys. Rev. xxxiii. p. 113 (1929).
(8) J. M. Eglin, Jr. Opt. Soc. Amer. & Rev. Sci. Inst. xviii. p. 393 (1929).
(9) P. J. Mulder and J. Razek, Phys. Rev. xxxiii. p. 284 (1929).
(10) J. Razek and P. J. Mulder, Phys. Rev. xxxiii. p. 284 (1929).

(11) P. J. Mulder and J. Razek, Jr. Opt. Soc. Amer. & Rev. Sc. Inst. xviii. p. 466 (1929).
(12) J. Razek and P. J. Mulder, Jr. Opt. Soc. Amer. & Rev. Sc. Inst. xix. p. 390 (1929).
(13) H. J. Van der Bijl, Phys. Rev. xii. p. 171 (1918).
(14) W. B. Nottingham, Jr. Frank. Inst. ccix. p. 287 (1930).

II. *On the Initiation of Gaseous Explosions by Small Flames.* *By* John M. Holm, *B.Sc., Research Student in the University of Glasgow* *.

[Plate I.]

Introduction.

SINCE 1815 it has been known that the flame of an inflammable gaseous mixture will not travel along a tube containing the mixture when the diameter of the tube is small, but nevertheless finite. This fact, which was discovered by Sir Humphrey Davy, was the starting-point of the invention of the safety-lamp which bears his name.

Davy [1] found that with methane-air mixtures no flame could propagate along a metal tube less than $\frac{1}{7}$ inch in diameter, and that metal tubes were more effective than glass ones in preventing flame propagation. He also observed that the addition of an inert gas, such as carbon dioxide or nitrogen, reduced the explosibility of the mixture. From these and similar experiments he deduced that the effect of the tubes and the inert gases in preventing propagation depended on their cooling powers, *i. e.*, upon their thermal conductivities. Hence it was easy to explain why the metal tubes extinguished the flame more readily than the glass ones.

The idea that the limiting diameter of tube just sufficient to prevent flame propagation depends to a considerable extent upon the thermal conductivity of the tube, is, the writer believes, fairly widely accepted. It must be admitted that, at first sight, it is a very reasonable assumption to make. Thus Messrs. Payman and Wheeler [2], when investigating the increase of uniform flame speed with diameter of tube, came to the conclusion "that the higher the coefficient of conductibility of the material of which tubes of small diameter are made . . . the larger is the diameter of tube capable of preventing the spread of flame in any mixture."

* Communicated by Professor E. Taylor Jones, D.Sc.

Although Mallard and Le Chatelier [3] found that the velocity of uniform flame propagation in a tube of given diameter was independent of the material of which the tube was made, and therefore of the thermal conductivity or cooling effect of the walls, yet they came to the rather paradoxical conclusion that the decrease in flame speed due to a decrease in diameter of tube was caused by the increased cooling effect of the walls. They showed, however, that the diameter of tube necessary to extinguish the flame of a given mixture was smaller the greater the flame velocity in the mixture.

It would appear from the experiments described in Part II. that the above assumption was not justified, *i. e.*, that the limiting diameter of tube just great enough to allow flame propagation to take place was determined primarily by the thermal conductivity of the walls of the tube. In these experiments it has been found that for all coal-gas air and methane-air mixtures examined, the limiting diameter for copper and glass tubes is the same with a maximum error of 2·5 per cent. Thus it is difficult to believe that the extinction of the flame depends largely on the cooling effect of the walls, since altering the thermal conductivity in the ratio of approximately 460 : 1 does not change the limiting diameter by more than 2·5 per cent.

Further, if this assumption was true, one would expect the limiting diameter for propagation through circular holes in thin plates to be considerably less than that for propagation along a tube of the same material, since in this case the effect of the walls would be greatly reduced. Yet the experiments show that the difference is comparatively small and less than experimental error for the strongest coal-gas air mixtures.

A similar phenomenon arises in the case of spark ignition. The theory of this has been successfully developed by Professor Taylor Jones, Dr. J. D. Morgan, and Professor R. V. Wheeler [4] upon the assumption that general ignition of the mixture depends on the volume of gas which the spark, by its own heat, can raise to the ignition temperature of the mixture. The underlying idea [5] is that when the radius of the spherical flame starting out from the spark is very small, the ratio of the rate at which heat is being lost by conduction from the surface of the flame to the rate at which heat is being produced inside the flame by the chemical combination, is very large. Hence, unless the radius of the sphere exceeds a certain minimum value, the small flame will fail to spread throughout the gas and produce general

ignition, since it will be extinguished by too rapid conduction from its surface.

The energy of the minimum spark required for general ignition is thus the balance of heat which is necessary to keep the surface of the flame at the ignition temperature as the flame spreads out to the minimum radius, where it becomes self-supporting and can propagate indefinitely by its own heat. The actual value of the radius of the maximum sphere, which can be raised to the ignition temperature by a condenser spark without producing general ignition, has been determined experimentally by Messrs. Coward and Meiter [6] and found to be about ·62 mm. for an 11·2 per cent. methane-air mixture. The value of the radius as calculated by Messrs. Taylor Jones, Morgan, and Wheeler [4] was about ·91 mm., which is of the the same order of magnitude as the above.

A similar explanation could be applied to the popular form of petrol lighter. If the spark from the flint and steel does not contain sufficient heat to enable the flame to expand out to the limiting diameter, no general ignition of the petrol is produced. It is exceedingly interesting to note that, previous to the introduction of the Davy and similar safety-lamps, a glimmering light was obtained in dangerous coal mines from flint and steel mills [7]. By pressing a piece of flint against the periphery of a rapidly rotating steel disk, a stream of glowing particles in quick succession was produced. The success of the method was due to the comparatively high ignition temperature and low flame speed of methane-air mixtures. The mills were known to be dangerous to use in atmospheres containing hydrogen.

From these phenomena it is evident that the cooling effect of the unburnt gas in contact with the outer flame surface is sufficient to extinguish the flame when its diameter is small, and it is suggested that the same effect is the primary cause in preventing propagation along narrow tubes or through small apertures in thin plates.

When a flame is travelling along a tube of diameter slightly greater than that required for propagation, the flame is, with the exception of those in mixtures approaching the usual lower limit of inflammability, practically a hemisphere of radius slightly less than that of the tube. It is evident that the flame can never actually touch the surface of the cold tube, as that would involve an infinite temperature gradient. Thus the flame is not cooled by the material of the tube directly, as it is always separated from its surface by a layer of usually unburnt gas. The chief effect of reducing the

diameter of the tube is to force the flame to burn as a smaller hemisphere, which is therefore more efficiently cooled by the gas in contact with its external surface. The presence of the tube will affect the distribution of temperature from the flame surface, because it presents a finite boundary which is maintained at practically the temperature of the cold unburnt mixture.

A formula connecting the limiting diameter for propagation along tubes with various constants of the gaseous mixture can be derived in the following manner. While it is not claimed to be anything more than a first approximation, it certainly indicates correctly the manner in which the limiting diameter changes with the constants involved, and on calculation yields a result which is of the correct order of magnitude.

Fig. 1.

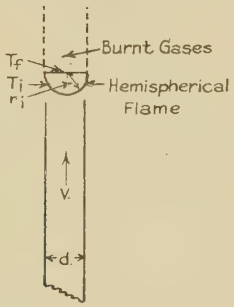

Suppose we have a vertical tube of diameter d, up which a steady stream of an explosive mixture is passing with velocity V. Let the rate of flow be such that it will permit a small self-supporting flame to burn at the top of the tube. If the velocity V is just greater than v, the velocity of the flame down the tube through the stationary mixture, then this flame is approximately a hemisphere of radius r_i, slightly greater than that of the tube. When V is reduced, the flame contracts and travels slowly down the tube when V is just less than v and r is slightly less than $\frac{d}{2}$.

If d is just less than the limiting diameter then the hemispherical flame goes out abruptly when the rate of flow is still finite and the radius r_i is approximately equal to the radius of the tube. In this case, if the concentration of the mixture is not greater than that for theoretically

complete combustion, the lowest point of the flame does not sink below the level of the top of the tube.

Let T_0 be the temperature of the unburnt gaseous mixture and T_i its ignition temperature, which must therefore be the temperature of the surface of the hemispherical flame of radius r_i. Let Q be the total quantity of heat evolved when 1 c.c. of the explosive mixture at temperature T_0 and atmospheric pressure is burnt at constant (atmospheric) pressure, and let C_p be the mean specific heat of the resulting products of combustion between T_0 and T_f, the average temperature of the burnt gases escaping through the plane surface of the hemisphere. Let k be the thermal conductivity of the mixture at temperature T° C.

Consider the heat produced inside this hemispherical flame in a short interval of time dt. Assuming that all the gas escaping from the tube is burnt inside the flame, which is probably true for the small rates of flow employed and for mixtures not too rich in combustible gas, the heat produced from this source is

$$\pi \frac{d^2}{4} \mathrm{V}\, \mathrm{Q}\, dt.$$

The quantity carried out of the hemisphere by the upward flow of burnt gas through the horizontal circle of radius r_i is

$$\pi \frac{d^2}{4} \mathrm{V}\, dt\, \overline{\mathrm{C}}_p(\mathrm{T}_f - \mathrm{T}_0).$$

The quantity lost by conduction through the hemispherical surface of the flame is

$$-2\pi r_i^2 k \overline{\frac{\partial \mathrm{T}}{\partial r}}\Big|_{r=r_i} dt,$$

where T is the temperature at a distance r from the centre of the hemisphere. This assumes that the distribution of T is spherically symmetrical.

There will be practically no conduction of heat through the plane surface of the hemisphere since the temperature gradient will be almost zero there.

It is obvious that the flame cannot continue to exist if the rate at which heat is being generated inside its volume is less than the rate at which heat is being lost through its external surface. If the rate of generation is greater, then the flame is easily self-supporting, and the limiting condition when the flame is on the point of being extinguished is given by

$$d^2 \mathrm{V}\, \mathrm{Q} = d^2 \mathrm{V}\, \overline{\mathrm{C}}_p(\mathrm{T}_f - \mathrm{T}_0) - 8 r_i^2 k \overline{\frac{\partial \mathrm{T}}{\partial r}}\Big|_{r=r_i} \quad . \quad . \quad . \quad (1)$$

The exact determination of the heat lost by conduction from the spherical surface of the flame is decidedly difficult and rather ideal conditions have to be assumed. These assumptions make it impossible to obtain the exact numerical value of the limiting diameter for propagation in any particular case, but still give a formula which is substantially correct.

To calculate the temperature gradient, $\frac{\partial T}{\partial r}$, consider the flame to be a *sphere* of radius r_i, maintained at the constant temperature T_i. The equation for the spherically symmetrical conduction of heat in the steady state is

$$\frac{\partial}{\partial r} kr^2 \frac{\partial T}{\partial r} = 0 \quad . \quad . \quad . \quad . \quad . \quad . \quad (2)$$

Let k, the thermal conductivity of the mixture at temperature T, be $f(T)$ and let

$$\int f(T) dT = F(T) \quad . \quad . \quad . \quad . \quad . \quad . \quad (3)$$

Integrating (2) twice with respect to r and eliminating the constant of integration by substituting

$$T = T_i \quad \text{when} \quad r = r_i$$

and

$$T = T_0 \quad \text{when} \quad r = \infty,$$

we obtain

$$F(T) = \frac{r_i}{r} \{F(T_i) - F(T_0)\} + F(T_0) \quad . \quad . \quad . \quad (4)$$

Therefore on differentiating,

$$k \frac{\partial T}{\partial r} = - \frac{r_i}{r^2} \{F(T_i) - F(T_0)\} \quad . \quad . \quad . \quad . \quad (5)$$

Let $\bar{k}$ be the average value of k between the temperatures T_0 and T_i. Therefore

$$\bar{k} = \frac{F(T_i) - F(T_0)}{T_i - T_0} \quad . \quad . \quad . \quad . \quad . \quad . \quad (6)$$

Substituting from (6) in (5) we have

$$\overline{k \frac{\partial T}{\partial r}}\Bigg|_{r=r_i} = - \frac{\bar{k}(T_i - T_0)}{r_i} \quad . \quad . \quad . \quad . \quad . \quad (7)$$

Hence we obtain from (7) and (1)

$$d^2 V \{Q - \overline{C}_p (T_f - T_0)\} = 8 r_i \bar{k} (T_i - T_0) \quad . \quad . \quad . \quad (8)$$

If V is reduced to v, the velocity of propagation down the tube, the radius of the flame decreases to practically the radius of the tube, and the flame will travel down if

$$d > \frac{4\bar{k}(T_i - T_0)}{v\{Q - \bar{C}_p(T_f - T_0)\}} \quad . \quad . \quad . \quad . \quad . \quad (9)$$

When the right-hand side of (9) is greater than the left, the flame is not self-supporting and is therefore extinguished.

Thus the limiting diameter necessary for propagation is given by

$$d = \frac{4\bar{k}(T_i - T_0)}{v\{Q - \bar{C}_p(T_f - T_0)\}}, \quad . \quad . \quad . \quad . \quad (10)$$

where v is the limiting value to which the velocity of flame propagation approaches as the diameter of tube tends to the limiting value.

The formula indicates the manner of variation of the limiting diameter fairly successfully. Thus d decreases with increase in velocity of propagation, which is in agreement with Mallard and Le Chatelier's observation and also with those about to be described. Also d will decrease if the thermal conductivity of the mixture decreases, which is necessary, since the efficiency of the cooling will then be less. It also indicates that gases having low ignition temperatures will, *ceteris paribus*, pass through tubes of smaller diameter.

The limiting diameter is infinite if

$$Q = \bar{C}_p(T_f - T_0), \quad . \quad . \quad . \quad . \quad . \quad (11)$$

that is, if all the heat from the chemical combination is contained in the burnt gases. Provided the average flame temperatures are known, this gives a method of calculating the usual limits of inflammability which are obtained in tubes of large diameter. Alternatively, if the percentage compositions of the mixtures at the usual limits of inflammability are known, the average flame temperatures at these limits can be calculated.

It should be pointed out that v is not zero at the usual limits of inflammability. This is evident from the curves given by Messrs Burgess and Wheeler [8], which even suggest that v in equation (10) is independent of the concentration.

In some mixtures, probably those in which the thermal conductivities of the components are practically identical, the maximum flame speed occurs at nearly the same concentration as the maximum of Q, *i. e.*, at c_0, the concentration for

theoretically complete combustion. Thus with methane-air mixtures the maximum flame speed is obtained with a mixture containing between 9·5 and 10·0 per cent. methane by volume, whereas the mixture for maximum Q is

$$CH_4 + 2O_2 + 7{\cdot}52N_2,$$

or 9·51 per cent. methane by volume. The minimum limiting diameter for propagation in methane-air mixtures occurs at 9·63 per cent. See Part II. below.

When we start to calculate the absolute value of the limiting diameter given by equation (10) in any particular case, we are faced with the problem of obtaining the correct values for the constants at the high temperatures involved. The greatest difficulty is experienced with $\bar{k}$, the mean thermal conductivity of the mixture between the room temperature and its ignition temperature. It would appear that, up to the present, all measurements of k have been made at temperatures below 100° C. The usual way of expressing the result is

$$k = k_0(1 + \alpha T) \quad . \quad . \quad . \quad . \quad . \quad . \quad (12)$$

where k is the thermal conductivity at T° C.

Thus Gregory and Archer [9] give for air,

$$k_0 = {\cdot}0000583 \text{ in C.G.S. units}$$

and $\alpha = {\cdot}00297$ over the range from 7 to 12° C.,

while Schneider [10] finds

$$k_0 = {\cdot}000059$$

and $\alpha = {\cdot}00395$ over the range from 8 to 40° C.

As will be readily observed, there is a considerable discrepancy between the two values of α, which suggests that α increases fairly rapidly with rise in temperature. If this is true then the following calculation will give values of d which are too small. For lack of a better value at present, the thermal conductivity of methane has been assumed to be the same as that of air.

The values of the mean specific heats of the gases involved have been found from the tables given by Messrs. Partington and Shilling [11], which in most cases extend up to 2000° C.

In order to calculate the limiting diameter for the theoretical methane-air mixture,

$$CH_4 + 2O_2 + 7{\cdot}52N_2 = CO_2 + 2H_2O + 7{\cdot}52N_2 \quad . \quad (13)$$

the following values have been used,

T_i = Ignition temperature = 750° C. [12].

T_f = Average flame temperature = 1670° C. [13]

T_0 = Room temperature = 18° C.,

and the heat of combustion of 1 gm. mol. of methane $= 212.10^3$ cal.[14] when burnt completely to carbon dioxide and water at 18° C.

Therefore for this 9·51 per cent. methane-air mixture,

$$Q = Q_0 = \frac{212.10^3.273.9{\cdot}51}{22{\cdot}4.10^3.291.100} = {\cdot}844 \text{ cal./c.c. of mixture.} \quad (14)$$

From the specific heat tables referred to, the amount of heat evolved when the gases on the right-hand side of (13) are cooled down from T_f to T_0 is found to be $161{\cdot}3.10^3$ cal., *i. e.*, for 10·52 gm. mol. of unburnt mixture. Hence

$$\overline{C_p}(T_f - T_0) = {\cdot}654 \text{ cal./c.c. of mixture at } 18° \text{ C.}$$

Assuming that equation (12) can be extrapolated up to 570° C., which is rather doubtful, we have

$$k = k_0\left(1 + \frac{\alpha}{2}(T_i + T_0)\right)$$

$= {\cdot}0001248$ using Gregory and Archer's value,

and $= {\cdot}0001483$ using Schneider's value.

The limiting value, to which the velocity of flame propagation tends as the diameter of the tube approaches the limiting diameter, has been determined by Bunsen's Method [15]. This consists in measuring the time taken for a known volume of the mixture (500 c.c. in this case) to flow through a tube of known diameter, the rate of flow being adjusted so that the flame burning at the top of the tube is just prevented from travelling down. Measurements were made with several tubes slightly greater than the limiting diameter and the results extrapolated to the limiting diameter. The value obtained in this way for the 9·5 per cent. methane-air mixture was 15 cm./sec.

Hence we have from equation (10)

$d = 1{\cdot}28$ mm. using the first value for k,

and $d = 1{\cdot}53$ mm. using the second value for k.

The actual limiting diameter found for the 9·5 per cent. methane-air mixture was 3·80 mm.

Thus the formula gives the correct order of magnitude for the diameter, but the actual value is too small. The

uncertainty of the value of k at high temperatures and the ideal conditions assumed for the calculation of the cooling by conduction from the flame surface would probably account for this discrepancy.

Let us apply equation (11) to calculate the percentage of methane in the methane-air mixture at the usual lower limit of inflammability.

If c is the percentage by volume of methane in the mixture, then one gm. mol. can be represented by

$$\frac{c}{100}CH_4+\frac{100-c}{476}(O_2+3{\cdot}76\,N_2), \quad . \quad . \quad . \quad (15)$$

which gives on combustion

$$\frac{3{\cdot}76}{4{\cdot}76}N_2+\frac{1}{4{\cdot}76}O_2+\frac{c}{100}\left(CO_2+2H_2O-\frac{10{\cdot}52}{4{\cdot}76}O_2-\frac{3{\cdot}76}{4{\cdot}76}N_2\right)$$
$$. \quad . \quad . \quad . \quad . \quad . \quad . \quad (16)$$

The calculation of the amount of heat which is evolved when this latter quantity of burnt gas is cooled down from T_f to T_0 is simplified by the fact that the specific heats of oxygen and nitrogen are identical. See Partington and Shilling [11].

Let $\overline{C}_{pn}$ and $\overline{C}_{pc}$ be the mean specific heats per gm. mol. of nitrogen and carbon dioxide between T_f and T_0, and let $\overline{C}_{ps}$ be the mean specific heat per gm. mol. of steam between T_f and 100° C.

Since (16) are the products of combustion of one gm. mol. of mixture, we have

$$\overline{C}_p(T_f-T_0)=\frac{1}{V}\left\{\left[\overline{C}_{pn}+\frac{c}{100}\left(\overline{C}_{pc}-\frac{14{\cdot}28}{4{\cdot}76}\overline{C}_{pn}\right)\right](T_f-T_0)\right.$$
$$\left.+\frac{2c}{100}(\overline{C}_{ps}(T_f-100°)+L+18(100°-T))\right\},$$
$$. \quad . \quad . \quad . \quad . \quad . \quad . \quad (17)$$

where V is the volume of one gm. mol. at T_0 and normal pressure, and L the latent heat of steam per gm. mol.

For given values of T_f and T_0 we can evaluate the right-hand side of equation (17) from the specific heat tables referred to above. If we assume, as before, $T_f=1670°$ C. and $T_0=18°$ C., then we obtain

$$\overline{C}_p(T_f-T_0)=\cdot5111+\cdot0151\,c \text{ cal./c.c.}, \quad . \quad . \quad (18)$$

which gives $\overline{C}_p(T_f-T_0)=\cdot654$ cal./c.c.

when $c=9{\cdot}51$ per cent. (*vide ut supra*).

Let Q_0 and c_0 be the values of Q and c for the theoretical mixture for complete combustion. Then, if c is less than c_0,

$$Q = \frac{c}{c_0} Q_0 = \cdot 08876\ c \text{ for methane-air mixtures.}$$

Hence, assuming that the average flame temperature at the usual lower limit of inflammability is 1670° C., we have, for c', the percentage concentration at that limit,

$$\cdot 08876\ c' = \cdot 5111 + \cdot 0151\ c'$$

or
$$c' = 6 \cdot 93 \text{ per cent.} \quad . \quad . \quad . \quad . \quad . \quad (19)$$

If the average flame temperature at the usual lower limit is only the ignition temperature, *i. e.*, $T_f = T_i = 750°$ C., we have, from (17),

$$\overline{C}_p(T_f - T_0) = \cdot 2175 + \cdot 0108\ c,$$

giving
$$c' = 2 \cdot 79 \text{ per cent.} \quad . \quad . \quad . \quad . \quad . \quad (20)$$

The average of 28 values of c' under normal conditions given by Bone [16] is 5·66 per cent. Hence the average flame temperature at the lower limit lies between 750 and 1670° C., and by successive approximation we can deduce the value of T_f which will give c' equal to 5·66 per cent.

In this way we find that if $T_f = 1425°$ C., then

$$\overline{C}_p(T_f - T_0) = \cdot 4305 + \cdot 01323\ c,$$

giving
$$c' = 5 \cdot 67 \text{ per cent.} \quad . \quad . \quad . \quad . \quad . \quad (21)$$

The limiting conditions for the propagation of a flame along a tube, the section of which is a rectangle whose length is large compared with its breadth b, can be treated in a similar manner. If such a tube is arranged as previously described for the circular tubes, then, when the rate of flow, V, is just sufficient to prevent the flame from travelling down, the shape of the flame is that of the lower half of a horizontal cylinder cut by a horizontal plane through its axis.

Let the radius of this semicylindrical flame be R_1, then, with the same notation as before, we must have, when unit length of the flame is considered,

$$bVQ\,dt = bV\overline{C}_p(T_f - T_0)\,dt - \pi k R \overline{\left.\frac{\partial T}{\partial R}\right|_{R=R_1}}\,dt, \quad . \quad (22)$$

where T is now the temperature at a distance R from the axis of the flame.

Assuming that the distribution of T can be represented with sufficient accuracy by that from a complete cylinder, we

have, if the length of the flame is large compared with its breadth,

$$\frac{\partial}{\partial \mathrm{R}} k\mathrm{R}\frac{\partial \mathrm{T}}{\partial \mathrm{R}}=0,$$

which when integrated twice gives,

$$\mathrm{F(T)}=\frac{\mathrm{F(T}_i)-\mathrm{F(T}_0)}{\log \mathrm{R}_i-\log \mathrm{R}_0}\log \mathrm{R}+\frac{\mathrm{F(T}_0)\log \mathrm{R}_i-\mathrm{F(T}_i)\log \mathrm{R}_0}{\log \mathrm{R}_i-\log \mathrm{R}_0}, \quad . \quad . \quad . \quad . \quad . \quad . \quad (23)$$

if $\mathrm{T}=\mathrm{T}_0$ when $\mathrm{R}=\mathrm{R}_0$ and $\mathrm{T}=\mathrm{T}_i$ when $\mathrm{R}=\mathrm{R}_i$.

On differentiating (23) we obtain,

$$\overline{k\mathrm{R}\frac{\partial \mathrm{T}}{\partial \mathrm{R}}}\Big|_{\mathrm{R}=\mathrm{R}_i}=\frac{\bar{k}(\mathrm{T}_i-\mathrm{T}_0)}{\log \mathrm{R}_i-\log \mathrm{R}_0}. \quad . \quad . \quad . \quad (24)$$

On substituting from (24) in (22) we have, finally,

$$b=\frac{\pi\bar{k}(\mathrm{T}_i-\mathrm{T}_0)}{v'\{\mathrm{Q}-\mathrm{C}_p(\mathrm{T}_f-\mathrm{T}_0)\}(\log \mathrm{R}_0-\log \mathrm{R}_i)}. \quad . \quad (25)$$

From equations (10) and (25) we can find the ratio of the limiting diameter for propagation along a circular tube to the limiting breadth for propagation along a tube of the above description. It is

$$\frac{d}{b}=\frac{4v'(\log \mathrm{R}_0-\log \mathrm{R}_i)}{\pi v}, \quad . \quad . \quad . \quad . \quad (26)$$

where v' is the limiting velocity of flame propagation along the long rectangular tube.

R_0 is of the same order of magnitude as the length of the flame and R_i is practically equal to $b/2$. In the actual slots used the length was ten times the breadth, so that the value of $\log \mathrm{R}_0-\log \mathrm{R}_i$ would be about $\log_e 20$ or 3·0.

Hence in this case

$$\frac{b}{d}=\frac{12v'}{\pi v}=3\cdot 83\frac{v'}{v}.$$

The actual values of d and b for the 20 per cent. coal-gas air mixture were found to be 1·80 and 1·05 mm., which gives

$$\frac{d}{b}=1\cdot 71.$$

This suggests that v' is less than v in the ratio of about

$$\frac{v'}{v}=\cdot 446. \quad . \quad . \quad . \quad . \quad . \quad . \quad (27)$$

Experimental Work.

Part I.—*Times of Contact for Failure of Ignition by Flames.*

The initial experiments on the limiting conditions for ignition of a gaseous mixture by flames were based upon the assumption that there existed a definite, measurable interval of time, during which a given flame could remain in contact with the explosive mixture without producing general ignition. The object was to obtain a curve showing the variation of the maximum time of contact for failure of ignition, with the percentage of inflammable gas in the mixture and then to determine how the curve changed for various flames having different rates of generation of heat, size, and temperature. It was not found possible to carry out this programme, as, using coal-gas air mixtures ignited by small coal-gas flames, no definite and repeatable ignition curve of the above description could be obtained. It is doubtful, however, if the results would have been of much value, since they would be obtained under conditions in which it would be difficult to interpret exactly what was taking place.

The experiments involve bringing a small flame burning in air into contact, for a very short interval of time, with a volume of the explosive mixture contained in a closed vessel. Hence the flame and mixture must be in rapid relative motion at the time of contact, or else a rapidly moving partition separating the two, uncovers an aperture which allows them to come into contact. One of the main difficulties in the experiments is to make certain that what is taken as failure of ignition is not really failure of the surface of the flame to come into contact with the mixture. Another inherent difficulty is encountered with mixtures containing more combustible gas than the theoretical mixture for complete combustion. When such a mixture comes into contact first with the air surrounding the flame, it forms a layer of the strongest mixture possible between the flame and the mixture being investigated. The matter is much more complicated than the corresponding problem of spark ignition, since a very small spark, lasting for a very short interval of time, can readily be produced inside a closed vessel containing a homogeneous quiescent mixture of known and definite composition.

In the first type of apparatus tried, a horizontal glass explosion tube, 40 cm. long and 3·0 cm. in internal diameter, was used. At one end of the explosion tube there was a brass plate pierced by a circular hole, 1 cm. in diameter

and concentric with the tube. This opening could be closed by a thin brass plate acting as a slide-valve The mixture could be drawn into the explosion tube from the gas container through the hollow stem of a piston which closed the other end of the tube. A piece of strong brass tubing (40 cm. long and 5/8 inch external diameter) was mounted so that it could rotate freely in the horizontal plane containing the axis of the explosion tube. Into the outer end of this tube a glass jet, which was bent at right angles to the tube, could be inserted by means of a long rubber stopper. The jet and rotating tube were so adjusted that the jet would pass centrally through the hole at the end of the explosion tube. A rigid stop, against which the rotating tube struck, was arranged so that the jet would only travel about 5 mm. into the explosion tube. Just before the jet reached the hole, the rotating tube actuated a trigger which drew aside the sliding plate covering the hole. A flexible rubber tube was connected to the end of the rotating tube nearest to the axis of rotation, so that a stream of coal gas could be passed along the tube and a small flame maintained at the jet.

On the same axle as that carrying the horizontal brass tube, a wooden pulley about 20 cm. in diameter was mounted. By means of a flexible steel wire attached to the periphery of this pulley and passing over another small metal pulley, a weight of about 2640 gm. was lifted from the floor as the brass tube was drawn away from the end of the explosion tube. The weight could be held at various predetermined heights by engaging a catch in one of the teeth of a serrated sector screwed on to the large wooden pulley.

When the weight was released from a height of about 20 cm., the rotating tube moved rapidly round towards the explosion tube, and the small flame burning at the jet went out at the instant when the tube struck against the stop. By varying the height through which the weight dropped and the distance which the jet entered the explosion tube, it was hoped that it would be possible to bring the small flame into the tube for a sufficiently short time to fail to ignite the mixture.

From the dynamics of the system, the linear speed, v, of the jet at the moment of entering the explosion tube was calculated to be given by,

$$v = 147{\cdot}8\sqrt{h}\ \text{cm./sec.},$$

where h was the height in cm. through which the weight dropped.

The apparatus did not, however, prove successful, and no reliable and consistent results could be obtained.

The greatest difficulty was experienced in obtaining a small flame which would remain lit at very high speeds. With the usual type of small flame, the inner blue cone being about 3·5 mm. long and the total length visible in the dark about 7 mm., the maximum speed attainable was about 5·7 metres per second, giving a minimum time of contact of about 1·6 milliseconds.

A considerable number of experiments were made to determine the optimum conditions of producing a small flame which would remain lit at very high speeds.

To this end experiments were made on the variation of the maximum speed attainable with the pressure of the coal gas supplied to it. The graphs showed that the speed was a maximum for a certain pressure, but that for the type of small flames used, the optimum pressure was practically that of the supply mains, *i. e.*, about 12 cm. of water.

The next type of experiment was on the variation of the maximum speed with the direction in which the flame was pointing with respect to the direction of motion, the jet being supplied with coal gas at constant pressure.

The apparatus (described below) which was used in these experiments enabled the flame to be rotated continuously in a horizontal circle, 50 cm. in radius, at any linear speed up to 35 metres per second. The jet could be turned so that the flame pointed in any direction in the vertical plane containing the direction of motion.

From the results it was evident that the optimum direction for the flame was not along the direction of motion but one making an angle of from 45° to 90°, either upwards or downwards with the direction of motion, the speeds in these directions being from 2·5 to 3·5 times greater. The minimum speed was usually obtained when the angle between the flame and the direction of motion was between 90° and 120°.

The highest speed obtained with this apparatus was 30·8 metres/second, or 68·8 miles/hour. The dimensions of this flame were :—Total length = 6 cm., inner blue cone = 3 cm., while the cross-section at 1·5 cm. from the base was approximately an ellipse having a major axis of 6 mm. and a minor axis of 4 mm.

The maximum speed at which a given flame would just remain lit appeared to be fairly consistent and definite.

In the first type of apparatus it was impossible to use speeds much higher than about 10 metres/second with safety, as the large impulse developed when the rotating arm was

suddenly stopped, produced a severe strain in the whole of the rotating system. To overcome this difficulty a new piece of apparatus was constructed, allowing the flame to be rotated continuously at much higher speeds.

The original idea was to obtain a small flame rotating at as high a speed as possible and then to bring a soap-bubble (about 1 cm. in diameter) filled with the explosive mixture, quickly into its path. However, this was soon abandoned, as the large draught caused by the rotating tube made it impossible to keep sufficient control over the bubble, which was blown away before it could be brought into the path of the flame.

The actual apparatus consisted of a piece of strong brass tubing, 1 metre long, mounted at its mid-point to a vertical shaft so that it could rotate in a horizontal plane. The vertical shaft was driven by an electric motor, the speed of which could be controlled by a rheostat. Into one end of the horizontal tube a glass jet was inserted by means of a long rubber stopper. A mercury trap was fitted to the top of the vertical shaft so that coal-gas could be supplied continuously to the jet when it was rotating rapidly.

The tip of the jet, which was bent downwards, was arranged so that it passed freely through the middle of a slot which terminated the top of a small vertical tube 3 mm. in internal diameter. This slot was about 3 mm. wide and 5 mm. deep. The lower end of this small vertical tube was connected through a needle-valve, a "safety tube" packed with long strips of copper gauze and a stop-cock, to a glass gas-holder filled with a 20 per cent. coal-gas air mixture.

By opening the stop-cock and the needle-valve, this mixture was allowed to escape slowly up the small vertical tube, and at the same the horizontal tube was set in motion by the electric motor. The glass tap was closed regularly for half a second every five seconds, and the number of times which a flame travelled down the small vertical tube in a given time counted. It was found for a given rate of flow that this number was independent of the speed of the rotating flame from very small velocites up to 30 metres per second. The actual horizontal length of the flame at these high speeds was certainly less than 2 cm., and we thus had ignition with a time of contact of about ·0007 seconds.

Following these experiments, the small vertical tube was replaced by a horizontal sheet of copper foil pierced by a hole 2·06 mm. in diameter. The copper foil, which was arranged to close the upper end of a vertical glass tube 1 cm. in internal diameter, was ·085 mm. thick.

Similar experiments were tried with the flame from the jet passing right over the hole, and when the tap was closed ignition was produced, although the flame was travelling at 30 metres per second.

However, when this experiment was tried with a 1·51 mm. hole in copper foil, it was almost impossible to get ignition at all, even if a horizontal flame was played against the surface of the hole for two minutes. If, however, the flame was held vertically so that the end of the flame shot through the hole then ignition was produced immediately.

These experiments, while not actually disproving the existence of a maximum time of contact for failure of ignition, show that the size of the flame exposed to the mixture is of considerable importance.

Part II.—*Measurements of Limiting Diameters.*

Following the above work, the experiments were changed from measurements of times of contact to measurements of limiting diameters for ignition or propagation. These experiments have been characterized by their remarkable definiteness and consistency, in marked distinction to those just described. At the same time, several interesting and it is believed new phenomena have been observed.

The apparatus used was exceedingly simple and is shown in fig. 2. AB was a vertical glass tube 15 cm. in length and 2 cm. in internal diameter ; the lower end, A, just dipping under a water surface, WW′. Attached to the upper end of this tube was a horizontal brass disk, PQ (8 cm. in diameter and 2·5 mm. thick). This disk had a 2 cm. hole turned out of the centre so that it did not constrict the upper end of AB. The horizontal side tube, CD, which was joined to the valve, NN′, by a short piece of rubber tubing, RR′, was packed with a roll of fine copper gauze to prevent the explosion which took place in AB from travelling along to the needle-valve. Between this valve and the stop-cock of a 10·7 litre glass gas container, a *safety device*, SS′, was inserted. This consisted of nine disks of fine copper gauze, 3·5 cm. in diameter, pressed close together in a suitable holder so as to form a flame-proof partition in the tube joining the gas container to the explosion tube AB.

A number of rectangular plates of copper foil, ·085 mm. thick, were cut and circular holes of diameters from 1·51 up to 9·50 mm. drilled through their centres. The diameters were chosen so that the percentage difference in diameter between any two successive holes was less than 7 per cent.,

the average percentage difference being 5·16 per cent. The diameters were determined by measuring, with a micrometer screw-gauge, the diameter of that part of the corresponding drill-shank which would just pass through the hole. The holes were made by a completely new set of twist-drills which bored very true to their diameter. In order to obtain circular holes the copper-foil was clamped between two brass plates of thickness at least equal to the radius of the hole to be drilled and the drill put through the three plates.

Fig. 2.

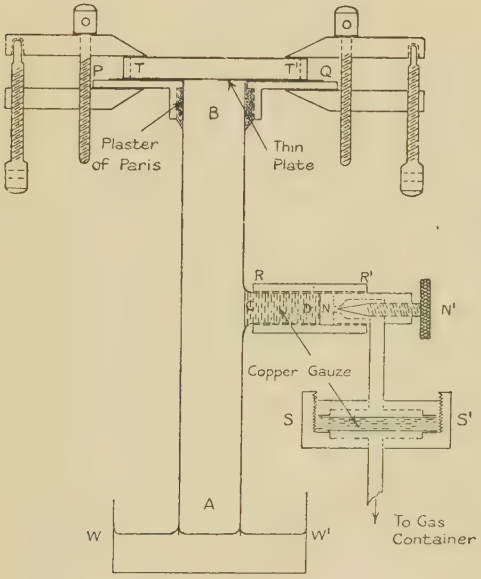

A similar series of mica plates pierced by the same drills was prepared, the thickness of the plates ranging from ·06 to ·22 mm.

By means of two parallel jaw-tool clamps and a brass ring, TT', any of these plates could be made to close the upper end of AB, with the hole in the plate concentric with the tube.

A series of copper tubes was made by drilling copper rod with the same drills as were used for making the copper-foil and mica series. The length of each tube was made to be exactly ten times its internal diameter. For diameters up

to 3·78 mm. $\frac{1}{4}$ inch rod was used, from 3·98 to 5·62 mm. $\frac{3}{8}$ inch, and from 5·95 to 9·50 mm. $\frac{1}{2}$ inch.

A collection of glass tubing was procured, the pieces being selected to be as near to the diameters of the drills used for the other series as possible. From each piece of tubing selected, two lengths were cut, one about ten times the internal diameter and the other about twenty-five times, thus giving rise to two sets of glass tubes, referred to as A and B.

Any of these tubes could be inserted into the upper end of AB by means of a suitable rubber stopper.

Coal-Gas Air Mixtures.*

The method of experimenting with the plates was as follows:—Having made up a coal-gas air mixture of known concentration (say 20 per cent.) in the gas container, a copper plate was fixed over the upper end of AB and the mixture allowed to flow through the hole in the plate and to bubble through the water surface, WW′, so as to fill the vertical tube completely with the mixture.

A small coal-gas flame (inner blue cone 1·5 mm. long and total length 3 mm.) was then brought into contact with the mixture escaping from the hole and the needle-valve adjusted till a self-supporting flame was obtained. The shape of this flame was conical for high rates of flow, for medium rates it took the form of a flat disk, while for very low rates it was almost hemispherical. (See Pl. I. (*b*), (*c*), and (*d*)). The diameter of the circular disk was slightly greater than, while that of the hemisphere was practically the same as, that of the hole below it.

When the rate of flow was increased from that giving a conical flame, an unstable type of flame, shown in Pl. I. (*a*) was formed. This flame was practically elliptical in shape, the centre of the ellipse lying on the axis of the orifice, while its plane was inclined to the vertical at an angle between 20° and 70°. For greater rates of flow it was not possible to maintain a self-supporting flame, as this flame was carried upward by the flow of the mixture.

In Pl. I. the first four photographs represent flames burning at the top of a copper tube 4·76 mm. in internal diameter. For (*a*) and (*b*) a 9·5 per cent. methane-air

* I am indebted to the Glasgow Corporation Gas Department for supplying the analyses from which the following average is compiled:

H_2.	CH_4.	CO.	N_2.	CO_2.	C_nH_m.	O_2.
51·4	19·1	17·7	5·7	3·5	2·3	·3 per cent.

mixture was used, while for (*c*) and (*d*) the concentration was reduced to 7·85 per cent., which is very near the lower limiting concentration for that diameter. In (*d*) the lowest part of the hemisphere is obscured as it lay just below the level of the top of the tube. When these photographs were taken the axis of the camera lay in the horizontal plane passing through the top of the tube and the flames appear about ·85 times their actual size.

Once a self-supporting flame was obtained the small coal-gas flame was removed, and the rate of flow was such that the mixture no longer bubbled through the water surface WW′.

Method I.

The rate of flow was adjusted so that when the escaping mixture was lit, the flame which formed was of the flat disk type shown in (*c*), and within a few seconds the rate of flow was reduced so as to give the hemispherical type of flame. By closing the needle-valve very slowly this hemispherical flame either passed down through the hole and produced immediate ignition (*i*, *e.*, in less than $\frac{1}{5}$ second) of the mixture contained in the tube AB, or went out abruptly on the top side of the plate without giving ignition, according as the diameter of the hole was greater or less than a certain limiting value. For example, with a 20 per cent. coal-gas air mixture, the hemispherical flame went out on the top side of the plate for diameters up to 1·78 mm., but travelled down and gave ignition, which at this concentration was fairly violent, for diameters of 1·85 mm. and greater.

This criterion of obtaining a limiting diameter for failure of ignition was found to be applicable without change for coal-gas air mixtures containing more than 12·5 per cent. of coal gas.

Method II.

For concentrations of 12·5 per cent. and less, it was not found possible to maintain a self-supporting flame above the holes in the plates, so that the method of experimenting had to be slightly changed.

If, say, an 11·5 per cent. mixture was escaping through a 3·95 mm. hole in copper foil and the small coal-gas flame held horizontally about 4 or 5 mm. above it, then a bluish aureole formed on the underside of the flame. When the needle was closed slowly, the aureole separated from the flame and, passing down through the hole, ignited the

rest of the mixture in AB. The aureole was obviously in unstable equilibrium above the hole for small rates of flow. If, however, the plate was changed for one having a hole 3·80 mm. in diameter, the aureole was in stable equilibrium above the plate, showing no tendency to travel down through the hole and produce ignition when the needle-valve was closed slowly.

As may be seen from the graphs, the curve obtained by this method gives a good continuation of that from 12·5 to 31·5 per cent. by Method I.

With concentrations greater than 24 per cent. an exceedingly interesting, though fairly complicated, phenomenon was observed. This was virtually an almost spherical flame formed by the mixture burning under the hole in the thin plate, and which might, in some circumstances, last for 20 seconds without producing general ignition. Sometimes the flame expanded, vibrated at an audible frequency, and gave ignition of the rest of the mixture in AB, and sometimes it did not.

(*e*) (Pl. I.) shows a disk flame burning above a 3·25 mm. hole in copper foil, while (*f*) is a photograph of the almost spherical flame burning below a circular aperture in a mica plate, the diameter of the aperture being 2·78 mm. In both cases a 29·5 coal-gas air mixture was used. The photographs were taken looking down on the top side of the plate, so that in (*f*) the spherical flame is viewed partly through the mica itself and partly through the actual aperture, which appears as a small ellipse above the lower part of the flame. The duration of this spherical flame under the plate was about 16 seconds, and yet no general ignition of the mixture in the vertical tube AB was produced.

The phenomena obtained were very consistent, though they varied considerably with the concentration of the mixture, the diameter of hole and the manner of closing the needle-valve, *i. e.*, either quickly or slowly. They are best described by considering the changes which take place with a 28·5 per cent. coal-gas air mixture.

Starting with a 1·67 mm. hole in copper foil, a self-supporting disk flame could be maintained on the top side of the plate. This flame went out abruptly above the plate without producing ignition, when the needle-valve was closed either quickly or slowly. With holes of 1·78 and 1·85 mm. in diameter, the disk flame went out on the top side of the plate when the valve was closed slowly, but sank down through the hole and stayed in the mixture for 1·2 and 3 seconds respectively, when the valve was closed smartly.

No ignition of the rest of the mixture in the tube AB was then produced, and the flame under the plate was approximately a small sphere 2 mm. in diameter.

The phenomena were independent of the manner of closing the needle-valve for holes in copper foil of diameters from 1·93 to 2·77 mm. A spherical flame, which sang during the last second of its 3 seconds existence but which did not expand, was obtained under the hole in plates of diameters 1·93, 1·96, and 2·06 mm. This singing flame went out sharply without producing general ignition, and did not expand to a diameter greater than that of the hole above it. The rest of the mixture was ignited in about 2·8 seconds by a singing expanding flame under the plate with holes of diameters from 2·16 to 2·47 mm. The fact that the flame expanded could easily be seen by using the mica plates, which behaved in the same manner as the copper ones. The flame was not perfectly spherical, as a small cap cut off by the plane of the hole was missing, and it usually expanded to a diameter about double that of the hole above. With a 2·64 mm. hole in copper foil, no ignition was produced by a singing flame lasting for 17 seconds under the plate. This flame contracted to a sphere about 2·5 mm. in diameter before going out. A non-singing but expanding flame burning for 20 seconds without giving general ignition was observed with a 2·77 mm. hole in copper foil.

Immediate ignition (*i. e.*, in less than $\frac{1}{5}$ sec.) was obtained when the disk flame burning above holes of from 2·94 mm. to 3·44 mm. in diameter was slowly reduced by closing the valve. When the valve was closed smartly with these apertures, a non-singing flame, which did not produce general ignition, formed under the plate and lasted for about 20 seconds. With holes of 3·59 mm. and greater, immediate ignition of the mixture in the vertical tube AB was effected whether the rate of flow of the mixture through the aperture was reduced quickly or slowly.

These results are shown more briefly in Table I.

It was sometimes possible, by opening the needle-valve slowly, to cause the spherical flame burning below the plate to rise up through the hole and give a disk flame burning, as previously, on the top side of the plate. This process if possible once could be repeated indefinitely, and took place most readily with concentrations greater than 28 per cent.

With stronger mixtures, such as 25 per cent., the phenomena corresponding to those found with holes of diameters from 2·64 to 3·44 mm. were missing, while with concentrations greater than 28·5 per cent. their range was extended and

that of ignition from a singing expanding flame curtailed. In general, as the concentration changed from 24 towards 32 per cent., the time of duration of the various flames under the plate increased and the probability of ignition from them decreased.

TABLE I.

28·5 per cent. coal-gas air mixture. Copper-foil plates.

Diameter of hole in mm.	Needle-valve closed slowly.	Needle-valve closed quickly.
1·67	Disk flame out above plate. No ignition.	The same.
1·78 1·85	As above.	Non-singing, non-expanding flame under plate. Duration 1·2 and 3 sec. No ignition.
1·93 1·96	Singing, non-expanding flame under plate. Duration 3·0 sec. No ignition.	The same.
2·06 2·16	Ignition from a singing, expanding flame under the plate. Duration 2·8 sec.	The same.
2·26 2·36		
2·47 2·64	No ignition. Singing, expanding flame under plate. Duration 17 sec.	The same.
2·77 2·94	No ignition. Non-singing, non-expanding flame. Duration 20 sec.	The same.
3·17 3·25	Immediate ignition. No spherical flame under plate.	No ignition from a non-singing, non-expanding flame under plate. Duration 20 sec.
3·44 3·59 and greater.	Immediate ignition.	The same.

As may be seen from Table I., there are no fewer than four limiting diameters for the 28·5 per cent. mixture. These are bracketed together. The limiting diameters corresponding to the largest two have been determined for holes in copper foil and are shown in the accompanying graphs. It is believed that the curve given by the smaller one is the correct continuation of the curve from 13 to 23 per cent. obtained by Method I.

Method III.

This is applicable between 23 and 32 per cent. and is the determination of the maximum diameter, which does not give immediate ignition when the disk flame burning above the hole is reduced by closing the needle-valve quickly, *i. e.*, corresponding to the largest limiting diameter in Table I.

Method IV.

Perhaps it might not be inappropriate to point out that there is yet another limiting diameter referring to the flames burning above the aperture in the plates and at the top of the tubes. This is the minimum diameter of hole which will just allow a self-supporting flame to be maintained on the upper side of the plate (or at the top of tube), independently of the rate of flow of the mixture through the aperture (or along the tube). Thus with a 1·67 mm. hole in copper foil no flame could be maintained with an 18 per cent. mixture for any rate of flow whatever, but a self-supporting disk flame could be obtained with a 1·78 mm. hole by suitably adjusting the rate of flow. With a 13 per cent. mixture this limiting diameter was between 2·77 and 2·94 mm., while with a "pure" coal gas it was very small though finite. Part of the curve showing the variation of this limiting diameter with concentration is shown in Graph III., which refers to circular holes in copper foil.

Tubes.

The method of experimenting with the tubes was similar to that for the copper foil and mica plates. Having fitted one of the tubes by means of a suitable rubber stopper into the upper end of AB (fig. 2), a hemispherical flame was produced at its upper end by Method I. It was always found possible to obtain two tubes of neighbouring diameter, such that, when the needle-valve was closed slowly, this flame would travel steadily down the tube of greater diameter for a distance at least equal to half its length, but would not propagate down that of smaller diameter for a distance greater than the diameter.

When the diameter of the tube was slightly greater than that required for propagation, the surface of the flame which travelled down the tube was approximately hemispherical. The radius of this hemisphere was slightly less than that of the tube for concentrations greater than 16 per cent., but with weaker mixtures, such as 12 per cent., it might only be about $\frac{3}{4}$ that of the tube.

With concentrations between 14 and 26 per cent., the rest of the mixture in the tube AB was ignited immediately by the flame travelling down the tube of greater diameter. This was true for all three sets of tubes, *i. e.*, copper and glass, A and B. Outside these limits the diameter of tube required to give ignition of the mixture in AB was greater than that for propagation alone, although the exact value was not determined in each case.

With the tubes it was possible to maintain a self-supporting flame down to 11·5 per cent., but for concentrations lower than this Method II. had to be employed.

The phenomenon of the spherical flame inside AB, corresponding to that observed with the plates, was not obtained with the tubes. This indicates that the former was due to the mixture in the vicinity of the hole not being homogeneous.

With concentrations greater than 25 per cent., the well-known phenomenon of flame separation took place. This could be observed most readily with the glass tubes. When the flame burning at the top of the tube (assumed greater in diameter than the minimum for propagation) was slowly reduced in size by decreasing the rate of flow, a bright green hemispherical flame travelled steadily down the tube, leaving a pale blue cone burning at the top. When the diameter was less than the minimum for propagation, the bright green flame sank down the tube for a distance not greater than the diameter of the tube, started to oscillate with a very low frequency and amplitude about equal to the radius of the tube, and then went out abruptly.

The flame burning at the top of the tube was bright blue in colour for concentrations less than 24 per cent, and went out abruptly without sinking down below the level of the top of the tube if the diameter was less than that required for propagation. If the diameter was greater, then the flame travelled steadily down the tube without any flame separation.

It should be pointed out that the spherical flames burning under the holes in the plates were always blue in colour. Usually, however, the under surface of the disk flame burning above the plate was bright green for concentrations greater than 25 per cent. This green part disappeared as the flame travelled down through the hole when the needle-valve was closed.

Provided the following precautions were taken, the limiting diameters determined by Methods I., II., III., and IV. were very sharply defined and consistent:—

(1) To make sure that exactly the same criterion of failure of ignition or propagation was employed each time.

(2) To clear away all the burnt gas from the previous explosion in the vertical tube AB by allowing the mixture to flow through for a sufficient length of time.

(3) To avoid heating up the edges of the holes or the tops of the tubes unduly by successive trials, or by allowing the disk flame to burn for too long before it was reduced to a hemispherical flame.

(4) To wait till the surface of the water at the lower end of AB was perfectly still before closing the needle-valve. This is necessary since if the surface was oscillating, due to the mixture bubbling through it just previously, the hemispherical flame was given a vertical vibration which might carry it through a smaller hole than usual.

(5) To have a reliable method of ascertaining the concentration of the mixture. Since the coal gas used in the experiments was drawn direct from the supply mains each time, the small changes occurring in its composition from day to day undoubtedly affected the results. As a rule, however, the change produced in the limiting diameter was less than the experimental error (*i. e.*, about 2·5 per cent.) and passed unobserved.

Altogether about 500 observations of limiting diameters for coal-gas air mixture have been made. The most consistent and reliable are given in the accompanying graphs and tables. The limiting diameter was usually taken to be the mean of the experimental upper and lower limiting diameters ; but in some cases it was obvious, from the behaviour of the flames, that the correct limiting diameter was nearer to that of one hole than it was to that of the other. In these cases the limiting diameter was taken to be the average between the mean diameter and the diameter considered to be nearer the correct limiting diameter. If two concentrations had the same upper and lower limits, say d and d', the limiting diameters were taken to be

$$d+\frac{d'-d}{4} \quad \text{and} \quad d+\frac{3(d'-d)}{4},$$

and if three concentrations had the same limits, the limiting diameters were taken to be

$$d+\frac{d'-d}{6}, \qquad d+\frac{d'-d}{2}, \quad \text{and} \quad d+\frac{5(d'-d)}{6}.$$

Results with Coal-gas Air Mixtures.

Copper Foil.—The complete curve showing the variation with concentration of the limiting diameter obtained by

Graph I.

A. Copper foil. Methods I. and II.
B. Copper tubes. „ „ „
C. Copper foil. Method III.

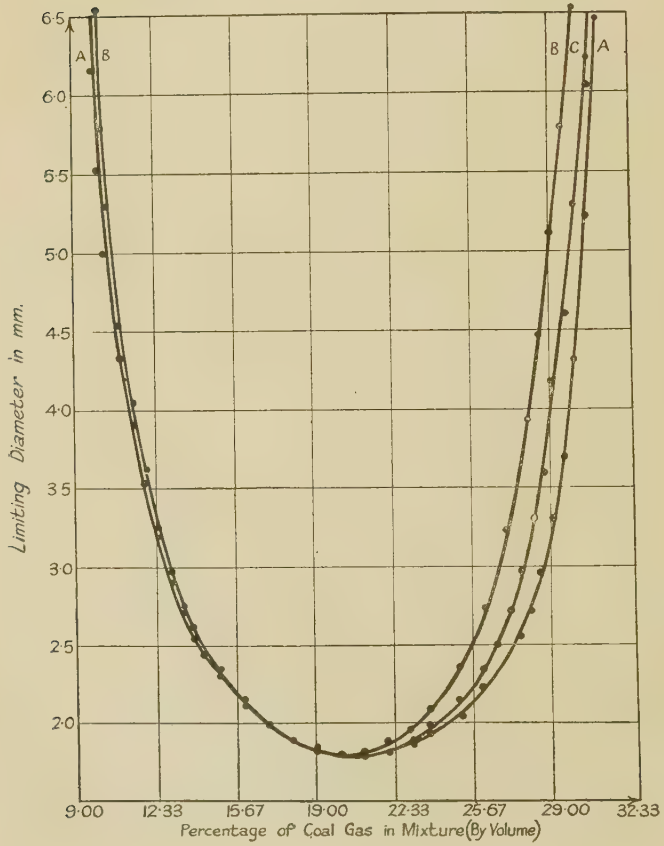

Methods I. and II. is drawn in Graph I. The curve is definitely not symmetrical about the minimum at 20·5 per cent., at which concentration the explosion, as judged roughly by its sound, was the most violent. Above part of this curve, that given by Method III., from 23 to 31·5 per cent.

is inserted. It is almost, but not exactly, symmetrical about 20·5 per cent. with the other half of the curve for copper foil.

Mica Plates.—From 9·75 to 16 per cent. the curve for the mica plates was identical with the corresponding part of the curve for copper foil. The curve lay definitely below that for copper foil from 16 to 26 per cent. For higher concentrations the limiting diameter given by Method I. has not been determined on account of the ease with which the edges of the holes became red hot. The diameters obtained by Method III. were identical with those for copper foil.

Tubes.—The limiting diameters, determined as described above, were the same for the copper and glass tubes for all concentrations between 9·75 and 31·5 per cent. The curve, shown in Graph I., lies slightly, but definitely, above that for copper foil from 9·75 to 20·5 per cent. From the latter percentage onwards, the curve rises more steeply than that for the plates and lies distinctly above it. The minimum occurs at the same percentage as that on the curves for the plates, *i. e.*, at 20·5 per cent.

From the coal-gas analysis given above, it has been calculated, assuming $n=m=6$, that the theoretical coal-gas air mixture for complete combustion contains 19·0 per cent. coal-gas.

Following these experiments, the effect of changing the shape of the aperture in the copper foil was investigated. The experiments showed definitely that the area of the limiting hole did not remain constant when its shape was changed.

The new apertures were made by drilling two holes of equal diameter, b, through sheets of copper foil at a distance L apart (between centres). The part between the centres of breadth b was then cut out with the aid of a sharp knife and a fine file. Thus a slot having rounded ends was obtained. Two such series were made, one in which the average value of $\frac{L}{b}$ was 1·18 and another in which the average value was 7·99.

With the first series, if b was the limiting breadth for failure of ignition and d the limiting diameter for failure through circular holes for the same concentration, then it was found that

$$\frac{b}{d}=\cdot 725$$

over the range from 12 to 26 per cent. within the experimental error. Or, expressed in terms of area, A_s being that of the slot and A_c that of the circle,

$$\frac{A_s}{A_c} = 1{\cdot}25,$$

i. e., the area of the slot had to be about one and a quarter times that of the circular hole.

It was easy to show, by means of the other longer slots, that the actual area of the aperture, considered by itself, had very little to do with determining whether ignition did or did not take place. Thus the area of these might be as much as 3·60 times that of the corresponding circular hole without giving ignition.

The average value of the ratio $\frac{b}{d}$ for these long slots over the range from 16 to 24 per cent. was ·584, or in terms of area, $\frac{A_s}{A_c} = 3{\cdot}80$.

The two ratios, $\frac{b}{d}$ and $\frac{A_s}{A_c}$, are, of course, not independent for a series of apertures of similar shape. Thus, with these slots, if $\frac{L}{b} = \gamma$, we have

$$\frac{A_s}{A_c} = \frac{\pi + 4\gamma}{\pi}\left(\frac{b}{d}\right)^2.$$

The explanation of the increase of limiting area with change of shape of the aperture is that the flame is extinguished by conduction from the flame surface, the shape of which in three dimensions determines the efficiency of the cooling effect. Thus the cooling effect per unit area, per unit time, C_s, at the surface of a sphere is from equation (8),

$$C_s = \frac{\bar{k}(T_i - T_0)}{r_i}, \quad \ldots \ldots \quad (8)$$

while that at the surface of a cylinder, C_c, is, from equation (29),

$$C_c = \frac{\bar{k}(T_i - T_0)}{R_i(\log R_0 - \log R_i)} \cdot \quad \ldots \ldots \quad (29)$$

If the radii of the sphere and cylinder are equal, then we have

$$\frac{C_s}{C_c} = \log \frac{R_0}{R_i}.$$

Hence if the radius R_i is small, the cooling effect of the sphere is larger than that of the cylinder. Thus to produce the same cooling effect per unit area, the radius of the cylinder must be smaller than that of the sphere.

For infinitely long slots it is evident that the limiting area would be infinite, while the actual limiting breadth might not be much less than half the diameter of the limiting circular hole.

Methane-air Mixtures.

Similar experiments were carried out using methane-air * mixtures, most of the results being substantially the same as those obtained with the coal-gas air mixtures. Apart from the very noticeable diminution in violence of the methane explosions, the most striking difference was observed when examining the limiting diameters for propagation down the tubes and ignition of the mixture in the vertical tube AB.

With the coal-gas air mixtures, see above, ignition of the mixture in the tube AB was produced when the flame travelled down the smallest tube which would give propagation, if the concentration of the mixture was between 14 and 26 per cent. Outside these limits, the diameter necessary to give ignition in AB was greater than that for propagation alone, but was not determined exactly in each case. With the methane mixtures the phenomenon was reversed. Using vertical copper tubes, the limiting diameters for propagation and for propagation and ignition of the mixture in AB were identical for concentrations between 6·5 and 7·25 per cent. and also between 11·75 and 12·5 per cent. Between 7·5 and 11·75 per cent., however (*i. e.*, the strongest mixtures), the diameters for propagation and ignition were considerably greater than those for propagation alone. Similarly, with horizontal copper tubes, the two limiting diameters were the same from 6·5 to 7·75 per cent. and again from 11·75 to 12·5 per cent. Between 7·75 and 11·75 per cent., however, the diameters for propagation and ignition were greater than those for propagation alone, but less than those for propaga-

* The methane used was kindly supplied in a metal cylinder by Messrs. Imperial Chemical Industries, Ltd., Stevenston.

tion and ignition down vertical tubes. These results are shown in Graph IV.

The explanation of this peculiar behaviour of the methane mixtures between 7·5 and 11·75 per cent. is that with these mixtures the flame goes into vibration in the lower half of the tube and extinguishes itself when the amplitude upwards into the burnt gas above the flame becomes too great. Thus it is not really a case of failure of ignition, but one of failure of the flame to reach the mixture in the tube AB. The amplitude of the vibration was sometimes quite large and could readily be observed by using the glass tubes. By suitably adjusting the rate of flow, a stationary flame which vibrated continuously at an audible frequency could usually be obtained at a point about $\frac{3}{4}$ down the tube.

This was not observed with the coal-gas mixtures, except for the very small concentrations, nor was it obtained with the methane mixtures outside the above limits, *i.e.*, 7·5 to 11·75 per cent. In these cases the flame travelled steadily down the tube without vibrating.

The phenomenon appears to be very similar to that occurring in a Rijke Sounding Tube[17]. This consists simply of a fairly large vertical tube having a piece of wire gauze stretched across the tube at a distance of about $\frac{1}{5}$ of its length from the lower end. When the gauze is heated red hot by a bunsen flame and the flame removed, the tube emits a most powerful note as the gauze cools. No sound is produced if the tube is horizontal. The effect is dependent on the upwards convection current of air through the tube and on the fact that the gauze forms a sharply marked surface of separation between two volumes of air, one hot and the other cold. When the tube is horizontal there is no unidirectional convection current and no sharply marked surface of separation.

With flame propagation along horizontal tubes the same effect is obtained as with vertical tubes. The reason for this is that there is still a steady flow of gas along the tube and a sharply marked surface (the flame front) separating the cold unburnt gas from its heated products of combustion.

The phenomenon of the spherical flame under the holes in the thin plates was also obtained, though slightly modified, with the methane mixtures of concentration greater than 12·25 per cent. This almost hemispherical flame differed from those observed in coal-gas mixtures, in that it neither expanded to a diameter greater than that of the hole above, nor vibrated at an audible frequency. It also lasted for

a shorter time under the plate, usually about 2 and never more than 5 seconds.

Flame separation took place with methane-air mixture of concentration greater than 12·0 per cent., a bright green

Graph II.

A. Copper foil. Methods I. and II,
B. Copper tubes. „ „ „
C. Copper foil. Method III.

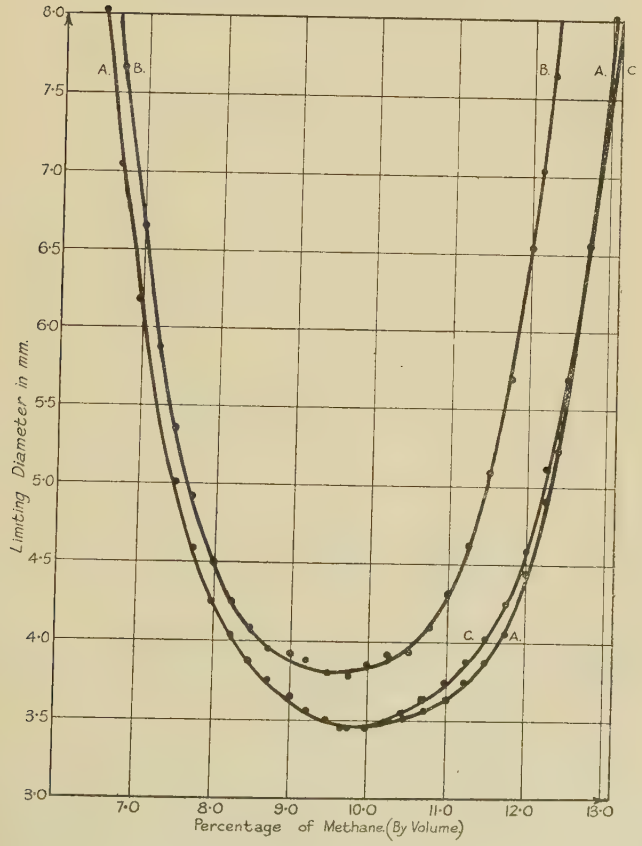

hemispherical flame travelling down the tube, leaving a pale blue cone burning at the top.

This latter phenomenon is probably responsible for the fact that the limiting diameter for propagation along tubes increases more rapidly with concentrations greater than c_0,

than it does for concentrations less than c_0. Thus since the combustion in the hemispherical flame is incomplete, the amount of heat liberated therein is less than would be given by the equation

$$Q = \frac{100-c}{100-c_0} \cdot Q_0,$$

Graph III.

Method IV. Copper foil.
A. Methane-air mixtures.
B. Coal-gas air „

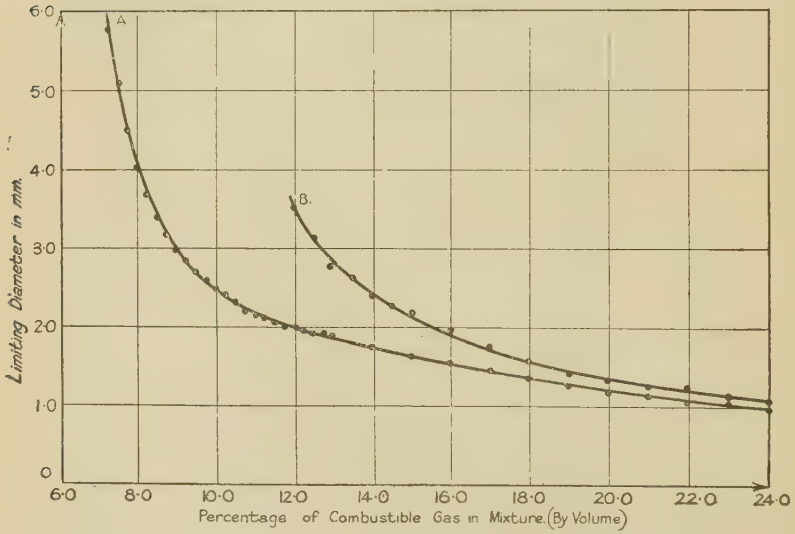

where Q_0 is the amount of heat liberated by the complete combustion of 1 c.c. of the theoretical mixture of concentration c_0.

Results with Methane-air Mixtures.

Copper Foil.—The graphs of the limiting diameters obtained by Methods I., II., and III. are shown in Graph II., and it may be seen that they are very similar to the corresponding ones for coal-gas air mixtures. The minimum diameter is 3·46 mm., which is 1·92 times the minimum for coal-gas air mixtures and occurs at 9·88 per cent. Graph III. shows the variation with concentration of the minimum diameter of hole which will just give a self-supporting flame, *i. e.*, Method IV. above.

Mica Plates.—From 6·5 to 9·25 per cent., the limiting diameters for the mica and copper foil series were identical. For greater concentrations the diameters for the mica plates were slightly less than those for the copper foil (see Table II.). The curve given by Method III., from 10·5 to 13·0 per cent., was the same, within the experimental error, as the corresponding curve for copper foil.

Tubes.—In agreement with the results for coal-gas air mixtures, the limiting diameters for propagation along copper

Graph IV.

A. Vertical copper tubes. } Propagation
B. Horizontal „ „ } and ignition.

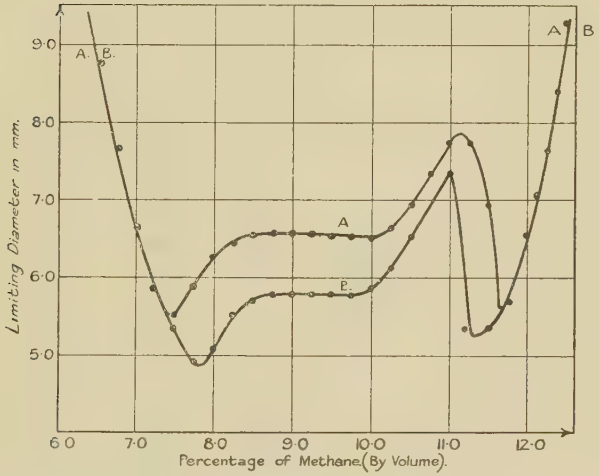

and glass tubes were the same for all concentrations examined, *i. e.*, from 6·38 to 12·5 per cent. The minimum diameter for propagation along the tubes is 3·80 mm. and occurs at a concentration of 9·63 per cent. This is 2·11 times the minimum diameter for the coal-gas mixtures. With the methane mixtures, the difference between the diameters for propagation along tubes and for ignition through holes in thin plates was more distinctly marked than with the coal-gas mixtures.

A piece of apparatus was assembled which allowed the limiting diameters for horizontal propagation to be determined. With this it was found that the limiting diameters for horizontal and vertically downward propagation were the same for all methane mixtures examined.

A considerable amount of work has been done in order to arrive at an equation which would represent, within the experimental error, the variation of limiting diameter with concentration.

TABLE II.

Methane-air Mixtures.

Limiting diameters for ignition through circular apertures in copper foil and mica plates, by Methods I. and II.

Conc. per cent.	Copper foil.	Calc. diam.	Mica plates.	Conc. per cent.	Copper foil.	Calc. diam.	Mica plates.
	mm.	mm.	mm.		mm.	mm.	mm.
6·38	8·65	8·59	—	10·00	3·46	3·46	3·29
6·50	8·03	8·03	—	10·25	3·49	3·47	3·29
6·75	7·05	7·03	7·04	10·50	3·53	3·49	3·37
7·00	6·17	6·22	6·15	10·75	3·57	3·54	3·45
7·25	5·52	5·56	5·51	11·00	3·64	3·61	3·53
7·50	5·00	5·03	5·09	11·25	3·75	3·72	3·63
7·75	4·59	4·61	4·62	11·50	3·88	3·88	3·74
8·00	4·25	4·29	4·24	11·75	4·06	4·12	3·92
8·25	4·03	4·03	4·04	12·00	4·45	4·47	4·24
8·50	3·88	3·84	3·88	12·25	4·92	4·96	4·82
8·75	3·75	3·69	3·74	12·38	5·25	5·28	5·14
9·00	3·64	3·59	3·63	12·50	5·70	5·66	5·51
9·25	3·56	3·52	3·53	12·75	6·66	6·64	6·43
9·50	3·50	3·48	3·42	13·00	8·03	7·98	7·57
9·75	3·47	3·46	3·31	13·13	8·84	8·85	—
				13·25	9·88	9·85	—

The following are the equations tried, arranged in chronological order :—

$$d = d_0 + \alpha(c - c_0)^2, \quad . \quad . \quad . \quad . \quad . \quad . \quad . \quad . \quad . \quad (1)$$

$$d = d_0 + \alpha(c - c_0)^3 + \beta(c - c_0)^4, \quad . \quad . \quad . \quad . \quad . \quad (2)$$

$$d = d_0 + \alpha(c - c_0)^\beta, \quad . \quad . \quad . \quad . \quad . \quad . \quad . \quad . \quad . \quad (3)$$

$$d = d_0 + \alpha(e^{\beta(c-c_0)} - 1), \quad . \quad . \quad . \quad . \quad . \quad . \quad . \quad . \quad (4)$$

$$d = d_0 + \alpha(e^{\beta(c-c_0)} - \beta(c - c_0) - 1), \quad . \quad . \quad . \quad . \quad (5)$$

$$d = d_0 + \alpha(c - c_0)(e^{\beta(c-c_0)} - 1), \quad . \quad . \quad . \quad . \quad . \quad (6)$$

where d is the limiting diameter at concentration c, (c_0, d_0) the coordinates of the minimum, and α and β constants chosen from the experimental curve.

In general the values of α and β are different for the two parts of the curve on either side of the minimum. If c is less than c_0, then $(c-c_0)$ is taken to be the positive difference between these two quantities.

Of the above equations the best is (6), which can be fitted to most of the curves within the experimental error. For example, for propagation along tubes with methane-air mixtures, the limiting diameter can be represented by

$$d=3{\cdot}80+{\cdot}2326\,(9{\cdot}63-c)(e^{{\cdot}6580\,(9{\cdot}63-c)}-1) \text{ mm.}$$

if c is less than 9·63 per cent., and by

$$d=3{\cdot}80+{\cdot}1553\,(c-9{\cdot}63)\,(e^{{\cdot}8974\,(c-9{\cdot}63)}-1) \text{ mm.}$$

if c is greater than 9·63 per cent.

TABLE III.

Methane-air Mixtures. Equation (6).

Graph.	c_0.	d_0.	Range.	α.	β.
	Per cent.	mm.	Per cent.	mm.	
Copper foil. Methods I., II.	9·88	3·46	$6{\cdot}38 \leq c \leq 9{\cdot}88$	·2233	·5780
			$9{\cdot}88 \leq c \leq 13{\cdot}25$	·05868	1·039
Copper foil. Method III.	9·88	3·46	$9{\cdot}88 \leq c \leq 13{\cdot}25$	·1613	·7109
Copper tubes. Methods I., II.	9·63	3·80	$6{\cdot}38 \leq c \leq 9{\cdot}63$	·2326	·6580
			$9{\cdot}63 \leq c \leq 12{\cdot}50$	·1553	·8974

The agreement between the experimental and calculated values for copper foil is shown in Table II. Further values of the constants for other curves are given in Table III.

In some cases equation (4) gives fairly good agreement, and although it has the theoretical disadvantage of not having a minimum at (c_0, d_0), it has the advantage of simplicity.

The method of obtaining the values of α and β for equations (4) and (6) is interesting, since unless it is used, an equation, which can only be solved by successive approximation, is obtained for β.

α and β are determined from the coordinates of two other points on the curve beside those of the minimum. Let these two points be chosen so that the value of $(c-c_0)$ for one is exactly twice the value for the other. Thus if (c', d') are the coordinates of a point about half way along the curve from the minimum, find, from a large scale graph if necessary,

the diameter corresponding to the concentration $2c'-c_0$ and let it be d''.

On substituting in equation (6) say, we have

$$d'=d_0+\alpha(c'-c_0)(e^{\beta(c'-c_0)}-1),$$

and

$$d''=d_0+2\alpha(c-c_0)(e^{2\beta(c'-c_0)}-1).$$

Whence on eliminating $e^{\beta(c'-c_0)}$ by squaring and solving for α, we have

$$\alpha=\frac{2(d'-d_0)}{(c'-c_0)\left(\frac{d''-d_0}{d'-d_0}-4\right)}.$$

Eliminating α from one of the previous equations, we obtain

$$\beta=\frac{1}{(c'-c_0)}\log_e\left[\frac{(d''-d_0)}{2(d'-d_0)}-1\right].$$

Summary.

Introduction.

A theory of the failure of flames to travel along small tubes containing an explosive mixture is developed on the assumption that the extinction of the flame is caused primarily by the cooling effect of the unburnt gas in contact with the flame front. This is contrary to the usual assumption, *i. e.*, that the extinction is due chiefly to the cooling effect of the walls of the tube. An approximate formula connecting the limiting diameter required for propagation with various constants of the gaseous mixture is deduced. This formula indicates correctly the manner of variation of the limiting diameter with these constants, and on calculation gives a result which is of the required order of magnitude.

Experimental Work.

Part I.

Experiments are described in an attempt to measure the maximum time of contact for failure of ignition when a flame is brought into contact with an explosive mixture. No satisfactory evidence of the existence of such a time of contact could be obtained, and it is shown that, under the conditions used, it must have been exceedingly short and less than ·0007 second for a 20 per cent. coal-gas air mixture.

However, it is shown that the actual size of the flame exposed to the mixture has a very important bearing on whether ignition does, or does not, take place.

Part II.

The actual arrangements and methods used for determining the limiting diameters for propagation along tubes and for ignition through circular apertures in thin plates are described. It is found that for all coal-gas air and methane-air mixtures the limiting diameters for propagation along copper and glass tubes are identical, which is also true over part of the explosive range for ignition through circular holes in copper foil and thin mica plates.

A detailed description and photographs are given of an almost spherical flame which may burn inside the explosive mixture for several seconds without producing general ignition.

It is shown that the area of the limiting aperture for ignition through thin plates does not remain constant as its shape is changed.

The curves connecting the limiting diameter, d, with the percentage concentration of the combustible gas in the mixture, c, can be represented by an equation of the type

$$d = d_0 + \alpha(c - c_0)(e^{\beta(c-c_0)} - 1),$$

where (c_0, d_0) are the coordinates of the minimum and α and β are constants.

The writer would like to take this opportunity of expressing his thanks to Messrs. Imperial Chemical Industries, Ltd., Stevenston, for suggesting the above work, for providing a personal grant, and for giving permission to publish the results ; also to Dr. J. Weir for the interest which he took in the investigation. It again affords the writer much pleasure to acknowledge his indebtedness to Professor Taylor Jones for his helpful advice and encouragement.

The experimental part of the above work was carried out in the Research Laboratories of the Natural Philosophy Department of Glasgow University.

References.

(1) H. Davy, Roy. Soc. Phil. Trans. 1816, p. 1.
(2) W. Payman and R. V. Wheeler, Journ. Chem. Soc. 1918, p. 658.
(3) Mallard and Le Chatelier, *Annales des Mines*, p. 274 (1883).
(4) E Taylor Jones, J. D. Morgan, and R. V. Wheeler, Phil. Mag. ser. 6, lxiii. p. 359 (1922).
(5) R. V. Wheeler, Journ. Chem. Soc. cxvii. p. 903 (1920).

(6) Coward and Meiter, Journ. Amer. Chem. Soc. 1927, p. 396.
(7) F. W. Hardwick and L. T. O'Shea, Trans. Inst. Min. Eng. li. p. 553, (1915).
(8) W. A. Bone and D. T. A. Fraser, 'Flame and Combustion in Gases,' 1927 ed., p. 111.
(9) Gregory and Archer, Proc. Roy. Soc. A, cx. p. 91 (1926).
(10) Schneider, *Ann. der Phys.* 4, lxxix. p. 177 (1926).
(11) J. R. Partington and W. G. Schilling, 'The Specific Heats of Gases,' 1924 ed., p. 204.
(12) *Vide* 8 above, p. 480.
(13) *Vide* 8 above, p. 199.
(14) Julius Thomsen, 'Th ermochemische Untersuchungen,' or *vide* 8 above, p. 47.
(15) *Vide* 8 above, p. 39.
(16) *Vide* 8 above, p. 490.
(17) J. H. Poynting and J. J. Thomson, 'Sound,' 1899 ed., p. 139.

December 1931.

III. *The Electrostatic Potential of some Cubic Crystal Lattices.* *By* T. S. Wheeler, *Ph.D., F.R.C.Sc.I., F.I.C.* *

Introduction.

THE general methods[1] available for the calculation of the electrostatic potentials of crystal lattices are based on transformations of Epstein's formulæ[2] for the generalized zeta-function. The following simple method of calculating the potentials of some cubic crystals may be of interest, as it gives results in close agreement with those obtained by the more elaborate formulæ.

The method is based on the calculation of the potential of a simple cubic lattice with regard to the central lattice point, and the relating of the potential of the crystals considered to the results of this calculation.

The Potential of a Simple Cubic Lattice with regard to the Central Lattice Point.

It is assumed that the charges at the lattice points are unit charges of the same sign, and that the unit of distance is an edge of the lattice cube. The sign of the potential is taken to be positive for repulsive forces, and the necessary constraints to prevent the lattice disintegrating are postulated.

We consider the crystal to be built up of cubical layers around the central point ; it is easy to compute that the

* Communicated by the Author.

nth layer will contain $(2n+1)^3-(2n-1)^3=24n^2+2$ lattice points. In order to calculate the potential of the nth layer by direct summation, we take one face of the layer and consider the points constituting one-half of one side of the mth square, counting outwards from the centre of the face. This half-side is repeated 48 times in the layer. Accordingly, making allowance for the fact that the points at the corners of the square and at the centres of the sides are shared between two half-sides, we can write the potential of the mth squares in the nth layer,

$$\frac{24}{\sqrt{n^2+m^2}}+48\sum_{x=1}^{x=(m-1)}\left(\frac{1}{\sqrt{n^2+m^2+x^2}}\right)+\frac{24}{\sqrt{n^2+2m^2}}=\text{M-units say.}$$

The potential of the whole nth layer will be

$$\frac{6}{n}+\sum_{m=1}^{m=(n-1)}\text{M}+\left[\frac{12}{\sqrt{2n^2}}+\sum_{x=1}^{x=(n-1)}\left(\frac{24}{\sqrt{2n^2+x^2}}\right)+\frac{8}{\sqrt{3n^2}}\right].$$

The quantity in square brackets refers to the edges of the layer.

By direct calculation we find for the numerical value of the potentials :—

	Units.
Potential of the first layer =	19·103
Potential of the second layer =	38·083 = 2 × 19·042
Potential of the third layer =	57·122 = 3 × 19·041
Potential of the fourth layer =	76·165 = 4 × 19·041
Potential of the fifth layer =	95·202 = 5 × 19·040
Potential of the tenth layer =	190·407 = 10 × 19·041

It would appear, empirically, that the value for the potential of the nth layer should be $19{\cdot}041n$ units.

We can substantiate this result if we consider that the nth layer contains $24n^2+2$ unit charges, and has a total area of $24n^2$ units. When n is large, the difference in the distances of two adjacent charges from the central lattice point is small compared with these distances, so that we can replace each face of the layer by a charged plane of the same dimensions, with unit density of charge.

The potential of this plane with regard to the central point is given by

$$24 \int_{y=0}^{y=n} \int_{x=0}^{x=n} dy\, dx / \sqrt{(x^2+y^2+n^2)}\,*,$$

that is, by

$$24n(2 \sinh^{-1} 1/\sqrt{2} - \tan^{-1} 1/\sqrt{3})\,\dagger,$$

which is equal to $19{\cdot}041n$.

We may assume, therefore, that the potential of each layer after the first is given by $19{\cdot}041n$.

The Potential of the Edge of a Layer.

An edge of the nth layer can be replaced by a rod with unit density of charge. The potential with regard to the central point is given by

$$2 \int_{x=0}^{x=n} \frac{dx}{\sqrt{(2n^2+x^2)}} = 2 \sinh^{-1}(1/\sqrt{2}),$$

a result which is independent of n.

The Potential of a Cubic Lattice with regard to a Point at the Centre of one of the Cubes.

This potential, which is necessary for our calculations, can readily be deduced from the previous result.

We can regard the given cubic lattice as being made up of a cubic lattice of half the given lattice distance containing the given reference point in which every even-numbered layer, counting from the reference point, is empty, and each odd-numbered layer contains charges at one-fourth of the lattice points. The nth layer of the original lattice corresponds to the $(2n-1)$th layer of the more closely-spaced lattice; remembering that the spacing of this lattice is half the unit length, and that one-fourth of the points of the $(2n-1)$th layer are occupied, we deduce that the potential of this layer, the nth layer of the original lattice, will, as n increases, approach the value

$$\frac{19{\cdot}041}{2}(2n-1).$$

* The author is indebted to his colleague Mr. E. F. Burns for the solution of this integral.

† This asymptotic expression for the potential of a layer of lattice points at its centre may be of interest in other connexions.

We calculate by direct summation the following values :—

Potential of the first layer around the central reference point = 9·238 units.

This layer is formed by the lattice cube, at the centre of which is placed the charge to which the potential is referred.

Units.

Potential of the second layer = $28{\cdot}563 = \frac{3}{2} \times 19{\cdot}042$

Potential of the third layer = $47{\cdot}602 = \frac{5}{2} \times 19{\cdot}041$

Potential of the fourth layer = $66{\cdot}643 = \frac{7}{2} \times 19{\cdot}041$

These figures confirm the previous deduction.

The Potential of a Face-centred Cubic Lattice with regard to the Central Lattice Point.

Let W_1 be the required potential taking the unit distance to be half the distance between two charges measured along an axis of the lattice.

Let W_2 be the corresponding potential of charges placed at the vacant points of the cubic lattice on which the face-centred lattice is based.

Then

$$W_1 + W_2 = 19{\cdot}103 + 19{\cdot}041(2 + 3 + 4 + \ldots n).$$

If the charges corresponding to W_2 are reversed in sign, we have a lattice of the sodium chloride type, the potential of which is known [3]. We can, in fact, when n is large, write

$$W_1 - W_2 = -1{\cdot}748,$$

whence

$$W_1 = (1/2)[19{\cdot}103 - 1{\cdot}748 + 19{\cdot}041(2 + 3 + 4 \ldots n)].$$

The Potential of a Cube-centred Lattice with regard to the Central Lattice Point.

This lattice can be regarded as made up of two cubic lattices, the reference point being on one of the lattices, and at the centre of a unit cube of the second. Taking the side of a unit cube of one of these lattices as the unit of distance, we have for the potential

$$\begin{aligned} &9{\cdot}238 + \frac{19{\cdot}041}{2}(3 + 5 + 7 + \ldots) \\ &\quad + 19{\cdot}103 + 19{\cdot}041(2 + 3 + 4 + \ldots) \\ &\quad = 28{\cdot}341 + \frac{19{\cdot}041}{2}(3 + 4 + 5 + 6 + 7 + \ldots). \end{aligned}$$

The Potential of a Crystal of the Cæsium Chloride Type.

This crystal consists of two interpenetrating cubic lattices, the ions of one kind being at the centre of cubes formed by the other ions.

We consider a crystal with a cæsium ion at the centre, surrounded by alternate layers of chlorine and cæsium ions. Each molecule of cæsium chloride can be regarded as being made up of a cæsium ion and one-eighth of each of the surrounding chlorine ions. If, therefore, we have n-layers of cæsium ions, the crystal under consideration will contain an integral number of molecules if, in addition to the n intermediate layers of chlorine ions, we add a boundary $(n+1)$th, chlorine layer, consisting of one-eighth of a chlorine ion at each corner, one-fourth of a chlorine ion at the remaining points on the edges, and one-half of a chlorine ion at the remaining layer points.

We have now to determine the potential of this crystal with regard to the central cæsium ion, and one of the eight adjacent chlorine ions.

We can disregard the charges at the corners of the external layer in calculating the potential of the crystal, since the quantity involved has the dimensions n^{-1}, while, as shown below, the total potential to be calculated does not involve n.

Since the potential of the edge of a layer is independent of n, the potentials of the edges of the crystal with regard to the central cæsium and chlorine ions will cancel one another; the additional lattice point which we must add to each edge to make it the complete edge of a layer around the chlorine ion under consideration does not sensibly affect the potential.

We can, accordingly, regard the $(n+1)$th chlorine layer, charged as postulated above, as having a half charge at every lattice point, and neglect the deficiency at the corners and edges.

Potential of the Crystal with regard to the Central Cæsium Ion.

The potential of the cæsium layers with regard to the central cæsium ion is

$$19{\cdot}103+19{\cdot}041(2+3+4+\ \ldots\ n)\text{ units},$$

the unit distance being the edge of one of the lattice cubes.

The potential of the chlorine layers with regard to the central cæsium ion is

$$-\left[9{\cdot}238+\frac{19{\cdot}041}{2}\left[3+5+7\ldots(2n-1)+\frac{(2n+1)}{2}\right]\right].$$

The total potential of the crystal with regard to the central cæsium ion is therefore

$$19{\cdot}103-9{\cdot}238-\left(\frac{19{\cdot}041}{2}\right)\binom{3}{2}=-4{\cdot}416 \text{ units.}$$

Potential of the Crystal with regard to a Central Chlorine Ion.

Owing to the displacement of the chlorine ion from the centre of the lattice, we find that it is surrounded by n complete layers of cæsium ions, and three faces of the $(n+1)$th layer less the boundary edges associated with these faces, that is, less six edges with half the normal charge density.

There are also $(n-1)$ complete layers of chlorine ions, and an nth layer, which we may consider as being made up of a complete layer with half the normal charge density, and a half layer with half the normal charge density, less six edges with quarter of the normal charge density. This distribution arises from the fact that three faces of the layer are formed by the external layer with half the normal charge density, postulated above.

Finally, there is an incomplete $(n+1)$th layer of chlorine ions with half the normal charge density which requires the addition of six edges with quarter the normal charge density to complete the half layer with half the normal charge density.

We neglect various adjustments in the charges of corner points.

The potential of the six cæsium edges with half the normal charge density which we add to complete half of the $(n+1)$th layer of cæsium ions, cancels out with the potential of the two sets of six edges of chlorine ions with one quarter the normal charge density which we add to the nth and $(n+1)$th layers.

We have, accordingly, for the potential of the cæsium ions with regard to the chlorine ion under consideration the expression:

$$-\left[9{\cdot}238+\frac{19{\cdot}041}{2}\left[3+5+7+\ldots(2n-1)+\frac{(2n+1)}{2}\right]\right]^{*},$$

* As a check we note that this is identical with the potential of the chlorine layers with regard to the central cæsium ion.

and for the potential of the chlorine ions,

$$19{\cdot}103+19{\cdot}041\left[2+3+\ldots(n-1)+\frac{3n}{4}+\frac{n+1}{4}\right],$$

so that the potential of the crystal with regard to the chlorine ion is

$$19{\cdot}103+9{\cdot}238-\frac{19{\cdot}041}{2}={\cdot}344 \text{ units.}$$

The total potential of the crystal with regard to a central molecule is, accordingly,

$$-4{\cdot}416+{\cdot}344=-4{\cdot}072 \text{ units.}$$

If there are N molecules in the crystal the total potential energy is given by

$$\frac{-N}{2}(4{\cdot}072)=-N(2{\cdot}036),$$

division by 2 being required, since in summation over the crystal, each molecule is counted twice.

If e is the charge on a univalent ion, and a is the distance between two ions of the same kind measured along an axis of the lattice, then the potential is given by

$$\frac{-Ne^2}{a}(2{\cdot}036).$$

Emersleben[4], using Epstein's zeta-functions as a basis, has calculated 2·0354 for the coefficient; the figure here given differs from this by ·03 per cent.

The potential of a large crystal of any shape will be the same as that calculated for the finite cubical crystal, since this can be divided up into a number of cubical crystals.

The Potential of a Crystal of the Fluorspar Type.

We transform a crystal of the cæsium chloride type into one of the fluorspar type, by suppressing, symmetrically as regards the negative charges, one-half of the positive charges, and doubling the charges of the other half, so that we are left with the double positive charges on a face-centred lattice.

We consider the potential of the crystal with regard to half a molecule, a negative ion, and half a positive doubly-charged ion; we see that the potential with regard to the negative ion is the same as the potential of the cæsium

chloride crystal with regard to the chlorine ion, since the negative ions are arranged in the same manner in both crystals, while the suppressed positive ions, and those which have their charges doubled, are symmetrically situated as regards the negative ion. The potential of the fluorine ions with regard to half the central calcium ion is the same as the potential of the chlorine ions with regard to the central cæsium ion; the potential of the calcium ions on the face-centred lattice with regard to the central half calcium ion will be the same as the cæsium ions with regard to the central cæsium ion, less 1·748, since this potential is equal to $2W_1$.

Hence the total potential of the crystal with regard to the half molecule is

$$-4{\cdot}072-1{\cdot}748=-5{\cdot}820 \text{ units.}$$

If a is the unit distance, that is the shortest distance between two fluorine ions, then, as before, the total potential of N molecules will be

$$\frac{-Ne^2}{a}(5{\cdot}820).$$

Emersleben's[4] value for the coefficient, calculated by means of series, is 5·81828 which is within ·03 per cent. of the value deduced above. Ewald[5], using his rapidly converging series calculated 5·816, and Bormann[6], using the more slowly convergent series of Madelung[1], corrected an earlier calculation of Landé[7] and obtained a value of 5·87.

The Potential of a Crystal of the Zinc-Blende Type.

The zinc-blende lattice is obtained from the fluorspar lattice by suppressing symmetrically one-half of the negative ions, and doubling the charges on the other half. This is a repetition of the process involved in passing from a cæsium chloride to a fluorspar lattice.

The potential of the crystal with regard to a central half-molecule is, accordingly,

$$-5{\cdot}820-1{\cdot}748=-7{\cdot}568.$$

The total potential of N molecules is therefore

$$\frac{-Ne^2}{a}(7{\cdot}568).$$

a is half the distance measured along an axis of the lattice between two adjacent atoms of the same kind.

Emersleben's [4] value for the coefficient is 7·566. Born and Bormann [8], using Madelung's [1] series, obtained 7·65.

It is clear that the simple direct methods here outlined give, for the crystals considered above, values for the electrostatic potential which are close to the best values hitherto obtained by the more elaborate series methods. They are definitely better than the values obtained by Madelung's method.

The Potential of a Crystal of the Cuprite Type.

Starting with a crystal of the calcium fluoride type, we transform it into the cuprite type by first interchanging the signs of the charges, which does not alter the value of the potential. We then suppress, symmetrically with regard to the positive ions, the charges on three out of every four negative ions and quadruple the charge on the fourth negative ion. Halving the charges at all the occupied points gives us the required crystal lattice.

The potential of a fluorspar lattice with regard to a central half-molecule is $-5{\cdot}820$ units. If x is the increase in the positive potential involved in the suppression, detailed above, of three-fourths of the negative ions, and the quadrupling of the remaining negative charges, the total potential with regard to the half-molecule will be $-5{\cdot}820+x$.

Dividing by two, the total potential of the cuprite lattice with regard to a central half-molecule will be

$$\frac{-(5{\cdot}820+x)}{2}.$$

We calculate x as follows :—

The potential of a cube-centred lattice with regard to a unit charge at the central point, if there are quadruple charges at the lattice points, unit distance being the edge of a cube is

$$4(28{\cdot}341+\frac{19{\cdot}041}{2}-(3+4+5+\ldots))$$

If the unit distance is half the edge of a cube, the potential will be

$$2(28{\cdot}341+\frac{19{\cdot}041}{2}(3+4+5+\ldots)).$$

The potential of the complete cubic lattice, from which

the cube-centred lattice can be obtained by suppression of three-fourths of the lattice points and quadrupling the charges on the remainder, is

$$19{\cdot}103 + 19{\cdot}041(2+3+4+5+\ \ldots)),$$

from which we find $x = -{\cdot}503$, whence the total potential of the cuprite lattice with regard to a central half-molecule is

$$\frac{-5{\cdot}820 - {\cdot}503}{2} = -3{\cdot}162 \text{ units.}$$

The potential of N molecules is then

$$\frac{-Ne^2}{a}(3{\cdot}162).$$

Emersleben's [4] value for the coefficient is 4·7522, which is 1·503 times the value here calculated.

On general principles Emersleben's value seems high, since comparing the unit cube of cuprite with that of fluorspar, there being half the number of molecules associated with it, one would expect roughly half the potential in place of 80 per cent. of it. Emersleben's paper is highly compressed, being a précis of a previous Dissertation [9], and on that account it is difficult to check his results.

The author's best thanks are due to Prof. H. E. Lennard-Jones and Dr. J. McAulay for their help.

Summary.

1 A simple method is given for the calculation of the electrostatic potential of a cubic lattice with regard to the central lattice point.

2. The result is applied to the calculation of the potential of a cubic lattice with regard to a point at the centre of one of the cubes, and the potentials of a face-centred and cube-centred cubic lattices with regard to central lattice points.

3. From these results the potentials of crystals involving these lattices can readily be obtained.

References.

(1) Madelung, *Phys. Zeit.* xix. p. 524 (1918); Ewald, *Ann. d. Phys.* (iv.) lxiv. p. 253 (1921); Emersleben, *Phys. Zeit.* xxiv. pp. 73, 97 (1923).

(2) Epstein, *Math. Annalen*, lvi. p. 615 (1903); lxiii. p. 205 (1907).

(3) Madelung, *loc. cit.* p. 531; Ewald, *loc. cit.* pp. 279, 280; Emersleben, *loc. cit.* p. 104; Kendall, J. Amer. Chem. Soc. xliv. p. 719 (1922). Kendall used a simple method involving direct summation.

(4) Emersleben, *loc. cit.* p. 104.
(5) Ewald, *loc. cit.* p. 284.
(6) Bormann, *Zeit f. Physik* i. p 55 (1920).
(7) Landé, *Verh. D. Phys. Ges.* xx. p. 217 (1918).
(8) Born and Bormann, *Ann. d. Phys.* (iv.) lxii. p. 218 (1920).
(9) Emersleben, Dissertation, Göttingen (1922).

Royal Institute of Science,
Bombay.

IV. *A Reciprocal Theorem in the Theory of Diffraction.* *By* F. D. Smith, *M.Sc.*, *A.M.I.E.E.* *

1. THE angular distribution of radiation in the neighbourhood of a source of radiation depends mainly upon the dimensions of the source in comparison with the wave-length. Large sources tend to produce a concentration of radiation in a particular direction, whereas small sources tend to produce a more uniform distribution. This property of a large source has an important practical application in the production of directed beams of wireless radiation. Numerous arrangements of transmitting aerials, sometimes in combination with reflectors, have been proposed for the production of a beam of wireless waves, and some of them have developed to a useful practical stage.

It is generally possible to calculate the angular distribution of radiation which will be produced at a distance by a specified aerial array having a specified distribution of current in all its elements. In practice, the distribution of current in the aerial array may depart appreciably from that assumed in the calculation, and a measurement of the angular distribution of radiation produced by the aerial array must be made. This measurement may indicate an insufficient concentration of radiation in the required direction, and it becomes necessary to modify the aerial array, to repeat the measurement of angular distribution and so, by a process of trial and error, to arrive at a satisfactory arrangement. Now an examination of the process by which the angular distribution of radiation from a specified aerial array is calculated, reveals the fact that some of the integrals involved are those used in the stages of Fourier analysis. This suggests that, by a process similar to Fourier analysis, it should be possible to infer the current distribution in the aerial array from the measured angular distribution of radiation and thereby to

* Communicated by the Author.

shorten the process of trial and error described above. It is the object of this paper to show how this calculation may be made.

The same fundamental principles are involved in the phenomena of optical diffraction. An illuminated pinhole, or slit, or a diffraction grating effects a concentration of light in a particular direction, closely analogous to the concentration of electromagnetic radiation produced by an array of wireless aerials. It should be equally possible to infer the distribution of intensity over the surface of a small source of light from the observed diffraction pattern produced by it.

These considerations apply with equal force to sources of sound. For example, the cone of a loud speaker vibrating in a baffle produces an angular distribution of sound in its vicinity which depends upon the frequency and mode of vibration. It is well known that over the upper part of its frequency range, the cone vibrates in a complex manner, and that nodal circles are formed. If the angular distribution of sound in its vicinity at a particular frequency of vibration is known from experiment, it should be possible to infer the mode of vibration of the cone. Numerous other acoustical devices in which use is made of a concentration of sound by a source in a particular direction, such as directional receivers for location of aircraft, directional receivers and transmitters for echo depth sounding and so on, may perhaps be profitably studied by the methods outlined in this paper.

The mathematical part of this paper is presented as a problem in the diffraction of sound; it might equally well have been written, however, with the symbols and nomenclature appropriate to electromagnetic radiation. To fix ideas, three idealized sources of sound and the angular distributions of sound produced by them have been selected to illustrate the process of Fourier analysis indicated above. The more general theory then follows.

Let the source of sound be a plane surface vibrating with simple harmonic motion at right angles to its plane, and let it vibrate in a closely-fitting aperture cut in an indefinite rigid plane and radiate sound into a semi-infinite medium bounded by the rigid plane. The xy plane in fig. 1 represents this rigid plane, and the space defined by positive values of z represents the medium. The small element of area ds at the origin represents a source vibrating with simple harmonic velocity $\dot{\xi}$ about O along the z-axis. The velocity potential $d\phi$ produced at any point P in the medium, defined by

coordinates r, ψ, θ, has been shown by Rayleigh[1] to be given by

$$d\phi = -\frac{1}{2\pi}\dot{\xi}\frac{\epsilon^{-ikr}}{r}ds, \quad . \quad . \quad . \quad . \quad . \quad (1)$$

in which $k = 2\pi/\lambda$, λ being the wave-length. The velocity and pressure at the point P may be found by differentiation with respect to space and time respectively in the usual manner. The velocity potential at P, due to a more extensive

Fig. 1.

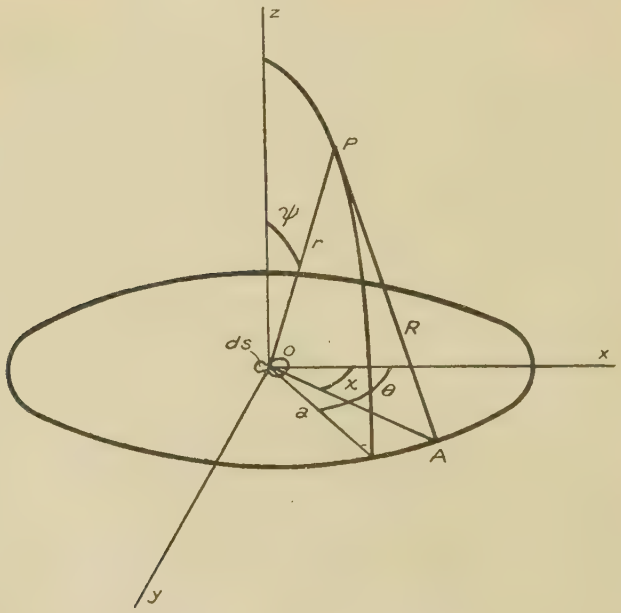

source, that is, a more extensive velocity distribution over the xy plane, is found by dividing the source into elements ds, evaluating the contributions $d\phi$ to the velocity potential separately and adding. The process is equivalent to a double integration over the xy plane as follows :

$$\phi = -\frac{1}{2\pi}\iint\dot{\xi}\frac{\epsilon^{-ikR}}{R}ds, \quad . \quad . \quad . \quad . \quad (2)$$

where R is the distance of the element ds from P. This integral has been evaluated for a number of simple sources of symmetrical shape, generally with the assumption that

ξ is constant over the vibrating area [2–11]. These references, 2–11, have been selected to illustrate the similarity between the formulæ for the directional radiation of sound and of electromagnetic radiation.

It will be shown that a kind of reciprocal relation exists between the mathematical formulæ for velocity distribution in a source and velocity potential in a medium. This reciprocal relation is used to calculate a velocity distribution which will produce a specified distribution of velocity potential. Consider an idealized source in which the velocity distribution over the source is uniform within a circle of radius a_0 and zero outside the circle, that is,

$$\left.\begin{aligned} &a_0 > a, && \dot{\xi} = \dot{\xi}_0 \text{ (constant)}, \\ &a > a_0, && \dot{\xi} = 0. \end{aligned}\right\} \quad . \quad . \quad . \quad (3\,a)$$

The distance R from P of any point A in the xy plane, distant a from O, fig. 1, is given by

$$R^2 = a^2 + r^2 - 2ar \sin\psi \cos(\theta - \chi).$$

If r is large in comparison with a,

$$R \doteqdot r - a \sin\psi \cos(\theta - \chi),$$

so that, using this value of R in (2),

$$\phi = -\frac{1}{2\pi} \iint \dot{\xi} \frac{\epsilon^{-ik\{r - a\sin\psi\cos(\theta-\chi)\}}}{r} ds,$$

where the small quantity $a \sin\psi \cos(\theta - \chi)$ has been neglected in the denominator. The integration over the area of the circle may be carried out in two steps, first by an integration with respect to $\theta - \chi$ and, second, by an integration with respect to a.

$$\phi = -\frac{\epsilon^{-ikr}\,\dot{\xi}_0}{2\pi r} \int_0^{a_0} \int_0^{2\pi} \epsilon^{ika\sin\psi\cos(\theta-\chi)}\, a.da.d(\theta - \chi).$$

The imaginary part of the integral vanishes by symmetry, and the real part in

$$\phi = -\frac{\epsilon^{-ikr}\,\dot{\xi}_0}{2\pi r} \int_0^{a_0} 2\pi\, J_0(ka \sin\psi).a.da,$$

where J_0 is a Bessel function, so that, by completing the integration,

$$\phi = -\dot{\xi}_0 a_0^2 \frac{\epsilon^{-ikr}}{2r} \frac{2J_1(ka_0 \sin\psi)}{(ka_0 \sin\psi)} . \quad . \quad . \quad (3\,b)$$

Reference to tables of Bessel functions shows that ϕ is maximum in the direction $\psi=0$; it decreases as ψ increases becoming zero at the first root of $J_1(ka_0 \sin\psi)=0$; it increases with further increase of ψ, and again decreases to zero at the second root of $J_1(ka_0 \sin\psi)=0$. The angular distribution of velocity potential consists of a central conical zone surrounded by annular zones decreasing progressively in strength and alternatively negative and positive in sign. It corresponds to the well-known optical diffraction pattern from a small disk source of light.

The angular distribution of velocity potential of sound produced by a ring source defined as follows:

$$\left\{\begin{array}{ll} a_0>a>0, & \dot{\xi}=0, \\ a_0+t>a>a_0, & \dot{\xi}=\dot{\xi}_0 \text{ (constant)}, \\ a>(a_0+t), & \dot{\xi}=0, \end{array}\right\} \qquad (4a)$$

is given by

$$\phi=-\dot{\xi}_0 \frac{a_0 t\, \epsilon^{-ikr}}{r} J_0(ka_0 \sin\psi), \quad . \quad . \quad . \quad (4b)$$

provided that t/a_0 is small. This result has already been obtained in the course of the integration for the disk source.

Again, the angular distribution of velocity potential from a line source, defined as follows:

$$\left\{\begin{array}{lll} x_0>x>-x_0, & t/2>y>-t/2, & \dot{\xi}=\dot{\xi}_0 \text{ (constant)}, \\ -x_0>x>x_0, & -t/2>y>t/2 & \dot{\xi}=0, \end{array}\right\}$$
$$. \quad . \quad . \quad (5a)$$

using rectangular coordinates as shown in fig. 2, is given by the well-known formula

$$\phi=-\frac{\dot{\xi}_0 t\, x_0 \epsilon^{-ikr}}{\pi r} \frac{\sin(k x_0 \sin\psi)}{k x_0 \sin\psi}, \quad . \quad . \quad (5b)$$

provided that t/λ is small.

2. The reciprocal relation referred to above can be proved for a disk source as follows. Consider a velocity distribution over the xy plane, fig. 1, having a circular symmetry about the origin O. Let it be imagined to consist of elementary sources distributed in a series of concentric annuli, and let the velocity of all the elements on a circle of radius a be $\dot{\xi}$. Using polar coordinates r, ψ, θ from the origin,

$$R^2=r^2+a^2-2ar\sin\psi\cos(\theta-\chi), \quad . \quad . \quad . \quad (6)$$

and, if a/r is small,

$$\mathrm{R}=r-a\sin\psi\cos(\theta-\chi). \quad . \quad . \quad . \quad . \quad (7)$$

On substituting in (2) and integrating,

$$\phi=-\frac{\epsilon^{-ikr}}{2\pi r}\int_0^{\infty}\dot{\xi}\,a\,da\int_0^{2\pi}\epsilon^{ika\sin\psi\cos(\theta-\chi)}d(\theta-\chi). \quad (8)$$

$$=-\frac{\epsilon^{-ikr}}{r}\int_0^{\infty}\dot{\xi}\,a\,\mathrm{J}_0(ka\sin\psi).da, \quad . \quad . \quad . \quad . \quad (9)$$

Fig. 2.

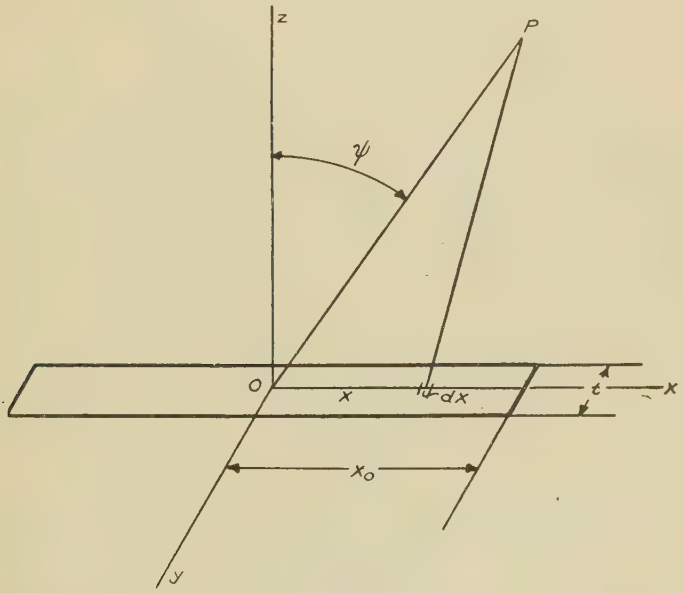

when the small quantity $a\sin\psi\cos(\theta-\chi)$ has been neglected in the denominator. Let $\dot{\xi}$ vary with a as follows:

$$\dot{\xi}=\dot{\xi}_0\frac{2\mathrm{J}_1(ka\,s)}{ka\,s}, \quad . \quad . \quad . \quad . \quad . \quad (10a)$$

an expression of the same form as (3 *b*), which represents the angular distribution of velocity potential from a disk source. On substitution in (9), and putting

$$ka\,s=u \quad \text{and} \quad \sin\psi=bs,$$

it appears that, after some reduction,

$$\phi = -\frac{2\dot{\xi}_0}{k^2 s^2} \cdot \frac{\epsilon^{-ikr}}{r} \int_0^\infty \mathrm{J}_1(u) \cdot \mathrm{J}_0(bu)\, du.$$

It is a well-known result, due to Weber, that

$$\begin{aligned} \int_0^\infty \mathrm{J}_1(u) \cdot \mathrm{J}_0(bu)\, du &= 1, & b &< 1 \\ &= 1/2, & b &= 1 \\ &= 0, & b &> 1, \end{aligned}$$

so that

$$\left.\begin{aligned} \phi &= -\frac{2\dot{\xi}_0}{k^2 s^2} \cdot \frac{\epsilon^{-ikr}}{r}, & s &> \sin\psi, \\ \phi &= 0, & \sin\psi &> s. \end{aligned}\right\} \quad . \quad . \quad (10\,b)$$

Now this represents a velocity potential uniform within the range of ψ defined by $\sin\psi < s$ and zero outside this range. In fact, it bears a close resemblance to $(3\,a)$ which defines a disk source. Summarizing the results for the disk source, it appears that a velocity distribution in the source

$$\left.\begin{aligned} a_0 &> a, & \dot{\xi} &= \dot{\xi}_0 \text{ (constant)}, \\ a &> a_0, & \dot{\xi} &= 0, \end{aligned}\right\}$$

produces a velocity potential in the medium proportional to

$$\frac{2\mathrm{J}_1(ka_0 \sin\psi)}{ka_0 \sin\psi},$$

and that a velocity distribution in the source

$$\dot{\xi} = \dot{\xi}_0 \frac{2\mathrm{J}_1(ka\,s)}{ka\,s},$$

produces a velocity potential in the medium

$$\left.\begin{aligned} s &> \sin\psi, & \phi &= -\frac{2\dot{\xi}_0}{k^2 s^2} \cdot \frac{\epsilon^{-ikr}}{r}, \\ \sin\psi &> s, & \phi &= 0. \end{aligned}\right\}.$$

An examination of these four expressions reveals the fact that the first pair have the same mathematical form as the second. They indicate the existence of a more general relationship between velocity distribution in a source and velocity potential in a medium.

It is instructive to repeat the calculation, given above for the disk, for the ring and the strip. Let the velocity distribution in the source take the form

$$\dot{\xi}=\dot{\xi}_0 \mathrm{J}_0(ka\,s), \quad . \quad . \quad . \quad . \quad . \quad (11a)$$

suggested by (4*b*). Substituting in (9) and putting

$$ka\,s=u \quad \text{and} \quad \sin\psi=bs$$

as before, it appears that, after some reduction,

$$\phi = -\frac{\dot{\xi}_0}{k^2 s^2}\frac{\epsilon^{-ikr}}{r}\int_0^\infty u\,\mathrm{J}_0(u)\,\mathrm{J}_0(bu)\,du.$$

Now

$$\int_0^\infty u\,\mathrm{J}_0(u)\,\mathrm{J}_0(bu)\,du=\infty, \qquad b=1$$
$$=0, \qquad b\neq 1,$$

so that

$$\left.\begin{aligned} &\phi=0, && \sin\psi<s,\\ &\phi=\infty, && \sin\psi=s,\\ &\phi=0, && \sin\psi>s. \end{aligned}\right\} \quad . \quad . \quad . \quad . \quad (11b)$$

This expression for velocity potential is identical in form with (4*a*), so that a similar reciprocal relation between velocity distribution in the source and velocity potential in the medium exists in this special case also.

Referring now to fig. 2 for the strip source, suppose the velocity distribution to take the form

$$\dot{\xi}=\dot{\xi}_0\frac{\sin(kxs)}{kxs}, \quad . \quad . \quad . \quad . \quad (12a)$$

suggested by (5*b*), and to extend between the limits $t/2>y>-t/2$ in the direction of the y axis, t/λ being assumed small. The contribution of an element to the velocity potential at a distant point P in the xz plane is approximately

$$\dot{\xi}\,t\,dx\,\frac{\epsilon^{-ikr}\,\epsilon^{ikx\sin\psi}}{2\pi r},$$

when the small quantity, $x\sin\psi$, in the denominator has been neglected. Hence the velocity potential due to the whole velocity distribution is

$$\phi = -\frac{t\epsilon^{-ikr}}{2\pi r}\int_{-\infty}^{+\infty}\dot{\xi}\,\epsilon^{ikx\sin\psi}\,dx,$$
$$= -\frac{t\epsilon^{-ikr}}{\pi r}\int_0^\infty \dot{\xi}\cos(kx\sin\psi).dx,$$

the second step being valid because of the assumed even distribution of $\dot{\xi}$ in (12 *a*). Substituting for $\dot{\xi}$ from (12 *a*) and putting

$$kxs = u \quad \text{and} \quad \sin\psi = bs,$$

$$\phi = -\frac{\dot{\xi}_0 t\epsilon^{-ikr}}{\pi rks}\int_0^\infty \sin u\cos bu \,.\, \frac{du}{u}$$

$$= -\frac{\dot{\xi}_0 t\epsilon^{-ikr}}{\pi rks}\,.\,\frac{1}{2}\left[\int_0^\infty \sin\{(1+b)u\}\frac{du}{u} + \int_0^\infty \sin\{(1-b)u\}\frac{du}{u}\right].$$

The integral has the value $\frac{\pi}{2}$ when $1>b>-1$ and is zero outside these limits. The velocity potential at P is therefore

$$\left.\begin{aligned} \phi &= \frac{1}{2}\frac{t\dot{\xi}_0\epsilon^{-ikr}}{s\,.\,kr}, && s>\sin\psi>-s, \\ \phi &= 0, && -s>\sin\psi>+s. \end{aligned}\right\} \qquad (12\,b)$$

This expression for velocity potential is identical with (5 *a*). The reciprocal relation also holds for a particular linear source distribution. It remains to show that the relation between velocity potential in the medium and velocity distribution in the source, shown to exist in three special cases, is more general.

3. Let two arbitrary functions, $\phi(\mu)$ and $f(ka)$, be related as follows:

$$\phi(\mu) = \int_0^\infty (ka) f(ka)\, \mathrm{J}_0(ka\mu)\, d(ka), \quad . \quad . \quad (15)$$

$\phi(\mu)$ may be expressed as a Fourier-Bessel integral thus

$$\phi(\mu) = \int_0^\infty (ka)\, \mathrm{J}_0(ka\mu)\, d(ka) \int_0^\infty (ka')\, \phi(ka')\, \mathrm{J}_0(ka\, ka')\, d\,(ka'), \quad . \quad . \quad . \quad (16)$$

subject to suitable restrictions on the form of the function $\phi(\mu)$. By comparison with (15),

$$f(ka) = \int_0^\infty (ka')\, \phi(ka')\, \mathrm{J}_0(ka\,.\,ka')\, d(ka'), \quad . \quad (17)$$

whence replacing ka by μ and a' by a

$$f(\mu) = \int_0^\infty (ka)\, \phi(ka)\, \mathrm{J}_0(ka\mu)\, d(ka), \quad . \quad . \quad (18)$$

which is (15) with ϕ and f interchanged. This theorem is due to Hankel [12].

Let $f(ka)$ in (15) represent a velocity distribution in a source having circular symmetry; $\phi(\mu)$ must be proportional to the resulting velocity potential by analogy with (9), if $\mu = \sin\psi$. Similarly, $\phi(ka)$ in (18) may represent a velocity distribution and $f(\mu)$ the resulting velocity potential if $\mu = \sin\psi$. The functions representing velocity distribution and velocity potential are, with some restrictions, interchangeable.

The velocity potential resulting from a specified velocity distribution proportional to $f(ka)$ is found by evaluating the integral in (15). If, however, the velocity potential $\phi(\mu)$ is specified, we can infer a velocity distribution which will produce it, that is, $f(ka)$ by evaluating the integral in (18). Since $\mu = \sin\psi$ and the range of ψ, $1 \geq \sin\psi \geq 0$, completely defines the velocity potential, $\phi(\mu)$ is specified within these limits. But the integration in (18) is carried to infinity, and the form of $\phi(ka)$ for $ka > 1$ must be specified in order to complete the integration. Since the choice of the form of $\phi(ka)$ for $ka > 1$ is unrestricted, except for the limitations imposed in the derivation of (16), there must be an infinite number of velocity distributions $f(ka)$ which produce the specified velocity potential. In a practical application, it may be evident from other considerations, that $\phi(\mu)$ should be assumed zero for $\mu > 1$, thereby eliminating all but one of the possible velocity distributions. For example, if $\phi(\mu)$ is negligibly small except for small values of μ, it is reasonable to assume that $\phi(ka)$ vanishes for $ka > 1$.

Suppose that $\phi(\mu)$, that is $\phi(\sin\psi)$, is constant over the range $1 \geq \sin\psi \geq 0$. It is well known that a velocity potential of this type is produced by a single source small in comparison with the wave-length. But, by putting $s = 1$ in (10 *a*) and (10 *b*), it is clear that a velocity potential independent of ψ is also produced by a velocity distribution,

$$f(ka) = \frac{2J_1(ka)}{ka} \quad . \quad . \quad . \quad . \quad . \quad . \quad (19)$$

In this case there is no physical consideration which indicates the form of the function $\phi(ka)$ for $ka > 1$.

Let two arbitrary functions $\phi(\mu)$ and $f(ka)$ be related as follows:

$$\phi(\mu) = \sqrt{\frac{2}{\pi}} \int_0^\infty f(ka) \cos(ka\mu)\, d(ka) \; ; \quad . \quad (20)$$

$\phi(\mu)$ may be expressed as a Fourier integral [13], thus:

$$\phi(\mu) = \frac{2}{\pi}\int_0^\infty \cos(ka\mu)\,d(ka)\int_0^\infty \phi(ka')\cos(ka.ka')\,d(ka'), \quad . \ . \ . \quad (21)$$

subject to suitable restrictions on the form of the function $\phi(\mu)$. By comparison with (20),

$$f(ka) = \sqrt{\frac{2}{\pi}}\int_0^\infty \phi(ka')\cos(ka.ka')\,d(ka'),$$

whence, replacing ka by μ and a' by a,

$$f(\mu) = \sqrt{\frac{2}{\pi}}\int_0^\infty \phi(ka)\cos(ka\mu)\,d(ka),$$

which is (20) with ϕ and f interchanged.

Let $f(ka)$ in (20) represent the velocity distribution in an even linear source; $\phi(\mu)$ must be proportional to the resulting velocity potential. The conclusions reached with respect to velocity distance having circular symmetry apply also to even linear velocity distributions.

4. An alternative method of finding a velocity distribution which produces a specified velocity potential depends upon a theorem due to Schlömilch [14] which states that any function $f(x)$ can be expanded in the form

$$f(x) = \tfrac{1}{2}b_0 + b_1 J_0(x) + b_2 J_0(2x) + \ \ldots \ + b_n J_0(nx),$$

where

$$b_0 = \frac{2}{\pi}\int_0^\pi \left\{ f(0) + u\int_0^1 \frac{f'(\mu\xi)\,d\xi}{\sqrt{1-\xi^2}} \right\} du$$

and

$$b_n = \frac{2}{\pi}\int_0^\pi u\cos nu \int_0^1 \frac{f'(\mu\xi)\,d\xi}{\sqrt{1-\xi^2}}\,du,$$

provided that $f(x)$ is continuous from 0 to x, and that $f'(x)$ exists and is continuous for $0 < x \leq \pi$.

If $x = ka_0 \sin\psi$, the terms $J_0(x)$, $J_0(2x)$, etc. may be regarded as proportional to the velocity potential produced by ring sources, as defined by equation (4 *a*) of radii, a_0, $2a_0$, etc. respectively. The constant term $\frac{1}{2}a_0$ may be regarded as proportional to the velocity potential produced by a small point source. If $f(x)$ represents the specified velocity potential, then the expansion gives a velocity distribution, consisting of a point source surrounded by ring sources whose radii increase in arithmetical proportion, which will produce the specified velocity potential.

Another solution of the problem applicable to a linear velocity distribution has been suggested by L. C. Martin in 'Nature' (15).

5. It has been shown that, by means of the integrals given in the previous section, an infinite number of velocity distributions which produce a specified velocity potential over a hemisphere of large radius may be determined and that, in a practical application, physical considerations may eliminate all but one of the possible velocity distributions. In other words, if the velocity potential over a large hemisphere with a plane source of sound located on its base and centrally placed is known, it is sometimes possible to infer the mode of vibration of the source.

The process of calculating a distribution of radiators from a distribution of radiation has been described with particular reference to sound. The fundamental principles on which it rests are, however, closely analogous to those involved in the study of the propagation of electromagnetic radiation. The formulæ of section 1 are to be found in the theory of diffraction in optics, and some of them in the theory of directive arrays of aerials. It is therefore possible that the integrals given above may be applied to the problem of finding the distribution of intensity in a source of light from an observed diffraction pattern, and to the problem of finding the distribution of currents in an aerial array from an observed radiation distribution.

6. The author's thanks are due to Mr. S. Butterworth, M.Sc., for his invaluable help and advice throughout the work, and to the Admiralty for permission to publish this paper.

Summary.

The problem of calculating the velocity potential produced in a medium by a plane source of sound has been solved in a large number of special cases. The more difficult converse problem of calculating a source of sound which will produce a specified distribution of velocity potential in the medium is treated in this paper. It is shown that a general theorem exists which enables a problem of the latter type to be converted to a related problem of the former type. The solution, obtained thus by an indirect method, is not unique.

A possible application of the same method to the calculation of an aerial array which will produce a specified angular distribution of electromagnetic radiation is suggested.

References.

(1) Lord Rayleigh, 'Theory of Sound,' ii. p 107 (1894). Macmillan.
(2) Grey, Matthews, and Macrobert, 'Treatise on Bessel Functions,' chap. xiv. (1922). Macmillan.
(3) H. Stenzel, "Über die Richtcharacteristik von Schallstrahlern," *Elektrische Nachrichten Technik*. iv. pp. 239–253 (1927).
(4) H. Stenzel, "Über die Richtcharacteristik von in einer Ebene angeordneten Strahlern," *E. N. T.* vi. pp. 165–181 (1929).
(5) H. Stenzel, "Über die Berechnung und Bewertung der Frequenzkurven von Membranen," *E. N. T.* vii. pp. 87–99 (1930).
(6) H. Stenzel, "Über die akustische Strahlung von Membranen," *Ann. der Phys.* v. pp. 947–982 (1930).
(7) I. Wolff and L. Malter, "Directional Radiation of Sound," Journ. Acous. Soc. of Am. ii. pp. 201–241 (1930).
(8) R. M. Wilmotte, "General Formulæ for the Radiation Distribution of Antenna Systems,' Proc. I. E. E. v. pp. 1174–1189 (1930).
(9) R. M. Wilmotte, "The Radiation Distribution of Antennæ in Vertical Planes," Proc. I. E. E. v. pp. 1191–1204 (1930).
(10) G. C. Southworth, "Factors Affecting Gain of Directive Aerials," Proc. Inst. Radio Eng. xviii. p. 1502 (1930).
(11) G. Gresky, "Richtcharacteristiken von Antennenkombinationen deren einzelne Elemente in Oberschwingen erregt werden," *Zeits. f. Hoch.* xxxiv. pp. 132–140 (1929).
(12) Gray, Matthews, and Macrobert, *loc. cit.* p. 243, ex. 13.
(13) Carslaw, 'Fourier's Series and Integrals,' chap. viii. (1906). Macmillan.
(14) Gray, Mathews, and Macrobert, *loc. cit.* p. 39.
(15) L. C. Martin, "A Point in the Theory of Critical Illumination in the Microscope," 'Nature,' cxxv. p. 741 (1930).

V. *Generalized Division and Heaviside Operators.*

By A. Press *.

Summary.

The methods of Fractional Differentiation were mainly employed by Oliver Heaviside in his Electromagnetic Theory to develop the needed subject of Bessel's Functions. In contradistinction a Generalized Division Method is herewith suggested which in no way depends on fractional differentiation. Yet the results achieved are substantially the same. It is shown that where approximate solutions of the one-way-series type are obtained the degree of approximation depends, even with convergence, on the presence of a "persistency term," which latter calls for a slightly modified form of the original differential equation investigated. The

* Communicated by the Author.

generalized division method thus acts as a check on the fractional differentiation processes due to Oliver Heaviside, and actually substantiates his preference for handling "divergent" forms in the manner in which he did. This is because the persistency term becomes reduced by the later necessary operational manipulations.

Developing the persistency term so as to produce a series by generalized division, it becomes possible at times so to "extend" the original convergent development that the effects of the persistency term altogether vanish. When this is the case the original differential equation is found to require no modification. Otherwise the "last convergent term" acts as the new reduced persistency term. The types of solution obtained conform in the main to those suggested by Heaviside having a so-called two-way-series form. Application is then made both to the Heaviside Generalized Exponential and to the Generalized Bessels. The need of the "satellite functions" to explain away the difference between "equivalent" and "identical" solutions is led back to the factor of the main argument of the initial fractional index terms occurring in the series. It is the latter factor that comes out definite as to character by adopting the proposed new method of Generalized Division.

---

1. TAKING such a simple differential equation as

$$\frac{dy}{dx} - ay = 0, \quad . \quad . \quad . \quad . \quad . \quad . \quad (1.1)$$

we have operationally that

$$\left(\frac{d}{dx} - a\right) y = 0. \quad . \quad . \quad . \quad . \quad . \quad (1.2)$$

The usual operational method is based upon the idea that an inverse operator process exists, namely $(d/dx - a)^{-1}$, which, acting on both sides of (2), leads to the result first that

$$\left(\frac{d}{dx} - a\right)^{-1} . \left(\frac{d}{dx} - a\right) = 1, \quad . \quad . \quad . \quad (1.3)$$

indicating thereby operationally that

$$y = \left(\frac{d}{dx} - a\right)^{-1} . 0. \quad . \quad . \quad . \quad . \quad . \quad (1.4)$$

The operand of the right-hand side is zero, but since we have by virtue of the index law that

$$\left(\frac{d}{dx}-a\right)^{-1} \equiv 1\Big/\left(\frac{d}{dx}-a\right), \quad . \ . \ . \quad (1.5)$$

it has been suggested (see Forsyth, Diff. Eqs. p. 72, ed. 1929) that an algebraic type of expansion can be resorted to, at least in terms of the operator symbol d/dx. For the present we can adopt with Forsyth the notation

$$\mathrm{D} = d/dx. \quad . \ . \ . \ . \ . \ . \quad (1.6)$$

Thus by ordinary division we have that

$$\frac{1}{\mathrm{D}-a} = \frac{1}{(1-\mathrm{D}/a)} \cdot \frac{1}{a}$$

$$= \left\{1+\left[\frac{1}{a}.\mathrm{D}\right]+\left[\frac{1}{a}\mathrm{D}\right]^2+\left[\ \right]^3+\ldots \text{etc.}\right\}.\frac{1}{a}. \quad (1.7)$$

Heaviside, on the other hand, had long since suggested that an integrating process other than (1.7) is of very practical value, so that in effect we have operationally that

$$\frac{1}{\mathrm{D}-a} = \frac{1}{1-a/\mathrm{D}} \cdot \frac{1}{\mathrm{D}}$$

$$= \{1+[a\mathrm{D}^{-1}]+[a\mathrm{D}^{-1}]^2+[\ ]^3+\ldots \text{etc.}\}.\mathrm{D}^{-1}. \quad (1.8)$$

The methods (1.7) and (1.8), however, are not the only types available.

2. Instead of developing the operator functions in (1.7) and (1.8), after the manner of Forsyth and Heaviside, and later applying the expanded operators to the operand zero of (1.4), one of the methods comprised in the Generalized Division contemplated is to act *directly* on the operand zero. The method, however, which has its major application to fractional Heaviside operators, involves the adoption of a purely arbitrary first term taken in the quotient. This is algebraically regular, for it is easily seen that

$$\frac{0}{a-x} = \frac{a.\alpha_m x^m}{a-x} - \frac{a.\alpha_m x^m}{a-x}. \quad . \ . \ . \quad (2.1)$$

If, then, the first right-hand term is developed by ordinary division, we have

$$\frac{a\alpha_m x^m}{a-x} = \alpha_m x^m \left\{1+\frac{x}{a}+\frac{x^2}{a^2}+\ldots \text{etc.}\right\}. \quad . \quad (2.2)$$

That is, it follows,

$$\frac{0}{a-x} = \alpha_m x^m \left\{ 1 + \frac{x}{a} + \frac{x^2}{a^2} + \ldots \text{etc.} \right\} - \left(\frac{a \cdot \alpha_m x^m}{a-x} \right). \quad (2.3)$$

The identity (2.3), however, has important consequences when applied operationally to differential equations. The undeveloped portion, namely $\left(\frac{a\alpha_m x^m}{a-x} \right)$, corresponds to a "persistency term" and acts as a check, giving the degree of approximation resulting by taking the operationally developed portion. Strictly speaking we have that

$$\frac{0}{a-x} = \alpha_m x^m \left\{ 1 + \frac{x}{a} + \ldots \frac{x^n}{a^n} \right\} + \left[\frac{\frac{\alpha_m}{a^{n+1}} \cdot x^{n+1}}{a-x} \right]_{\text{RT}} - \left(a\alpha_m \cdot \frac{x^m}{a-x} \right)_{\text{PT}}, \quad (2.4)$$

with the remainder term as the middle right-hand expression of (2.4) and the persistency term that to the extreme right.

3. Applying such a type of arbitrary first term division to the differential equation (1.1) with initial m arbitrarily assumed, it follows

$$\begin{array}{l|l} \text{D}-a)\,0 & \alpha_m x^m + a \cdot \frac{\alpha_m}{m+1} \cdot x^{m+1} + \ldots \text{etc.} \quad . \quad (3.1) \\ \hline & -a\alpha_m x^m + (m\alpha_m x^{m-1})_{\text{PT}} \\ \hline & a\alpha_m x^m - (\text{PT}) \\ \hline & a \cdot \alpha_m x^m - a^2 \cdot \frac{\alpha_m}{m+1} \cdot x^{m+1} \\ \hline & a^2 \cdot \frac{\alpha_m}{m+1} \cdot x^{m+1} - (\text{PT}) \\ \hline & \ldots\ldots\ldots \end{array}$$

Here (PT) stands for the unreduced or "persistency term" $(m\alpha_m x^{m-1})$.

The complete solution is therefore given by

$$y = \frac{\alpha_m}{a^m} \cdot \lfloor \underline{m} \cdot \left\{ \sum_0^n \frac{(ax)^{m+n}}{\lfloor \underline{m+n}} + \left[\frac{1}{\text{D}-a} \frac{(ax)^{m+n+1}}{\lfloor \underline{m+n+1}} \right]_{\text{RT}} \right\} - \left(\frac{m\alpha_m x^{m-1}}{\text{D}-a} \right)_{\text{PT}}. \quad (3.2)$$

The remainder term in (3·2) is [RT] with the unaffected or "persistency term" as (PT).

If the series Σ is convergent in (3.2), then the remainder term [RT] can be neglected, so that the solution reduces to the form

$$y = \frac{\alpha_m \lfloor m}{a^m} \sum_0^n - (\mathrm{PT}) \quad . \quad . \quad . \quad . \quad . \quad (3.3)$$

The usual solution for equation (1.1) is of course that

$$y = \alpha_0 e^{ax} = \alpha_m \Sigma \frac{(ax)^{m+n}}{\lfloor m+n}, \quad . \quad . \quad . \quad . \quad . \quad (3.4)$$

where the arbitrarily taken initial m is placed equal to zero.

4. The (PT) or last term of (3.2) offers of course a difficulty which so far has not been surmounted, but its significance can be easily demonstrated. Thus it follows that had the original equation been of the form

$$\frac{dy'}{dx} - ay' = (m\alpha_m x^{m-1})_{\mathrm{PT}} \quad . \quad . \quad . \quad . \quad (4.1)$$

instead of

$$\frac{dy}{dx} - ay = 0 \quad . \quad . \quad . \quad . \quad . \quad (1.1)$$

then the solution would have been

$$y' = \alpha_m \cdot \frac{\lfloor m}{a^m} \sum_0^n \frac{(ax)^{m+n}}{\lfloor m+n} \quad . \quad . \quad . \quad . \quad (4.2)$$

for all possible values of m, fractional or integral. It thus appears that for all those cases where the magnitude of $m\alpha_m x^{m-1}$ is negligibly small relative to zero (4.2) would indeed be a proper type of approximate solution.

The persistency term, as in (4.1), indicates to what extent the original differential equation has been approximated. Yet the approximated algebrized solution, namely

$$y \equiv y' = \alpha^m \frac{\lfloor m}{a_m} \cdot \sum_0^n \frac{(ax)^{m+n}}{\lfloor m+n}, \quad . \quad . \quad . \quad (4.3)$$

can be improved upon by including in y at least a partial development of the operationally additive or persistency term $(\mathrm{D}-a)^{-1}.m\alpha_m x^{m-1}$ in (3.2). This development should be con inued to a point where the original magnitude of the persistency term no longer reduces for the value of x taken.

Any further development would only result in what Heaviside has designated as a divergent series addition. The point of stopping has been called by him the "last convergent term" (see *l. c.* ii. p. 484). The above theory justifies theoretically his treatment of divergent series. The reduced persistency term can then be written down. It will be shown that it amounts to obtaining the two-way generalized developments which become so useful for calculation purposes.

Thus, turning again to the matter of Generalized Division, a dual first term of the form $\{\alpha_m x^m + \alpha_{m-1}x^{m-1}\}$ can be employed in the quotient instead of what had been indicated in (3.1) and (3.2). The expression $\alpha_{m-1}x^{m-1}$ for a *descending series* development (as against the former ascending development based on $\alpha_m x^m$) is introduced in order to avoid (as far as possible) the persistency term. That is, we have

$$\mathrm{D}-a)\,0 \;\Big|\; \underline{\{\alpha_{m-1}x^{m-1}+\alpha_m x^m\}+\{\alpha_{m+1}x^{m+1}+\alpha_{m-2}x^{m-2}\}+\ldots\text{etc.}} \qquad (4.4)$$

$$\frac{\{(m-1)\alpha_{m-1}x^{m-2}+m\alpha_m x^{m-1}\}-a(\alpha_{m-1}x^{m-1}+\alpha_m x^m)}{a\alpha_m x^m+(a\alpha_{m-1}-m\alpha_m)_1 x^{m-1}-(m-1)\alpha_{m-1}x^{m-2}}$$

$$\frac{\{(m+1)\alpha_{m+1}x^m+(m-2)\alpha_{m-2}x^{m-3}\}-a(\alpha_{m+1}x^{m+1}+\alpha_{m-2}x^{m-2})}{a\alpha_{m+1}x^{m+1}+(a\alpha_m-(m+1)\alpha_{m+1})_2\cdot x^m}$$

$$+\left(a\alpha_{m-2}-m(m-1)\frac{\alpha_m}{a^2}\right)_3 x^{m-2}-(m-2)\alpha_{m-2}x^{m-3}$$

. . . . . .

It will be noted that in the third line of (4.4), as well as in the fifth line, in order to avoid persistency terms the coefficients $(\,)_1$ and $(\,)_2$ as well as $(\,)_3$ have been so chosen that we take

$$\left.\begin{aligned} \alpha_{m-1} &= \frac{m}{a}\cdot\alpha_m\,; & (\,)_1 &= 0,\\ \alpha_{m+1} &= \frac{a}{m+1}\cdot\alpha_m\,; & (\,)_2 &= 0,\\ \alpha_{m-2} &= \frac{m(m-1)}{a^2}\cdot\alpha_m\,; & (\,)_3 &= 0. \end{aligned}\right\} \qquad (4.5)$$

. . . . . .

The general law of the coefficients follows really by substituting $(m+1)$ and also $(m-1)$ for m in the first line of (4.5).

The solution of y is evidently one where we have

$$y = \alpha_m \frac{\lfloor m}{a^m} \sum_{-n}^{n} \frac{(ax)^{m+n}}{\lfloor m+n} . + (\mathrm{RT}) \quad . \quad . \quad . \quad (4.6)$$

Thus n can start to right or left from $x=0$ by integral increments for any arbitrarily assumed value for m fractional or integral, provided of course that for n-plus and n-minus at least one branch is convergent. If a branch is divergent then a persistency term must be allowed to subsist so as to modify to this extent the original differential equation. The solution would then be of approximate character only, or of so-called asymptotic type.

The standard solution being, with $m=0$, that

$$y = \alpha_0 \sum_{0}^{n} \frac{(ax)^n}{\lfloor n}, \quad . \quad . \quad . \quad . \quad . \quad . \quad (4.7)$$

Heaviside has suggested (see his Elec. Mag. Theory, ii. p. 439) that we take

$$y = \mathrm{A} \sum_{n}^{-n} \frac{(ax)^{m+n}}{\lfloor m+n} . \quad . \quad . \quad . \quad . \quad . \quad (4.8)$$

The series was to be extended both ways with $m \neq 0$. Difficulties, however, were later encountered which suggested the use of a so-called "satellite term" (see, for example, *l. c.* equations (44) and (45), p. 249). In reality the difficulty, quite apart from divergence, is now seen to rest on the proper m-development to take for e^{ax}. Thus, in view of (4.6), we should take that

$$\mathrm{A}e^{ax} = \left(\alpha_m \frac{\lfloor m}{a^m}\right) \sum_{n}^{-n} \frac{(ax)^{m+n}}{\lfloor m+n} . \quad . \quad . \quad . \quad (4.9)$$

Changing arbitrarily from one m-value to another, though permitted for a proper change in α_m, is rather to be avoided in any one application of the generalized series—that is to say, α_m needs to be standardized. This feature is of particular interest when dealing with the Heaviside Generalized Bessels $\mathrm{B}_\mu(qx, r)$ (see *l. c.* ii. p. 249, equation (43), and also p. 468).

5. The Bessel's Equation can be expressed as

$$\frac{d^2y}{dx^2} + \frac{n}{x}\frac{dy}{dx} - q^2y = 0. \quad . \quad . \quad . \quad . \quad (5.1)$$

For purposes of obtaining a solution (5.1) can be symbolically written as

$$\left.\begin{aligned} &\left\{\left(\mathrm{D}^2+\frac{n}{x}\mathrm{D}\right)-q^2\right\}y=0,\\ &y=\frac{0}{\left(\mathrm{D}^2+\frac{n}{x}\mathrm{D}\right)-q^2}. \end{aligned}\right\} \quad . \quad . \quad . \quad (5.2)$$

Generalized operational division will again be adopted wherein, similarly to (3.1), the first term is taken arbitrarily to be $\alpha_m x^m$. That is, we have, by equating the possible persistency terms equal to zero, so as to obtain regularly ascending and descending terms, that

$$\alpha_{m+2}=\frac{q^2}{(m+2)(m+n-1)}\cdot\alpha_m; \quad \alpha_{m-2}=\frac{m(m+n+1)}{q^2}\cdot\alpha_m. \quad . \quad . \quad . \quad (5.3)$$

All the remaining coefficients can now be obtained by adopting the expedient referred to with regard to (4·5).

If now, in order to obtain Heaviside's evaluation for the Generalized Bessels, we write

$$m=2r \quad \text{and} \quad n=1+2\mu, \quad . \quad . \quad . \quad (5.4)$$

the solution of (5.2) becomes

$$y=\mathrm{B}_n=\alpha_{2r}\left[\text{etc. ...}+\frac{2^2r(r+\mu)x^{2r-2}}{q^2}+x^{2r}+\frac{q^2x^{2r+2}}{2^2(r+1)(r+\mu+1)}+\text{... etc.}\right]. \quad (5.5)$$

Thus, dividing through with $\lfloor\underline{r}\,\lfloor\underline{r+\mu}$, the latter transforms to

$$y=\mathrm{B}_n=\alpha_{2r}\left(\frac{q}{2}\right)^{-2}\lfloor\underline{r}\,\lfloor\underline{r+\mu}\left[\text{etc. ...}+\frac{\left(\frac{qx}{2}\right)^{2r-2}}{\lfloor\underline{r-1}\,\lfloor\underline{r+\mu-1}}+\frac{\left(\frac{qx}{2}\right)^{2r}}{\lfloor\underline{r}\,\lfloor\underline{r+\mu}}+\frac{\left(\frac{qx}{2}\right)^{2r+2}}{\lfloor\underline{r+1}\,\lfloor\underline{r+\mu+1}}+\text{... etc.}\right]. \quad . \quad . \quad . \quad (5.6)$$

The latter (*l. c.*) agrees exactly with the spirit of Heaviside's work. However, he preferred to define the Bessels by writing

$$\mathrm{B}_n=x^{-\mu}.\mathrm{B}_\mu, \quad . \quad . \quad . \quad . \quad . \quad . \quad (5.7)$$

and referring to B_μ as the Generalized Bessel of the μth order. Thus, multiplying through with x^μ within the bracketed expression of (5.5), we have

$$B_\mu = \alpha_{2r}.\left(\frac{q}{2}\right)^{-2r} \frac{}{r}\,\frac{}{r+\mu}\left[\text{etc.} \ldots + \frac{(\frac{1}{2}qx)^{\mu+2r-2}}{\frac{}{\mu+r-1}\,\frac{}{r-1}}\right.$$

$$\left. + \frac{(\frac{1}{2}qx)^{\mu+2r}}{\frac{}{\mu+r}\,\frac{}{r}} + \frac{(\frac{1}{2}qx)^{\mu+2r+2}}{\frac{}{\mu+r+1}\,\frac{}{r+1}} + \ldots \text{etc.}\right]. \quad \ldots \quad (5.8)$$

The factor, $\alpha_{2r}.(q/2)^{-2r}.\ \frac{}{r}\,\frac{}{r+\mu}$, explains why Heaviside was driven to the concept of a satellite term. It arises from ignoring the fact that, as μ and r change within the square bracket of (5.8), that in reality the proportionality coefficient to the left acted as the so-called satellite function.

The H and K Bessels of divergent form, as well as many other interesting new developments, can be obtained in quite an analogous manner if only the generalized type of division is adhered to.

New York.
Nov. 1931.

VI. *Classicism and the Electromagnetic Equations of Lorentz.* *By* A. Press *.

Summary.

Discussions of Electromagnetic Theory have in the main been centred on subdividing vectors into two classes, namely, those having divergence and those having curl. It is shown this is a faulty classification. In Heaviside's 'Electromagnetic Theory,' vols. i. to iii., on the contrary, the classification is that of divergence as opposed to circuitality. It is shown definitely that curl, solenoidality, and circuitality are far from being synonymous terms.

Applications are then made to the "Electromagnetic Equations" of Lorentz as against those of Heaviside. The vector conditions are then discussed for bringing the two into possible accord with each other. Later, it is shown that the Lorentz conception of a time-rate of change of

* Communicated by the Author.

electrical displacement $\bar{d}$ due to an array of electrons of density ρ moving with circuital velocity u is utterly at variance with classical electromagnetic theory. Indeed, according to the Maxwellian theory of a dielectric displacement current the only time a circuital current element is possible with $\rho\bar{u}$ is when the variable displacement of Lorentz's $\bar{d}$ indicates $\dot{\bar{d}}=0$. For the classical case when the $\bar{d}$ due to ρ is such that $\dot{\bar{d}}\neq 0$ there is actually no current effect. With Lorentz's characterization of the displacement $\bar{d}$ therefore, there can be no true correlation. Finally, the Lorentzian equation div. $\rho\bar{u}=\frac{d\rho}{dt}$ is discussed and shown to be vectorially inconsistent with taking $\frac{\partial\rho}{\partial t}=\frac{\partial}{\partial t}$ div e. To avoid inherent self-contradiction the Heaviside-Maxwell-Hertz equations must be resorted to.

REFERRING to Professor Marcus's criticism of my paper in the November issue of the Phil. Mag. for 1931, I appreciate the point which he makes regarding the $d\rho$ properties in the discussion of the equation

$$d(\rho u)=\rho.du+u.d\rho. \quad . \quad . \quad . \quad . \quad . \quad (1)$$

As a condition precedent to making

$$\rho\, du=d\,(\rho u) \quad . \quad . \quad . \quad . \quad . \quad . \quad . \quad (2)$$

in the Lorentz equation

$$\frac{d\rho}{dt}=\text{div}\,\rho u \quad . \quad . \quad . \quad . \quad . \quad . \quad . \quad (3)$$

there was some loss of generality in considering only the individual parts of the total differential $d\rho$. At the same time there are a number of other points raised by Prof. Marcus, particularly in connexion with div and curl that make it important enough to enter into more vectorial and physical detail. Hence the subjoined analysis.

At the outset it must be insisted upon, as with the vector $\bar{d}$ in my equations (23), (24), and (25), which Prof. Marcus appears to have overlooked, that a vector $\rho\bar{u}$ can always be split up into two distinctive parts, one of which is wholly circuital, and the other wholly divergent or non-circuital

(*see* Heaviside, E.M.T. vol. i. p. 207). In this way we have that

$$\rho\underline{u}=\rho\underline{u}_{\text{div}}+\rho\underline{u}_{\text{cir}} \quad . \quad . \quad . \quad . \quad . \quad (4)$$

$$\text{div}\,\rho\underline{u}=\text{div}\,\rho\underline{u}_{\text{div}} \quad . \quad . \quad . \quad . \quad . \quad . \quad (4')$$

$$\underline{d}=\underline{\text{D}}_{\text{div}}+\underline{\text{D}}_{\text{cir}} \quad . \quad . \quad . \quad . \quad . \quad . \quad (5)$$

$$\text{div}\,\underline{d}=\text{div}\,\underline{\text{D}}_{\text{div}} \quad . \quad . \quad . \quad . \quad . \quad . \quad (5')$$

There is a further relationship which needs to be justified, namely, that under certain circumstances to be discussed herewith,

$$\text{curl}\,\rho\underline{u}=\text{curl}\,\rho\underline{u}_{\text{cir}} \quad . \quad . \quad . \quad . \quad . \quad (6)$$

$$\text{curl}\,\underline{d}=\text{curl}\,\underline{\text{D}}_{\text{cir}} \quad . \quad . \quad . \quad . \quad . \quad (6')$$

The last equations (6) will be more easily acceptable if we first bear in mind the two fundamental "Circuital Laws" of electrodynamics. These, of course, are due to Heaviside, Maxwell, and Hertz. Thus we have for the first that the total current $\underline{\text{J}}$ passing through a unit cross-section measured a circuital line integral about such cross-section.

Prof. Marcus, however, appears to object to such distinctively geometrical characterization. In any event the relation is defined mathematically by the equation

$$\text{curl}\,\underline{h}=\frac{d\underline{d}}{dt}+\rho\underline{u} \quad . \quad . \quad . \quad . \quad . \quad . \quad (7)$$

The current involved therefore becomes the Heavisidean,

$$\underline{\text{J}}=\frac{d\underline{d}}{dt}+\rho\underline{u}. \quad . \quad . \quad . \quad . \quad . \quad . \quad (7')$$

The law so far does not stipulate, as it stands, the circuitality of $\underline{\text{J}}$ but it does insist on the circuitality of $\underline{h}$. *Per contra*, the circuitality of $\underline{\text{J}}$ is insisted upon in the second law.

The second law, originally due to Maxwell and Faraday, states that the magnetic current passing the unit cross-section (designated by Heaviside as $d\underline{\text{B}}/dt$) measures the circuital line integral about such section. This defines mathematically the relation

$$-\frac{d\underline{\text{B}}}{dt}=\text{curl}\,\underline{e}. \quad . \quad . \quad . \quad . \quad . \quad . \quad (8)$$

The vector e is therefore defined as a circuital vector whose total or line integral measures the voltage used in electrical engineering calculations. It is such aggregate voltage $\int e \cdot ds$ of the circuit that becomes a measure of the circuital current J set up by virtue of the electrical constants of the circuit peculiar to the materials employed.

Similarly, we have the aggregate gaussage $\int h \cdot d_s$ (see Perry's 'Calculus for Engineers,' p. 135) that becomes a measure of the circuital electric current J set up. Here, however, the magnetic constants of the circuit need to be known. These, again, depend upon the materials of the circuit. If then for convenience we write

$$\frac{1}{c^2} = \mu k, \quad . \quad . \quad . \quad . \quad . \quad . \quad . \quad (9)$$

equation (8) can be written in the form

$$\frac{1}{c^2} \cdot \frac{dh}{dt} = \text{curl } d \, . \quad . \quad . \quad . \quad . \quad . \quad (10)$$

This equation has been objected to by Prof. Marcus, and I imagine on the ground that Lorentz in his electron theory of matter has attempted to do away, as far as possible, with the classical interpretations of μ and k (see Cunningham, 'The Principle of Relativity,' chap. iii. p. 23). Whatever the grounds of objection, it yet remains true, nevertheless, that electrical engineers in their researches and designs still employ the classical ideas here expressed.

The upshot of the above is that in classical electromagnetic theory the vectors h and J, in addition to possessing curl, also possess circuitality. The current J being therefore defined by the relation

$$\text{J} = \frac{dd}{dt} + \rho u, \quad . \quad . \quad . \quad . \quad . \quad . \quad (7)$$

both d and ρu in this theory must therefore possess circuitality as well as curl. In other words, if we operate with curl on (4) it is true we have formally that

$$\text{curl } \rho u = \text{curl } \rho u_{\text{div}} + \text{curl } \rho u_{\text{cir}} \, , \quad . \quad . \quad . \quad (11)$$

but by the two circuital laws ρu_{div} does not enter into current considerations so far as h is concerned. The separation

$$\text{curl } \rho u = \text{curl } \rho u_{\text{cir}} \quad . \quad . \quad . \quad . \quad . \quad (12)$$

is then justified on these grounds. Were it contemplated that an electric current J could flow away from some source without ever returning (thereby making the current non-circuital) then there would be justification in including the term curl ρu_{div}. Physical and engineering difficulties have arisen with just such a system in the calculation of the self-induction coefficient L for a finite length of wire with no return conductor. Thus, since at any point r from a wire with diameter 2R the value of H is given as $1/5r$ per ampere of current (see Perry's 'Calculus for Engineers,' p. 135), we have for the flux per centimetre ampere or L that

$$\mathrm{L}=\int_{r=\mathrm{R}}^{\infty} 1/5r.dr=(1g\infty-1g\mathrm{R})/5=\infty \quad . \quad . \quad (13)$$

This is obviously an absurd result.

It would seem, however, that Prof. Marcus includes just such a term as curl ρu_{div} probably because it appears, at least formally, to be included in the electromagnetic system of Lorentz. This point is so vital that it will be better to show the two systems side by side. Thus we have

Lorentz (see Cunningham, *l. c.*).	Heaviside.
$\operatorname{curl} \underline{h}=\frac{1}{c}\left(\frac{\partial \underline{e}}{\partial t}+\rho \underline{u}\right)$.	$\operatorname{curl} \underline{h}=\frac{d\underline{d}}{dt}+\rho \underline{u}=\frac{d\underline{\mathrm{D}}_{\text{cir}}}{dt}+\rho \underline{u}_{\text{cir}}$.
$\operatorname{curl} \underline{e}=-\frac{1}{c}\frac{\partial \underline{h}}{\partial t}$.	$\operatorname{curl} \underline{d}=\operatorname{curl} \underline{\mathrm{D}}_{\text{cir}}=-\frac{1}{c^2}\frac{d\underline{h}}{dt}$.
$\rho=\operatorname{div} \underline{e}$.	$\rho=\operatorname{div} \underline{d}=\operatorname{div} \underline{\mathrm{D}}_{\text{div}}$.
$0=\operatorname{div} \underline{h}$.	$0=\operatorname{div} \underline{h}$.

. . . . (14)

Operating now with curl on the first of equations (14) it follows :

Lorentz.	Heaviside.
$\operatorname{curl}^2 \underline{h}=\frac{1}{c}\left[\frac{\partial}{\partial t}\operatorname{curl} \underline{e}+\operatorname{curl} \rho \underline{u}\right]$	$\operatorname{curl}^2 \underline{h}=\frac{d}{dt}\operatorname{curl} \underline{\mathrm{D}}_{\text{cir}}+\operatorname{curl} \rho \underline{u}_{\text{cir}}$.

. . . . (15)

In the Heaviside system both elements of current $\underline{d}$ and $\rho \underline{u}$ are already circuital. To assume otherwise is to throw overboard at least one of the two circuital laws fundamental

to classical theory. Then there is the engineering difficulty with regard to the calculation of the self-induction coefficient L outlined above. If ρu in curl ρu on the left-hand side of (15) has divergence as well as circuitality, we would then be entitled to write and then only that,

$$\text{curl}\,\rho u\ (\text{Lorentz}) = \text{curl}\,\rho u_{\text{cir}} + \text{curl}\,\rho u_{\text{div}} \quad . \quad . \quad (16)$$

Let us therefore operate on (14) with div on both sides. This will give

Lorentz.	Heaviside.
$\text{div curl}\,h = 0 =$	$\text{div curl}\,h = 0 = \text{div}\,J$
$\frac{1}{c}\left(\frac{\partial}{\partial t}\,\text{div}\,e + \text{div}\,\rho u\right).$	$= \text{div}\,D_{\text{cir}} + \text{div}\,\rho u_{\text{cir}}.$

. . . . (17)

The right-hand side, that is the Heaviside system, is consistent enough, but on the left-hand side making use of the Lorentzian third equation

$$\rho = \text{div}\,e \quad . \quad . \quad . \quad . \quad . \quad . \quad . \quad (18)$$

it appears that

$$\frac{\partial \rho}{\partial t} = \frac{\partial}{\partial t}\,\text{div}\,e = \text{div}\,\rho u. \quad . \quad . \quad . \quad . \quad (19)$$

Thus the question arises can the ρu of (19) be identically the same ρu which the first line of (14) contains and appears to have the curl property? This can be answered by writing ρu in the form

$$\rho u = \rho u_{\text{div}} + \rho u_{\text{cir}} \quad . \quad . \quad . \quad . \quad . \quad . \quad (20)$$

which proves at once that the e in the third line of the Lorentz system is not circuital at all.

If consistency with the Heaviside system of equations is to prevail then the ρu in equation (19), that is

$$\frac{\partial \rho}{\partial t} = \text{div}\,\rho u \quad . \quad . \quad . \quad . \quad . \quad . \quad . \quad (21)$$

must not be considered as having any circuitality. It is to be considered as wholly divergent so as to offer nothing toward curl h in the Lorentz system of equations (14). The same applies to a divergent part of e also included.

Thus far from making an equation of the form (21) the basis for building-up a system of equations applying to electromagnetism, on the Heaviside system it is circuitality

rather than divergence that is made the keynote. To this extent Prof. Marcus has wholly misunderstood my position.

A word or two about the total current J and the contribution of Lorentz would now be in order. The Maxwellian conduction current C was not based on a convection of charges, or even on a chain of pulsating separated charges, that is, with the Lorentzian type of "polarization." In a condenser circuit therefore a dielectric displacement current was introduced to provide circuitality. Again no convection of charges was contemplated. The electric fluid, as it were, within the conductor was driven over from one side of the condenser armatures to the other through the conductor. Heaviside states (vol. i. p. 21, *l. c.*) that "Away from matter (in the ordinary sense) the medium concerned is the ether, and μ and c absolute constants. The presence of matter, to a first approximation, merely alters the value of these constants." In the interspace between the condenser plates the same non-convective type of electric fluid was assumed to exist. The conduction current in the Maxwell-Heaviside system had nothing to do with electrons so far. Later the possible convection of charges with a circuital velocity u was added. Clearly this constituted an electric current stream of entirely different nature to the one originally suggested by Maxwell. Yet if ρu as a current exists at all it must be wholly circuital, which means that if an ionized conductor forms the conduction portion of a condenser circuit with a hard vacuum between plates, there can be no electron current ρu taking part in the phenomenon at all. On the other hand, the original Maxwellian type of displacement current should exist and can still give rise to a conductive dielectric dissipation of energy within the conductor after the original manner. This does not preclude the possibility that when the space between condenser plates as in a hard Crookes' vacuum tube is filled with thermions or the like, that the circuital convection current ρu may not now give rise to additional convective losses. The latter is the contribution of Lorentz to electromagnetic theory.

Despite the above possible reconciliation of the two systems of equations there are still difficulties to be surmounted. For if we turn to Lorentz's 'Theory of Electrons,' section (2) page 4, we have the statement that "If the divergence of a vector is 0 at all points, its distribution over space is said to be *solenoidal*." On page 13, section (8), however, we find the following:—"ρ is ... connected with . . . the equation (17) [div. $d = \rho$]. We may

say that . . . in general this vector $[\underline{d}]$ is solenoidally distributed, but that there are some places which form an exception to this rule, the divergence of $\underline{d}$ having a certain value ρ different from 0."

The two statements are not reconcilable. It would have been better had a distinction been made between solenoidal and circuital. Taking two charges, plus and minus, as in fig. 1, then on integrating over the surface A it would indicate that no divergence existed within and therefore such region was solenoidal. By integrating over the surface B, however, a divergence would be discovered, and therefore within B the region would not be wholly solenoidal. Nevertheless, so far as both charges plus and minus are concerned, the electrical displacement vector $\underline{d}$ is not circuital, though within certain envelopes $\underline{d}$ can be solenoidal. It is not

Fig. 1.

necessary, in spite of Lorentz's first statement, that the divergence of a vector needs to be zero at all points to be solenoidal. This is mixing up solenoidality with circuitality.

A second difficulty occurs on page 232 referring back to the above section (2). It is aimed to prove that

$$\text{div}\,(\dot{\underline{d}}+\underline{\rho v})=0$$

by requiring "that the total current which is composed of the displacement current $\dot{\underline{d}}$ and the convection current $\underline{\rho v}$ be solenoidally distributed." Lorentz then goes on to say "we shall fix our attention on an element of charged matter" and then proceeds to discuss a change in volume due to an infinitesimal time-displacement along $\underline{v}$. But why this change in volume? Moreover, if $\underline{d}$ by section (2) is really a divergent displacement vector set up by ρ, it is no longer a circuital Maxwellian displacement vector of a type independent of any ρ. Yet, so far as moving electrons are concerned, a circuital current can be produced if the motion

v is circuital and not "transverse." Thus, if the electrons constituting ρ form a circuital array and move parallel to the circuital array path in the direction of circuital v, then the a and a' Maxwellian displacement currents, together with the b and b' currents, form a reinforced circuital current effect. The current elements (see fig. 2) lying between the a and a paths will nullify each other, and the only resultant will be a

Fig. 2.

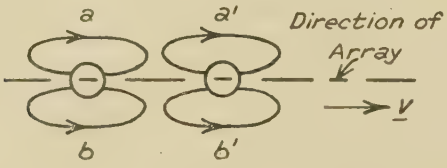

circuital effect already mentioned. The distance between the plus and minus charges can remain constant, and with it the Lorentzian d. In fact, we have $\dot{d}=0$.

If now the motion of the same electrons in circuital array is such that they move "transverse" to the circuital path of the array (see fig. 3), then no circuital current effect will follow along the circuital path of the array. This will be so despite the fact that the distance between plus and minus

Fig. 3.

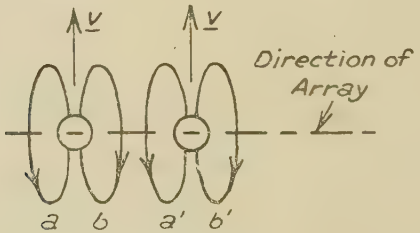

charges vary, and with it the Lorentzian displacement d giving rise to $\dot{d}\neq 0$. In this case, so far as the circuital array path is concerned, the a and b of the one, together with the a' and b' of the neighbouring electrons, nullify each other, and we are left with non-circuital displacements in the transverse direction.

The $\dot{d}$ of Lorentz it is seen has had nothing to do with the matter of current circuitality in the direction of the array

as here developed on a purely Heavisidean basis. The circuital displacement currents in the direction of the array produced by ρu have been wholly Maxwellian and only set up actually when motion characterized by the Lorentzian $\dot{d}=0$ occurs. Thus it has been shown there is no need of changing either the Heavisidean D_{div} or the Lorentzian d to produce a Heavisidean convection current element because of ρu. The two systems are, in fact, totally different.

Some additional light can now be shed on the opening remarks of this paper. Dealing with vectors, we have

$$\text{div } \rho u = \rho n . \frac{d}{dn} . u + u . n \frac{d\rho}{dn} = \rho . \text{div } u + u . \nabla \rho . \quad (22)$$

The vector u must be either circuital or divergent. If circuital then, despite the remarks regarding equations (19) and (21), we have by the Heaviside classification of vectors that, necessarily,

$$\rho . \text{div } u = 0 . \quad . \quad . \quad . \quad . \quad . \quad . \quad (23)$$

The necessary and sufficient condition following from (22) and (23) becomes

$$\text{div } \rho u = \frac{\partial}{\partial x}(\rho u_x) + \frac{\partial}{\partial y}(\rho u_y) + \frac{\partial}{\partial z}(\rho u_z) \equiv u . \nabla \equiv \frac{dn}{dt}\frac{d\rho}{dn} \equiv \frac{d\rho}{dt}$$

$$\equiv u_x . \frac{\partial \rho}{\partial x} + u_y . \frac{\partial \rho}{\partial y} + u_z . \frac{\partial \rho}{\partial z} \quad . \quad . \quad . \quad . \quad . \quad . \quad . \quad (24)$$

This appears to be contrary to Prof. Marcus's expressed opinion. At the same time in view of (21) a Lorentzian contradiction is involved. Moreover, it must again be insisted upon that only my three original equations (33), namely,

$$u_x = u_x(y, z, t), \quad u_y = u_y(x, z, t), \quad u_z = u_z(x, y, t) \quad (25)$$

permit mathematically of bringing the ρ's under the respective partial differential signs of (24). The meaning of $\frac{d\rho}{dt}$ in my original equation (32), or (24) above, is that the former refers to the time-streaming of ρ across a face at right angles to u.

As to the interpretation of equations (25) which has been objected to, it now more easily follows, because of the discussion regarding Lorentz's $\dot{d}$, that with (23) and (25) the circuital state is a steady one and therefore no resultant voluminal distortion or deformation can take place. It is

only in this sense that my own characterization " partaking of a rigid body movement " can be justified. On the other hand, when u is non-circuital and therefore (23) does not prevail there is distortion, but then equations (24) would not apply, Prof. Marcus's views notwithstanding. This contingency regarding u in view of the $\dot{d}$ relation developed need hardly be considered further. It is best and safest, therefore, to keep once more to the classical Heaviside-Maxwell-Hertz system of equations. These at least have no inherent self-contradiction.

VII. *The Calibration of a McLeod Gauge in a Vacuum System**. *By* K. H. Ramaswamy, *M.A.*†.

THE calibration of a McLeod Gauge, by measuring the volumes of the bulb and the capillary tube respectively, becomes difficult when once it is connected to a vacuum system by means of all-glass joints. It seems possible to effect this without going to the extent of breaking up a ready-made gauge for this purpose. The method described below has been tested and found to give very satisfactory results.

The gauge is generally found connected to a very efficient vacuum system, which can be used to exhaust the system to such a low pressure that the gauge fails to read it. In our case a Cenco Hyvac Pump coupled in series with two mercury-vapour pumps of the Waran type ‡ produces the necessary high vacuum where all-glass connexions alone are employed, as in the figure.

Beyond the stopcock A of the pump system is a T-piece, with a burette joined to it, as in fig. 4. The free end of the T-piece B is provided with a stopcock and can be made to communicate with the atmosphere. The end of the graduated tube is kept under mercury contained in the beaker. The stopcock at A is closed, and the pumps are put into action until the pressure within reads zero, as indicated by the gauge. Next the stopcock B is slightly opened to

* Phil. Mag. xlvii. p. 110 (1874).
† Communicated by Prof. H. P. Waran, M.A., D.Sc., F.Inst.P.
‡ Journ. Sci. Inst. 1923.

the atmosphere, so that the levels of the mercury inside and outside the burette read the same, and is then kept closed. Now by opening the stopcock A a definite volume of air can be made to escape into the vacuum system. The pressure exerted by this air within is indicated by the fall of mercury level in the McLeod Gauge at M, fig. 3. This fall being of the order of 5 or 6 cm., the error introduced in the assumption of a perfect vacuum for the system becomes negligible. Applying Boyle's law, we have, if

V = volume of air let in,

P = the initial mean pressure,

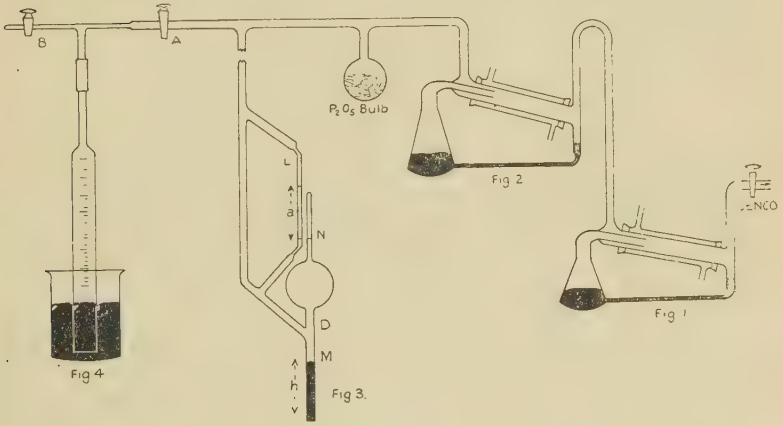

and h = fall in the mercury level in McLeod Gauge (pressure exerted by air within),

then X = volume of the system

$$= \frac{PV}{h}.$$

In the second stage of the experiment a very small volume of air is sent into the system, such that its pressure within can be easily read off on the gauge. For this the burette tube of the T-piece is replaced by a fine capillary tube whose diameter is accurately known. Since mercury is opaque and produces a capillary depression due to surface tension it has to be replaced with concentrated sulphuric acid.

If the small volume of air let into the system be v, then in

this case it can be assumed to be initially at atmospheric pressure P, so that within the system it exerts the pressure

$$p = \frac{v\mathrm{P}}{\mathrm{X}}.$$

Let dv = volume of the capillary tube of gauge up to mark N,

V = total volume beyond D (*i. e.*, vol. of bulb, capillary tube, and connecting tube at D).

The pressure exerted within is now p. On compressing the volume of the air in bulb to that of the volume dv of capillary tube above the mark N, then the new pressure exerted by the air will be

$$p' dv = p\mathrm{V};$$

$$\therefore \qquad \frac{dv}{\mathrm{V}} = \frac{p}{p'}.$$

If now the mercury in the limb L stands a cm. above that in N, we have

$$p' - p = a,$$

i. e.,
$$\frac{p'}{p} - 1 = \frac{a}{p}.$$

Let
$$\frac{dv}{\mathrm{V}} = \alpha = \frac{p}{p'}.$$

Then
$$\frac{p'}{p} - 1 = \frac{a}{p}$$

becomes
$$\frac{1}{\alpha} - 1 = \frac{a}{p},$$

or
$$\frac{1}{\alpha} = 1 + \frac{a}{p} = \frac{a+p}{p} = \frac{a}{p}$$

(since p is very small).

Hence
$$\alpha = \frac{p}{a} = \frac{v\mathrm{P}}{a\mathrm{X}}.$$

Since all the values in the above are known, that of α can be easily calculated.

The following results were obtained in the actual experiment:—

Volume of air let in V.	Mean pressure P.	Fall in height of gauge h.	Total volume $X = \frac{PV}{h}$.
c.c.	cm.	cm.	c.c.
11·1	71·77	2·1	379
15·0	70·17	2·8	376
		Mean	377·5

Area of cross-section of the capillary tube = ·02087 sq. cm.
Atmosphere pressure = 75·97 cm.

Volume of air let in v.	Difference in height in gauge a.	Ratio $\frac{dv}{V}$.
c.c.	cm.	
·09809	9·4	·002100

On calculating the pressure corresponding to the mark on the gauge indicating a pressure of ·001 mm. with the above value for $\frac{dv}{V}$ it was found to be ·0009780 mm. The error herein is as low as 2 per cent., thereby showing the efficiency of the method employed.

I beg to acknowledge my indebtedness to Prof. H. P. Waran, M.A., D.Sc., Ph.D., F.Inst.P., at whose suggestion the experiment was carried out.

The Presidency College, Madras.
1st Dec. 1931.

VIII. *The Absorption of Scattered X-rays.* *By* S. R. Khastgir, *D.Sc.* (*Edin.*), *Reader in Physics, University of Dacca* *.

Introduction.

IT has been shown by Barkla and Khastgir † that the difference between the scattered and the primary X-radiations in their penetrating power is the result of

* Communicated by the Author.
† Barkla and Khastgir, Phil. Mag., Jan. 1925, Nov. 1925, Sept. 1926.

the J-transformation which occurs during transmission of the scattered radiation through matter. Two distinct cases have been recorded. In what has been described as case A the difference appears abruptly in steps at particular values of the mass-absorption coefficients of the incident primary radiation, showing that the "modification" of the scattered beam is subsequent to the process of scattering. In case B, on the other hand, the difference in the absorbabilities of the scattered and the primary radiations is observed over a wide range, from low to high frequencies, without any sign of equality of absorption or of sudden changes of absorption referred to in case A. O. Gaertner *, R. T. Dunbar †, B. L. Worsnop ‡, and N. S. Alexander § have published some experimental results which also do not show any discontinuity. These results, however, add nothing to those already given by Barkla and Khastgir. The conditions in the experiments of Gaertner, Dunbar, and others must be the same as those prevailing in the experiments which yielded results described as case B. The absence of any discontinuity has, however, been taken by some of these experimenters to suggest that "the J-phenomenon has no real existence as an X-ray absorption effect" ‖. In view of such statements it is necessary to emphasize that, even when no discontinuity is observed and the experiments show a persistent difference between the absorbabilities of the scattered and the primary radiations, the difference follows a simple law, viz., $\frac{\mu'}{\rho} - \frac{\mu}{\rho} = \text{constant}$—a law which is a characteristic of Barkla's J-transformation of X-rays. *Discontinuity or no discontinuity, the J-phenomenon is there, whatever be its ultimate explanation.* Experimental evidence is also definite that, whatever be the difference between the conditions of the experiments in case A and those in case B of Barkla and Khastgir's experiments, the process by which the difference between the scattered and the primary beams is produced is *identical* in the two cases (*vide* Phil. Mag., Sept. 1926 and Oct. 1927). Any hypothesis of wave-length change (at least in these absorption experiments) has also been shown to be untenable.

The object of the present paper is twofold :—(1) It is proposed to direct attention to the case B of the absorption

* Gaertner, *Phys. Zeits.* xxviii. p. 493 (1927).
† Dunbar, Phil. Mag. Jan. 1925, May 1928.
‡ Worsnop, Proc. Phys. Soc. xxxix. p. 305 (1927).
§ Alexander, Proc. Phys. Soc. xlii. p. 82 (1930).
‖ Alexander, *loc. cit.*

experiments. Taking into account the energy distribution in the different constituents of the heterogeneous radiation employed, it has been shown that these experiments do not agree with Compton's formula for wave-length change. (2) It has been shown that the experiments of Gaertner, Dunbar, and others agree rather closely with the experiments of Barkla and Khastgir, and that they reveal one significant feature of the J-phenomenon, viz., the difference between the absorbabilities of the scattered and the primary radiations is constant.

I. *Comparison of the Absorbabilities of the Scattered and the Primary X-radiations and Compton's Theory of Scattering.*

To compare the absorbabilities of the scattered and the primary X-rays, the method of Barkla and Khastgir is to measure the ratio of the ionizations produced by the scattered and the primary beams when they are *first* unintercepted and *then* intercepted by similar sheets of any absorbing material. A difference between the "unintercepted" ratio S/P and the "intercepted" ratio S′/P′ indicates a difference in the absorbabilities of the scattered and the primary radiations. In case B of these experiments a constant difference between the ratios S/P and S′/P′ has been observed over a wide range of wave-lengths without any sign of equality. The significant feature in these experiments is the constancy of both the ratios from low to high frequencies.

Compton's formula for wave-length change is

$$\delta = \lambda' - \lambda = 2\Lambda \sin^2\frac{\theta}{2},$$

and that for the intensity of the radiation scattered is

$$\frac{I_S}{I_P} = \frac{C}{\left[1+\frac{\Lambda}{\lambda}(1-\cos\theta)\right]^5} \left\{\frac{1+\cos^2\theta}{2} + \frac{\Lambda}{\lambda}\left(1+\frac{\Lambda}{\lambda}\right)(1-\cos\theta)^2\right\}^*,$$

where I_S = intensity of the radiation scattered at an angle θ to a distance r.

I_P = intensity of the primary beam.

λ' = "modified" wave-length.

* Wentzel, *Phys. Zeits.* xxvi. p. 450 (1925). Klein-Nishina's formula does not materially differ from this formula in the region of wave-lengths under investigation.

λ = "unmodified" wave-length.

θ = angle of scattering.

$$\Lambda = \frac{h}{mc} = \cdot 0242 \text{ Å}.$$

$$C = \frac{e^4}{c^4 m^2 \gamma^2}.$$

Now the ratio of the ionizations produced by the "unintercepted" beams can, to a first approximation, be written as follows:

$$S/P = K \cdot \left(\frac{\lambda'}{\lambda}\right)^3 \cdot \frac{I_S}{I_P}. \quad . \quad . \quad . \quad . \quad . \quad (1)$$

In a similar way, for the beams intercepted by x cm. of an absorbing substance, we can write

$$S'/P' = K \cdot \left(\frac{\lambda'}{\lambda}\right)^3 \frac{I_S}{I_P} \cdot e^{-(\mu'-\mu)x}, \quad . \quad . \quad . \quad (2)$$

where $\frac{\mu'}{\rho}$ = "modified" mass-absorption coefficient,

$\frac{\mu}{\rho}$ = "unmodified" mass-absorption coefficient.

If we substitute in these two relations the value of $\frac{I_S}{I_P}$, as required by Compton's intensity formula, we can write to a first approximation, for $\theta = 90^c$,

$$S/P = \text{constant} \cdot \left(\frac{\lambda'}{\lambda}\right)^3 \frac{1}{1+\frac{3\Lambda}{\lambda}}, \quad . \quad . \quad . \quad . \quad . \quad . \quad . \quad (1.1)$$

$$S'/P' = \text{constant} \cdot \left(\frac{\lambda'}{\lambda}\right)^3 \cdot \frac{1}{1+\frac{3\Lambda}{\lambda}} \cdot e^{-(\mu'-\mu)x} = S/P \cdot e^{-(\mu'-\mu)x}. \quad . \quad . \quad (2.1)$$

Obviously the "unintercepted" ratio S/P is constant except for very short radiations. Now it can be shown that

$$\frac{\mu'-\mu}{\rho} = 3K\lambda^2 \cdot \delta,$$

where δ = Compton's change of wave-length. (Here $\frac{\mu}{\rho} = \frac{\sigma}{\rho} + K\lambda^3$ has been assumed.) Again, since experiments

have shown that both S′/P′ and S/P are practically constant, it follows that $\delta \propto \frac{1}{\lambda^2}$, which is contrary to Compton's theory of scattering.

The above deduction is on the assumption that the radiation employed is *homogeneous*, but since in many cases the general unfiltered radiation from the target has been experimented upon, the energy distribution among the different constituents of the general radiation should be taken into account in order that Compton's theory could be tested.

Calculations of S/P and S′/P′ are based on C. T. Ulrey's * energy distribution curves of tungsten for voltages 20, 25, 30, 35, 40, and 50 kilovolts. The area of each curve obtained by employing Simpson's formula gives the total ionization produced by the primary radiation emitted at each voltage. Now the ratio of the ionizations produced by the "unintercepted" scattered and primary beams may be written as $\frac{i_s}{i_p}$ for an individual wave-length. Thus

$$\frac{i_s}{i_p} = \frac{I_S}{I_P} \cdot \left(\frac{\lambda'}{\lambda}\right)^3.$$

And the corresponding "intercepted" ratio, which may be written as $\frac{i_s'}{i_p'}$ for a single wave-length, is given by

$$\frac{i_s'}{i_p'} = \frac{I_S}{I_P} \cdot \left(\frac{\lambda'}{\lambda}\right)^3 \cdot e^{-(\mu'-\mu)x}.$$

Now the ionization for each constituent wave-length of the primary beam is known from the distribution curve. The values of $\frac{I_S}{I_P}$ and $\left(\frac{\lambda'}{\lambda}\right)^3$ are known from Compton's intensity and wave-length formulæ. Therefore the ionization produced by the scattered radiation for each constituent wave-length can be calculated. The ionization-wave-length curve for the scattered beam is thus constructed for each voltage. The area of each curve gives the total ionization produced by the heterogeneous scattered beam. The ratio of this total ionization produced by the scattered beam to the total ionization produced by the primary beam is then a measure of $\frac{\Sigma i_s}{\Sigma i_p}$ or S/P. From Ulrey's distribution curves, again, the corresponding ones are constructed for both primary and

* C. T. Ulrey, Phys. Rev., May 1918.

scattered beams after each beam has been intercepted by an equal thickness of an absorbing substance. The exponential law of absorption has been employed. In the case of the scattered beam the increased value of the absorption coefficient corresponding to Compton's wave-length change has been used. The calculation is based on the experimental results of Hewlett* and Richtmyer †. The presence of the "unmodified" radiation in the scattered beam is also taken into account ‡. Thus, for six different voltages six pairs of distribution curves for the "intercepted" scattered and primary beams are obtained. The ratio of the areas of each pair is then a measure of $\frac{\Sigma i_s'}{\Sigma i_p'}$ or S′/P′.

Table I.

Voltage.	Average wave-length.	S/P, arbitrary units.	S′/P′, Intercepted by ·15 cm. of aluminium.
Kv.	Å.U.	$\times x$.	$\times x$.
50	·55	1·0	·93
40	·57	1·0	·94
35	·59	1·0	·93
30	·63	1·0	·95
25	·67	1·01	·90
20	·75	1·01	·89

The aluminium absorber considered is of thickness ·15 cm. In Table I. are given the computed values of S/P and S′/P′ for different voltages. The average wave-length of the general radiation corresponding to each voltage is also calculated from each distribution curve. The results are graphically shown in fig. 1. The computed value of S/P is remarkably constant. The experimental curve for S′/P′ is also drawn in the figure for comparison from the results obtained with a Coolidge tube (*vide* Barkla and Khastgir, Phil. Mag., Oct. 1927).

* Hewlett, Phys. Rev. xvii. p. 284 (1921).
† Richtmyer, Phys. Rev. xviii. p. 13 (1921).
‡ Ross, Proc. Nat. Acad. Sci. (Sept. 1925). The change in the proportion of unmodified wave-length in the scattered beam with the change of wave-length had not been allowed for.

Thus, if Ulrey's curves can be taken to represent the real distribution of energy among the different constituents of the general radiation from the tungsten anticathode of the Coolidge tube used, it can be said that Compton's theory of scattering does not agree with the experimental results.

II. *Comparison of Results by different Experimenters.*

It will be interesting to notice a very close agreement between the results obtained by different experimenters at different places and times. We shall consider here the measurements of the ratio of the ionizations produced by the scattered and the primary beams when both the beams are intercepted by successively increasing equal thicknesses of an absorbing substance. The curves showing S′/P′ against

Fig. 1.

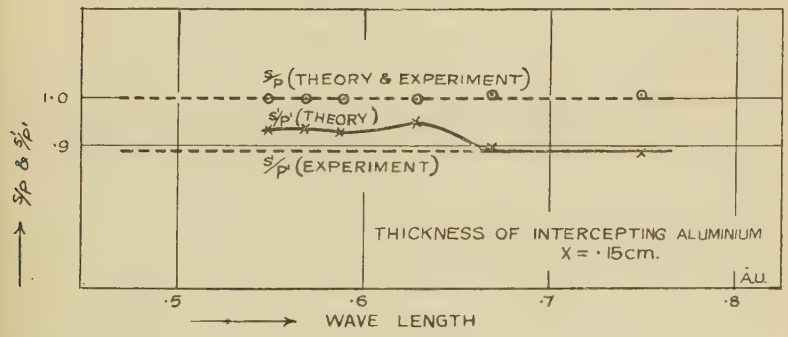

the thickness of the filters drawn from the results of the experiments by Crowther, Barkla and Khastgir, and Gaertner are practically coincident. The results are given in Table II. (see fig. 2). Moderately soft radiation was used by all the experimenters.

The slope of the curve from the experimental results of Dunbar is distinctly less. Before discussing this point the striking feature in the results of Dunbar should be pointed out. Table III. is made out of the curves drawn from his published data. This is shown in fig. 3.

The ratio S′/P′ or at least the ratio $S'/P' \Big/ \frac{S}{P}$ in Dunbar's experiments can thus be regarded as practically constant *.

* It is possible that Dunbar's value of S/P has been conveniently adjusted to be equal to unity for each observation.

TABLE II.*.

Thickness of filter (Aluminium).	S′/P′, arbitrary units.	Remarks.
Barkla & Khastgir.		
cm.		
0·0	1·0	Gas-filled tube.
·02	·96	
·04	·93	Filter paper
·048	·915	radiator.
·06	·90	
·08	·88	
·10	·855	
Crowther.		
0·0	1·0	Gas-filled tube.
·071	·87	Aluminium radiator.
·12	·81	
·21	·75	
Gaertner.		
cm.		
0·0	1·0	Hot cathode tube
·01	·97	excited by valve-
·02	·95	rectified A. C.
·03	·946	current.
·04	·93	Paraffin-wax
·05	·92	radiator.
·06	·90	
·07	·89	
·08	·88	
·09	·875	
·10	·86	
Dunbar.		
0·0	1·0	Coolidge tube.
·046	·941	
·055	·934	Filter paper
·065	·929	radiator.
·075	·921	
·091	·914	
·11	·898	

Vide Crowther, Phil. Mag., Nov. 1921.

Fig. 2.

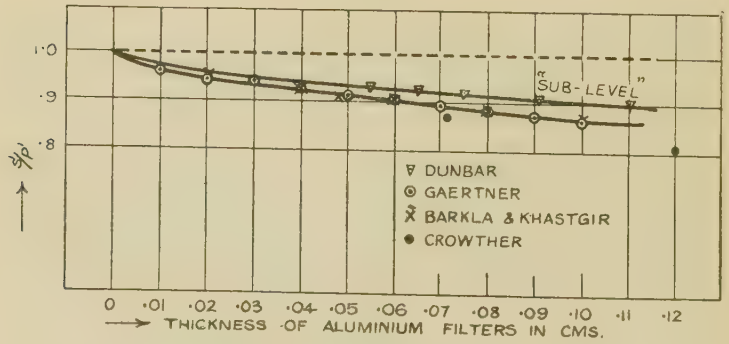

* It is not important that the source of X-rays in all the cases should have exactly the same hardness. The slope has been found to be the same *whatever be the original absorbability of the X-rays.*

TABLE III.

$\left(\frac{\mu}{\rho}\right)_{Al}$ Primary.	Unintercepted S/P.	Intercepted by ·05 cm. of al. S′/P′.	Intercepted by ·09 cm. of al. S′/P′.
	×x.	×x.	×x.
4·7	1·0	·94	—
4·2	1·0	·94	·91
4·2	1·0	·94	—
3·7	1·0	·95	—
3·4	1·0	·96*	—
3·4	1·0	·94	·91
3·0	1·0	·94	·91
3·0	{ 1·0 1·017 }	·955	·93
3·0	1·0	·94	·91
2·9	1·0	·955	·92
2·3	{ 1·0 ·99 }	·94	·92

* Dunbar's curve in this case is very irregular. See Phil. Mag., May 1928, p. 978.

Fig. 3.

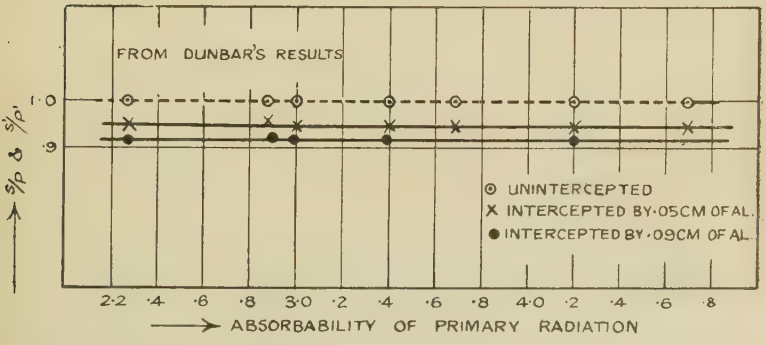

This is in perfect agreement with the law of the J-phenomenon, viz.,

$$\frac{\mu'}{\rho} - \frac{\mu}{\rho} = 0 \text{ or } a \text{ or } b \text{ or } c.$$

The smaller slope of the curve (fig. 2) in Dunbar's experiments, when the ratio of the ionizations produced by the

scattered and the primary beams is plotted against the thickness of the filters placed in the paths of both the beams, indicates a smaller difference in the absorbabilities of the scattered and the primary radiations. This smaller constant difference has also been recorded in Prof. Barkla's laboratory. Some of the results showing the "sublevel" are still unpublished. In Table IV. the results obtained by the author in Prof. Barkla's laboratory in one series of experiments are given, where the difference in the mass-absorption coefficients (in aluminium) is decidedly less than that generally obtained in case B or after the J_1-discontinuity in case A. Fig. 4 illustrates the experimental results. The ratio S′/P′ of the

TABLE IV.

$\left(\frac{\mu}{\rho}\right)_{Al}$ primary.	S/P.	S′/P′, Thickness of aluminium ·045 cm.
	$\times x$.	$\times x$.
1·68	0·99	·90
1·73	1·0	·91
1·88	1·0	·91
1·96	1·0	·91
2·01	1·0	·91
2·26	0·99	·91
2·39	1·005	·945
2·75	1·0	·945
2·85	1·0	·945
2·99	1·0	·945
3·1	1·0	·945
3·46	1·0	·945

ionizations produced by the scattered and the primary radiations, when each is intercepted by ·05 cm. of aluminium, is constant for various absorbabilities of the primary radiation and is less than the constant "unintercepted" ratio S/P by only 5 per cent., whereas the difference usually observed is 9 per cent. (see Crowther, Barkla and Khastgir, and Gaertner). The fixed values of S′/P′, however, lie on two distinct horizontal lines. The scattering angle is 90°. The "sublevel" has also been observed for the angle of scattering equal to 60°. These facts are all explained in terms of the J-phenomenon—indicating that there are different possible levels of X-ray absorption.

The values of $\left(\frac{\mu'}{\rho} - \frac{\mu}{\rho}\right)$, corresponding to the horizontal lines in fig. 4, are found on calculation to be ·4 and ·7 respectively. The smaller value agrees rather well with the observed difference in the half-value mass-absorption coefficients for aluminium between the primary and scattered X-rays at 90° from filter-paper, as given in Dunbar's paper. The constant difference of ·4 is evident, at least from

$$\left(\frac{\mu}{\rho}\right)_{Al} = 3 \quad \text{to} \quad \left(\frac{\mu}{\rho}\right)_{Al} = 5.$$

Dunbar's results are shown in Table V.

Fig. 4.

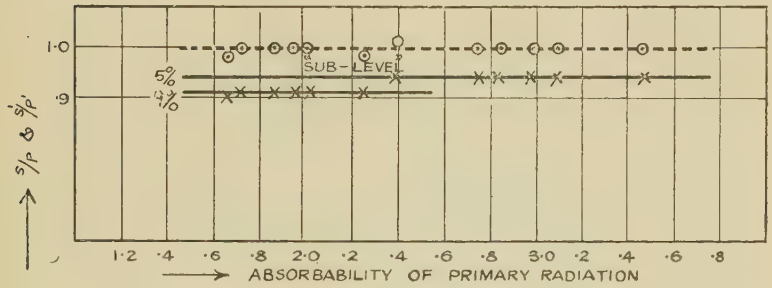

TABLE V.

(R. T. Dunbar, Phil. Mag., May 1928, p. 971.)

$\left(\frac{\mu}{\rho}\right)_{Al}$ primary.	$d\left(\frac{\mu}{\rho}\right)$.	$\left(\frac{\mu}{\rho}\right)_{Al}$ primary.	$d\left(\frac{\mu}{\rho}\right)$.
3·2	·40	4·02	·47 *
3·39	·35	4·12	·46 *
3·42	·34 *	4·15	·39
3·5	·38	4·25	·39
3·58	·33 *	4·39	·36
3·63	·40	4·43	·42
3·8	·39	4·66	·43
3·86	·38	4·92	·53 *
3·97	·39	5·0	·43

* These values are discrepant.

The agreement is satisfactory considering that the percentage error in the direct measurements of the half-value mass-absorption coefficients cannot be very small. It appears, on the other hand, that there is good agreement between Dunbar's values of $\frac{\delta\mu}{\rho}$ and the corresponding values computed from Compton's theory for harder radiations; but one should remember that to test Compton's theory the presence of the "unmodified" scattered radiation must be considered. It is curious that even Compton's own measurements * (absorption experiments) showed agreement with his theory, in spite of the fact that the unmodified part was not allowed for.

The results of Worsnop and Alexander cannot be utilized for comparison. Worsnop follows an indirect method, and, besides, the scattering substance is placed in most cases in the "reflecting" position, so that a true comparison of the scattered and the primary radiations is not possible. When, however, the scattering substance is placed in the right position, avoiding error due to differential absorption of the scattered and the primary beams, the experimental data are not available. Judging by the two lines marked S/P and S′/P′ in one diagram, running parallel to each other †, the constancy of the difference in the absorbabilities of the scattered and the primary radiations seems to be substantiated. Alexander's results are "not calculated to measure difference in absorption."

Summary.

In the present paper attention is directed to the case B of the experiments of Barkla and Khastgir, where a constant difference between the absorbabilities of the scattered and the primary beams is observed over a wide range of frequencies. An attempt has been made to test Compton's theory, taking into account the heterogeneity of the X-radiation experimented upon. Calculations are based on Ulrey's energy-distribution curves for general radiations from tungsten at various voltages. The presence of the "unmodified" radiation in the scattered beam has been considered in the computation. The experiments are shown *not* to agree with Compton's theory.

The results of other experimenters have been discussed. It has been shown that the experiments of Crowther,

* A. H. Compton, Phil. Mag. Nov, 1923.

† Worsnop, Proc. Phys. Soc. xxxix. p. 305, fig. 6 (*b*).

Gaertner, and Dunbar agree closely with the experiments of Barkla and Khastgir—thus revealing a feature of the J-phenomenon, viz.,

$$\left(\frac{\mu'}{\rho}\right) - \left(\frac{\mu}{\rho}\right) = \text{constant.}$$

In conclusion, I wish to express thanks to Prof. C. G. Barkla, under whose direction the experiments described in this paper were performed in the Physical Laboratory of the University of Edinburgh.

Supplementary Note.—Since writing the paper I. Backhurst has published some experimental results in Phil. Mag., Jan. 1932. Employing a full-wave rectification "constant potential" high-tension generator, he has attempted to repeat the experiments on superposed X-radiations (scattered) described by Prof. Barkla and Sen-Gupta in Phil. Mag., April 1929. Backhurst's absorption curves for X-radiations scattered from paraffin wax at 90°, do not, however, show any discontinuity. It should be mentioned here that a striking feature in all the experimental results on the subject is that whenever the J-discontinuities appear, there is always a law governing the position and the magnitude of the effects. Backhurst's assertion that the discontinuities are due to "stray" effects and fluctuations in the voltage-time curve of the high-tension generator, ignores altogether this fact of a regular law behind the phenomenon. Besides, as has already been pointed out in the paper, the absence of a discontinuity does not necessarily mean an absence of the J-absorption. *Even* if we disregard the discontinuities, it has been shown that the *observed constancy* of the difference between the absorption coefficients of the scattered and primary beams from wave-length to wave-length is not compatible with Compton's theory, according to which $\delta\mu \propto \lambda^2$. As wave-length increases, the proportion of unmodified wave-length in the scattered beam is, however, expected to increase, tending thereby to diminish the value of $\delta\left(\frac{\mu}{\rho}\right)$ to some extent. Again, the effect of heterogeneity of the beam has been shown to diminish its value to a certain extent. It is, however, extremely difficult to believe that there is an exact compensation to make the change of absorption coefficient (in different substances) independent of wave-length.

A comparison between the actual values of $\delta\left(\frac{\mu}{\rho}\right)$ and those calculated from Compton's theory has been made elsewhere. The change in the mass-absorption coefficient can be evaluated from the constant difference between the ratio (S/P) of the ionizations produced by the scattered and the primary beams and the corresponding ratio (S′/P′), when both the beams are intercepted by similar sheets of an absorbing substance. The values of $\delta\left(\frac{\mu}{\rho}\right)$ have been calculated for various absorbing substances, *e. g.*, filter paper, aluminium, copper, silver, tin, and gold. The experimental values have been compared with the values calculated according to Compton's theory for $\lambda = \cdot 7$ Å., since for this wave-length the proportion of unmodified wave-length in the scattered beam is known from the measurements of Ross. The effect of heterogeneity has been neglected. The comparison shows discrepancies. The agreement, if there is any, is only accidental. Multiple scattering in the body of the scattering substance cannot explain the discrepancies. Barkla and Khastgir have also shown that the value of $\delta\left(\frac{\mu}{\rho}\right)$ is independent of the angle of scattering. (*Vide* Phil. Mag., Sept. 1926.)

Physics Department,
Dacca University.
May 3rd, 1932.

IX. *The Kinetics of Chemical Change in Solution.* *By* E. A. Moelwyn-Hughes *.

IT is a well known fact that the variation with temperature of the velocity constant for any uncomplicated chemical reaction in a homogeneous system is given by the Arrhenius[1] equation :

$$k = Z.e^{-E/RT}. \quad . \quad . \quad . \quad . \quad . \quad . \quad (1)$$

The quantity E, termed the critical increment for the reaction, has not yet been evaluated from independently determined quantities, although attempts are at present being made to do so. The true meaning of the term Z was first understood by

* Communicated by the Author.

Lewis[2], who identified it in the case of two bimolecular gaseous reactions with the collision number for the systems. Since then, the collision theory of chemical reaction rate has developed considerably, particularly in the hands of Hinshelwood[3], who has shown how, by considering the critical energy increment to be distributed among internal degrees of freedom of the colliding molecules, the kinetics of gaseous unimolecular reactions could be explained. It is the object of this paper to examine various types of reactions in solution in the light of the collision theory.

The numerical values of the constants E and Z are obtained from the experimental values of the velocity coefficient (k) determined at various temperatures (T), by plotting $\ln k$ against $\frac{1}{T}$; the slope of the curve is $-\frac{E}{R}$, and Z is the value of R corresponding to $T=\infty$.

This method of dealing with experimental data must, however, be used with circumspection where reactions in solution are involved, for several of these, which appear at first sight to be uncomplicated, prove, on closer inspection, to be anything but simple. For example, the hydration of acid anhydrides[4], the decomposition of β-keto-carboxylic acids[5], and certain coordination reactions[6] are kinetically unimolecular in water, but the reaction rate is sensitive to hydrogen ion and hydroxyl ion, so that the observed rate at any given temperature is represented by an equation of the type

$$k_{obs.} = k_0 + k_1 f_1[H^+] + k_2 f_2[OH^-]. \quad . \quad . \quad (1)$$

The point to observe is that, if the observed velocity constant ($k_{obs.}$), which is clearly a composite value, is treated in the manner described, the resulting equation (1) gives an entirely misleading conception of the true energetics of the processes involved. The peculiarities of such reactions are not revealed until the nature of f_1 and f_2 is known and k_0, k_1, and k_2 can be examined separately. In the present work we will confine our attention to chemical changes the rates of which are due either (1) predominantly to an elementary reaction (e.g., $k_0 >> \{k_1 + k_2\}$) or (2) to two simultaneous reactions with reactivities of the same order (e.g., $k_1 \cong k_2$).

The collision theory of chemical reaction rate states that for thermal reactions undergone by simple molecules, or by complex molecules undergoing elementary changes, the number of molecules reacting per second $\left(\frac{dn}{dt}\right)$ is equal to the number of collisions per second ($_1Z_2$) multiplied by

the fraction ($e^{-E/RT}$) of these which have a total kinetic energy of approach equal to or greater than the energy of activation (E). The total number of collisions per c.c. per second between gas molecules of types 1 and 2 is given by the kinetic theory [7]

$$_1Z_2 = 2n_1n_2\sigma_{12}^2 \left\{ 2\pi RT\left(\frac{1}{M_1} + \frac{1}{M_2}\right)\right\}^{\frac{1}{2}} . \quad . \quad . \quad (2)$$

M_1 and M_2 are the molecular weights of the two types of molecules, and n_1 and n_2 the number of molecules of each type in 1 c.c. of gas at temperature T; σ_{12} is the sum of the molecular radii. It has sometimes been assumed that this equation requires some correction before it can be applied to estimate the number of collisions between dissolved molecules, but in the present work no such correction will be introduced. There are two reasons for applying the formula directly. The identity of the osmotic pressure of a dilute solution with the gas pressure, which has long been known in the case of aqueous solutions, has recently been shown to hold for non-aqueous solutions also [8]; this is experimental confirmation of what is predicted by the kinetic theory, namely, that the average kinetic energy, and consequently the root-mean-square velocity, of a dissolved molecule is equal to that of a gaseous molecule with the same mass and at the same temperature. Secondly, we have the experimental observation that the decomposition of chlorine monoxide in the gaseous phase—a reaction involving consecutive bimolecular changes—is identical in all respects with its decomposition in carbon tetrachloride solution [9]; since the above equation accounts for the rate of bimolecular gaseous reactions, it is to be concluded that it gives also a true value of the number of collisions between dissolved molecules in simple cases. The bimolecular velocity constant (k), expressed in litres per gram-molecule per second, is

$$-\frac{dn}{dt} \cdot \frac{1}{n_1n_2} \cdot \frac{N_0}{1000},$$

where N_0 is the Avogadro constant; hence the calculated collision frequency in these units is

$$_1Z_2 = \frac{2N_0\sigma_{12}^2}{1000} \cdot \left\{ 2\pi RT\left(\frac{1}{M_1} + \frac{1}{M_2}\right)\right\}^{\frac{1}{2}} . \quad . \quad (2a)$$

An approximate value for the molecular diameters may be obtained by assuming the molecules of the reactants to be closely packed in the pure liquid or solid state at low

tempertures[10]; σ is then related to the molecular volume V_m by the equation

$$\sigma = 1{\cdot}33 \times 10^{-8} \times V_m^{\frac{1}{3}} \quad . \quad . \quad . \quad . \quad . \quad (3)$$

The values of σ obtained in this way are in quite good agreement with those determined from the study of surface films[11] and with the size of ions in solution as measured by means of their electrical conductivity[12].

We shall now proceed to compare the observed rates of certain reactions with those calculated on the collision theory, applying the gas formula directly to the case of dilute solutions.

Bimolecular Reactions between Neutral Solute Molecules.

Data relating to various bimolecular reactions in solution are summarized in Table I. The critical increment and the observed collision number have been found by plotting the logarithm of the velocity coefficient (expressed in litres/gram-molecule seconds) against $\frac{1}{T}$. In the only example—that of the conversion of ammonium cyanate into urea—where a reverse reaction is detectable, allowance has been made for this in calculating the velocity constant. The agreement between the experimental collision frequencies and those calculated by equation ($2a$) is always within the limit of experimental uncertainty, and is in some cases quite striking when it is recalled that the absolute values of the velocity constants differ by a factor of more than 10^4. It is true that all but one of these reactions are of the same type ($R_1ONa + R_2I \rightarrow R_1OR_2 + NaI$), that all the solvents are hydroxy compounds, and that the range of critical increment values is not great, but other instances are known which show a similar agreement[21]. The examples given in Table I. have been selected as representative instances from a large mass of data, concerning all of which it may be said that the gas-collision formula gives rates which are always of the right order of magnitude.

The observed collision numbers for the reactions between methyl iodide and the sodium cresolates show how, in a disubstituted benzene nucleus, the rate at which one substituent is attacked (in this case the $-ONa$ group) can be influenced by the proximity of a second substituent (here the $-CH_3$ group). It is a matter of interest to inquire how the relative reactivities of such compounds can be interpreted on a purely mechanical basis, such as Ingold has

TABLE I.

Reaction.	Reference.	Solvent.	E (calories).	$Z \times 10^{-11}$. Observed.	$Z \times 10^{-11}$. Calculated	$\frac{k_{calc.}}{k_{obs.}}$
$CH_3ONa + 1:2:4ClC_6H_3(NO_2)_2$	(13)	CH_3OH	17,450	1·91	2·42	1·3
$C_2H_5ONa + 1:2:4ClC_6H_3(NO_2)_2$	(13)	C_2H_5OH	16,760	1·80	2·39	1·3
$C_2H_5ONa + CH_3I$	(14)	C_2H_5OH	19,490	2·42	1·93	0·8
$C_2H_5ONa + C_2H_5I$	(15)	C_2H_5OH	20,650	1·49	2·23	1·5
$C_2H_5ONa + C_6H_5CH_2I$	(15)	C_2H_5OH	19,900	0·15	2·17	14·5
$C_6H_5ONa + C_3H_7I$	(16)	C_2H_5OH	22,450	3·53	2·31	0·7
$C_6H_5ONa + iso\ C_3H_7I$	(16)	C_2H_5OH	22,100	1·74	2·31	1·3
$C_6H_5ONa + C_{16}H_{33}I$	(16)	C_2H_5OH	22,430	2·78	2·92	1·0
$C_6H_5CH_2I + C_4H_9I$	(17)	C_2H_5OH	21,560	2·92	2·43	0·8
$C_6H_5CH_2I + iso\ C_4H_9I$	(17)	C_2H_5OH	21,350	2·45	2·43	1·0
$C_6H_5CH_2I + C_{16}H_{33}I$	(17)	C_2H_5OH	21,090	1·26	3·12	2·5
$o\ CH_3C_6H_4ONa + CH_3I$	(18)	C_2H_5OH	21,180	1·30	1·99	1·5
$m\ CH_3C_6H_4ONa + CH_3I$	(18)	C_2H_5OH	19,490	2·27	1·99	0·9
$p\ CH_3C_6H_4ONa + CH_3I$	(18)	C_2H_5OH	20,900	8·49	1·99	0·2
$\beta\ C_{10}H_7ONa + C_2H_5I$	(19)	CH_3OH	21,010	0·10	2·21	22·1
$\beta\ C_{10}H_7ONa + C_2H_5I$	(19)	C_2H_5OH	19,840	0·11	2·21	20·1
$\beta\ C_{10}H_7ONa + C_2H_5I$	(19)	C_3H_7OH	21,300	0·40	2·21	5·5
$NH_4CNO \rightarrow (NH_2)_2CO$	(20)	H_2O	23,170	42·7	4·05	0·1

adopted to explain the relative rates of hydrolysis by alkalies of substituted malonic acid esters[22]. A vast volume of work, commencing with that of Meyer and of Menschutkin, has been carried out on the relative rates of reactions of *o*-, *m*-, and *p*-disubstituted compounds, and much useful data are given by Wittig[23]. The results reveal but few regularities, as may be expected from the fact that the relative ease with which one group can be attacked will generally depend not only on the position of the second substituent, but also on the nature of the reaction[24]. It would appear, however, that one general observation can be made with some confidence, *i. e.*, in the majority of cases the probability that an activated molecule shall undergo chemical change is greater for the meta- and the para-compounds than for the ortho-compound. This is precisely what is to be anticipated on a collision basis for a set of reactions with a common critical increment, for steric hindrance in the ortho-compound must be greater than in the others. For the particular example under discussion, the relative steric factors appear to be

$$o : m : p : : 7{\cdot}5 : 4{\cdot}5 : 1.$$

Another way of describing the same thing is to say that, before the three results can give equal agreement with theory, the effective diameters for collision purposes must be in the ratio

$$o : m : p : : 1 : 1{\cdot}3 : 2{\cdot}6.$$

Attention has been directed by Christiansen[25] and by Norrish and Smith[26] to several reactions—notably the formation of ternary ammonium salts—which have rates about 10^8 times slower than those calculated in the above manner. The suggestion, which at one time seemed probable, that the discrepancy could be attributed to the deactivating influence of solvent molecules, must, however, be abandoned, since recent experiments have shown that the velocity of these reactions is, roughly, the same in certain solvents as in the gaseous phase, where, moreover, there is considerable catalysis by the walls of the reaction vessel[27]. The real reason for the slowness of these reactions is not yet fully understood. It is possible that one of the reactants must ionize before being able to undergo chemical change. So far as the information at present available on the minute ionization of such bodies allows us to go, this view is quite consistent with the facts[28]; but other explanations are equally logical, although not so easy to test.

Bimolecular Reactions between Ions and Neutral Molecules.

It is, of course, not justifiable to apply to the kinetics of reactions which depend upon ions colliding with neutral molecules a collision formula which has been deduced for gaseous systems. Nevertheless, it will be interesting to compare the observed rates of a few reactions involving ions with those rates calculated on the assumption that, for purposes of determining the number of collisions between a neutral solute molecule and an ion, the ion can be regarded as moving with the same velocity as a neutral gas molecule of the same mass. It should be observed that the reactions treated in the previous section are to some extent ionic. In calculating the rates given in Table II. the ions have been assumed to be unsolvated, but this does not introduce a large error. The first two instances are of particular interest since, although the absolute rates differ by a factor of 10^{10}, the theoretical velocities are in both cases of the right order of magnitude. This at least suggests that even for reactions of this category the predominant factor determining the rate is the fraction of molecules which are in an activated state: compared with this term ($e^{-E/RT}$) an error in the collision frequency must be small. For seven other reactions the discrepancy is no greater than can be allowed for by an error of some 200 calories in the experimental values of the energy of activation; and since velocity constants for some of these reactions were determined over a small range of temperature only, an error to this extent is easily accounted for. On the other hand, the hydrolysis of the aliphatic esters by alkalies and certain cases of the Finkelstein reaction show discrepancies which at once suggest that, either the collision formula cannot hold even approximately, or that the reactions are in some way subject to disturbing influences which are absent in other cases. The possible nature of these influences will be discussed later.

Catalyzed Unimolecular Reactions.

A catalyzed reaction possessing a unimolecular velocity constant which is proportional to the concentration of the catalyst must be bimolecular in character, and the rate of chemical change must depend on the number of encounters between catalyst and reactant molecules. From the point of view of chemical kinetics the chief difference between a catalyzed unimolecular reaction and a true bimolecular reaction is that in the former case only one of the interacting species is changed chemically, so that the second

TABLE II.

Reaction.	Reference.	Solvent.	E.	$Z \times 10^{-11}$. Observed.	$Z \times 10^{-11}$. Calculated.	$\frac{k_{obs.}}{k_{calc.}}$
$CH_2Cl.COOH + OH^-$	(29)	H_2O	25,850	4·55	2·86	0·6
$C_6H_4\langle^{CH_2}_{CO}\rangle O + OH^-$	(30)	H_2O	12,500	41·7	2·93	0·07
$CH_3COOC_2H_5 + OH^-$	(31)	H_2O	11,210	0·00017	2·95	17,400
iso $CH_3COOC_5H_{11} + OH^-$	(31)	H_2O	11,040	0·00011	3·80	34,600
$CH_2I.COOH + Cl^-$	(32)	H_2O	22,850	7·9	2·66	0·3
$CH_2Cl.COOH + I^-$	(32)	H_2O	19,770	0·13	1·47	11·3
$CH_2I.COOH + SCN^-$	(32)	H_2O	18,190	0·40	2·17	5·4
$CH_3[CH_2]_3Cl + I^-$	(33)	$(CH_3)_2CO$	23,500	2·24	1·64	0·7
$C_6H_5CO[CH_2]_2Cl + I^-$	(33)	$(CH_3)_2CO$	22,160	10·5	1·88	0·2
$CH_3S[CH_2]_2Cl + I^-$	(34)	$(CH_3)_2CO$	20,740	0·085	1·57	18·5
$\left.\begin{matrix}\alpha\\ \beta\end{matrix}\right\} C_{10}H_7O[CH_2]_2Cl + I^-$	(34)	$(CH_3)_2CO$	22,420	0·15	1·73	11·5
$C_3H_7Cl + I^-$	(35)	$(CH_3)_2CO$	18,610	0·0013	2·69	2,070
$C_{16}H_{33}Cl + I^-$	(35)	$(CH_3)_2CO$	19,040	0·0020	4·76	2,580

species retains its initial concentration throughout. Some of the most important reactions occurring in solution belong to this category. All the reactions referred to in Table III. are catalyzed by hydrogen ion, with the exception of the decomposition of nitrosotriacetonamine, which is catalyzed by hydroxyl ion. The true (bimolecular) constant for these reactions is obtained by dividing the observed unimolecular constant by the concentration of the catalyst. This is a simple matter where $k_{\text{uni.}}$ is proportional to $[H^+]$, as, for

Table III.

Reaction catalyzed by H^+.	Reference.	$E_{observed.}$	$Z_{observed.}$
Hydrolysis of Methyl Acetate	(36)	16,920	$3{\cdot}86\times10^{8}$
Hydrolysis of Ethyl Acetate	(37)	16,830	$1{\cdot}66\times10^{8}$
Hydrolysis of Acetamide	(38)	18,780	$9{\cdot}43\times10^{9}$
Conversion of Creatine into Creatinine	(39)	19,690	$4{\cdot}35\times10^{8}$
Hydrolysis of Benzoyl Glycine	(40)	22,100	$1{\cdot}72\times10^{9}$
Hydrolysis of Acetyl Glycine.....	(40)	22,100	$7{\cdot}41\times10^{9}$
Conversion of γ-Hydroxyvaleric Acid into Lactone.....	(41)	16,630	$4{\cdot}55\times10^{8}$
Mutarotation of α-Glucose	(42)	17,100	$3{\cdot}89\times10^{10}$
Enolization of Acetone	(43)	20,580	$3{\cdot}94\times10^{10}$
Decomposition of Nitrosotriacetonamine (catalyzed by OH^-)	(44)	16,040	$4{\cdot}69\times10^{9}$
Decomposition of Diazoacetic Ester ...	(45)	17,480	$4{\cdot}64\times10^{12}$
Hydrolysis of Lactose	(46)	24,680	$3{\cdot}21\times10^{11}$
Hydrolysis of Sucrose	(47)	25,560	$8{\cdot}89\times10^{14}$
Hydrolysis of Maltose	(48)	30,970	$1{\cdot}86\times10^{15}$
Hydrolysis of Cellobiose	(48)	30,710	$9{\cdot}78\times10^{14}$

example, in the case of the decomposition of diazoacetic ester [45] and the conversion of creatine into creatinine [39]; similarly, $k_{\text{uni.}}$ for the decomposition of nitrosotriacetonamine [44] is proportional to $[OH^-]$. In certain other cases, however, this linear relation does not hold, the observed unimolecular constant being more closely proportional to the activity of the hydrogen ion: this is true for the hydrolysis of lactose [46] and the substituted glycines [40]. The true bimolecular constant in these instances is $k_{\text{uni.}}/a_{H^+}$, since the activity of hydrogen ion becomes equal to its concentration at great dilutions. Wherever it has been possible to compare

values of $k_{\text{uni.}}/a_{H^+}$ determined at fairly high concentrations of acids with values of $k/[H^+]$ measured in dilute solutions the agreement is quite good. Thus, for the conversion of γ-hydroxyvaleric acid into valerolactone at 30° C., Garrett and Lewis give $k_{\text{uni.}}/a_{H^+} = 4{\cdot}45 \times 10^{-3}$, while Taylor and Close find $k_{\text{uni.}}/[H^+]$ to be $4{\cdot}31 \times 10^{-3}$ litres/gram-molecule-seconds [41]. Similarly, for the hydrolysis of sucrose at 25° C. the bimolecular constant given by Moelwyn-Hughes from the activity of hydrogen ion is $1{\cdot}47 \times 10^{-4}$; $k_{\text{uni.}}/[H^+]$ in very dilute solutions is found by Lamble and Lewis to be $1{\cdot}35 \times 10^{-4}$ litres/gram-molecule-seconds [47]. The experimental velocity constants have been corrected for the attainment of an equilibrium stage in certain instances (*e.g.*, the mutarotation of α-glucose [42], the hydrolysis of methyl acetate [36], and the formation of valerolactone) and for auto-catalysis in the case of the enolization of acetone—the measurable process in the reaction between iodine and acetone in acid solution.

The logarithm of the bimolecular constants thus obtained, when plotted against $\frac{1}{T}$, give the Arrhenius critical increments E. Again, wherever possible the results of different investigators were plotted on one graph. E for the hydrolysis of sucrose [47] by acids is the average of 36 values in very close agreement; E for the enolization of acetone [43] is the average of 25 values. These are probably the most accurately known values of the energy of activation for reactions in solution. The constants obtained by Meehan, by Euler and Rudberg, and by von Peskoff and Meyer for the hydrolysis of acetamide [38], taken jointly, give E = 18,780 calories, which is in fair agreement with Crocker's value of 18,320. The present value of the critical increment for the hydrolysis of lactose [46] was obtained from the data of Bleyer and Schmidt at six temperatures, and is considered to be a more reliable value than that previously quoted by Moelwyn-Hughes.

The kinetics of these reactions in dilute solution may be summarized in the form of equation (1), the numerical values of the constants E and Z being given in Table III. Assuming equation (2) to give the number of collisions between molecules of reactant and hydrated hydrogen ions (H_3O^+), the theoretical value of Z is in all cases about 2×10^{11}. Now, although these are fairly representative instances of a large number of catalyzed reactions, it is to be observed that only in one case—the hydrolysis of lactose—does the observed

collision term approximate to this calculated value. Since the other values of Z range well above and below this figure, the agreement in this particular instance must be regarded as accidental. We therefore conclude that the use of equation (2) to determine the number of collisions of this type is not admissible, and that the Arrhenius equation does not give the true energy of activation.

Discussion.

On general grounds we may say that chief among the causes responsible for reducing below its normal value the rate of a second-order reaction in a homogeneous system are: (1) exothermic formation of a complex prior to the reaction proper; (2) the necessity for the ionization of either or both of the reactants; (3) deactivation by solvent molecules; and (4) stringent conditions of orientation or of internal phase of the reacting molecules at the moment of impact. On the other hand, some of the factors which will allow a faster reaction velocity than that permitted by the simple collision theory are: (*a*) endothermic formation of a complex prior to the reaction proper; (*b*) the distribution of the energy of activation among a number of internal degrees of freedom of the reacting molecules; (*c*) the propagation of reaction chains; and (*d*) activation by some means other than by collision, *e. g.*, by radiation. There is no evidence that either (*c*) or (*d*) enters into the problem so far as the present reactions are concerned. The possibility of the formation of complexes (in aqueous solutions, hydrates) by combination of the reactant molecules with solvent molecules cannot be denied, and may yet prove to be of great importance, but the magnitude of the energy terms involved in those instances where heats of hydration are known is not great enough to account for the discrepancy. Ionization also complicates the kinetics of reactions of this type, but substances such as sucrose can confidently be regarded as almost completely unionized in acid solution. Recent experiments carried out by Moelwyn-Hughes and Hinshelwood [49] on the kinetics of five different reactions in the gaseous state and in solution have demonstrated deactivations by solvent molecules to be absent in each case, so that this factor does not play as prominent a part as was at one time, quite naturally, supposed. With regard to the possible influence of the orientation of the molecules during collision, it may be stated that the steric factor is known to be small for gaseous reactions, and for several reactions in solution amounts to no more than is

already allowed for in the necessarily approximate values ascribed to the molecular diameters. The idea that reaction occurs only when molecules in a particular internal phase collide has not yet received sufficient experimental support. It should here be mentioned that the rates of most of these reactions have been determined in the presence of sucrose, glucose, glycerol, methyl alcohol, potassium chloride, and other substances ; k is increased in all cases, but the critical increment is not altered.

The introduction of internal degrees of freedom is the most probable explanation for the rates of those reactions which exceed those given by the simple collision theory. If we assume, for example, that the number of collisions between sucrose molecules and H_3O^+ can be given by equation (2), and that the Arrhenius value for the critical increment is the true value, then each collision of this type results in the transformation of some 4000 molecules of sucrose. If, however, E is regarded as distributed among five degrees of freedom, the observed rate can be accounted for almost quantitatively. On the other hand, adopting the same basis for our calculations, only one collision out of every 500 between methyl acetate and H_3O^+ (with combined kinetic energy exceeding 17,000 calories) results in hydrolysis of the ester. It is thus clear that some other correction is required before the rate of these apparently slow reactions can be understood.

The Nature and Number of Collisions between Hydrogen Ions and Neutral Molecules in Aqueous Solution.

In dealing with liquid systems, two distinct types of collisions must be recognized. A solute molecule may collide with a second solute molecule, of the same or of a different species, in which case formula (2) as deduced for gases gives the number of encounters in dilute solution at least approximately. The number of collisions of this type is proportional to $\sqrt{T}$, and is therefore sensibly constant within the narrow temperature range to which most reactions in solution are confined. Secondly, a solute molecule may collide with a solvent molecule, in which case the collision frequency is proportional to the viscosity of the solvent, and thus diminishes rapidly with a rise in temperature. The distinction between these two types of collisions was realized by Jowett[10]. It is quite possible that catalysis by hydrogen ions in aqueous solution entails collisions of this second type.

Considering a neutral aqueous solution, the number of

collisions per c.c. per second between solute molecules and water molecules is

$$ {}_sZ_w = \frac{3\pi n_s \eta \sigma}{2m_s}, $$

where σ is the diameter of the solute molecule, m_s is its mass, n_s is the number of solute molecules per c.c. of solution, and η is the viscosity of water [50]. If hydrogen ion be present in the form of H_3O^+ and at a concentration of n_H molecules per c.c., then of this number, ${}_sZ_w$, a fraction, n_H/n_w, will be collisions between solute molecules and hydrogen ion; n_w is the total number of water molecules per c.c. Hence *

$$ {}_sZ_H = \frac{3\pi n_s n_H \eta \sigma}{2m_s n_w} \quad . \quad . \quad . \quad . \quad . \quad . \quad (4) $$

The probability that such a collision possesses total kinetic energy in excess of E′ calories per gram-molecule is $e^{-E'/RT}$, so that the instantaneous rate of reaction is

$$ \frac{dn}{dt} = {}_sZ_H \cdot e^{-E'/RT}. $$

Now the bimolecular constant expressed in litres per gram-molecule per second is

$$ k = \frac{N_0}{1000} \cdot \frac{dn}{dt} \cdot \frac{1}{n_s n_H}, $$

hence

$$ k = \frac{3\pi N_0 \eta \sigma}{2M_s[H_2O]} \cdot e^{-E'/RT}; \quad . \quad . \quad . \quad . \quad (5) $$

N_0 is the Avogadro constant, M_s the molecular weight of the solute, and $[H_2O]$ the number of gram-molecules of water per litre of solution. The collision term in equation (5) is very similar numerically to that in equation $(2\,a)$. The important point is that E′, the true critical increment of the reaction, is greater than the Arrhenius term E, which is evaluated on the false assumption that the collision rate is independent of temperature. Values of E′, obtained from the experimental results by plotting the logarithm of $\frac{k}{\eta}$ against $\frac{1}{T}$, will be found in Table IV.

* This equation is similar to an empirical relation which has often been used by Lewis and his collaborators, in that it involves not only the concentration of the two reactants, but also the "concentration" of water and the viscosity of the solution.

TABLE IV.

Reaction catalyzed by Hydrogen Ion.	E′.	$t°$ C.	$k=k_1/[\text{Catalyst}]$. Observed.	$k=k_1/[\text{Catalyst}]$. Calculated.	F.
Hydrolysis of Methyl Acetate	20,790	30	$2{\cdot}16\times10^{-4}$	$2{\cdot}55\times10^{-4}$	—
Hydrolysis of Ethyl Acetate	20,840	25	$9{\cdot}38\times10^{-5}$	$1{\cdot}23\times10^{-4}$	—
Hydrolysis of Acetamide	22,790	25	$6{\cdot}60\times10^{-6}$	$6{\cdot}79\times10^{-6}$	—
Conversion of Creatine into Creatinine	22,810	78	$2{\cdot}18\times10^{-4}$	$4{\cdot}08\times10^{-4}$	—
Hydrolysis of Benzoyl Glycine	25,210	80	$5{\cdot}05\times10^{-6}$	$1{\cdot}13\times10^{-5}$	—
Hydrolysis Acetyl Glycine	25,430	60	$2{\cdot}05\times10^{-5}$	$2{\cdot}77\times10^{-5}$	1
Conversion of Hydroxyvaleric Acid into Lactone	20,500	30	$4{\cdot}38\times10^{-3}$	$3{\cdot}38\times10^{-3}$	1
Mutarotation of Glucose	21,100	25	$7{\cdot}63\times10^{-3}$	$3{\cdot}72\times10^{-3}$	2
Enolization of Acetone	24,620	24	$2{\cdot}53\times10^{-5}$	$3{\cdot}63\times10^{-5}$	2
Decomposition of Nitrosotriacetonamine (catalyzed by Hydroxyl Ion)	19,910	30	$3{\cdot}04\times10^{-2}$	$4{\cdot}09\times10^{-2}$	2
Decomposition of Diazoacetic Ester	21,490	25	$6{\cdot}42\times10^{-1}$	$1{\cdot}63\times10^{-1}$	4
Hydrolysis of Lactose	28,690	25	$3{\cdot}24\times10^{-7}$	$3{\cdot}12\times10^{-7}$	4
Hydrolysis of Sucrose	29,570	25	$1{\cdot}41\times10^{-4}$	$9{\cdot}82\times10^{-5}$	10
Hydrolysis of Maltose	34,300	60	$1{\cdot}68\times10^{-5}$	$2{\cdot}00\times10^{-5}$	9
Hydrolysis of Cellobiose	34,040	60	$5{\cdot}89\times10^{-6}$	$5{\cdot}47\times10^{-6}$	9

Equation (5) has been used to calculate the rates of hydrolysis of esters, amides, etc., taking σ to be 5×10^{-8} cm. and $[H_2O] = 55$ gram-molecules per litre. The results (Table IV.) are in good agreement with observation when it is recalled that the calculation is absolute and the observed k's at 25° C. differ by a factor of 2000. It should be noted that the corrected values of the critical increment (E′) are greater than the Arrhenius values (E) by a quantity dependent on the temperature to which the kinetic measurements refer.

The rates of the remaining reactions are greater than equation (5) will allow. We therefore conclude that the activation process is here more complicated and involves energy other than kinetic. By combining the collision formula (4) with the Hinshelwood-Fowler-Rideal expression[51] for the probability that such a collision possesses energy of activation distributed among F internal degrees of freedom,

$$k = \frac{3\pi N_0 \eta \sigma}{2M_s[H_2O]} \cdot e^{-E/RT} \cdot \left(\frac{E}{RT}\right)^F \cdot \frac{1}{\lfloor F}, \quad . \quad . \quad . \quad (6)$$

E is now equal to $(E' + F.RT)$. The values of F given in Table IV. are the nearest whole numbers which, when substituted in equation (6), give values of k equal to, or nearly equal to, the observed values. These figures must be accepted with reserve at present, since there is some uncertainty regarding the assumption that complex formation is entirely absent: the collision formula, moreover, may yet need revision. Nevertheless, they reveal in an interesting manner the relative complexity of the activation process in these different reactions. The decomposition of diazo-acetic ester, for example

$$\left(-CH\begin{matrix}N \\ \| \\ N\end{matrix} + H_3O^+ \rightarrow -CH_2OH + N_2 + H^+\right),$$

requires energy drawn from four internal degrees of freedom, whereas the hydrolysis of esters

$$(-COOR + H_3O^+ \rightarrow -COOH + ROH + H^+)$$

requires kinetic energy only. The hydrolysis of sucrose, which almost certainly entails the opening of the five-membered γ-fructoside link, involves ten internal degrees of freedom, while the mutarotation of glucose, which is concerned with the relative positions of the hydrogen atom and

hydroxyl group attached to a terminal carbon atom, involves two only *.

The decomposition of nitrosotriacetonamine indicates that, from the kinetic standpoint, there is no essential difference between hydroxyl ion catalysis and hydrogen ion catalysis. This suggests that the saponification of esters by alkalies (Table II.) may be treated in the manner described above. On applying equation (5) it is found that $k_{calc.}/k_{obs.}$ for a series of these reactions is 14. The disparity is now not serious, as it was when the gas-collision formula was employed and the Arrhenius E was taken to be the true energy of activation. It is also possible that the solute-solvent type of collision is effective in certain instances quoted in Table I., where one of the reactants has an ion in common with the solvent.

Finally, it is of interest to note that the hydrolysis of sucrose, although apparently involving several degrees of freedom, is kinetically bimolecular. Now for gaseous reactions when F is large the reaction is unimolecular except at fairly low pressures. It would appear, therefore, that the time of relaxation of an activated molecule in solution is much less than the corresponding quantity for a gaseous molecule. But the contrast may well be due to the specific chemical character of the reacting molecules, and not to any inherent difference in the reaction mechanism for the two systems.

Summary.

The kinetics of reactions in solution have been investigated from the standpoint of the collision theory of chemical change by comparing the observed rates of reaction with those calculated by means of the relation: Number of molecules reacting per second = number of collisions per second × the fractional number of collisions with energy equal to or exceeding the energy of activation.

For several bimolecular reactions in dilute solution, whether between two neutral solute molecules or between a neutral solute and an ion, the observed rates agree with the theoretical values when for the total number of encounters the gas-collision formula is used, and the fraction of these which is fruitful is given by $e^{-E/RT}$. E is the Arrhenius value for

* In dealing with the values of F given in Table IV. it should be observed that equation (6) does not reduce to equation (5) when F=0. This is because the Hinshelwood-Fowler-Rideal expression is an approximation, being the first and usually the significant term in a series.

energy of activation. The possibility is discussed of explaining on a mechanical basis the relative reactivities of *o*-, *m*-, and *p*-disubstituted compounds.

The rate of hydrolysis of esters, amides, and substituted glycines, catalyzed by hydrogen ion in aqueous solution, is given quantitatively by an equation of this form, but the gas-collision formula is no longer applicable, and must be replaced by the expression : Number of collisions per second per c.c. $=3\pi n_s n_H \eta\sigma/2m_s n_w$, where n_s, n_H, and n_w are the number of molecules of solute, hydrogen ion (H_3O^+), and water per c.c. ; σ is the diameter, and m_s the mass of the solute molecule ; η is the viscosity of water. The fractional number of collisions which is chemically successful is still $e^{-E/RT}$, but E is no longer the Arrhenius term, and is obtained by plotting $\ln\left(\frac{k}{\eta}\right)$ against $\frac{1}{T}$.

The rate at which more complicated reactions (*e. g.*, the decomposition of diazoacetic ester and the hydrolysis of disaccharides) proceed can be explained on the Hinshelwood-Fowler-Rideal theory. The values found for F—the number of internal degrees of freedom contributing to the energy of activation—vary in a regular and interesting manner with the complexity of the molecules and with the nature of the chemical change concerned.

The writer is indebted to the Department of Scientific and Industrial Research for the award of a Senior Research Scholarship.

References.

(1) Arrhenius, *Z. physikal. Chem.* iv. p. 226 (1889).
(2) Lewis, Trans. Chem. Soc. cxiii. p. 471 (1918).
(3) Hinshelwood, 'The Kinetics of Chemical Change in Gaseous Systems,' 2nd ed., Oxford (1929).
(4) Orton and Jones, Trans. Chem. Soc. ci. p. 1708 (1912) ; Verkade, *Rec. trav. chim. Pays-bas*, xxxv. p. 299 (1915).
(5) Pedersen, J. Amer. Chem. Soc. li. p. 3098 (1929).
(6) Brönsted, *Z. physikal. Chem.* cxxii. p. 383 (1926).
(7) See, for example, Jeans, 'The Dynamical Theory of Gases,' 4th ed., Cambridge (1925).
(8) Eichelberger, J. Amer. Chem. Soc. liii. p. 2025 (1931).
(9) Moelwyn-Hughes and Hinshelwood, Proc. Roy. Soc. cxxxi. A, p. 186 (1931) ; see also Bowen, Moelwyn-Hughes, and Hinshelwood, *ibid.* cxxxiv. A, p. 211 (1931).
(10) Jowett, Phil. Mag. viii. p. 1059 (1929).
(11) Kosakewitsch and Uschakowa, *Z. physikal. Chem.* clvii. A, p. 188 (1931).

(12) Hartley and Raikes, Trans. Faraday Soc. xxiii. p. 393 (1927).
(13) Thalen, 'Thesis,' Leiden (1927): see *Tables Annuelles*, 1931.
(14) Conrad, *Z. physikal. Chem.* iii. p. 450 (1889).
(15) Hecht, Conrad, and Brückner, *ibid.* iv. p. 273 (1889).
(16) Segallar, Trans. Chem. Soc. cv. p. 106 (1914).
(17) Haywood, *ibid.* cxxi. p. 1904 (1922).
(18) Conrad and Brückner, *Z. physikal. Chem.* vii. p. 274 (1891).
(19) Cox, Trans. Chem. Soc. cxix. p. 142 (1921).
(20) Walker and Hambly, *ibid.* lxvii. p. 746 (1895).
(21) Moelwyn-Hughes, Chemical Review, x. p. 241 (1932).
(22) Ingold, Trans. Chem. Soc. p. 1375 (1930).
(23) Wittig, 'Stereochemie,' Leipzig (1930).
(24) *Cf.* Allan, Oxford, Robinson, and Smith, Trans. Chem. Soc. p. 401 (1926).
(25) Christiansen, *Z. physikal. Chem.* cxiii. p. 35 (1924).
(26) Norrish and Smith, Trans. Chem. Soc. cxxxi. p. 129 (1928).
(27) Moelwyn-Hughes and Hinshelwood, Trans. Chem. Soc. p. 230 (1932).
(28) Moelwyn-Hughes and Rolfe, *ibid.* p. 241 (1932).
(29) Schwab, quoted by van't Hoff, 'Studies in Chemical Dynamics' (1896).
(30) Tasman, 'Thesis,' Leiden (1927): vide *Tables Annuelles*, 1931.
(31) Smith and Olsson, *Z. physikal. Chem.* cxviii. p. 99 (1925).
(32) Wagner, *ibid.* cxv. p. 121 (1925).
(33) Conant and Kirner, J. Amer. Soc. xlvi. p. 232 (1924).
(34) Kirner and Richter, *ibid.* li. p. 3409 (1929).
(35) Conant and Hussey, *ibid.* xlvii. p. 476 (1925).
(36) Lamble and Lewis Trans. Chem. Soc. cv. p. 2330 (1914).
(37) Taylor, J. Amer. Chem. Soc. xxxvii. p. 551 (1915).
(38) Meehan, 'Thesis,' Liverpool (1923); Euler and Rudberg, *Z. anorg. Chem.* cxxvii. p. 244 (1923); von Peskoff and Meyer, *Z. physikal. Chem.* lxxxii. p. 129 (1913); Crocker, Trans. Chem. Soc. xci. p. 573 (1907).
(39) Edgar and Wakefield, J. Amer. Chem. Soc. xlv. p. 2242 (1923).
(40) Escolme and Lewis, Trans. Faraday Soc. xxiii. p. 651 (1927).
(41) Garrett and Lewis, J. Amer. Chem. Soc. xlv. p. 1091 (1923); Taylor and Close, J. Phys. Chem. xxix. p. 1085 (1925).
(42) Hudson and Dale, J. Amer Chem. Soc. xxxix. p. 320 (1917); Moelwyn-Hughes, Trans. Faraday Soc. xxv. p. 88 (1929).
(43) Rice, Fryling, and Wesolewski, J. Amer. Chem. Soc. xlvi. p. 2405 (1924); Rice and Kilpatrick, *ibid.* xlv. p. 1401 (1923); Dawson and Powis, Trans. Chem. Soc. ci. p. 1502 (1912); see also Dawson and co-workers in subsequent issues of this journal.
(44) Clibbens and Francis, *ibid.* ci. p. 101 (1912); Colvin, Trans. Faraday Soc. xxii. p. 241 (1926).
(45) Fraenkel, *Z. physikal. Chem.* lx. p. 202 (1907).
(46) Bleyer and Schmidt, *Biochem. Z.* cxxxv. p. 546 (1923); Moelwyn-Hughes, Trans. Faraday Soc. xxiv. p. 309 (1928).
(47) Urech, *Berichte*, xvii. p. 2175 (1884); Spohr, *Z. physikal. Chem.* ii. p. 195 (1888); Arrhenius, *ibid.* iv. p. 226 (1889); Lamble and Lewis, Trans. Chem. Soc. cvii. p. 233 (1915); Moelwyn-Hughes, Trans. Faraday Soc. xxv. p. 81 (1929).
(48) Moelwyn-Hughes, *ibid.* xxv. p. 503 (1929).
(49) Moelwyn-Hughes and Hinshelwood, Trans. Chem. Soc. (1932).

(50) Moelwyn-Hughes, Trans. Chem. Soc. p. 230 (1932). The kinetics of unimolecular reactions in solution are dealt with in this paper, and are therefore omitted from the present work.
(51) Hinshelwood, Proc. Roy. Soc. A, cxiii. p. 230 (1926); Fowler and Rideal, *ibid.* p. 570.

Magdalen College,
Oxford.
January 15th, 1932.

X. *Lattice Dimensions in Copper–Silver Alloys.* *By* Miss Helen Dick Megaw, *B.A., The Mineralogical Laboratory, Cambridge* *.

[Plate II.]

An X-ray method, introduced by Van Arkel †, which can be applied to the investigation of alloys consists in the examination of the powder lines given by high-angle reflexions. From Bragg's Law,

$$n\lambda = 2d \sin \theta,$$

it is apparent that the dispersion becomes infinite as θ approaches 90°, and it is thus possible by using such high angles to detect and measure very small changes in spacing.

For a pure substance the spacing is constant. If a second substance forms a solid solution with the first, its atoms replace those of the latter, probably arranging themselves statistically in the lattice. If the atoms of the two substances are not of the same size, a change in the lattice spacing is to be expected on substitution, and the simplest assumption is that suggested by Vegard ‡, of a linear relation between spacing and composition. This, however, is not in general true; that is to say, the atoms do not retain the same effective radius as in the pure element, but may show on the average either an expansion or a contraction. The curve connecting spacing and composition in mixed crystals can be traced by X-ray investigation of specimens of different compositions. It is continuous over the range in which mixed crystals are formed, and often approximates to the straight line of Vegard's hypothesis.

* Communicated by J. D. Bernal, M.A.
† A. E. van Arkel, *Zeits. für Krist.* lxvii. p. 235 (1928).
‡ L. Vegard, *Zeits. für Phys.* v. p. 17 (1921). L Vegard and H. Dale, *Zeits. für Krist.* lxvii. p. 148 (1928).

Now, if there is more than enough of the second element present to form a saturated solution, a second phase appears. This gives rise to new powder lines, but they are of small intensity, and have not been looked for in our investigation. But the composition of the saturated mixed crystals remains constant at a given temperature, however much of the second phase is present, and therefore their spacing at that temperature also remains constant. Thus the composition at which the spacing attains its constant value indicates the saturation composition of the mixed crystals, and hence gives the solubility of the second substance in the first at that temperature. If the substance can be examined at the temperature to be investigated, no further discussion is necessary. This is not practicable in the case of the high temperatures; but if a specimen is suddenly quenched from a high temperature to one very much below its melting-point and kept there, any subsequent readjustments are completely negligible. Then investigation at this low temperature reveals the composition at the temperature from which the specimen was quenched. In the case of copper–silver alloys, quenching to room temperature is sufficient to make any further changes negligibly slow. It is thus possible, by using specimens of different composition quenched from a series of different temperatures, to trace the equilibrium diagram relating solubility to temperature. The attainment of equilibrium at any temperature can also be followed, for if a specimen is quenched before equilibrium is reached, the variation of composition shows up as a variation in spacing.

The system Cu–Ag has been investigated by Sachs * and others. Our work has been confined to the extreme ends of the series, where we have investigated alloys nearer the pure metals than theirs, thus tracing in more detail these parts of the spacing-composition curve. An important difference in our method consists in the use of a small oscillation for the specimen instead of a complete rotation. This, together with the use of a limiting slit for the X-rays, means that the rays fall on a small area only of the specimen, and therefore relatively few of its crystals contribute to the reflexion. Thus the powder line is not a line of uniform intensity, but consists of small spots each given by one crystal in the specimen, whose separate effects can therefore be distinguished. Thus when equilibrium has not been

* G. Sachs and J. Weerts, *Zeits. für Phys.* lx. p. 481 (1930). N. Ageew and G. Sachs, *Zeits. für Phys.* lxiii. p. 293 (1930). N. Ageew, M. Hansen, and G. Sachs, *Zeits. für Phys.* lxvi. p. 350 (1930).

reached, and different crystals have different compositions, the crystals are arranged at non-uniform distances from the centre; when the composition varies throughout single crystals the spots are drawn out in a direction perpendicular to the line. These two effects cannot be distinguished by Sachs's method, as both result in a broadening of the line. Sachs, in fact, obtains an average of all the crystals in the specimen, while we take a sample of them. It is probable that the variation which causes the broadening of the spot occurs during the tempering process, the excess atoms of the second element being expelled at the boundaries of the crystal, and a concentration gradient thus set up inside the crystal. There is certain evidence that the equilibrium curve is different for single crystals and for polycrystalline material *.

Theory.

Copper and silver both form face-centred cubic lattices. If the spacing of the cube-planes is a_0, the glancing angle for a reflexion from the face (hkl) is θ, then

$$\lambda = 2d \sin \theta$$

where $$d = \frac{a_0}{\sqrt{h^2+k^2+l^2}}.$$

Now, if $2a$ is the diameter of the powder ring, b the distance from specimen to film,

$$\tan(\pi - 2\theta) = \frac{a}{b}.$$

Hence from measurements of $2a$ the spacing can be calculated.

The dispersion is high when θ approaches 90°. If the wave-length λ is taken as constant, the change $\Delta\theta$ in the glancing angle for a small change Δd in the spacing is given by

$$\frac{\Delta d}{d} = \cot\theta \,.\, \Delta\theta \;;$$

therefore when θ is nearly 90°, quite a large change of glancing angle corresponds to a very small change in spacing. Expressed in terms of a and b,

$$\frac{\Delta d}{d} = \sin 4\theta \,.\, \cot\theta \left(\frac{\Delta a}{a} + \frac{\Delta b}{b}\right).$$

* U. Dehlinger, 'Ergebnisse der Exakten Naturwissenschaften,' Bd. x. p. 325 (1931); *Zeits. für Phys.* lxxiv. p. 267 (1932). P. Wiest, *Zeits. für Phys.* lxxiv. p. 225 (1932).

Hence errors in the measurement of a and b give a very small percentage error in the calculated value of the spacing, and very small changes in the spacing give measurable differences in a.

Material.

The specimens used were prepared, analysed, and supplied to us by Dr. Stockdale, who also investigated the series by examination under the microscope and measurement of the electrical resistance *. The specimens were in the form of wires of about 1 mm. diameter. The compositions were as follows :

	Per cent. gm. Cu.	Per cent. atoms Cu.
Silver-rich :—(*a*)	0·0	0·0
(*b*)	0·79	1·33
(*c*)	1·41	2·37
(*d*)	2·21	3·69

	Per cent. gm. Ag.	Per cent. atoms Ag.
Copper-rich :—(*a*)	0·0	0·0
(*b*)	0·96	0·57
(*c*)	1·91	1·13
(*d*)	2·89	1·72

The copper used in preparing the specimens contained ·077 per cent. of oxygen, less than ·0015 per cent. of iron, and less than ·002 per cent. of other impurities; the silver was at least 999·7 fine.

Three sets of these alloys were subjected to different heat treatments as follows :

(1) Annealed at 728° C. for 3 days and quenched.

(2) Annealed at 728° C. for 2 days. Cooled to 480° C. in 4 days. Cooled to 452° C. in 2 days. Annealed at 452° C. for 1 day and quenched.

(3) Annealed at 728° C. for 3 days. Cooled to 452° C. in 4 days. Cooled to 150° C. in 9 days. Cooled to 100° C. in 2 days and allowed to cool slowly in a heavy furnace.

* D. Stockdale, J. Inst. Metals, xlv. p. 127 (1931).

Experimental Method.

The specimen was set vertically on the axis of a Bernal photogoniometer, and given an oscillation of about 1°. The film was enclosed in a camera set at right angles to the X-ray beam and penetrated by the slit system through which the beam passed (fig. 1). The distance from specimen to film was about 7 cm. There were two slits. The first was about ·5 mm. wide; this determined the width of the spot, because, the distances from slit to specimen and from specimen to film being approximately equal, the focussing effect came into play. The second slit, about 1 mm. wide, was placed nearer the specimen to limit the area of the

Fig. 1.

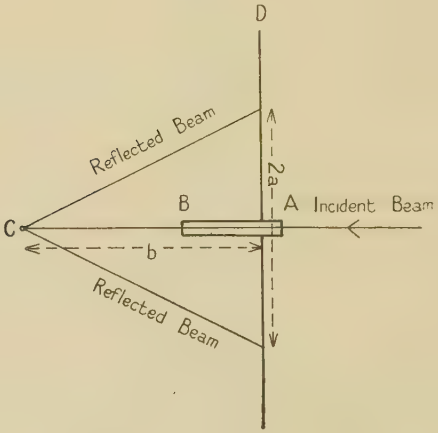

Diagrammatic representation of back-camera.

A. Focussing slit, width ·5 mm.
B. Slit limiting area, width 1 mm.
C. Specimen.
D. Film.

specimen on which the beam fell. The X-rays were obtained from a Shearer tube, run at about 2–10 milliamps., exposures of from 5–15 hours being needed. A copper anticathode was used for the silver-rich specimens; with these the {511} faces give a reflexion of the Kα doublet at about 80°. For the copper-rich specimens a brass anticathode was substituted, giving a reflexion of CuKα from {420} at about 63°, and of ZnKα from {422} at about 70°; the former was rather far out, and only the latter was actually used for measurement.

The diameter of the ring on the photograph was found by direct measurement on an accurate glass scale against an illuminated background. Measurement with a travelling microscope of low magnification was also tried, but gave no higher accuracy. The natural width of the line was equal to the width of the focussing slit, ·5 mm., and the diameter of the ring could thus be measured correct to ·1 mm. on the photographs of the silver-rich alloys; on the copper-rich photographs the lines were fainter and measurement therefore rather less accurate. When the spots were drawn out measurements were made to both edges. The distance from specimen to film was found by taking two photographs at different distances; the position of the camera on the scale could be read to ·05 mm., and from measurement of the diameters of the rings, a simple geometrical calculation gave the absolute distance, with a possible error of ·3 mm.

Accuracy of Results.

The accuracy of determination of the spacing is limited chiefly by the accuracy with which $2a$ can be measured. The possible error of ·1 mm. in this gives a possible error of ·0003 Å. in the spacing. The possible error of ·3 mm. in the absolute value of b corresponds to ·0005 Å. in the spacing, but this is a systematic error and does not affect their relative values. The distance b was unfortunately not kept the same for all the photographs at the silver-rich end, so they are not directly comparable, but since their settings were known to ·05 mm., the error in the spacings due to this source is less than ·0001 Å., which is negligible.

A correction must be made for the shrinkage of the film. Measurements made on films before and after development showed that this amounted to ·3 per cent.; therefore the measured value of $2a$ has been multiplied by 1·003 to give the true value from which to calculate θ. This corresponds to a systematic correction of ·0005 Å. in all the spacings.

The wave-lengths assumed in the calculation are those given by Siegbahn *:

$$\mathrm{Cu\,K}\alpha_1 = 1{\cdot}537395\ \text{Å}.$$
$$\mathrm{K}\alpha_2 = 1{\cdot}541232\ \text{Å}.$$
$$\mathrm{Zn\,K}\alpha_1 = 1{\cdot}43217\ \text{Å}.$$
$$\mathrm{K}\alpha_2 = 1{\cdot}43603\ \text{Å}.$$

* M. Siegbahn, 'Spektroskopie der Röntgenstrahlen,' 2nd ed. (1931).

TABLE I.—Silver-rich alloys.

		Composition Cu atoms per cent.	Distance from specimen to film. cm.	Diameter of ring (corrected for shrinkage of film).		Spacing.		
						Calculated from		Mean.
				Ka_1. cm.	Ka_2. cm.	Ka_1. Å.U.	Ka_2. Å.U.	Å.U.
Quenched from 728° C.	1 *a*	0	6·84	5·86±·01	5·445±·01	4·0774±·0003	4·0772±·0003	4·0773±·0003
	b	1·33	6·93	5·72	5·315	4·0721	4·0725	4·0722
	.....	2·37	6·93	5·61	5·185	4·0694	4·0695	4·0694
	d	3·69	6·93	5·405	4·955	4·0644	4·0639	4·0642
Annealed at 452° C.	2 *b*	1·33	6·85	5·65	5·255	4·0722	4·0724	4·0723
	c	2·37	6·85	5·53	5·135	4·0690	4·0694	4·0691
	d	3·69	6·85	5·555	5·145	4·0695	4·0696	4·0695
Annealed to room temperature.	3 *a*	0	6·85	5·87	5·465	4·0775	4·0774	4·0775
	b	1·33	6·93	5·71	5·285	4·0718	4·0717	4·0718
	c	2·37	6·93	5·56 – 5·63	5·175	4·0680 – 4·0697	4·0690	4·0680 – 4·0697
	d	3·69	6·93	5·355 – 5·68	4·855 – 5·295	4·0641 – 4·0710	4·0617±4·0718	4·0633 – 4·0712

TABLE II.—Copper-rich alloys.

		Composition Ag atoms per cent.	Distance from specimen to film. cm.	Diameter of ring (corrected for shrinkage of film).		Spacing.		
						Calculated from		Mean.
				$K\alpha_1$. cm.	$K\alpha_2$. cm.	$K\alpha_1$. Å.U.	$K\alpha_2$. A.U.	Å.U.
Quenched from 728° C.	4 *a*	0	6·78	6·965±·01	6·57±·01	3·6093±·0005	3·6090±·0005	3·6092±·0005
	b	·57	,,	7·07	6·685	3·6119	3·6119	3·6119
	c	1·13	,,	7·20	6·84	3·6153	3·6157	3·6154
	d	1·72	,,	7·365	6·995	3·6196	3·6197	3·6196
Annealed at 452° C.	5 *a*	0	,,	6·955	6·57	3·6089	3·6090	3·6089
	b	·57	,,	7·08	6·725	3·6122	3·6128	3·6124
	c	1·13	,,	7·18	6·77	3·6147	3·6140	3·6145
	d	1·72	,,	7·15	6·78	3·6139	3·6141	3·6140
Annealed to room temperature.	6 *b*	·57	,,	7·12	6·715	3·6131	3·6134	3·6132
	c	1·13	,,	7·19	6·79	3·6150	3·6145	3·6148
	d	1·72	,,	7·155	6·755	3·6141	3·6136	3·6139

In taking the mean of the spacings calculated from the two lines, the weights of 2 and 1 were allotted to the α_1 and α_2 lines respectively, as the α_1 is twice as intense as the α_2, and measurements made on it are likely to be more accurate.

The correction for refraction of the X-rays is obtained from the formula * :

$$d = d'(1 + 5{\cdot}4\, d^2\rho \times 10^{-6}),$$

Fig. 3.

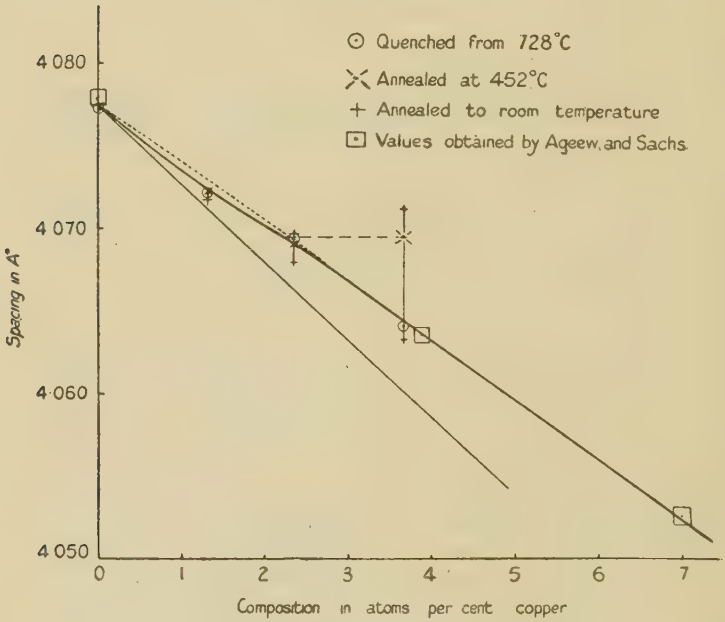

Variation of spacing with composition in silver-rich alloys.

where d is the spacing in Å., ρ the density. On substituting the values of d and ρ, the correction to be made to all the spacings works out as ·0001 Å., which is negligible.

Results.

The measurements of the photographs and the spacings calculated from them are set out in Tables I. and II. The photographs give an indication of the grain of the specimen. In most cases the ring consists of small discontinuous spots, each due to a single crystal (Pl. II. fig. 2, *a*) ; but in one

* *Ibid.*

or two the ring is of almost uniform intensity, indicating extremely small crystals. In the silver-rich alloys annealed to room temperature the spots on the photographs are markedly drawn out (Pl. II. fig. 2, *b*), showing that the spacing varies throughout single crystals of the specimen, and therefore that equilibrium has not been reached. This is particularly interesting, since the alloys annealed at 452° C. give no such effect; though it is to be noticed that the

Fig 4.

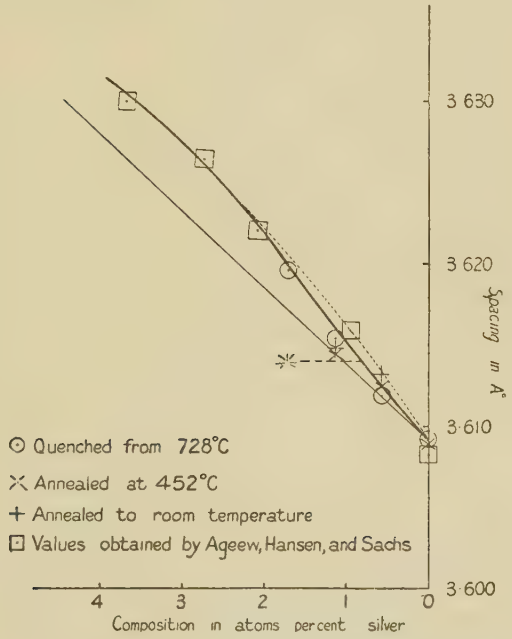

Variation of spacing with composition in copper-rich alloys.

latter took six days to cool from 728° C. to 452° C., as compared with four days for the specimens which were subsequently annealed to room temperature. Neither does the effect occur to an appreciable extent among the copper-rich alloys. In none of the other photographs are the spots at measurably different distances from the centre, so that equilibrium must be very nearly attained.

The results are shown graphically in figs. 3 and 4, where the spacings are plotted against the compositions of the three differently treated sets of alloys. One or two of the

values found by Ageew, Hansen, and Sachs * are shown for comparison ; their alloys are further from the pure metals than most of ours, but the points lie fairly well on the same curve. The silver-rich alloys quenched from 728° C. give a continuous curve, all the copper being in solid solution in the silver ; and the same is true of the copper-rich alloys quenched from 728° C. But for the alloys annealed at lower temperatures, saturation is reached ; and for specimens with more than the saturation amount of the second element the spacing remains constant.

The results give the spacing of pure silver as 4·0774 Å., and of pure copper as 3·6090 Å. Since the lattice is cubic face-centred, the radius of the atom is $\frac{1}{2\sqrt{2}}$ times the spacing, giving 1·4496 Å. for the silver atom and 1·2760 Å. for the copper. If the effective radii of the atoms of each element remained constant throughout the alloys, the relation between spacing and composition would be linear. This is shown by the thin line in figs. 3 and 4, and perhaps more clearly in fig. 5, where our values and those of Ageew, Hansen, and Sachs for both ends of the copper–silver series are plotted as part of the same curve, drawn on a much smaller scale. It is evident that the actual curve in this case always lies above the straight line, showing that the average radius in solid solution is greater than on Vegard's hypothesis. It is of interest to calculate the apparent radii. For a silver-rich alloy containing 3 atoms per cent. of copper, the spacing read from the graph is 4·0669 Å., corresponding to an average radius of 1·4379 Å. Therefore the apparent radius of the copper atom in this alloy is 1·319 Å. Similarly, for a copper-rich alloy containing 3 atoms per cent. of silver the spacing is 3·6271 Å., and the apparent radius of the silver atom therefore 1·489 Å.

Two features appearing from the graphs may have some significance. It is noticeable that the silver-rich alloys containing 1·33 atoms per cent. of copper, and the copper-rich alloys containing 0·57 and 1·13 atoms per cent. of silver, seem to lie below the smooth curve carrying the other points (shown dotted in figs. 3 and 4) by an amount which is rather more than the experimental error. This suggests that there may be inflexions at these parts of the curve

* N. Ageew, M. Hansen, and G. Sachs, *Zeits. für Phys.* lxvi. p. 350 (1930). They used an older value for the wave-lengths of the CuKα lines, 1·53729 and 1·5402 Å. respectively. Their figures for the spacings have here been corrected to refer to the newer values we have used.

which have not hitherto been noticed. The points in question lie much nearer the thin line than the others, so perhaps there may be a closer approximation to linear variation of spacing with composition when there is a very small amount of the second element present. It is not possible, however, to draw any definite conclusions without investigating more points in the neighbourhood. The second fact to be noticed occurs at the copper-rich end of the curve, where, if we take the alloy with 1·72 per cent. silver annealed at 452° C. as giving the solubility at that temperature, then the similarly-treated alloy with 1·13 per cent.

Fig. 5.

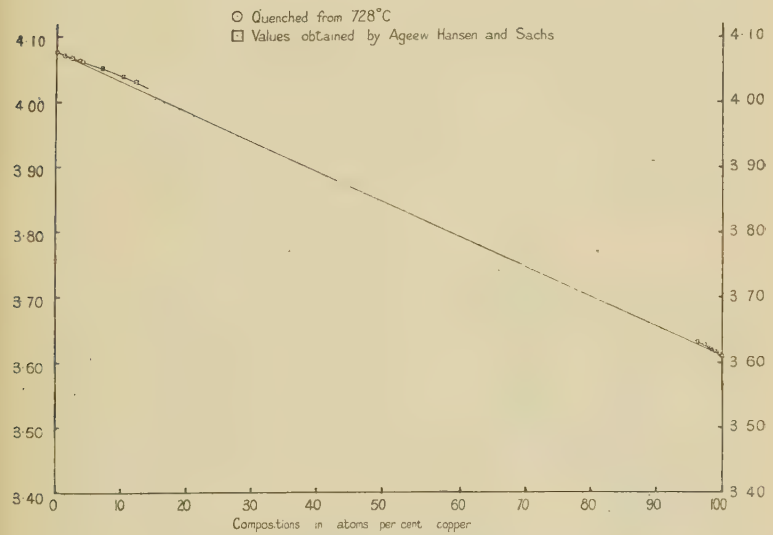

Variation of spacing with composition in silver-rich and copper-rich alloys.

silver must be slightly supersaturated. The difference is hardly more than the experimental error, but it seems reasonable to suppose that as the velocity of reaching equilibrium depends on the excess amount of silver present, which is in this case extremely small, the alloys in question might still remain supersaturated even when the excess silver had separated out from mixed crystals which initially contained more. In support of this suggestion is the fact that the spots on the corresponding photographs are not very sharp, but slightly broadened, as if equilibrium had not quite been reached.

It is possible to read from the graphs the solubility of silver in copper and copper in silver. At 452° C. the values are shown by the broken lines drawn in figs. 3 and 4. The solubility of copper in silver is 2·26 atoms per cent. or 1·34 gm. per cent.; this agrees fairly well with the value 1·2 gm. per cent. obtained by Ageew and Sachs, and that of 1·4 gm. per cent. obtained by Stockdale. The solubility of silver in copper, read from fig. 4, is 0·83 atoms per cent., or 1·40 gm. per cent. Ageew, Hansen, and Sachs obtain 1·0 gm., and this disagreement is probably to be explained by the difference in the course of our spacing-composition curve, for if the dotted curve is assumed to be correct, it gives a solubility of 1·1 gm. per cent. The solubility of silver in copper at room temperature does not appear to differ appreciably from that at 452° C., but this is very possibly because equilibrium had not been reached by the alloys annealed to room temperature. The solubility of copper in silver at room temperature cannot be determined either; it is quite certain from the drawn-out spots given by these alloys that they were not in equilibrium.

Acknowledgments.

The author is indebted to Dr. Stockdale for supplying the specimens used throughout the investigation, and for information about them. She wishes to give her sincerest thanks to Mr. J. D. Bernal for suggesting the problem, and for much helpful advice and criticism. The apparatus used was purchased by means of a grant from the Royal Society.

The investigation was carried out while the author was holding a Yarrow Research Studentship from Girton College, Cambridge.

XI. *The Steady Electric Current Field in a Circular Plate.* *By* H. Ataka, *Meidi College of Technology, Tobata, Japan* *.

I. *Introduction.*

THE steady electric current field in a rectangular plate having two electrodes on any parts of its boundary was first given by H. F. Moulton †. Extending his results we have obtained the steady electric current field in a

* Communicated by the Author.

† Proc. of London Math. Soc. p. 105 (Jan. 1905).

circular plate when a circular electrode is placed in it and the other electrode along a part of its circumference.

It will be noticed that the field in such a doubly-connected region can be obtained from that in a simply-connected region by means of conformal representation.

II. *The Field in a Circular Plate.*

In fig. 1 let PQRS be a rectangular plate having two adjacent sides on the axes of $z=x+iy$ plane.

Let the resistance of a square made of the same plate be R, when the whole of two opposite sides form the electrodes. Taking the length of the side PQ to be 2π, and that of the side PS α, we put one electrode AB just on the middle part of the side PQ and the other electrode on the whole of the

Fig. 1.

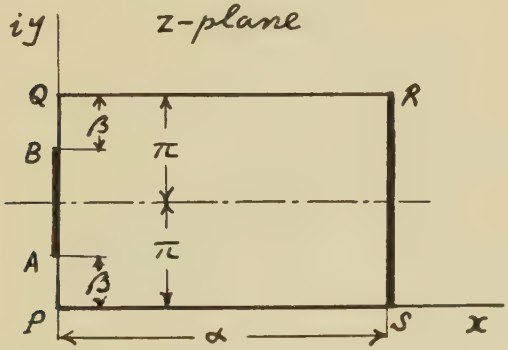

side RS. Then the coordinates Z_a, Z_b, Z_r, Z_s of the points A, B, R, S will be

$$\left.\begin{aligned} Z_a &= i\beta, \\ Z_b &= i(2\pi-\beta), \\ Z_r &= \alpha+i2\pi, \\ Z_s &= \alpha. \end{aligned}\right\} \quad \ldots\ldots \quad (1)$$

Let the current passing through the electrodes be I. By symmetry it will be clear that the distribution of the potential along the side QR is equal to that along the side PS.

Now we will transform the rectangle in the z-plane into an eccentric circular ring in the w-plane by means of the function

$$Z = \log\left(\frac{w-e^{\varphi}r}{e^{\varphi}w-r}\cdot e^{-i\theta}\right), \quad \ldots\ldots \quad (2)$$

where r, θ, and ϕ are all real constants. Then the side PQ is transformed into a circle P′Q′ of radius r, having its centre at O in fig. 2, and the side RS into the other circle R′S′ of radius r', having its centre at O′, while the sides QR and SP are transformed into circular arcs Q′R′ and S′P′ respectively, and along these two arcs the circular ring has an infinitely narrow gap.

But the distribution of potential along the arc Q′R′ is still equal to that along the arc P′S′, so that no disturbances will be given to the field in the plate, even if the arc Q′R′ were combined with the arc P′S′, to generate a complete eccentric circular ring.

Fig. 2.

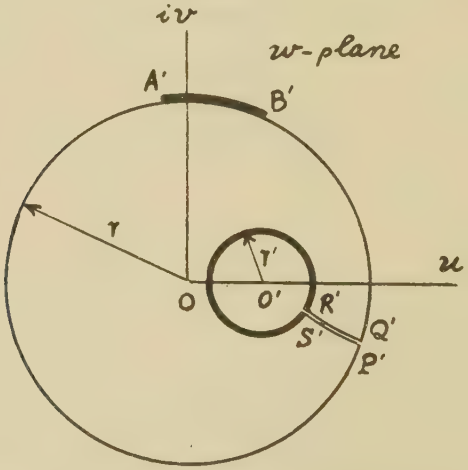

Denoting the potential function of the field in the circular plate with U and the current function with V, we put

$$W = U + iV. \quad . \quad . \quad . \quad . \quad . \quad . \quad (3)$$

The function W can be obtained by the substitutions of (1) and (2) in the results given by Moulton :

$$\mathrm{sn}^2(\mu W, \kappa) = \frac{(\mathrm{sn}^2 mZ - \mathrm{sn}^2 mZ_a)(\mathrm{sn}^2 mZ_b - \mathrm{sn}^2 mZ_s)}{(\mathrm{sn}^2 mZ - \mathrm{sn}^2 mZ_b)(\mathrm{sn}^2 mZ_a - \mathrm{sn}^2 mZ_s)} \ (\mathrm{mod.}\ \lambda,)$$

$$. \quad . \quad . \quad (4)$$

$$\kappa^2 = \frac{(\mathrm{sn}^2 mZ_a - \mathrm{sn}^2 mZ_s)(\mathrm{sn}^2 mZ_b - \mathrm{sn}^2 mZ_r)}{(\mathrm{sn}^2 mZ_b - \mathrm{sn}^2 mZ_s)(\mathrm{sn}^2 mZ_a - \mathrm{sn}^2 mZ_r)} \ (\mathrm{mod.}\ \lambda),$$

$$. \quad . \quad . \quad (5)$$

$$\mu = \frac{1}{\mathrm{RI}} \mathrm{K}',$$

where K′ is the complete elliptic integral of the first kind of modulus $\kappa' = \sqrt{1-\kappa^2}$.

The values of m and λ can be found from

$$\left.\begin{aligned} L &= \alpha m, \\ L' &= 2\pi m, \end{aligned}\right\}$$

where L and L′ are the complete elliptic integrals of the first kind of moduli λ and $\lambda' = \sqrt{1-\lambda^2}$ respectively.

Fig. 3.

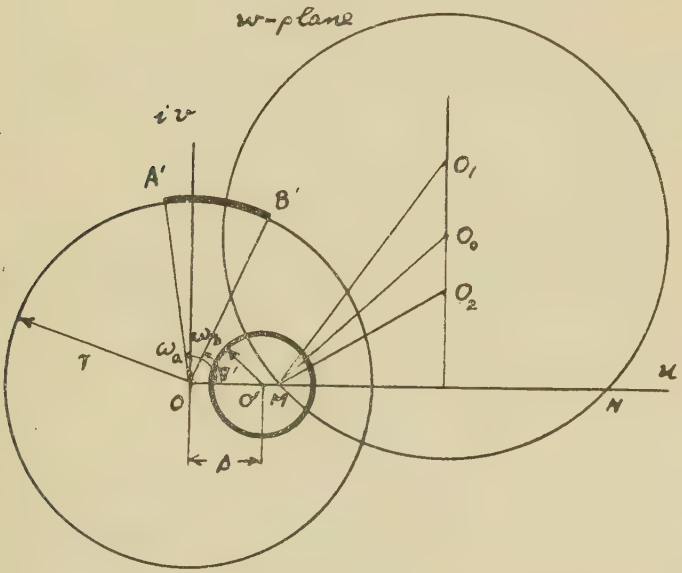

In fig. 3 let two circles in the w-plane be given by

$$\left.\begin{aligned} u^2 + v^2 &= r^2, \\ (u-s)^2 + v^2 &= r'^2, \end{aligned}\right\}$$

and let the electrode along the outer circle be determined by

$$\left.\begin{aligned} \text{L A}'\text{O}u &= \omega_a, \\ \text{L B}'\text{O}u &= \omega_b, \end{aligned}\right\}$$

where $\omega_a > \omega_b$, and along the arc subtended by the angle

A′OB′ the electrode is supposed to lie. Then the procedure determining the field in the circular plate is as follows:—

(i.) Find the values of α and ϕ from

$$\left.\begin{aligned}\cosh\alpha &= \frac{r^2+r'^2-s^2}{2rr'}\\ \cosh\phi &= \frac{r^2-r'^2+s^2}{2rs}\end{aligned}\right\}.$$

(ii.) Find the values of m and λ from

$$\left.\begin{aligned}\mathrm{L} &= \alpha m\\ \mathrm{L}' &= 2\pi m\end{aligned}\right\}$$

by using the table of $\log q = -\pi \mathrm{M}\dfrac{\mathrm{K}'}{\mathrm{K}}$ for κ, where $\mathrm{M} = \log_{10} e$.

(iii.) Calculate the value of β from

$$\tan 2\beta = \frac{2\sinh\phi(\sin\omega_a - \sin\omega_b) - \sinh 2\phi \sin(\omega_a-\omega_b)}{2+\cos(\omega_a+\omega_b) - 2\cosh\phi(\cos\omega_a+\cos\omega_b) + \cosh 2\phi\cos(\omega_a-\omega_b)}.$$

(iv.) Find the value of κ from (5), or

$$\kappa = \frac{\lambda}{\mathrm{dn}^2 m\beta} \text{ (mod. } \lambda'\text{)}.$$

If β is comparable to π, then it will be preferable to use

$$\kappa = \left\{\frac{1-(1-\lambda)\mathrm{sn}^2 m\beta'}{\mathrm{dn}m\beta' + (1-\lambda)\mathrm{sn}m\beta'\mathrm{cn}m\beta'}\right\}^2 \text{ (mod. } \lambda'\text{)},$$

where $$\beta' = \pi - \beta.$$

Finally, we can obtain the function W from (4).

In the field in the circular plate the lines of flow which are circular arcs intersecting both electrodes at right angles can be obtained by simple geometrical constructions. Let M and N in fig. 3 be the two common inverse points of the pair of circles. Let O_1 be the centre of a circle passing through the points A′, M, N, and O_2, the centre of a circle passing through the points B′, M, N. If O_0 is a point of intersection of a bisector of the angle $\mathrm{O}_1\mathrm{MO}_2$ and a line $\mathrm{O}_1\mathrm{O}_2$, then a circle having its centre at O_0 and passing through M will be the required lines of flow.

III. *The Equivalent Resistance.*

If we put $Z = Z_a$ in (4), then $\mathrm{sn}(\mu W, \kappa) = 0$ or $W = 0$ —that is, the potential of the electrode AB is zero. If we put $Z = Z_s$ in (4), then $\mathrm{sn}(\mu W, \kappa) = 1$, or $W = \frac{K}{\mu}$—that is, the potential of the electrode BC is $\frac{K}{\mu} = \mathrm{RI}\frac{K}{K'}$, where K is the complete elliptic integral of the first kind of modulus κ. Hence the equivalent resistance between the electrodes is

$$R\frac{K}{K'}.$$

Assuming that $r = 30$, $r' = 2$, and $s = 10$, we have calculated* the equivalent resistances of the circular plate in the following five cases :—

(1) ..... $\omega_a = 10°$, $\omega_b = 10°$,
(2) ..... $\omega_a = 55°$, $\omega_b = 35°$,
(3) ..... $\omega_a = 100°$, $\omega_b = 80°$,
(4) ..... $\omega_a = 145°$, $\omega_b = 125°$,
(5) ..... $\omega_a = 190°$, $\omega_b = 170°$.

Following to the procedure above-mentioned we obtain

$$\left.\begin{aligned} \alpha &= 2{\cdot}590, \\ \beta &= 1{\cdot}094, \\ \lambda &= \sin 5°4' = 0{\cdot}0883, \\ m &= 0{\cdot}5017. \end{aligned}\right\}$$

The values of β, κ, and RK/K', the equivalent resistances, are given in the accompanying table :—

Case.	β.	κ.	RK/K'.
(1)	$\pi - 0{\cdot}3479$	0·680	0·967 R
(2)	$\pi - 0{\cdot}2438$	0·764	1·08 R
(3)	$\pi - 0{\cdot}1399$	0·856	1·25 R
(4)	$\pi - 0{\cdot}0980$	0·897	1·37 R
(5)	$\pi - 0{\cdot}0872$	0·908	1·41 R

* The calculations were carried out by the aid of K. Hayashi's "Fünfstellige Tafeln der Kreis- und Hyperbelfunktionen" and E. Jahnke and F. Emde's "Funktionentafeln mit Formeln und Kurven."

XII. *The Resemblance between the Longitudinal Asymmetry of the Classical Field of an Accelerated Electron and the Distribution of Scattered Photoelectrons.* *By* LEWIS SIMONS, *D.Sc., Reader in Physics, Birkbeck College (University of London* *).

The Classical Problem of the Radiation Field of an Accelerated Electron.

IN the classical theory of the electromagnetic field around a moving electron the part of the field energy that involves the acceleration of the charge is usually written in the form $\frac{1}{2}(E^2+H^2)$, where $E^2/2$ and $H^2/2$ are the electric and magnetic energy densities respectively. It is well known that the rate of radiation of electromagnetic energy to the surrounding space is

$$\frac{dU}{dt}=\frac{e^2\Gamma^2}{6\pi c^3}\frac{(1-\beta^2\sin^2\epsilon)}{(1-\beta^2)^3}.$$

In this equation Γ is the acceleration of the charge e, ϵ is the angle between Γ and the velocity βc. The other symbols have their usual meanings. This energy spreads itself in the form of a set of excentric shells ; each shell represents an equi-phase surface in the action.

If the angle ϵ is zero it can be shown from the equations that the rate of radiation within the conical aperture between θ and $\theta+d\theta$, where θ is the semi-vertical angle of the cone and the charge moves at the apex axially, is

$$\left(\frac{dU}{dt}\right)_{\theta.d\theta}=\frac{e^2\Gamma^2}{8\pi c^3}\frac{\sin^3\theta\,d\theta}{(1-\beta\cos\theta)^5}=Af(\theta)d\theta,\text{where}A=e^2\Gamma^2/8\pi c^3.$$

It follows, therefore, that the electromagnetic radiation energy will not be divided equally by an equatorial plane. The semi-vertical angle θ_b of the cone dividing the energy into equal portions may be obtained from the expression

$$\int_0^{\theta_b}f(\theta)d\theta=\int_{\theta_b}^{\pi}f(\theta)d\theta. \quad . \quad . \quad . \quad . \quad \text{(i.)}$$

The integration is simply performed by writing

$$p=(1-\beta\cos\theta)$$

* Communicated by the Author.

and by changing the limits of integration

$$0 \text{ becomes } 1-\beta,$$
$$\theta_b \text{ becomes } 1-\beta\cos\theta_b,$$
$$\pi \text{ becomes } 1+\beta.$$

This results in the equation

$$\frac{3(1-\beta^2)-8(1-\beta\cos\theta_b)+6(1-\beta\cos\theta_b)^2}{(1-\beta\cos\theta_b)^4} = \frac{8\beta^3+(1-3\beta)(1+\beta)^3}{(1-\beta^2)^3}; \quad . \quad \text{(ii.)}$$

but if it is assumed that for small values of β the angle of bipartition θ_b will approximate to $\pi/2$ then the squares

Fig, 1.

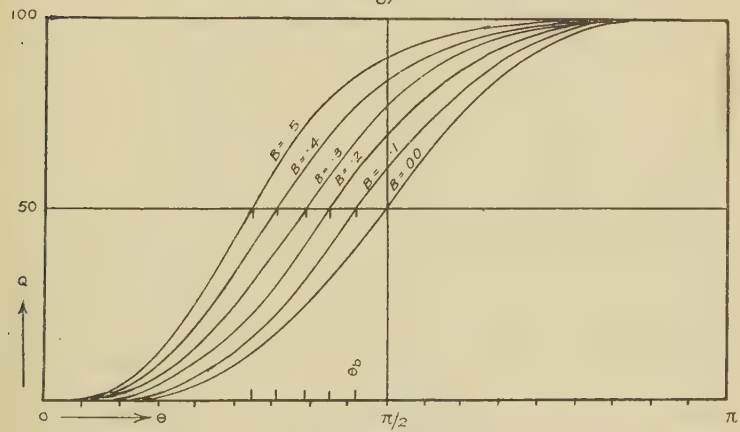

Curves showing the angles of bipartition θ_b of the energy of a radiation field of an accelerated electron moving with a velocity βc.

and higher powers of $\cos\theta_b$ may be neglected in comparison with unity, and as $\beta<1$ the equation gives nearly

$$\cos\theta_b = \tfrac{5}{4}\beta \quad . \quad . \quad . \quad . \quad . \quad . \quad \text{(iii.)}$$

As a check on this I have interpolated the formulæ

$$A_1\int_0^{\theta}\frac{\sin^3\theta\,d\theta}{(1-\beta_1\cos\theta)^5} = Q, \text{ where } A_1\int_0^{\pi}\frac{\sin^3\theta\,d\theta}{(1-\beta_1\cos\theta)^5} = 100 \quad \text{(iv.)}$$

for each value of β_1.

The values of β_1 range from 0 to ·5. A_1 is an adjustable factor which makes the rate of radiation 100 units to the whole of space for each value of β_1. Fig. 1 shows the

results. In this figure the value of θ_b will be given in each case where the curve has an ordinate of 50.

Table I. shows the comparison of the two methods, column I. by approximation from (iii.) and column II. by graphical interpolation from the exact formulæ (iv.).

The approximate formula $\cos\theta_b = \frac{5}{4}\beta$ will therefore hold for values of β up to about ·5, which corresponds to the maximum possible velocity of a photoelectron ejected by a wave-length of $1{\cdot}59 \times 10^{-9}$ cm. or, say, the K radiation from uranium.

Table I.

β_1.	I.	II.
0	90°	90°
·1	82·8	82
·2	75·5	75
·3	68	68·5
·4	60	61·3
·5	51·3	54

The Reciprocal Problem of the Production of Photoelectrons by Photons.

Now for very small values of β the energy of the radiation is distributed with the type of longitudinal symmetry given by

$$Q_\theta = A' \int_0^\theta \sin^3\theta \, d\theta,$$

where A′ is a constant depending upon the total energy available, whilst the symmetry round the direction of motion of the accelerated electrons as axis is complete. According to more recent ideas, the Maxwell field of radiation may be regarded as either a continuous distribution of energy denoted by this function or a frequency of probability distribution of energy quanta, each possessing the whole energy of the Maxwell field, but passing out from the origin in a given direction with a frequency of occurrence specified by this function. With this proviso the problem becomes mathematically similar to that of photoelectron distribution produced by exciting photons. This has been dealt with by Auger and Perrin *. For small velocities and low binding

* *Journal de Physique*, viii. (2) p. 93 (1927).

energy they found that the probability of an electron being ejected at an angle θ to the direction of the parent unpolarized photons was proportional to $\sin^2\theta$.

Let ξ be specified as the angle between the electric vector of the plane polarized light-wave and that of the path of the consequent photoelectron, then, as is explained by fig. 2, OP represents the probable direction of ejection of the photoelectron due to the plane polarized ray moving in the direction OA. This probability is proportional to $\cos^2\xi$ if OE represents the direction of the electric vector. If unpolarized light may be regarded as consisting of two non-coherent plane polarized rays with electric vectors of equal

Fig. 2.

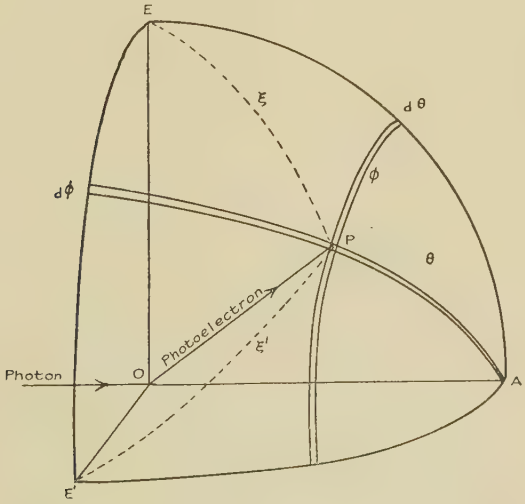

average intensities mutually perpendicular to each other arbitrarily chosen in the directions OE and OE′, then the probable frequency of the appearance of the photoelectrons within the aperture denoted by $\sin\theta\, d\theta\, d\phi$ will be

$$dN_{(\sin\theta\, d\theta\, d\varphi)} = \frac{3N}{8\pi}(\cos^2\xi + \cos^2\xi')\sin\theta\, d\theta\, d\phi,$$

where ϕ is the azimuth, and as $\cos\xi = \sin\theta\cos\phi$ and $\cos\xi' = \sin\theta\sin\phi$ the frequency of appearance within the conical aperture denoted by $\theta\, d\theta$ will be

$$dN_{\theta\ d\theta} = \frac{3N}{4}\sin^3\theta\, d\theta,$$

where N is the whole number of photoelectrons under consideration. This completes the reciprocity between the photon-photoelectron system for low energies which is the basis of de Broglie's principle of interference.

This is for very slow electrons, but just as the Maxwell field of an accelerated electron is distorted in the longitudinal direction of the velocity, so is the probability distribution of photoelectrons similarly distorted for higher values of the energy of the parent photons. For a bibliography of experimental work the reader is referred chiefly to the work of Auger *, to Williams, Nuttall, and Barlow †, and to the writer's experimental paper ‡.

The Theory of Auger and Perrin.

For completeness a brief account of the treatment due to Auger and Perrin of the forward distortion of the longitudinal and transverse symmetry denoted by the last expression must now be given. The need arises, as is amply shown by their experiments, when the exciting photon is of higher energy. With this higher energy they suppose that the equatorial plane of maximum probability EOE′ (fig. 2) inclines forward and becomes a conical surface on OA as axis and of semi-vertical angle θ_b. This conical surface therefore divides the total emission into equal parts under these new conditions. The actual amount of inclination forward is fixed by consideration of momentum and energy of the interacting parts. They are—(i.) the total energy of the photoelectron due to its motion, in whatever direction it may ultimately move, is constant and therefore the momentum is independent of direction: this is denoted by I in fig. 3; (ii.) the longitudinal distortion of the system is due to the fact that each photoelectron acquires a forward momentum i in the direction OA In the figure if OB represents the chance momentum of a photoelectron in conditions of longitudinal symmetry, the momentum $i = \mathrm{BC}$, of fixed amount, gives a resulting momentum OC of fixed amount. The same applies to a chance emission in the direction OB′ which becomes changed into the direction OC′ which defines the angle of bipartition θ_b. If

$$dN_{\theta' d\theta'} = \frac{3N}{4} \sin^3 \theta' \, d\theta'. \quad . \quad . \quad . \quad . \quad (v.)$$

* *Comptes Rendus*, clxxxviii. p. 447 (1929).
† Proc. Roy. Soc. A, cxxi. p. 611 (1928).
‡ Phil. Mag. x. p. 388 (1930).

represents the old distribution, the new distribution is obtained from the transformations

$$\sin\theta' = \sin\theta/\sqrt{1+\cos^2\theta_b - 2\cos\theta_b\cos\theta},$$

$$\cos\theta' = (\cos\theta - \cos\theta_b)/\sqrt{1+\cos^2\theta_b - 2\cos\theta_b\cos\theta},$$

$$d\theta' = \frac{1-\cos\theta_b\cos\theta}{1+\cos^2\theta_b - 2\cos\theta_b\cos\theta}\,d\theta.$$

The angles in azimuth remain unchanged, whence if

$$dN_{(\sin\theta'\,d\theta'\,d\phi)} = dN_{(\sin\theta\,d\theta\,d\phi)},$$

$$dN_{\theta,\,d\theta} = \frac{3N}{4}\left\{\frac{(1-\cos\theta_b\cos\theta)\sin^3\theta}{(1+\cos^2\theta - 2\cos\theta_b\cos\theta)^{5/2}}\right\}d\theta. \quad \text{(vi.)}$$

Fig. 3.

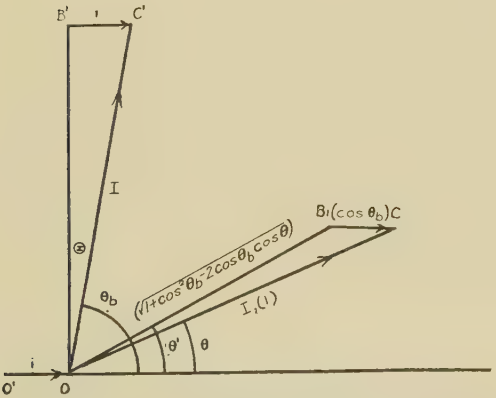

Vector diagram to illustrate Auger and Perrin's trigonometrical relations.

This gives the number of photoelectrons emerging between the angles θ and $\theta+d\theta$ to the direction of the photons and then

$$\int_0^\theta dN_{\theta\,d\theta} = \frac{N}{2}\left\{1 - \frac{\cos\theta-\cos\theta_b}{\sqrt{1+\cos^2\theta_b - 2\cos\theta_b\cos\theta}}\cdot\left(1+\frac{1}{2}\frac{\sin^2\theta}{1+\cos^2\theta_b - 2\cos\theta_b\cos\theta}\right)\right\} \quad \text{(vii.)}$$

with dispersion. Without dispersion or distortion this reduces to

$$\int_0^\theta dN_{\theta\,d\theta} = \frac{N}{2}\{1-\cos\theta\,(1+\tfrac{1}{2}\sin^2\theta)\}.$$

Expressions of this type * have been deduced from time to time and also a value of $\cos\theta_b$, but Auger and Perrin's equations are represented here in order to emphasize the fact that their expression (vii.) contains implicitly only the principles (i.) and (ii.) above, viz., that the final speed is independent of direction and each photoelectron is given a forward momentum of the same amount. There are no numerical relations amongst these quantities implied. The only other relation is that the original direction of projection of the photoelectrons possessed the symmetry given by equation (v.).

A similar approximation to that assumed in solving (ii.) may now be made. If the dispersion is small $\cos^2\theta_b$ may be neglected in comparison with unity ; (vi.) then becomes

$$dN_{\theta\, d\theta} = \frac{3N}{4}(1+4\cos\theta_b\cos\theta)\sin^3\theta\, d\theta,$$

which still gives θ_b as the angle of bipartition if the expression is suitably integrated as in (i.). But the expression is useful in this form for determining the average forward momentum of the photoelectrons in terms of $\cos\theta_b$. Thus if I is the resultant momentum of a photoelectron at an angle θ to the photon, the average forward momentum of all will be

$$\left\{ I\frac{3N}{4}\int_0^{\pi}(1+4\cos\theta_b\cos\theta)\sin^3\theta\cos\theta\, d\theta \right\} \Big/ N .$$

$$= \tfrac{4}{5} I\cos\theta_b = \tfrac{4}{5} i \quad . \quad . \quad . \quad \text{(viii.)}$$

Auger and Perrin's Theory applied to the Probability Radiation Field of Accelerated Electrons.

This theory may now be applied in a reciprocal manner to the production of photons by an accelerated electron for the following reasons : (i.) in both cases the distribution of energy follows the same $\sin^2\theta$ law in the limit ; (ii.) both systems involve a forward displacement when higher energies are involved ; (iii.) the energy of the Maxwell radiation field may be regarded as localized in photons, the energy depending upon β and Γ ; (iv.) the Maxwell field must acquire forward momentum from the electron apart altogether from that distributed radially.

Equation (iii.) gives the value of θ_b for a given value of β. If $\theta_b \sim \pi/2$ write $\sin\Theta = \cos\theta_b = \frac{5}{4}\beta$, where Θ is the complement of θ_b and represents the forward displacement of the angle of the cone bisecting the energy. Then as Θ is

* Compton, 'X-rays and Electrons,' p. 245 (1927).

practically a linear function of β, if the time variation of the velocity of the electron is uniform then the angle Θ will change from $\frac{5}{4}\beta$ to 0, with the result that the time average of the forward displacement of the angle of the bisecting cone $=\frac{5}{8}\beta$. If, now, a large number of similar electrons take part in the action, and the *whole* field of each be localized in direction, the value $\frac{5}{8}\beta$ may be substituted in (viii.), where I is now the mean resultant momentum of the localized field, thus:

$$\frac{\text{average forward momentum of field}}{\text{mean resultant momentum of field}} = \frac{\beta}{2} \quad . \quad \text{(ix.)}$$

The assumptions made in deducing this result are that each localized "field" of mean resultant momentum I receives the same forward momentum i. No numerical relation is implied between i and I except that the former is small in comparison with the latter.

Consider, now, the complementary phenomenon of the production of photoelectrons by photons of moderately low energy. The forward moving photon of momentum $h\nu/c$ disappears and in its place a scattered photoelectron appears with forward momentum, as one would expect, $i=h\nu/c$ and resultant momentum $\mathrm{I}=m\nu$. If this photoelectron started from rest the conditions are exactly analogous to those above, and, consequently, if the further simple relation $\frac{1}{2}m\nu^2=h\nu$ be applied we get

$$\frac{\text{forward momentum of electron}}{\text{mean resultant momentum of electron}} = \frac{h\nu/c}{m\nu} = \beta/2, \quad \text{(x.)}$$

a result pointed out by Richardson *.

Recently determined Value of θ_b.

The above is the earlier and simpler view. There is, however, a growing body of experiment which indicates that the value of sin Θ is greater than $\beta/2$ indicated by (x.), and (ix.) supplies the clue for this. Assume the complete reciprocity of the two systems dealt with in the first part of the paper. Now it can be shown on classical lines that there is no great departure in the nature of the radiation field if

* 'Electron Theory of Matter,' p. 481 (1916); see also Sommerfeld, 'Wave Mechanics,' p. 189 (1930). For a truer comparison of (ix.) and (x.) the latter should be written

$$\frac{\text{the average forward momentum of electrons}}{\text{mean resultant momentum of one}} = \frac{4}{5}\cdot\frac{h\nu/c}{m\nu} = \frac{4}{5}\cdot\frac{\beta}{2},$$

which follows from (viii.).

this be considered as being due to an electron accelerated in a direction at right angles to that of its speed, as is the case of an orbital electron for example. In this case the value of β would be maintained until the external electron had passed into the atom and the whole came into phase again. This would give a theoretical value of $\sin\Theta=\beta$, and, *mutatis mutandis*, if an orbital electron is removed from an atom by a photon *without change in speed* then for this, too, $\sin\Theta=\beta$. This satisfies the theory of Sommerfeld * in the case of the hydrogen atom derived from the purely wave mechanical view-point.

To determine θ_b stereoscopic observation is made on a sufficiently large number of Wilson tracks of the photo-electrons, and curves of longitudinal space distribution are

Table II.

Source of photoelectrons and energy of excitation P in kilovolts.		Energy of attributed level of origin in kilovolts.	Θ obs.	Θ calculated * from $\sin\Theta=\beta$.		
				P.	P—L.	P—K.
(1) argon	17·5	K 3	12°	15°4	...	15°3
(2) xenon	56	K 35 (L5)	14	25·8	24·9	16·3
(2) N_2 and O_2	20·6	...	14	..	...	16·1
(3) H_2 air argon	17·5	...	14·9	...	...	14·8
(4) argon	91·2	K 3	32	32	...	31·7

(1) Auger, *Comptes Rendus*, clxxxviii. p. 477 (1929).
(2) Williams, Nuttall, and Barlow, Proc. Roy. Soc. A, cxxi. p. 624 (1928).
(3) Loughridge, Phys. Rev. xxx. p. 492 (1927), calculated from $\cos\theta_b = \frac{2}{3}\cos\theta_{max}$.
(4) Lutze, *Ann. d. Physik* (9) vii. p. 853 (1931).

* $h\nu_P = m_0c^2(1/\sqrt{1-\beta^2}-1)$ gives $\beta = \sqrt{a^2+2a}/(1+a)$ where $a=h\nu_P/m_0c^2$.

plotted closely resembling those of fig. 1 ; the ordinate in this case is the number of photoelectrons. The value can then be taken directly from the curves.

In Table II. are collected some of the most recent results of observations from photoelectron distribution curves. In the last column the value of Θ is given for the attributed source of photoelectrons calculated on the basis $\sin\Theta=\beta$. Values for subsidiary electron groups are added tentatively in columns P and (P—L) in order to show what the effect would be on the main value of Θ in column (P—K) of the admixture of subsidiary electrons from the more loosely

* *Loc. cit.*

bound shells. These subsidiary values are calculated by substituting $h\nu_P$, $h\nu_P - h\nu_L$ for $h\nu_P - h\nu_K$ from which the last column is calculated.

The earlier experiments gave values of $\sin\Theta$ approaching $\beta/2$, but there is no doubt that the later ones show that the value is practically β. Recent theories have introduced the Döppler and Compton effects *, but they are refinements and make but little difference in the calculation.

Apart from the interesting analogy between photon and photoelectron distribution, there are, therefore, two distinct consequences involved in stating that $\cos\theta_b = \sin\Theta = \beta$. Either β has remained constant during the ejection or the speed has varied in such a way that the average value is βc.

Supposing the former of these alternatives, then the photon has merely destroyed the orbital acceleration of the electron (or its counterpart), but the kinetic energy and speed are the same before as after the ejection. In this connexion it is to be noted that the orbital momentum of a Bohr electron is $nh/2\pi a$, whilst the momentum of an electron external to the atom given by wave mechanical theory and recent experiment is $mv = h/\lambda = n'h/2\pi a$, where n and n' are whole numbers and a is the radius of the simple orbit. If $n = n'$ these two momenta would be numerically equal to each other. On the other hand, it has been pointed out that the kinetic energy of an orbital electron must be taken as $h\nu_P + h\nu_{K,\,L,\,etc}$, where $h\nu_{K,\,L,\,etc.}$, is the ionizing energy, in order that the change in energy before and after escaping, viz., $2h\nu_{K,\,L,\,etc.}$, shall be twice the ionizing potential.

If $\beta_1 c$ is the internal speed and $\beta_2 c$ the external speed then

$$\cos\theta_b = \beta = (\beta_1 + \beta_2)/2$$
$$= \sqrt{\tfrac{1}{2}m_0c^2}\{(h\nu_P + h\nu_{K,\,L,\,etc.})^{\frac{1}{2}} + (h\nu_P - h\nu_{K,\,L,\,etc.})^{\frac{1}{2}}\}$$
$$= \cdot 03152\{(V_P + V_{K,\,L,\,etc})^{\frac{1}{2}} + (V_P - V_{K,\,L,\,etc})^{\frac{1}{2}}\},$$

where V is in kilovolts corresponding to energies. This formula possesses a double advantage. It will explain the numerical values obtained for Θ or θ_b in recent experiments, for $\cos\theta_b$ reduces to $\sqrt{2\alpha}$ when $h\nu_{K,\,L}/h\nu_P$ is small. This will give the same results for the last column of Table II. It will also explain in a quantitative manner the important conclusions of Watson and van den Akker †, who found that Θ was smaller for K and L_I electrons than for L_{II} and L_{III} electrons—in other words, an increase in the binding energy

* Fischer, *Ann. d. Physik* (5), viii. p. 821 (1931).
† Proc. Roy. Soc. A, cxxvi. p. 138 (1929–30).

of the atomic electron decreased Θ. This will be apparent for Θ changes from $\sqrt{2\alpha}$ where $h\nu_{K,L}/h\nu_P$ is negligible down to $\sqrt{\alpha}$, where $h\nu_{K,L}=h\nu_P$ and $\alpha=h\nu_P/m_0c^2$.

Summary.

Auger and Perrin's trigonometrical formulæ describing the longitudinal asymmetry of photoelectric emission will fit the case of the similar asymmetry of the quantized Maxwell radiation field of accelerated electrons of velocity βc. The conclusion arrived at is

$$\frac{\text{average forward momentum of field}}{\text{resultant momentum of field}}=\beta.$$

It is shown by analogy, as well as by experiment, that

$$\frac{\text{the forward momentum of a photoelectron}}{\text{resultant momentum of one}}=\beta.$$

There is a short discussion as to the manner in which β enters for photoelectric emission. The alternatives are either (i.) the electron is expelled without change of speed, (ii.) βc is the mean speed of the electron before and after expulsion.

XIII. *On the Time of Combustion of Flashlight Powder.* *By* S. Kalyanaraman, *M.A., L.T., Assistant Professor of Physics, Presidency College, Madras* *.

[Plate III.]

Introduction.

IT was thought in connexion with sound-pulse photography that flashlight powder might be used as an illuminant in place of the usual magnesium light-gap †, since the intensity of the latter was not found to be sufficient. If it could give an instantaneous flash of the same order of duration as an electric spark it was thought its use might be an improvement over the usual method. Accordingly the time of combustion was determined as follows.

* Communicated by Prof. H. P. Waran, M.A., D.Sc., F.Inst.P.

† Davis and Fleming, Journ. Sci. Instr. iii. p. 393 (1926).

The Principle of the Method.

The duration of flash was measured by allowing the light from the flash to illuminate a glass bead attached to a metal pointer which was kept revolving at constant speed. The arc described by the bead during the time of flash as measured photographically, together with the speed of revolution of the pointer, gave the data for calculating the duration of flash.

Experiment.

The metal pointer was attached by means of a clamp to the axle of a speed-reducing gear which was connected by a belt to the shaft of a 60-volt motor. The motor speed could be regulated so that the metal pointer revolved at a rate of about 50 revolutions per minute. The pointer was coated black, so that it would not reflect any light, and a black cardboard was fixed behind the pointer, so that the track of the glass bead could be photographed against a black background.

Ignition of the powder was arranged in front of the revolving pointer, and an electric spark from an induction coil was used for its ignition. The powder was carried in a metal spoon to which one terminal of the coil was attached. The other terminal was connected to a metal pointer clamped vertically, with its tip at a height of about 1 inch above the powder in the spoon, so that when the coil was worked a flaming spark passed between the pointer and the spoon. A flaming spark was found essential for ignition, since a thick condenser spark was not found to ignite the powder. The spoon and the sparking arrangement were contained inside a box which was closed on all sides except the one facing the revolving pointer.

The photographic camera was arranged behind the box, and at such a height that when an incandescent lamp was placed in the position of the ignition powder the complete rotation of the bright glass bead was visible in the camera.

For giving an exposure the plate was kept exposed in its place, with the camera shutter on. Since the whole experiment was arranged in a dark room, exposure could be given by igniting the powder with an instantaneous spark for the coil after removing the camera shutter. The speed of revolution was immediately measured by finding the time for fifty revolutions of the pointer.

Exposures were given with the same quantity of powder (a spoonful each time) but with different speeds of revolution

of the pointer. For measuring the angles of rotation the negatives were projected on a large paper protractor and measurements taken.

Results.

Speed of rotation (time for fifty revolutions).	Angle of rotation.	Time of combustion.
sec.	o	sec.
55·5	17	·052
35·0	30	·058
35·5	29	·057
31·5	36	·063
30·0	36	·059

The average time of combustion for a spoonful of powder was therefore equal to ·058 sec. These results clearly show that the time of combustion is much too large for sound-pulse photography, for during the flash the sound-wave would be moving through a distance of 68 ft., and no instantaneous position could be recorded. Experiments were conducted with smaller amounts of powder. Even then, though the combustion was a bit quicker, the duration was found to be of the same order of magnitude.

Discussion of Results.

Apart from the definite conclusions to which the results of the experiments have led, the author does not believe that this time of combustion is anything of the nature of a physical constant for the powder, for it can be easily altered by the manner in which the powder is contained in the spoon, whether spread out or heaped up. From the photographs obtained (Pl. III.) one could easily see how the beginning and the end of the flash are not abrupt, but are gradual. The foregoing results were calculated for the bright portion of the arc.

I am indebted to Prof. H. P. Waran for suggesting this work and guiding me through it.

The Presidency College, Madras.
15th Dec. 1931.

XIV. *The Scattering of Light by Liquid Helium* *By* Prof. J. C. McLennan, *F.R.S.*, H. D. Smith, *M.A.**, *and* J. O. Wilhelm, *M.A.*†

[Plates IV. & V.]

Introduction.

AMONG the many interesting features encountered in the study of liquid helium is the existence of two distinct liquid states. This was first suggested by Keesom and Wolfke ‡ in 1927. They found that at 2·19° K. there is a triple point, at which temperature the two liquid phases exist together in equilibrium with the helium gas. One phase, stable at temperatures above the point, is designated liq. He I, and the other, stable at temperatures below, is known as liq. He II. The physical properties of the two liquids differ materially, and sudden changes in the values of the density, dielectric constant, specific heat, heat of vaporization, and surface tension, occur at the triple point. Abrupt changes of this nature are usually accompanied by molecular phenomena of some sort, such as an association of molecules, or a change in molecular structure. In order to investigate the possibility of the occurrence of molecular changes which might explain the observed phenomena, we carried out experiments in an endeavour to obtain the Raman spectra of liq. He I and liq. He II. A study was made also of the Rayleigh scattering of the two phases, especially in the neighbourhood of the transition point, and the intensity of the Rayleigh scattering at this point compared with that of benzene at room temperatures.

Apparatus.

The essential parts of the apparatus used in these experiments are exhibited in fig. 1. The liquid helium was siphoned over the liquefier into the Raman tube, A, until a column of clear liquid, about 30 cm. in height, was obtained. In order to preserve the liquid helium the inner Dewar flask was surrounded by a second Dewar flask B, containing liquid air. The top T, made of German silver, was fastened to the Raman flask by a rubber joint at the point C.

* Fellow of the National Research Council of Canada.
† Communicated by the Authors.
‡ Keesom and Wolfke, *Leiden Comm.* No. 190*b*.

The source of incident exciting radiation was placed near the outside of the flask, B. The light scattered by the liquid upwards along the axis of the Raman tube, passed through the window W, and the light scattered downwards was reflected back along the axis by the mirror M. Suitable blackened metal diaphragms and the blackened metal tube T_2, cut down the amount of extraneous light reaching the slit

Fig. 1.

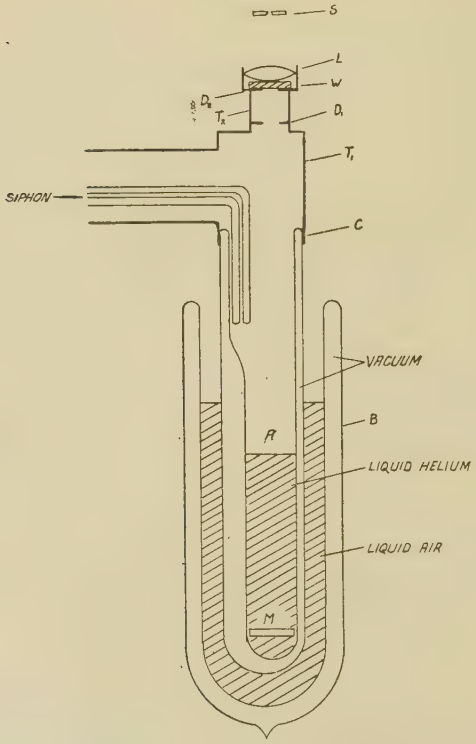

of the spectrograph. By this arrangement the light which arose from the walls of the Raman tube and was not cut out by the diaphragms was focussed off the slit on all sides.

In the first experiments the primary source of light consisted of a special mercury vapour lamp that had been used successfully in work on the Raman effects of liquid and of solid carbon dioxide. The lamp was constructed of pyrex tubing of 2 cm. diameter, in the form of a vertical helix

consisting of four turns, 15 cm. in diameter. The arc, approximately eight feet in length, when surrounded by a cylindrical polished aluminium reflector, gave a light of very great intensity along the axis of the helix. This axis coincided with that of the Raman tube during an exposure. The lamp carried 6 amps. when operated on the 220 volt D.C. circuit.

When this lamp was used the liquid helium boiled vigorously and the column lasted but 12 minutes. The light reflected by the large number of bubbles in the liquid caused

Fig. 2.

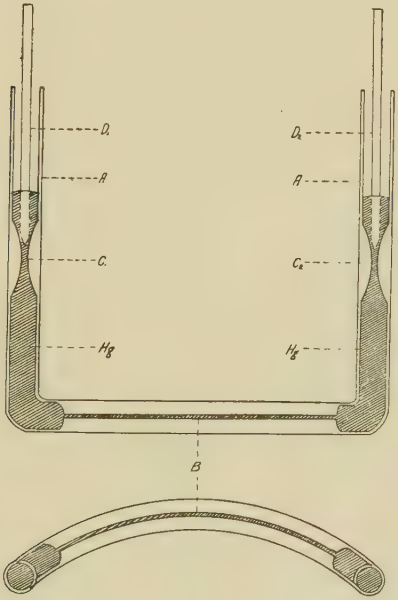

fogging of the photographic plate in a short time. It became necessary, then, to find a source of incident light which was accompanied by a smaller amount of infra-red radiation.

The capillary arc, shown in fig. 2, was finally employed. The two vertical arms A, of quartz tubing 1 cm. in diameter are joined to the ends of a piece of quartz capillary B, which is shaped so that it lies on the circumference of a circle concentric with, and at a short distance from, the outer wall of the flask B. The tubes are filled with very clean, gas-free

mercury. The steel rods D_1 and D_2 serve as electrodes and are supported by the constrictions C_1 and C_2.

The lamp, in series with a resistance of 110 ohms, is placed in the 220 volt D.C. circuit. The switch is closed and the capillary is heated by a small flame at a point midway between the vertical arms. When sufficient heat has been applied the arc suddenly strikes at this point, and the current drops to a quarter of its former value. The lamp is lowered at once into a bath of circulating cold water. The current is now brought up to a maximum of 1·5 amps. by decreasing the external resistance slowly. The length of the arc increases and gives a concentrated source of great intensity.

In the experiments with liquid helium the flask B was immersed in a continuous-flow water bath. The light was placed several cm. above the plane of the mirror M. This source of incident radiation proved very satisfactory and the amount of light which reached the slit of the spectrograph was equal to that which arose from the scattering medium when the spiral lamp had been employed. It was found that most of the heat from the arc was absorbed by the water; in fact, the liquid helium when irradiated by this source lasted for a period of five hours.

In order to lessen the continuous spectrum and cut out any particular group of lines in the spectrum of the mercury arc, various filtering solutions were used. These were contained in a glass cell placed between the arc and the flask B.

A direct vision spectrograph with a camera lens having a focal length of 8 cm., and providing a dispersion of about 70 A. per mm. gave good spectrograms. Ilford Golden Iso-Zenith plates H and D 1400 gave the best results for the region between λλ 4000 Å and 5000 Å.

Results and Discussion.

The apparatus was tested by photographing the light scattered by a column of liquid oxygen placed in the tube A. Spectrograms exhibiting the vibrational Raman lines clearly, were obtained with an exposure of one hour.

The light scattered by liquid helium at 4·2° K., the boiling-point of the liquid at normal pressure, was then investigated. At this temperature, however, it was impossible to keep the column of liquid free from bubbles, that moved rapidly to the surface. Due to this disturbance in the liquid, the photographic plate was blackened by reflected light in a short time.

It was decided that the experiment be repeated at some

temperature below the triple point. The pressure of the helium in the inner tube was reduced slowly and the liquid was watched closely as the triple point was approached. When a pressure of 38 mm. was reached, the appearance of the liquid underwent a marked change, and the rapid ebullition ceased instantly. The liquid became very quiet and the curvature at the edge of the meniscus appeared to be almost negligible.

Viewed through the window W_1 the surface of the liquid was indiscernible, while the lack of impurities and scattered light in the column caused the tube to appear empty. From the side, however, the surface could be seen distinctly. Photographs of this surface as viewed from different angles were taken. As far as we are aware, photographs of this nature have not been obtained previously, due, no doubt, to the fact that in most experiments liquid helium, with its small refractive index, is not easily seen.

Reproductions of pictures of the helium at 2° K. are shown in Pl. IV (*a*), (*b*), and (*c*). In Pl. IV. (*a*), the camera was placed in the plane of the surface of the helium, while in Pl. IV. (*b*) and (*c*) the photographs were taken from points above and below the surface respectively. A study of the plates exhibits clearly the tranquillity of the surface, the smallness of the meniscus, and the absence of scattered light.

Although it was apparent, visually, that the intensity of the classically scattered radiation was very small, nevertheless a search was made for any vibrational and rotational Raman lines arising from loosely-bound molecules that might be present in the liquid. The light scattered by the column, at a temperature of 1·95° K. and a pressure of 15 mm. was photographed with an exposure of 3 hrs. 40 mins.

After the evaporation of the liquid helium, with the scattering tube empty, an exposure of the same duration was made in order to photograph the amount of extraneous light reaching the slit of the spectrograph. A comparison of the two spectra showed that the intensities of corresponding unmodified lines were practically the same. This result substantiated the visual observation as to the extreme weakness of the classically scattered radiation. That this observation is in agreement with the theory may be shown by a consideration of the Einstein-Smoluchowski expression for the intensity of light-scattering in homogeneous media which may be written as follows:

$$I \propto \frac{T\beta(\mu^2-1)^2(\mu^2+2)^2}{\lambda^4},$$

where T is the absolute temperature of the liquid,
β is its compressibility,
μ is its refractive index,
and λ is the wave-length of the incident radiation.

Let us compare the scattering of liquid helium at 2° K. with that of benzene, say, at 300° K. for a given value of λ. The indices of refraction of liquid helium and benzene are approximately 1·02 and 1·5 respectively.

The compressibility of liquid helium is not known * but should be of the same order as that of benzene.

If subscripts He and B refer to liquid helium and benzene, respectively, the ratio of the light-scattering powers of these two liquids should be of the order of

$$\frac{T_{He}(\mu_{He}^2-1)^2}{T_B(\mu_B^2-1)^2}=\frac{1}{1{\cdot}4\times10^2}.$$

Insufficient time in the helium plant prevented more than a rough estimate of this ratio being made. With the Raman tube filled with Baker's chemically pure benzene, an exposure of 45 minutes' duration sufficed to bring out the unmodified lines with an intensity approximately equal to that of the corresponding lines obtained in the spectrum of liquid helium after an exposure of 3 hours 40 minutes. Raman lines of benzene also appeared clearly on the plate.

A comparison of the spectrograms obtained with liquid helium at 1·95° K., with the tube empty, and with benzene at 300° K. is shown in the reproductions, Pl. V. (*a*), (*b*), and (*c*).

A close examination of the spectrum reproduced in Pl. V. (*a*) revealed no isolated Raman lines. From this we may conclude that the intensity of any possible Raman lines in the spectrum of liquid helium is many times weaker than the faintest Raman line observed in the spectrum of the light scattered by liquid oxygen or liquid nitrogen. A slight difference between the spectra Pl. V. (*a*) and (*b*) was observed, however, in that the modified lines in Pl. V. (*b*) were sharply defined, while corresponding lines in Pl. V. (*a*) were accompanied by a faint broadening on both sides similar to the "wings" that appear in the Raman spectra of many liquids. It has been shown recently by Bhagavantam† that these wings, in most cases, arise from rotational Raman transitions of the molecules. It seems probable that the wings observed with liquid helium may

* Experiments now being carried out in this laboratory on the velocity of sound in liquid helium will give, if successful, a value for β.

† Bhagavantam, Ind. Jl. Phys. vi. p. 319 (1931).

have a similar origin, being due to rotational changes of loosely-bound molecules existing in the liquid. This view is supported by recent work of Weizel* on the energy levels of the He_2 molecules in which he shows that when two helium atoms each in the normal 1S state come together to form a molecule in the lowest energy state, there is possibly a very shallow minimum in the potential energy curve for very high inter-nuclear distances. In the liquid helium it is almost certain that all atoms present at a temperature of 2° K. are in the low 1S state and therefore possible molecules formed from these would have high inter-nuclear distances. This would result in a large value for the moment of inertia of the molecule and a corresponding low value for the rotational constant B. Raman rotational lines, therefore, would be in close proximity with the unmodified lines.

The work of Van Urk, Keesom, and Onnes † on the surface tension of liquid helium provides an argument which supports the view that there are molecules present below the triple point. If ψ_M, the molecular surface tension, is plotted against T a straight line is obtained for values of $T > 2{\cdot}19°$ K. This agrees with the simple theory of Eötvös which gives $\frac{d\psi_M}{dT} = k_{E\ddot{o}}$ (a constant). If we use the relation

$$\psi_M = \psi_\sigma \left(\frac{M}{\rho}\right)^{2/3}$$

when ψ_σ is the surface tension in dynes per cm., M is the molecular weight, and ρ is the density of the liquid, and take $M = 4$ for $T > 2{\cdot}19°$ K, *i. e.*, assume no molecular association of the helium atoms in liquid helium I, we obtain $k_{E\ddot{o}} = -1$. If the Eötvös constant is to have this value for $T < 2{\cdot}19°$ K, the value for M in the equation must be increased as T is decreased. For example, at $T = 1{\cdot}5°$ K the effective value of M would be 5. This indicates, on the basis of the rough considerations of Eötvös, that molecular association takes place in liquid helium II. the degree of association increasing as the temperature falls.

The authors desire to record their appreciation of the help kindly given them at times by Mr. C. Barnes during the investigation.

McLennan Laboratory,
University of Toronto.
May 9th, 1932.

* Weizel, Phys. Rev. xxxviii. p. 643 (1931).

† Van Urk, Keesom, and Kamerlingh Onnes, *Leiden Comm.* No. 179 *a* (1926).

XV. *The Strength of Persistent Currents in Superconductive Circuits.* *By* Prof. J. C. McLennan, *F.R.S.*, J. F. Allen, *M.A.**, *and* J. O. Wilhelm, *M.A.* †.

SOME years ago, Kamerlingh Onnes ‡ found that if a ring of lead were cooled to the temperature of liquid helium, a current of electricity could be induced in it which would persist at full strength so long as the ring was kept in the superconductive state. This current is characterized by no electromotive force and no heat loss; the sole energy which it possesses is in the form of the kinetic energy of the conduction electrons. Strengths of currents of this type were later measured by Tuyn §, who found them to be of the order of a hundred amperes in lead rings of a few square millimetres cross-section. The measurements, however, were made only on lead. We therefore decided to carry the investigation further and make comparative measurements of these currents in various superconductive metals. It was hoped from such an investigation that valuable information might be obtained, particularly as to the number of the electrons involved in current conduction.

Apparatus.

An investigation of this type involved considerable experimental difficulty. It was possible to make observations on only one metal at a time, and it was therefore necessary to maintain the same experimental and operating conditions over a succession of helium runs separated by several days. Also, since the most accurate method of measuring these currents is by a calibration device, the torsion, in order to ensure constancy, must be maintained at room temperature, while the ring of the metal, which forms the superconductive circuit, is immersed in liquid helium. We needed, therefore, a long rigid connexion between the torsion apparatus and the ring of metal in the helium. Tuyn used glass rods to form this connexion, but for our purpose glass was unsuitable and light metal tubes were used instead. It was found during the performance of the experiment that the liquid helium was very little disturbed by the presence of four German silver tubes which formed a direct metallic thermal connexion with the apparatus at room temperature.

* Student of the National Research Council of Canada.
† Communicated by the Authors.
‡ K. Onnes, *Leiden Comm.*, No. 141 *b*.
§ W. Tuyn, *Leiden Comm.*, No. 198.

Fig. 1.

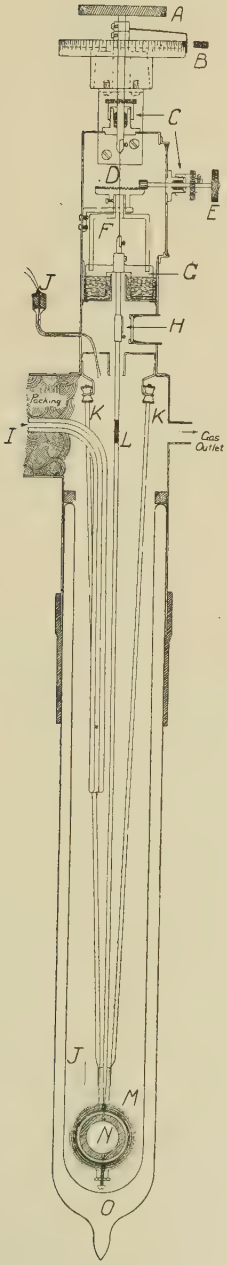

Measurements were obtained with the apparatus shown in fig. 1. The diagram is drawn to scale. The principle of the instrument is somewhat similar to that of the simple galvanometer with the swinging coil replaced by a metal ring. Rings were made of lead, tin, and tantalum. These rings, of identical dimensions and interchangeable in the apparatus, were 2·8 cm. in outside diameter, 2·0 cm. in inside diameter, and ·4 cm. thick. They are represented in the diagram by the ring N. In the apparatus, N was suspended inside a coil M. The coil was 3·9 cm. in outside diameter, 3·1 cm. in inside diameter, 1·2 cm. long, and contained 320 turns of fine copper wire. If a current is sent through the coil, a magnetic field is set up inside it. The change of flux that takes place causes an induced current to be set up in the ring N. Ordinarily, the induced current is only momentary, but when the ring is in the superconductive state, the induced current persists at a steady value, since there is no resistance to destroy it. The persistent induced current is in opposition to the primary current, and therefore a torsion of the ring takes place. The amount of this torsion was the quantity which was to be determined in the investigation.

The control mechanism was mounted above the helium cryostat O, in a brass cylinder. The latter formed a dead end in the gas-circuit and remained, therefore, at or near room temperature even when the flask below was filled with liquid helium. The moderate temperature of the brass cylinder facilitated manipulation and resulted in a constant torsion coefficient for the suspension. The position of the N was primarily controlled by means of the torsion head A. An attached pointer moved around a graduated cylinder and exact reproducible angular settings were made possible by the use of a stop B, which could be plugged in at any desired angle. The packing glands C, were necessary, since the system must be gas-tight. The suspension D, was a phosphor bronze ribbon 5 cm. long, 2 mm. wide, ·15 mm. thick, which provided the torsion to react against the turning force of the ring. The suspension D was fastened above to the torsion head, and below to a long rigid German silver tube L, which passed down the flask and supported the ring N. At L in the rigid tube a hard rubber insulator was inserted which insulated the ring N from the rest of the apparatus. A one-metre concave mirror H, mounted on the rigid suspension tube reflected a beam of light to a concave scale by means of which the angular position of the ring was observed. The scale was one metre in radius and

about one quadrant in length; its centre of curvature was the mirror H. The window in front of the mirror H was rectangular and wide enough to allow a 45° deflexion of the ring N to be observed. The coil M was held rigidly in position by means of a tripod of German silver tubes (of which two, K K, are shown) 42 cm. long. J J represent lead wires from the coil to the battery circuit outside the cryostat. Small brass tubes were set in the top and bottom of the coil M; the upper one allowed the brass tip of the suspension tube to pass through the coil and be fastened to the metal ring. The tube through the bottom of the coil carried a thin polished steel pin which entered a small fibre-lined hole in the bottom of the ring and served to restrict vibration and swaying, but left it perfectly free to swing on a vertical axis. The brass tip of the suspension rod contained a tiny threaded cross-hole. A clearance cross-hole, drilled through the ring, cut the hole in which the brass tip is inserted, at right angles. The cross-holes were lined up and a screw inserted, giving a rigid fastening for the ring and also allowing easy interchange of rings of different metals with negligible error in angular setting.

A paddle G, was attached to the top of the rigid tube L. The paddle, moving in an annular oil-trough, rendered the motion of the ring comparatively slow and very steady. In order to hold the ring in the position of coaxiality with the coil while the flux was changing, a yoke F was placed over the paddle blades. The yoke allowed complete freedom of the motion of the ring through only a small angle. The yoke was connected by means of a hollow shaft (through which the suspension D passed) to a pinion which was in gear with another pinion connected to the knob E. By these means full control was maintained over both the motion and the portion of the ring N.

Liquid helium was admitted to the cryostat O by means of the siphon tube I, which was attached to the bottom of the cryostat in which the liquid helium was made.

Method of Measurement.

When the persistent current is set up in the ring N, no motion will take place immediately, because the position of coaxiality of the ring and coil is one of unstable equilibrium. If the torsion head is turned through a small angle, however, the field of the ring will react against that of the coil, with the result that the ring will continue to turn until it comes into equilibrium with the torsion of the suspension.

In practice, the torsion head was first set by means of the stop B, at some angle (usually 20°), and by means of the knob E, the ring was brought back into the position of coaxiality with the coil M. The outside circuit was then closed, causing a small current from a six-volt storage battery to be sent through the coil, and the persistent current to be set up in the ring. The yoke was then turned back towards the 20° mark until the ring swung freely in equilibrium with the torsiou. The spot of light, reflected from the mirror H to the scale, recorded over 20°. The difference between the observed scale reading and the correct reading for 20° was, therefore, a measure of the strength of the persistent current in the ring. The yoke was then brought into play again to return the coil to its original position of coaxiality, after which the current was broken in the coil, causing the persistent current to disappear. After the resistance in the outside circuit had been altered so that a larger current could be sent through the coil, the switch was again closed and the whole procedure repeated until a complete curve was obtained for all inducing fields and persistent current strengths.

The experiment was performed three times, each time with a different ring. Conditions were maintained as nearly as possible the same for all three experiments. At the conclusion of these tests, a coil of the same dimensions as the rings and containing 150 turns of fine copper wire, was substituted for them, and calibration measurements were made so that absolute values of the strengths of the persistent currents in the various metals could be determined. These measurements were carried out at room temperature. The current in the outer coil was set at the various values used in the persistent current tests and the current in the calibrating coil adjusted until the proper deflexions (*i. e.*, the deflexions obtained with the rings) were obtained. Then, since the calibrating coil was of the same dimensions as the rings, the value of any one current in any ring was found by multiplying the number of turns in the calibrating coil by the value of current sent through it to produce the proper deflexion. In this way the values of persistent current strength were determined for three metals, lead, tin, and tantalum.

The experimental error in the persistent current measurements was surprisingly small, being not more than 1 per cent. When the calibration tests were made, however, the error was greater, mainly because of the necessity for using mercury cups for contacts to the calibration coil.

Discussion.

In Tables I., II., and III. are shown the data obtained for the three metals. The curves in fig. 2 show the quantities

TABLE I.

Persistent Current Strengths in Tantalum at 2·0° K.

Torsion head-angle setting.	Current in coil M. (amps.)	Total change of flux through ring. (Gauss.)	Scale deflexion of ring. (cm.)	Calibrated persistent current. (amps.)
20°	0·071	6·79	0·55	12·75
,,	·11	10·51	1·5	19 80
,,	·18	17·22	4·55	32 40
,,	·22	21·05	6·6	39·60
,,	·24	22·95	8·0	43·20
,,	·256	24·50	9·2	46·05
,,	·275	26·30	10·7	49·50
,,	·303	29·0	13·1	54·60
,,	·335	32·05	16·2	60·30
,,	·37	35·40	19·8	66·60
,,	·41	39·20	24·8	73·80
,,	·45	43·0	29·8	81·00
,,	·502	48·0	36·5	90·30
		Repetition.		
,,	·20	19·13	5·5	36·00
,,	·23	22·0	7·2	41·40
,,	·259	24·75	9·35	46·65
,,	·297	28·40	12·5	53·40
,,	·382	36·50	21·5	68·70
,,	·439	42·10	28·3	79·05
,,	·486	46·50	34·5	87·45
10°	·486	46·50	30·3	87·45
,,	·515	49·25	35·0	92·70
,,	·562	53·70	44·1	101·10
,,	·60	57·40	51·4	108·00
,,	·62	59·30	55 7	111·60
,,	·64	61·20	60·1	115·20
,,	·663	63·50	64·7	119·40
,,	·717	68 50	74·8	129·00
5°	·778	74·5	88·2	140·10
2·5°	·81	77·5	106·3	145·80
− 5°	·89	85·2	—	160·20
−11·5°	·98	93·7	—	176·40
−14°	1·04	99·5	—	187·20
−22°	1·10	105·1	—	198·00
−34°	1·25	119·6	—	225·00
−41°	1·34	128·20	—	241·20

which were directly measured when the torsion head was set at 20°. The graphs are plotted from the values of the currents in the coil M, and the deflexions produced on the

scale due to the torsion which results from the action of the persistent induced current on the primary. The scale deflexion values are taken considering the 20° mark on the scale as zero. In the case of tantalum, the inducing current

TABLE II.

Persistent Current Strengths in Tin at 2·0° K.

Torsion head-angle setting.	Current in coil M. (amps.)	Total change of flux through ring. (Gauss.)	Scale deflexion of ring. (cm.)	Calibrated persistent current. (amps.)
20°	0·07	6·7	0·5	12·6
,,	·09	8·62	0·9	16·2
,,	·115	11·01	1·7	20·7
,,	·15	14·37	3·0	27·0
,,	·168	16·07	3·8	30·25
,,	·18	17·22	4·5	32 40
,,	·184	18·56	5·2	34·90
,,	·206	19·73	5·9	37·1
,,	·22	21 05	6·7	39·6
,,	·233	22·3	7·7	42·3
,,	·25	23·93	8·85	45·0
,,	·264	25·27	9·95	47·5
,,	·28	26·8	11·2	50·3
,,	·295	28·25	12·35	52·8
,,	·31	29·7	13·7	55·0
,,	·326	31·2	15·2	57·8
,,	·345	33·0	17·0	60·9
,,	·365	35·0	19·1	64·2
,,	·38	36 4	20·7	66·7
,,	·395	37·8	22·4	69·5
,,	·416	39·8	24·4	72·5
,,	·435	41·7	26·6	75·7
,,	·459	44·0	28·85	77·7
,,	·481	46·0	29·5	75·2
,,	·51	48·8	28·8	68·8
,,	·54	51·7	26·2	62·5
,,	·575	55·0	23·9	54·7
,,	·615	58·8	21·3	45·3
,,	·77	73·7	10·6	15·0

was carried to values higher than those recordable on the scale with the torsion head set at 20°. In order to record these values the torsion-head angle was changed to 10°, then to 5°, and to 2·5°. Finally it was found necessary to continue the rotation of the torsion head past the zero position so that the spot of light could be returned to the scale. For the strongest inducing current used, 1·34 amperes, the torsion head had to be turned to 41° past the zero mark before the spot of light reappeared on the scale.

TABLE III.

Persistent Current Strengths in Lead.

(*a*) At 4·2° K.

Torsion head-angle setting.	Current in coil M. (amps.)	Total change of flux through ring (Gauss.)	Scale deflexion of ring. (cm.)	Calibrated persistent current. (amps.)
20°	0·07	6·7	0·6	12·6
,,	·089	8·52	1·1	16·0
,,	·105	10·04	1·5	18·9
,,	·129	12·33	2·3	23·2
	·152	14·54	3·2	27·4
,,	·165	15·77	3·8	29·7
,,	·18	17·22	4·5	32·4
,,	·19	18·17	5·1	34 2
,,	·20	19·13	5·85	36·0
,,	·212	20·27	6·25	38·2
,,	·225	21·50	7·2	40·5
,,	·24	22·95	8·30	43·2
,,	·255	24·38	9·45	45·9
,,	·27	25·82	10·6	48·6
,,	·289	27·65	12·05	52·0
,,	·31	29·65	13·8	55·8
,,	·33	31·53	15·9	59·4
,,	·35	33·50	17·85	63·0
,,	·37	35·40	20·1	66·6
,,	·386	36·9	21·9	69·5
,,	·403	38·6	23·9	72·6
,,	·421	40·2	26·05	75·8
,,	·444	42·4	28·7	80·0
,,	·466	44·5	31·6	83·9
,,	·493	47·1	34·9	88·8
,,	·509	48·7	36·7	91·7

(*b*) At 2·0° K.

,,	·075	7·17	0·7	13·5
,,	·094	8·98	1·0	16·9
,,	·113	10·8	1·8	20·3
,,	·138	13·2	2·55	24·8
,,	·157	15·01	3·4	28·3
,,	·18	17·22	4·5	32·4
,,	·20	19·13	5·75	36·0
,,	·212	20·27	6·4	38·2
,,	·226	21·6	7·3	40·7
,,	·24	22·95	8·4	43·2
,,	·255	24·38	9·4	45·9
,,	·289	27·65	11·95	52·0
,,	·325	31·4	15·25	58 5
,,	·35	33·5	17·75	63·0
,,	·37	35·40	20·0	66·6
,,	·403	38·6	23·8	72·6
,,	·421	40·2	26·0	75·8
,,	·466	44·5	31·55	83·9
,,	·48	45·8	33·15	86·4
,,	·506	48·4	36·65	91·2

In fig. 3 are shown the results of the calibration measurements carried out at room temperature and using a coil in place of the rings. Here the calculated currents in the rings are plotted against the various values of the change of flux through the ring. These flux values are not strictly correct, as it was not practicable to calculate exactly the flux through the ring, and an approximate value was taken

Fig. 2.

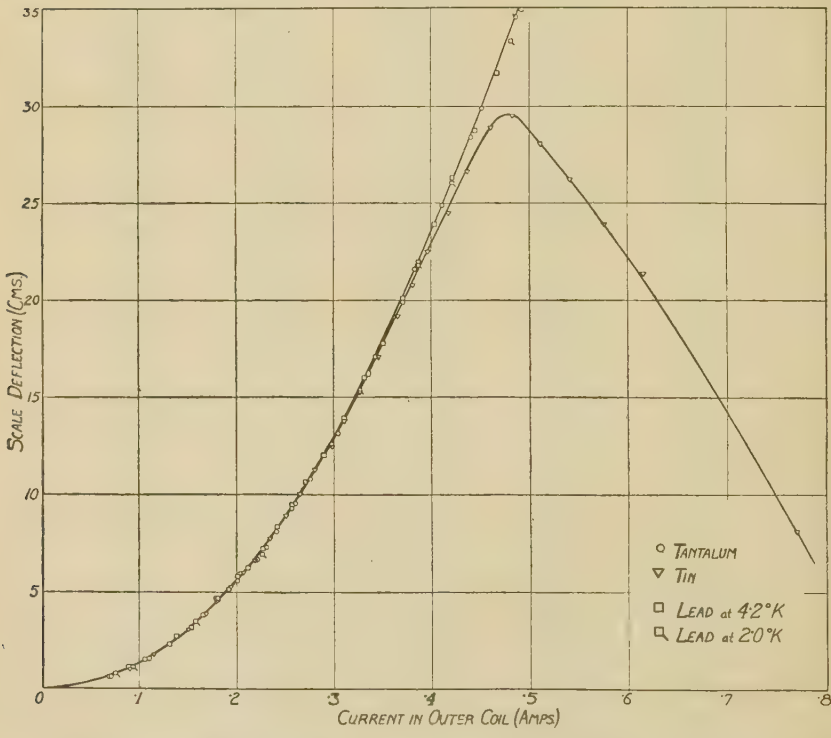

for the mutual inductance. The values of the flux plotted are values of the field at the centre of the coil M deduced from the simple formula. A more elaborate calculation, still using an approximate value for the mutual induction, gave results which were about 20 per cent. greater than those given in fig. 3. The final angular position of the ring, however, was always more than 20° from the position of coaxiality with the coil, and therefore the flux through part of the coil was lessened considerably. This would have reduced slightly the value calculated from the mutual

inductance. In view of this compensation the values of the field at the centre of the coil were considered to be accurate enough for our purpose, since the paper deals mainly with relative values of current for the different metals. In making the calibration measurements, the exact original scale deflexions were not used, except in the case of tin for inducing fields above 25 gauss. Instead, points were taken on the curve in fig. 2. The reason for using the curve as a

Fig. 3.

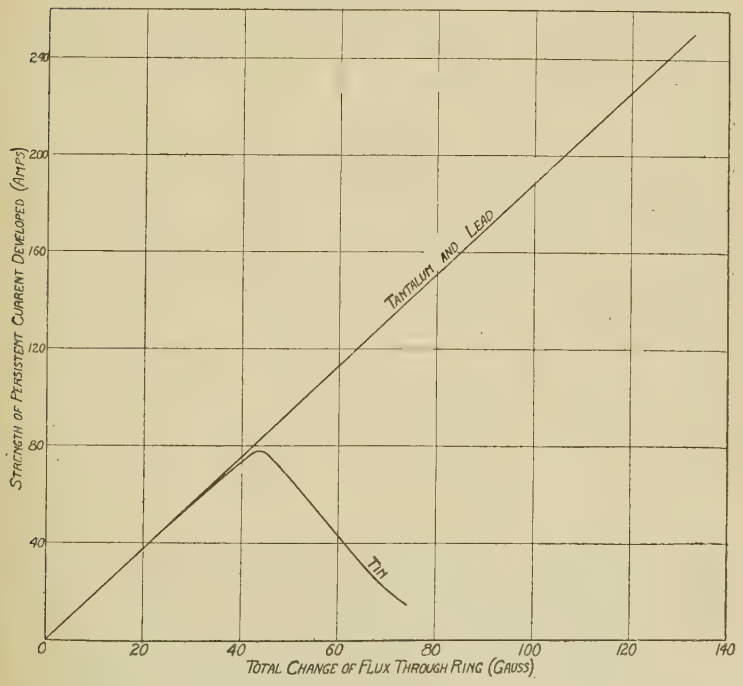

basis instead of the actual deflexion readings, was that the deflexion points were never very far off the curve, and the error in making the calibration readings was greater than the error in the persistent current measurements.

It was proved during the test on tantalum that the method of measuring the strength of persistent currents, as given in the preceding section, was valid for the whole curve. In obtaining the curve for tantalum, two sets of readings, shown in Table I. were made. For the first set the inducing

fields were carried up to 48 gauss ; the current in the coil M was made before and broken after each measurement. Then to test whether the persistent current was completely destroyed at the break of the primary circuit, a repetition of the set of readings was made. This second set agreed perfectly with the first, thus proving that, prior to every measurement, when there was no current in the primary circuit, no persistent current existed in the ring.

In order to find out whether the rate of change of flux exerted any influence on the strength of the current, a 1·7 henry inductance was inserted in the primary circuit in series with the coil M, which in itself possessed an inductance of approximately 10 millihenries. Measurements made with this hook-up do not vary appreciably from those obtained

Table IV.

Primary circuit inductance. 10 millihenries.		Primary circuit inductance. 1710 millihenries.	
Current in coil M. (amps.)	Scale deflexion of ring. (cms.)	Current in coil M. (amps.).	Scale deflexion of ring. (cms.)
·086	·09	·094	1·1
·094	1·1	·102	1·35
·11	1·5	·11	1·5
·12	1·85	·115	1·6

with no additional inductance in the circuit. These measurements are shown in Table IV., from which we can see that the rate of change of flux has no first-order effect on the magnitude of the persistent current.

We were desirous also of ascertaining whether or not the temperature of the ring played any part in determining the magnitude of the persistent current. Lead was a suitable metal on which to make this test, since it becomes superconducting at 7·2° K., and measurements could be made both at 4·2° K. and 2·0° K. From Table III. we see that measurements made at both these temperatures are almost identical, showing that the temperature below the superconducting point has no effect on the strength of the persistent current.

It has been shown that neither the temperature nor the rate of change of flux have any effect on the strength of the

persistent current. We are, therefore, in a position to compare the measurements as they stand in figs. 2 and 3 and Tables I., II., and III. We see at once that the same persistent current is developed in all rings by the same change of flux. That is, the magnitude of the induced current depends solely on the dimensions of the ring and not on the substance which composes it.

The case of tin is very interesting, since the values of the current in it agree with the others only up to about 25 gauss. For inducing fields higher than this the strength of the persistent current drops off. Above this point, then, part of the ring must be in a field, the strength of which has reached the critical value where resistance reappears; that is, an inner layer of the ring must have become non-superconducting. As the field is increased above this point, we can suppose the outside superconducting portion of the ring to become thinner and thinner, until the whole ring becomes non-superconducting. Incidentally this demonstrates that the field inside the coil is not homogeneous but possesses a gradient from the axis of the coil to the coil itself. It may be this lack of homogeneity explains the discrepancy between the critical field obtained by us (fig. 3) and that obtained by Onnes *, who found the critical field for tin at 2·0° K. to be in the neighbourhood of 200 gauss.

The fact that the same flux engenders the same persistent current in different superconducting metals having the same size and form follows from an application of the equation

$$\frac{L di}{dt} = \frac{d B_A}{dt} \qquad \text{or} \qquad i = \frac{B_A}{L}.$$

For rings of the same dimensions, the self-inductances will be identical; and in the superconducting state the resistances of the three metals are vanishingly small. These two factors produce the same magnitude of induced current in different superconductors.

Looking at the matter in another way we see that the induced currents in the three superconductors must be the same, since the magnetic flux of the persistent currents must be equal in magnitude and distribution, but opposite in direction to the flux of the exciting field.

Although the existence of any resistance whatsoever in superconductors seems incompatible with the results of this investigation, we have not definitely proved here the existence or non-existence of a micro-resistance in the super-

* K. Onnes, *Leiden Comm.*, Supplement No. 50.

conducting state. It may be that the results of defined measurements now being made by us on the decay of persistent currents will throw some light both on the existence of a micro-resistance and on its magnitude.

In conclusion the authors would like to express their thanks to Mr. C. Barnes for kind help given during the course of the investigation.

The McLennan Laboratory,
Department of Physics,
University of Toronto.
April 1932.

XVI. *Some Properties of Porous Building Materials.*—Part V. *The Absorption of Water in certain Special Cases.* *By* E. Madgwick, *M.C., M.Sc., Ph.D.**

Introduction.

THE experimental method described in the previous section in connexion with the examination of homogeneous specimens has been extensively used in the testing of building materials of various degrees of complexity. In this section some further principles underlying the interpretation of the absorption curves will be discussed.

The Absorption Constants of Compound Specimens.

The method may be extended in theory to the determination of the absorption constants of any number of materials intimately compounded as parallel slabs in a single specimen. Consider, as an illustration, the flow of water into and through two media, each of area A, under the action of a head h applied at the entering surface. Let the values of the thickness, resistivity, permeability, capillary head, total head, penetration constant, porosity, and absorptivity be l_1, σ_1, P_1, h_1', H_1, D_1, B_1, and Z_1 respectively for the first medium, and l, σ, P, h', H, D, B, and Z respectively for the second. The theoretical absorption curve is of the form shown in fig. 1. t_1 is the time taken to penetrate to the lower surface of the first medium ; t_0 the time taken by the water front to reach the lower surface of the second medium from the moment it enters that medium ; Q_0' the rate of absorption for a depth l_1

* Communicated by Sir F. E. Smith, K.C.B., C.B.E., Sec.R.S.

of penetration and under the action of a total head $h+l_1+h_1'$; Q_1' the rate of absorption for the same depth of penetration, but under the action of a total head $h+l_1+h'$; Q_0 the rate of absorption for a depth l_1+l of penetration and under the action of a head $h+l_1+l+h'$; and Q_1 the rate of transmission under the action of a head $h+l_1+l$. (Q_1' may be greater or less than Q_0'.) Then we have, by equation (18) (Part III.),

$$t_1 = \frac{B_1\sigma_1}{g}\left\{ l_1 - H_1 \log\left(1+\frac{l_1}{H_1}\right)\right\}, \quad . \quad . \quad (42)$$

Fig. 1.

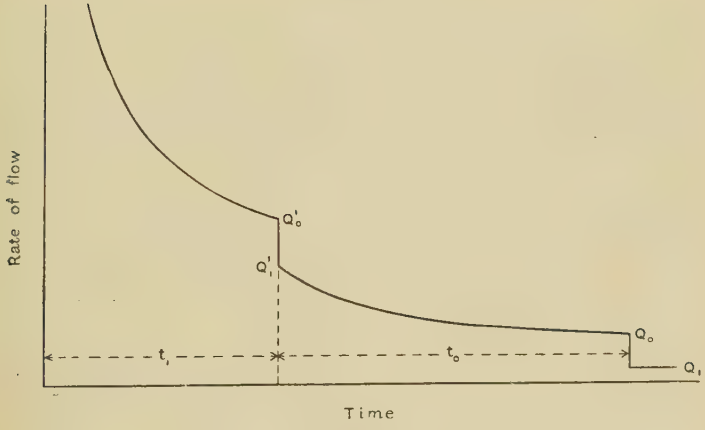

or, when l_1 is small compared with H_1,

$$t_1 = \frac{D_1 h_1' l_1^2}{H_1} \quad . \quad . \quad . \quad . \quad . \quad . \quad . \quad (42a)$$

By equation (14)

$$Q_0' = \frac{Ag(h+l_1+h_1')}{\sigma_1 l_1} \quad . \quad . \quad . \quad . \quad . \quad (43)$$

and

$$Q_1' = \frac{Ag(h+l_1+h')}{\sigma_1 l_1} \quad . \quad . \quad . \quad . \quad . \quad (44)$$

By equation (28)

$$t_0 = \frac{B(\sigma_1 l_1 - \sigma H)}{g} \log\left(1+\frac{l}{H}\right) + \frac{B\sigma l}{g}, \quad . \quad . \quad (45)$$

or, when l is small compared with H,

$$t_0 = \frac{Bl}{2Hg}(2\sigma_1 l_1 + \sigma l)$$

$$= \frac{Dh'}{H}\left(\frac{2\sigma_1 l_1 l}{\sigma} + l^2\right). \quad . \quad . \quad . \quad . \quad (45a)$$

Also, by equation (27),

$$Q_0 = \frac{Ag(h + l_1 + l + h')}{\sigma_1 l_1 + \sigma l} \quad . \quad . \quad . \quad . \quad (46)$$

and

$$Q_1 = \frac{Ag(h + l_1 + l)}{\sigma_1 l_1 + \sigma l}. \quad . \quad . \quad . \quad . \quad . \quad (47)$$

From these six equations the three independent constants for each material (h_1', σ_1, D_1, h', σ, and D, for example) may be readily calculated. In all cases in which the experimental conditions can be controlled l_1 and l would be small in comparison with H_1 and H; otherwise the time required by a test would be inordinately long. We can then write $h' + h + l_1 + l$ for $h' + h + l_1$ and $h_1' + h + l_1 + l$ for $h_1' + h + l_1$ when simple expressions for the absorption constants are obtained as follows. From equations (47) and (46)

$$h' = \frac{(h + l_1 + l)(Q_0 - Q_1)}{Q_1}. \quad . \quad . \quad . \quad . \quad (48)$$

Hence, by equation (44),

$$\sigma_1 = \frac{Ag(h + l_1 + l)Q_0}{l_1 Q_1 Q_1'}. \quad . \quad . \quad . \quad . \quad (49)$$

Thence, by equation (43),

$$h_1' = \frac{(h + l_1 + l)(Q_0 Q_0' - Q_1 Q_1')}{Q_1 Q_1'}, \quad . \quad . \quad . \quad (50)$$

by equation (47)

$$\sigma = \frac{Ag(h + l_1 + l)(Q_1' - Q_0)}{l Q_1 Q_1'}. \quad . \quad . \quad . \quad (51)$$

by equation (42*a*)

$$D_1 = \frac{t_1 Q_0 Q_0'}{l_1^2(Q_0 Q_0' - Q_1 Q_1')}, \quad . \quad . \quad . \quad . \quad . \quad (52)$$

and by equation (45*a*)

$$D = \frac{t_0 Q_0 (Q_1' - Q_0)}{l^2 (Q_0 - Q_1)(Q_1' + Q_0)}. \quad . \quad . \quad . \quad . \quad (53)$$

Further,

$$P_1 = \frac{1}{\sigma_1} \quad \text{and} \quad P = \frac{1}{\sigma}.$$

Also,

$$Z_1 = P_1 g h_1' = \frac{l_1(Q_0 Q_0' - Q_1 Q_1')}{A Q_0} \quad . \quad . \quad . \quad (54)$$

and

$$B_1 = \frac{2gh_1' D_1}{\sigma_1} = \frac{2t_1 Q_0'}{l_1 A} \quad . \quad . \quad . \quad . \quad . \quad . \quad . \quad (55)$$

Similarly,

$$Z = \frac{l Q_1'(Q_0 - Q_1)}{A(Q_1' - Q_0)} \quad . \quad . \quad . \quad . \quad . \quad (56)$$

and

$$B = \frac{2t_0 Q_0 Q_1'}{l A(Q_1' + Q_0)} \quad . \quad . \quad . \quad . \quad . \quad . \quad (57)$$

Tests on compound specimens have not yet been attempted, and a discussion of the practical aspects will be deferred. The method is described here for the sake of completeness.

Thin Coatings.

The laws governing the flow of water in successive media have been discussed in Part III. An important special case is that of a thin coating of, for example, size, distemper, paint, or "preservative" applied to the surface of such a porous material as plaster, stone, or brick. The effect of a homogeneous coating on the rates of absorption, penetration, and transmission can be calculated from the appropriate equations, provided the resistance $\sigma_1 l_1$ per unit area of the coating is known. This may be estimated by one of the methods discussed below.

(a) *The Absorption Curve.*—Suppose an ordinary absorption test to be carried out on a coated specimen. Let l, the thickness of the specimen, be small compared with the total head H. Then, assuming the penetration to be uniform, and measuring the time from the moment the coating is penetrated, we have, by equation (30), the time taken to penetrate a depth x,

$$t = \frac{Bx}{2gH}(2\sigma_1 l_1 + \sigma x). \quad . \quad . \quad . \quad . \quad (58)$$

The rate of absorption corresponding to this depth of penetration is, by equation (27),

$$Q = \frac{AgH}{\sigma_1 l_1 + \sigma x}, \quad . \quad . \quad . \quad . \quad . \quad . \quad (59)$$

and the equation to the absorption curve is, by equations (58) and (59),

$$t = \frac{K_1}{Q^2} - K_2 \quad . \quad . \quad . \quad . \quad . \quad . \quad (60)$$

(*cf.* equation (31)), where

$$K_1 = \frac{BA^2 g H}{2\sigma} \quad . \quad . \quad . \quad . \quad . \quad . \quad (61)$$

as in equation (32), and

$$K_2 = \frac{B(\sigma_1 l_1)^2}{2gH\sigma} \quad . \quad . \quad . \quad . \quad . \quad . \quad (62)$$

In some instances the time taken to penetrate the coating is extremely small, when t is measured, in the usual way, from the moment the specimen is wetted. We shall confine our attention at present to tests of this nature. Obtaining the values of t_0, Q_0, and Q_1 from the absorption curve in the manner described in Part IV., the rate of absorption for a depth l of penetration is, by equation (27),

$$Q_0 = \frac{Ag(h+l+h')}{\sigma_1 l_1 + \sigma l}, \quad . \quad . \quad . \quad . \quad . \quad (63)$$

and the rate of transmission is

$$Q_1 = \frac{Ag(h+l)}{\sigma_1 l_1 + \sigma l}. \quad . \quad . \quad . \quad . \quad . \quad (64)$$

Then from equations (63) and (64)

$$h' = \frac{(h+l)(Q_0 - Q_1)}{Q_1} \quad . \quad . \quad . \quad . \quad . \quad (65)$$

(*cf.* equations (36) and (48)), and from equations (61) and (62)

$$\sigma_1 l_1 = AgH\sqrt{\frac{K_2}{K_1}}$$

$$= Ag(h+l)\frac{Q_0}{Q_1}\sqrt{\frac{K_2}{K_1}} \quad . \quad . \quad . \quad . \quad (66)$$

by equation (65). Also, from equation (64),

$$\sigma = \frac{Ag(h+l)}{Q_1 l} - \frac{\sigma_1 l_1}{l}$$

$$= \frac{Ag(h+l)}{Q_1 l}\left(1 - Q_0\sqrt{\frac{K_2}{K_1}}\right) \quad . \quad . \quad . \quad (67)$$

by equation (66) (*cf.* equation (38)).

The time taken to penetrate to a depth equal to the thickness l of the specimen is (*cf.* equation (58))

$$t_0 = \frac{Bl}{2g\mathrm{H}}(2\sigma_1 l_1 + \sigma l) = \frac{Bl\sigma_1 l_1}{g\mathrm{H}} + \frac{Dh'l^2}{\mathrm{H}},$$

and, combining this with equations (65) and (66),

$$D = \frac{(t_0 - K_3)Q_0}{l^2(Q_0 - Q_1)} \quad . \quad . \quad . \quad . \quad . \quad (68)$$

cf. equation (40)), where

$$K_3 = BlA\sqrt{\frac{K_2}{K_1}}, \quad . \quad . \quad . \quad . \quad . \quad (69)$$

and BlA is the total volume of water which is absorbed by the specimen. This may be determined from the area under the curve; alternatively, it is equal to

$$\bar{Q} = \int_0^{t_0} Q\,dt = 2K_1^{\frac{1}{2}}\{(t_0 + K_2)^{\frac{1}{2}} - K_2^{\frac{1}{2}}\}, \quad . \quad . \quad (70)$$

K_1 and K_2 are evaluated by plotting $\frac{1}{Q^2}$ against t. Thus the absorption constants of the material are obtained from equations (65), (67), and (68), and the resistance per unit area of the coating from equation (66).

Occasionally the penetration proves to be so slow that it is inconvenient to follow out the complete absorption curve without the aid of the automatic device to be described in the next section. In such cases the steady rate of transmission Q_1 is read at some subsequent time, and the total quantity $\bar{Q}$ of water absorbed is found by measuring the loss of weight when the specimen is dried out. Q_0 and t_0 can then be found by exterpolation. With the type of curve we are now considering, we have

$$t_0 = \frac{\bar{Q}^2}{4K_1} + \bar{Q}\sqrt{\frac{K_2}{K_1}}$$

by equation (70), and hence Q_0 from equation (60).

The likelihood of the formation of a skin at the surface of certain materials during the process of drying has already been remarked (Part IV.). While the influence of such a skin is observable in some absorption curves, it is often associated with the random effects of inhomogeneity. Moreover, the resistance of a surface layer formed in such a manner

would be expected to decrease during the course of absorption. The isolation of the effect is therefore generally impossible. A number of tests on Whitbed stone, however, have yielded absorption curves which conform consistently to equation (60). The results of one experiment are embodied in curve *a*, fig. 2, depicting $\frac{1}{Q^2}$ plotted against *t*. To illus-

Fig. 2.

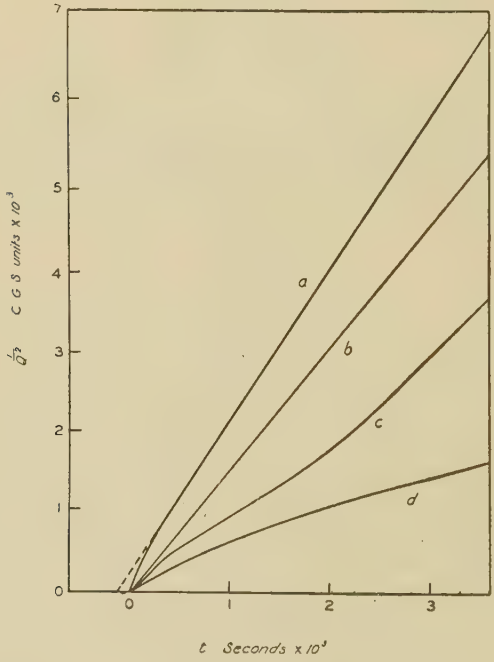

trate the general trend of such curves three others are shown, the scale in each case having been selected arbitrarily in order to bring them within the scope of the diagram *b*, which agrees excellently with equation (31) and represents the results of a test on a specimen of Box Ground stone; *c* and *d* are for specimens of Bath stone and gypsum plaster respectively. It is seen that the curve *a* becomes linear about five minutes after the commencement of the test, and the flow thereafter is consistent with the assumption of a skin of constant resistance at the entering surface. Calculating the absorption

constants in the manner described above, the following values in C.G.S. units are obtained:

$$h' = 298,$$
$$\sigma = 8{\cdot}4 \times 10^8,$$
$$\mathrm{D} = 208,$$
$$\sigma_1 l_1 = 6{\cdot}76 \times 10^8.$$

Those calculated on the simple theory from equations (36), (38), and (40) are:

$$h' = 298,$$
$$\sigma = 10{\cdot}2 \times 10^8,$$
$$\mathrm{D} = 295.$$

The first series of values closely interprets the experimental results, and would be employed in any series of experiments on the same specimen. But, in view of the inhomogeneity of the materials under consideration, the second series is sufficiently accurate for most practical purposes. For example, calculated from the first series of values the rate of absorption per square centimetre under the action of capillarity only, corresponding to a penetration x of 10 cm., is

$$q = \frac{gh'}{\sigma_1 l_1 + \sigma x} = 0{\cdot}32 \times 10^{-4} \text{ c.c. per sec.},$$

and the time which this penetration occupies is

$$t = \mathrm{D}\left(x^2 + \frac{2\sigma_1 l_1}{\sigma} . x\right) = 2{\cdot}41 \times 10^4 \text{ sec.}$$

Calculated from the second series these quantities are

$$q = \frac{gh'}{\sigma x} = 0{\cdot}29 \times 10^{-4} \text{ c.c. per sec.}$$

and

$$t = \mathrm{D}x^2 = 2{\cdot}95 \times 10^4 \text{ sec.}$$

The test specimen was 3·8 cm. thick. It will be seen from the table in Part IV. that, as a prediction to be applied to Whitbed stone taken from a particular bed, the second results are within the accuracy required. Industrial testing in such a case is therefore based on the simple theory.

(b) *Coatings of High Resistance.*—The coating is applied to the surface of a specimen whose absorption constants have

been determined previously, and an absorption test is carried out in the customary manner. Fig. 3 shows the results of a typical experiment on a painted specimen of gypsum plaster. The initial fall in the rate of flow during the first thousand seconds is ascribed to absorption by the coating itself; the succeeding rise to the gradual breaking down of the resistance of the coating; and the final decrease to the increasing resistance to flow as penetration proceeds. The

Fig. 3.

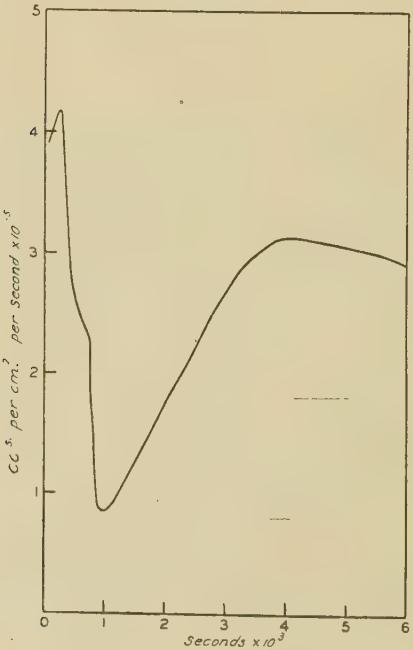

maximum value of $q = 3{\cdot}13 \times 10^{-5}$ c.c. per sq. cm. per sec. at about $t = 4000$ sec. thus represents the rate of flow through the coating under the action of the applied head h plus the capillary head h' of the plaster. Taking this value, we have, from equation (27) (Part III.),

$$\sigma_1 l_1 = \frac{g(h+h')}{q} - \sigma x,$$

where x is the average depth to which water has penetrated into the plaster. This can be estimated from the amount of

water which has been absorbed, but when the resistance of the coating is large the term σx is negligible. The value of $\sigma_1 l_1$ obtained from this particular test is $2{\cdot}14 \times 10^{10}$ C.G.S. units, which is equivalent to the resistance of rather more than 10 cm. of the plaster.

Caution is necessary in the application of such a result to practical problems. Experiments have shown that in many cases a pressure of a few centimetres of water is required to effect the initial penetration, after which the capillary pressure of the underlying material comes into operation ; so that a coating which admits the passage of water when applied to the outside of a building may be quite impermeable when applied to the inside.

(c) *Coatings of Low Resistance.*—The same procedure is followed as with coatings of high resistance, except that the rate of transmission of water through the coated specimen is measured. By equation (27) this is

$$Q = \frac{Ag(h+l)}{\sigma_1 l_1 + \sigma l},$$

from which $\sigma_1 l_1$ is calculated.

A coating of paraffin-wax applied to the surface of Whitbed stone in the manner described in the next paragraph was found in this way to have a resistance of $6{\cdot}59 \times 10^8$ C.G.S. units per sq. cm., which is equivalent to that of a thickness of 0·57 cm. of the stone itself.

Stone Preservatives.

With the object of preventing stone decay, various surface applications have been employed. Whatever the reason behind any particular treatment, it is of interest to know what is the effect on the absorptive properties of the stone. This may be determined as described above.

To be effective, any waterproofing agent must be impermeable under the maximum pressure due to wind, and is therefore tested under a head of 15 cm. of water. One coating which has for its object the sealing up of the surface pores is obtained by applying a $2\frac{1}{2}$ per cent. solution in ligroin of paraffin-wax of melting-point 105° F. This is done three times at intervals of 24 hours. A specimen of Whitbed coated in this way was tested and found to admit the flow of water, proving that the method is totally inadequate.

The Absorption and Transmission of Water by Cements.

The foregoing calculations are based on the assumption that the pore-spaces remain unchanged while water is being absorbed or transmitted: on the one hand, that there is no solvent action, and, on the other, that there is no swelling of the particles of the material. These conditions are sufficiently approached in the case of all the natural stones which have been tested. The addition of water to cements, however, is known to result in hydration and colloidal swelling,

Fig. 4.

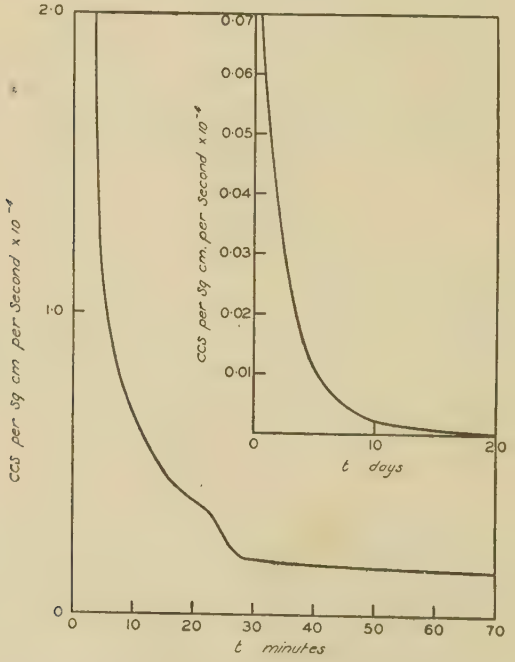

factors which must increase the resistivity. Fig. 4 shows the results of a test on a cement mortar. It will be observed that the rate of absorption decreases at a much greater rate than is required by the theory, and that the rate of transmission falls steadily until at the end of a fortnight the specimen is almost impermeable. The absorptive properties of a variable material of this kind are not amenable to calculation. Nevertheless, purely empirical tests by means of the absorption apparatus are of considerable practical value.

Prolonged Permeation in Stone.

It may not be out of place to refer here to an interesting experimental result. It has been observed that at the end of an absorption test on stone the rate of flow attains a steady value from which the permeability is calculated. By comparison with the permeability to air this rate of flow is less than is to be anticipated on viscosity considerations. The effect of prolonged permeation has therefore been investigated. After a time the rate of flow was found to increase, and with a specimen of Darley Dale had risen after three weeks to four times its original value without having become constant. This specimen was dried and the absorption test was repeated. The second curve was identical with the first, proving the change in permeability to be of a temporary character. To test whether the increased flow was due to the withdrawal of air, the specimen was again dried out and evacuated to a pressure of a few millimetres of mercury before the water was admitted. The rate of transmission was increased in this way by about 35 per cent. The matter has not been pursued beyond this point.

XVII. *Lattice Distortion and Carbide Formation in Tungsten Magnet Steels. By* W. A. Wood, *M.Sc., and* C. Wainwright, *M.Sc., Physics Department, National Physical Laboratory, Teddington, Middlesex* *.

[Plate VI.]

Introduction.

THE theory has been advanced by one of us [1] that a high value of the hardness and the coercive force of a steel is to be associated primarily with a high degree of lattice distortion; and that the peculiar changes in these properties, in the case of tungsten magnet steels, as a result of certain heat treatments, correspond with variations in distortion of the lattice. In pursuance of this point of view we have investigated the changes which occur in the carbide formation of the steels as the distortion of the lattice is altered. The aim was to find if a correlation existed between these two variables.

The term lattice distortion is applied to permanent irregular displacement of atoms from their normal positions at the

* Communicated by G. W. C. Kaye, O.B.E.

centres and corners of the unit cubes which build up the crystalline steel grains. This type of distortion influences the sharpness of X-ray reflexions from the material. If precautions are taken to preclude other causes of decreased definition, then the change in breadth of a suitable line in the X-ray spectrum affords a means of measuring the distortion. The chief precaution involves the use of specimens in which the average grain size is not less than about 10^{-5} cm. As shown in the previous paper [1], this point is observed in work on annealed specimens.

Experimental Procedure.

The chemical composition and the state of aggregation of the carbides were studied directly by X-rays. By this method, a narrow beam of approximately monochromatic X-rays is directed on to the surface of a specimen ; the crystalline constituents diffract the beam, each after its own pattern, and a composite spectrum is recorded on a suitably placed photographic film. Thus, in the present case, a system of lines due to iron is superposed on systems produced by the carbides. The latter can then be identified by comparing the carbide spectra with spectra of known substances. The sensitivity of the method depends mainly on the size and crystalline perfection of the carbide particles.

Variations in the distortion of the lattice were followed by observing the breadth of the line reflected from the (220) planes of the steel. Since the distortion affects the interplanar spacings, its effect is most marked on reflexions occurring at large angles where the rate of variation in reflexion angle with a spacing change is enhanced. The (220) line satisfies this condition and also is fairly strong. Normally, when the Kα radiation is used, the (220) is a doublet composed of reflexions of the α_1 and α_2 wavelengths. The resolution of the doublet permits of visual estimation of the distortion of the lattice. For example, as the lattice becomes more and more distorted, the doublet diffuses into a single broad line. The different specimens were photographed under exactly the same geometrical conditions, so that any change in the (220) line could be caused only by changes in the steel itself.

The following were the chief details of the experimental arrangements. A number of normal, "as rolled" specimens were obtained in the form of small blocks approximately $\frac{3}{4}'' \times \frac{3}{4}'' \times \frac{1}{4}''$ in size. These were of the same composition, namely, 5·63 per cent. by weight of tungsten, 0·64 carbon,

0·27 manganese, 0·23 silicon, 0·17 nickel, 0·014 phosphorus, 0·007 sulphur, and the remainder iron. A series of specimens were heated, by means of an electric furnace, in an atmosphere of argon for different periods of time at 850° C. and 900° C.; another set was heated at 1250° C., all being cooled in argon. From measurements of hardness, the first set was known to be spoiled and the second set to be recovered [1, 2].

Each specimen, in turn, was mounted at the centre of a cylindrical camera of radius 5 cm. A face of the specimen was placed parallel to and coincident with the camera axis. The incident X-ray beam from an iron anticathode entered the camera through a tubular slit, 4 cm. long and 1 mm. bore, in a direction perpendicular to the camera axis. The specimen was set with the face at an angle of either 30° or 80° to the beam The 30° setting brought into focus the main part of the carbide spectrum on a photographic film placed at the circumference of the camera. The 80° setting focussed the (220) steel line. Two photographs were secured in this way from each specimen. One showed the carbide spectra, and the other the condition of the (220) reflexion.

Finally, typically normal spoiled and recovered specimens were examined for a possible change in the dimensions of the unit cell. This was done by comparing the spacings of the (220) planes for each case. A special camera of high precision and resolution was employed for this purpose. It is hoped to describe the camera elsewhere.

Observations.

(a) "*As-rolled*" *specimens.*

It was found, firstly, that there was an almost complete absence of carbide lines in the spectra of the "as-rolled" steels. In general iron lines only were present. This state is illustrated by fig. 1*a* (Pl. VI.). Similarly, the carbide residues obtained from these steels by the method of Arnold and Read [3] gave no spectra, and, therefore, were amorphous also. In the second case, it was observed that the (220) line was invariably broad and diffuse (fig. 1*b*, Pl. VI.).

The characteristic of the normal material was a state of marked lattice distortion accompanied by no appreciable carbide aggregation.

(b) *Spoiled specimens.*

The photographs of the spoiled steels differed completely from those of the normal specimens. For, firstly, the carbide lines were numerous and comparable in intensity with the

Kβ lines. They were identified as (*a*) a transition compound which formed after a few minutes' heating, and then turned into the stable compound Fe_4W_2C, and (*b*) tungsten carbide which occurred in long heat treatments. The relative proportion of these carbides depended on the time of heating. The total amount increased as the heating period was extended. The carbide growth is illustrated by fig. 2*a* (Pl. VI.).

Secondly, the (220) line, which was diffuse in the case of the normal steels, exhibited sharp resolution into the α, α' components. This is shown in fig. 2*b* (Pl. VI.). Also, it was found that the sharpness of the doublet grew with longer periods of spoiling just as the carbide spectra increased in intensity.

The spoiled state appears, therefore, to be characterized by strong aggregation of carbides on the one hand and a lattice free from distortion on the other.

(c) *Recovered specimens.*

The carbide formation in the recovered steels was found to revert to the state associated with the as-rolled specimens. This coincides with the recovery in hardness and coercive force. Fig. 3*a* (Pl. VI.) shows the disappearance of the carbide lines from the spectra and should be compared with fig. 1*a* (Pl. VI.). Similarly, the lattice becomes distorted again as shown by fig. 3*b* (Pl. VI.). These observations apply not only to the original steels, which were heated to 1250° C., but also to specimens which were heated to that temperature after having been previously spoiled at 900° C. The residues from recovered steels were also found to be amorphous [4].

The recovered state consequently resembles the normal condition in that it is marked by no measurable carbide aggregation, but is accompanied by a high degree of lattice distortion.

(d) *Lattice parameter changes.*

The spacings of the (220) planes were compared with the following results. The spacings of the normal and recovered specimens were the same. The spacing of the spoiled steel was less. The difference between the two amounted to 0·33 per cent. This was calculated in the manner described below.

Let the photographic plate be set at an angle α to the direction of the incident beam, and let the length of the perpendicular to the plate from the point of incidence of beam and specimen be R. If x is the distance from the foot of this perpendicular to a line on the plate, then

$$x = \mathrm{R} \tan (2\theta - \alpha),$$

where θ is the glancing angle corresponding to the spectrum line considered. Hence

$$\delta x = 2\mathrm{R}\sec^2(2\theta-\alpha)\delta\theta.$$

For a change $\delta\alpha$ in the spacing d of the planes it follows from Bragg's law, $2d\sin\theta = \lambda$, that

$$\frac{\delta d}{d} = -\cot\theta\,\delta\theta,$$

so that from the last two equations

$$\frac{\delta d}{d} = \frac{-\cot\theta}{2\mathrm{R}\sec^2(2\theta-\alpha)}\delta x.$$

This relation gives the fractional change in spacing which would produce a shift δx on the photographic plate.

The difference in the position of the (220) lines for the spoiled and the normal specimens was as much as 2·5 mm. Now in the precision camera R was equal to 11·5 cm., α to 135°, and θ for the spoiled steels was 72·9°, so that the fractional change was 0·0033, and the percentage spacing change was 0·33.

The effect is illustrated by the reproductions (figs. 4*a* and 4*b*, Pl. VI.). The line AB is a line drawn between two reference points on the plate by means of a razor-blade edge. The points are shadows produced by pits in the plate-holder. The line occurs consequently in the same position on each plate. The difference in distance of the (220) line from AB gives the value δx. The measurements were taken from the middle of the (220) lines, so that it is the displacement of the lines as a whole with which we are concerned above.

In addition to this total displacement there is also the following aspect to be considered. A distorted system of planes, say, 220 planes, can be viewed as a collection of sets of planes of slightly different spacings. Each set will contribute to the reflexion from the whole system. But its contribution will be displaced in a photograph by an amount depending on the deviation of its spacing from the correct, undistorted spacing. The superposition of the contributions will produce the observed broad line. Therefore the change in breadth represents the variation of the change in spacing arising from the distortion. (The quantity δx in the above equation can be regarded as a result of the deviation δd of the distorted spacing from the value d; δx would be the measured increase in breadth of the (220) line.) On this assumption the maximum percentage deviation in spacing due to the distortion was 0·2 per cent.

Hence the spacings of the (220) planes of the normal and recovered steels are not only greater by 0·33 per cent. than the spoiled steels, but also, in addition, the former virtually vary amongst themselves up to a maximum of about 0·2 per cent. Whilst this latter view of distortion may not be rigorously correct it does give an idea of the comparative magnitude of the effect. A variation in the (220) planes involves an alteration in the other planes of the unit cell. Measurements on other lines would be of interest in consideration of directional effects.

Discussion.

The following points arise from the observations :—

(1) It is important to consider the change in the dimensions of the lattice from the point of view of a change in constitution of the tungsten-iron alloy which is the basis of the steel. The spacing of the (220) planes varies from 1·01 Å. for pure iron to 1·114 for pure tungsten ; that is, the spacing increases by 10·3 per cent. In a continuously varying solid solution alloy, formed by tungsten replacing iron atoms one by one in the cubic lattice, a replacement by 6 per cent. by weight of tungsten (or 2 per cent. by atomic proportion) would produce a proportional increase of about 0·2 per cent. This assumes a linear proportionality which would not be absolutely true. But it is sufficient to find that this percentage change is of the order measured (0·3 per cent.) in the transition of a steel from the spoiled to the normal state. Therefore, the difference in spacing must be caused by the entire removal of the 6 per cent. of tungsten, dissolved in the iron, during the spoiling process. The ejected tungsten presumably goes to form the carbide compounds then observed. In this condition the steel is reduced virtually to an ordinary carbon steel, with consequent loss in hardness, coercive force, and other properties.

(2) A correlation does exist between the degree of distortion of the steel lattice and the state of aggregation of the carbides. The less the distortion—as in the spoiled state—the greater the carbide formation. The tungsten and carbon atoms, therefore, are the agents controlling the distortion. In the lattice they cause distortion. Outside the lattice they permit the strain to be released.

At the spoiling temperatures these atoms combine. They form stable compounds. When the steel cools, therefore, they are unable to diffuse back into the lattice, which remains free from distortion. On the other hand, at the recovery

temperature of 1250° C., conditions are different because the mobility of the ions is enhanced, the stability of the carbides is less, and the iron lattice is no longer in the α body-centred form. Hence it is not unreasonable to suppose that the carbide components can re-enter the lattice at this temperature. Rapid cooling would then trap the atoms in the lattice and produce the observed distortion.

(3) It is suggested that it is the carbon atoms which are mainly responsible for the distortion; and that the tungsten atoms merely alter the spacings of the parent lattice as a whole, and its effective composition. For the entry of tungsten atoms into the lattice is by the method of replacing iron atoms and preserving the body-centred cubic structure. This process of substitutional solution is known not to produce distortion in cases like the present. The lattice expands uniformly in all directions. But the entry of carbon into the lattice is known to be of the type in which the small foreign atoms penetrate the interstices of the lattice. This process must produce distortion, and the degree of distortion which the lattice will stand before breaking down will be a function of the iron-tungsten composition.

(4) In the manufacture of these steels it is customary to heat them to 850° C. before quenching in order to secure maximum magnetic quality. Since 850° is a spoiling temperature, the time of heating is important. It is suggested that a routine X-ray examination of control samples from a batch of steels would provide a sensitive method of determining the maximum period for which the steels might be kept at 850° C. with safety.

This work was carried out on behalf of the X-ray Committee of the Department of Scientific and Industrial Research.

In conclusion, the authors wish to express their thanks to Dr. G. W. C. Kaye for his interest in the work, to Dr. G. Shearer with whom many points were discussed, and to Dr. W. H. Hatfield who kindly provided the specimens.

Summary.

A study has been made by X-ray methods of the relation between changes in the carbide formation and the state of the crystal lattice produced by the heat treatment of 6 per cent. tungsten magnet steels; and further light has been thrown on the phenomena of spoiling and recovery associated with these steels:—(*a*) It is shown that, in the spoiled state,

tungsten and carbon are ejected from the parent lattice to form carbides (Fe_4W_2C, WC), and thereby permit release of lattice strain. In the normal and recovered state these elements are dissolved in the lattice and produce distortion, with its accompaniment of enhanced coercive force and hardness. (*b*) The manner of solution is determined. It is found that the tungsten enters the lattice by substituting iron atoms, preserving the body-centred cubic structure, but producing measured spacing changes. The decrease in spacing occurring on spoiling indicates that the whole of the 6 per cent. of tungsten is removed from the lattice by that process. The carbon atoms, on the other hand, penetrate the interstices of the lattice. (*c*) It was concluded that it was the latter which are mainly responsible for the spoiling; and that the tungsten controls rather the composition of the parent lattice, its dimensions, and its ability to withstand high distortion.

References.

(1) Wood, Phil. Mag., Feb. 1932.
(2) Evershed, Journ. Inst. Elec. Eng. lxiii. p. 725 (1925).
(3) Arnold and Read, Proc. Inst. Mech. Eng. (1914).
(4) Wood, Phil. Mag. x. p. 660 (1930).

XVIII. *The Action of X-Rays on Ferrous Sulphate Solutions.*

By N. A. Shishacow, *Röntgen Institute, Moscow* *.

In the Phil. Mag. ser. 7, vii. p. 129 (1929) appeared a paper, under the above title, in which the authors, Fricke and Morse, have described only the results of their investigations concerning such solutions which were saturated with atmospheric air; furthermore, the authors do not say anything about the chemical properties of the sulphate solutions, which are so important from the point of view of the chemical action of the X-rays.

The object of my investigations was first to study these properties, and then to compare the action of the X-rays on ferrous sulphate under the above and under some other conditions. As the first part of the results of my experiments has been published in another magazine †, herein I will confine myself only to a brief description of these questions as far as they concern this röntgenochemical reaction.

* Communicated by the Author.

† N. A. Shishacow, Journ. of Gen. Chem. (Russ.) i. p. 1012 (1931).

The ferrosulphate solutions, especially when as strong as 0·1 molar, are apt to oxidize quickly and spontaneously; this oxidation does not cease even when the salt is one-half oxidized into ferrisulphate. It may be seen from this that the standard electrode, consisting of platinum wire dipped into $\frac{m}{10}$ to one-half oxidized ferrosulphate solution, which was used by Fricke and Morse at electrometric titration, was hardly suitable for exact work. It seems probable that, due to the oversight of some purely chemical properties, Fricke and Morse* have sometimes obtained irregular results, as, for example, the difference in the behaviour of the ferrosulphate solutions prepared from a strong standard solution.

In the presence of platinum wire this spontaneous oxidation of ferrosulphate solutions takes place very rapidly, and the excess of $Fe^{\cdots}$-ions accumulates around it; the potential of such unstable solutions have been found fairly high, when compared with true potential of the solutions of equal concentrations of $Fe^{\cdot\cdot}$ and $Fe^{\cdots}$-ions. This also proves that the choice of this standard electrode, made by Fricke and Morse, could not give thoroughly good results.

The incorrect choice of the end-point, *i. e.*, of the potential, at which the addition of the sodium bichromate to the analysed material had to be stopped, could also become a source of errors. My experiments have shown that this end-point depends on different conditions and mainly on the concentration of ferrosulphate solutions, while Fricke and Morse have chosen the potential plus 150 millivolts as the end-point for all concentrations. Instead of the ferrous-ferric standard electrode I have used the normal calomel electrode. As objects of investigations I also took ferrosulphate solutions in 0·8 normal sulphuric acid. The procedure of irradiation † was, in general, the same as by Fricke and Morse.

Experimental Results.

Figs. 1 and 2 show the dependence of oxidation of the ferrosulphate on the X-ray dose, which is expressed here in kiloröntgens. All these six curves refer only to the 0·002 molar solution. The curve 1 (fig. 1) shows the course of the oxidation in the case, when the surface of the liquids in

* 'Strahlentherapie,' xxvi. p. 759 (1927).

† The X-ray doses were measured by Dr. Ja. L. Schechtmann, to whom I wish to express my best thanks.

the cell was in contact with the atmosphere. In this case the straight line is obtained exactly of the same slope, as it has been found by Fricke and Morse. The only difference is that during my experiments the oxidation proceeds until a complete disappearance of the ferrosulphate takes place, but not to 94 per cent., as by Fricke and Morse. That my results are more exact, *i. e.*, that the reaction proceeds till the oxidation is complete, has been confirmed by the experiment on the irradiation of pure ferrisulphate solutions. In this case I have not observed any reduction of the ferric ion by all concentrations, ranging from $\frac{m}{1000}$ to $\frac{m}{20}$.

Fig. 1.

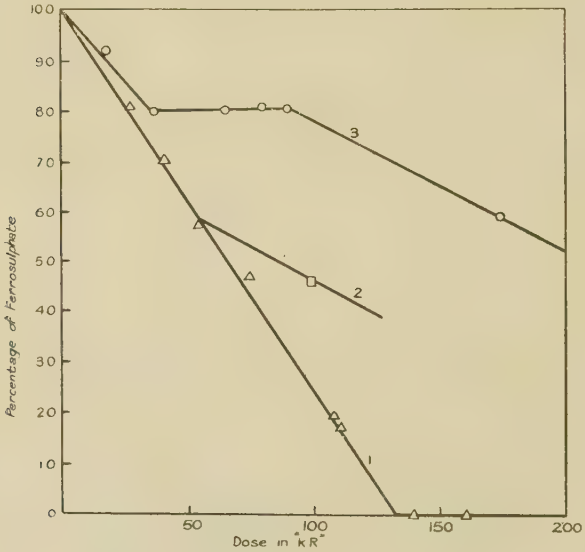

Oxidation of 0·0002 m. ferrosulphate solution.

Curve 1.—The surface of the liquid in contact with the atmosphere.
Curve 2.—The solution also saturated with atmospheric air but covered with a cover-glass.
Curve 3.—The boiled solution not in contact with the atmosphere.

The curve 2 (fig. 1) refers to the case when the solution, being also saturated with atmospheric air, was covered with a cover glass, *i. e.*, was not in contact with the atmosphere. Here we can notice a tendency of the curve to coincide with the one, drawn according to the results, published by Fricke and Morse (curve 4).

A quite different course has the curve 3, which refers to the case when the solution, having been previously boiled in order to eliminate all traces of dissolved air, was not in contact with the atmosphere during the irradiation. Here, in the first stage, the reaction is getting slower than under the above conditions; then it ceases completely, and finally it begins again, but at a relatively low rate. The fact that the oxygen accelerates the reaction may be seen from the initial parts of the curves. The middle parts of the curves, however, give us the possibility of drawing some additional

Fig. 2.

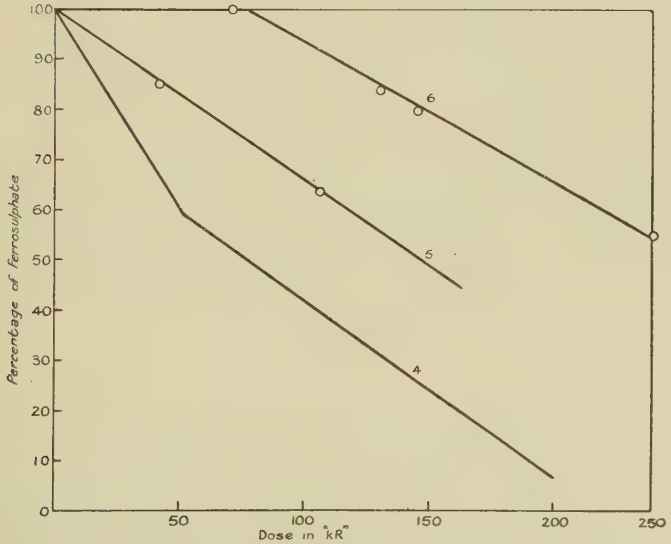

Oxidation of 0·002 m. ferrosulphate solution.

Curve 4.—Taken from data published by Fricke and Morse.
Curve 5.—The boiled solution in an exhausted and sealed-off bulb.
Curve 6.—The boiled solution saturated with hydrogen and sealed-off bulb.

conclusions. The interruption of the reaction in the region of doses from 46 to 89·5 kiloröntgens can hardly be explained only by the accumulation of hydrogen-peroxide as is done by Fricke and Morse, since the hydrogen peroxide, being present in such considerable quantities, must readily oxidize the ferrosulphate solution. That no hydrogen peroxide can actually be formed has been shown by J. A.

Crowther's experiments *, which have proved that colloidal solutions in the waterless medium (ethyl- and amyl-alcohol, etc.), being exposed to X-rays, are precipitated in the same way as in water solutions. Furthermore, even by means of the most delicate tests no traces of H_2O_2 could be detected during the process of the irradiation of pure water. We can see therefore that this effect is a direct one, *i. e.*, the hydrogen peroxide does not play an important part.

The only assumption remains, therefore, that during the exposure of ferrosulphate solutions an accumulation of hydrogen takes place, to which is due the delay of the oxidation. That the hydrogen plays an important part in this case is confirmed by curve 6 (fig. 2). In this case the solution, having been boiled in a small thin-walled bulb before the experiment, was cooled by blowing hydrogen through it. It will be seen that to 71 kiloröntgens, owing to the presence of hydrogen, no oxidation occurs. For the case when both the oxygen and the hydrogen are absent the course of the reaction is given by curve 5 (fig. 2). Here the gases have been eliminated from solution by means of boiling and simultaneous exhausting, the solution being also placed in a glass bulb. In this, as well as in all other cases, both the increase of concentration of the solution, due to the evaporation, and the absorption of the X-rays by the glass were, of course, taken into account.

Discussion.

When we look through these curves our attention is attracted to the fact that, after consumption of oxygen as well as hydrogen, the curves tend to go with equal slope, which is nearly the same as was observed by Fricke and Morse for 0·00878 and 0·00337 molar solutions. The part of the oxygen has been thoroughly well explained by these authors ; as to the hydrogen, the above results lead us to the conclusion that it is oxidized as well as the ferrosulphate. When the oxygen is present in the solution, the reaction proceeds with the formation of the water

$$2\,FeSO_4 + H_2SO_4 + O = Fe_2(SO_4)_3 + H_2O,$$

so that there is no delay in the reaction. But when the oxygen has been already consumed, the course of the reaction will be the following

$$2\,FeSO_4 + H_2SO_4 = Fe_2(SO_4)_3 + H_2,$$

* Phil. Mag. ser. 7, vii. p. 96 (1929).

and the reaction must be interrupted, due to the accumulation of adequate quantities of hydrogen, and this is actually observed on the curves 3 and 6. Sooner or later, however, the reaction begins again, but at half the rate, than it took place in the presence of oxygen. Therefore it is probable that the hydrogen not only accumulates gradually, but it also disappears at some rate, depending upon different conditions. It seems probable that the slow rate of the final reaction is the result of the elimination of hydrogen from solution, due to the slow heating of the cells and the bulbs, containing the solutions, since during my experiments, as well as by Fricke and Morse, they were placed relatively close to the X-ray tube, which, of course, was to some extent heated owing to the prolonged work. It is very probable also that simultaneously with this elimination of hydrogen, the oxygen emitted from the glass, due to the reduction of metallic oxides by the X-ray action *, had its influence, too. That the glass walls may actually play an important part has been confirmed by Fricke and Morse † themselves, who have found that "if immediately after the irradiation a cell in which a solution had been irradiated was filled and irradiated again, the results were different from the results of the first irradiation, this evidently being due to some change, produced in the glass during the irradiation."

XIX. *Adsorption at the Surface of a Solution.*

To the Editors of the Philosophical Magazine.

GENTLEMEN,—

IN a recent paper ‡ dealing with the adsorption of certain substances at the surface of their aqueous solutions I suggested that the data were compatible with the conception of a unimolecular layer provided that the total amount of solute and not merely the surface excess were considered. In a reply to this paper Dr. Schofield and Professor Rideal § state that I have claimed for my treatment freedom from the obvious thermodynamic requirement that, in the vicinity of the unimolecular layer of solute, there must be an excess of solvent corresponding to the amount of solute originally present at the surface. Actually, as is shown by a footnote

* See, for example, G. W. C. Kaye, 'X-Rays,' p. 87 (1923).
† Amer. Journ. of Roentgenology, xviii. p. 428 (1927).
‡ Phil. Mag. xii. p. 907 (1931).
† Phil. Mag. xiii. p. 806 (1932).

on page 909 of my paper, I neither made nor imagined any such claim, but merely ignored the *solvent* excess as being irrelevant to an argument dealing with the amount of *solute*. With the general thermodynamic considerations advanced by Dr. Schofield and Professor Rideal I am in complete agreement.

A further point raised by these authors is that I should have expressed the concentration not on a weight but on a volume basis; this is quite true, but I had previously satisfied myself by a rough calculation that the difference between the two scales did not significantly affect the value of U, the total amount at the surface.

With regard to their main criticism, "that the relation has no thermodynamic foundation and cannot, therefore, give results of any value . . . . . No theoretical foundation can be found for the relation proposed by Wynne-Jones," I can only plead that the words "thermodynamic" and "theoretical" are not synonymous, and that to reject a hypothesis merely because it cannot be proved thermodynamically would be to condemn a very large number of physical theories, including that of the unimolecular layer which has been so fruitfully employed by Dr. Schofield and Professor Rideal themselves.

I would add that I do not claim that my treatment is the only possible one, but that it offers a reasonable explanation of the data.

I am,

Yours faithfully,

W. F. K. Wynne-Jones.

The University, Reading.
May 29th, 1932.

XX. *Notices respecting New Books.*

Die elliptischen Funktionen von Jacobi: L. M. Milne-Thomson. (Verlagsbuchhandlung Julius Springer, Berlin. Preis, geb. R.M. 10.50.)

NEARLY fifty years ago, Glaisher remarked, in one of his early papers, that the quantities K and E (like the elliptic functions $sn\,u$, $cn\,u$, $dn\,u$ themselves), being rational functions of k^2, it is more proper to regard them as functions of k^2 than of k. Forty years later, tables of the complete elliptic integrals and theta functions were computed, using k^2 as argument, by Nagaoka and Sakurai. Prof. Milne-Thomson, adopting the same plan, has constructed five-place tables of $sn\,u$, $cn\,u$, $dn\,u$, for values of k^2 from 0·0 to 1·0 by 0·1 intervals, and u from 0 beyond the half or quarter period of the functions. Linear interpolation only is

required with regard to u, and generally, second differences are sufficient for interpolation with respect to m. A ten-place table of $dn\,u$ was first calculated, and from the simple relations between the three functions, tables of $sn\,u$ and $cn\,u$ were finally constructed. The claim that the entries reach a high degree of accuracy is thus well founded. The negative sign in the values of $cn\,u$ for u greater than K is not repeated in the following pages. The integrals K and E and q are tabulated to eight significant figures, m ranging from 0·00 to 1·00 by 0·01 intervals. A number of useful formulæ and integrals, with some numerical examples, are given in the introduction. Prof. Milne-Thomson's tables meet a long-felt want and will be warmly welcomed by those engaged in the many problems of physics and applied mathematics where numerical values of elliptic functions are so important.

British Association Mathematical Tables. Vol. I. (British Association for the Advancement of Science, Burlington House, London, W. 1. Prepared by the Committee for the Calculation of Mathematical Tables. Price 10*s*.)

This is the first instalment of the collected work of the "Tables" Committee of the British Association, which for so many years has been steadily progressing in its useful task. Commencing with the famous bibliographical report published in 1873 and gradually extending its activities, the Committee, in spite of numerous changes in membership and gaps in its grants, has accumulated both knowledge of what exists and what is wanted, and the means to satisfy those wants. Its influence on the progress of tabulation has been far wider than appears in its reports, since much work published elsewhere has been done in association with it, and its continued existence is an encouragement and witness to the value of such work. It should be emphasized that this volume is not a mere reprint of tables already published, either in the Reports or elsewhere. It represents the completion up to a given point, of the task of tabulating in modern form and with modern aids to use, certain functions of general value which require only single-entry tabulation, viz., $\sin x$, $\cos x$ (x in radians), hyperbolic sines and cosines of x and πx: exponential, sine, and cosine integrals: gamma function with its first four logarithmic derivatives, and the probability integral and its integrals. With one or two exceptions all the tables have appeared in the Reports of the Committee since publication was resumed ten years ago. But a mere list of contents does not indicate the completeness with which the tables have been prepared. In addition to the vast amount of work expended in the actual calculation of the tables, the rather tedious task of filling in gaps and supplying the necessary differences of even order to make each table self-sufficient has been successfully undertaken. An excellent introduction gives ample instruction for the user, who must, of course, be prepared to co-operate with the compilers in the

effort to make new tables available in convenient form by using the methods of interpolation chosen. Certain modifications in some of the printed differences are explained, though these do not affect the user who wants values of the functions themselves. The introduction also gives information about other existing tables which may supplement these in special cases.

Altogether it may be said that the volume is a model for future tables, not necessarily in details which must be varied to suit circumstances, but in general rightness for its purpose—type and format well chosen, price reasonable, volume of moderate size and opening readily at any page. Later volumes, which it is to be hoped will not be too long delayed by difficulties of finance, will involve difficulties such as double-entry, in regard to which we have as yet comparatively little to guide us, although the other great centre of tabulation work in this country, the school of Karl Pearson, with which the B.A. Committee has many personal links, has already published some useful tables of double-entry, and has others in preparation. To the mathematician, whether interested in seeing that the functions he uses are available to all in numerical form or specially concerned with statistical and other applications, this work is invaluable. The British Association is doing pioneer work in this field, as in so many others, and is doing it well.

The Essentials of Bacteriological Technique. By R. F. Hunwicke. With an Introduction by William G. Savage. [Pp. 108, 22 diagrams in the text.] (London: Williams & Norgate, Ltd. Price 6*s.* 6*d.* net.)

In the preface the author expresses the hope that this work may be suitable for students both of Medical and of General Bacteriology.

Chapters on laboratory equipment, apparatus, and microscopy are general in their treatment and might apply to several branches of Bacteriology. They abound in useful hints, many obviously the outcome of experience.

The chapter on the preparation of culture media will be particularly appreciated, as it gives a fairly wide range of formulæ with carefully worded instructions for their preparation. A description is given of the standardization of reactions of media by the hydrogen ion concentration method which has largely displaced the less satisfactory titration process. The account of methods of cultivation and study of micro-organisms provides admirable material for students in several branches of bacteriology. The cultivation of anærobes presents many practical difficulties and is the subject-matter of a special chapter. Formulæ for stains in general use and methods of staining are given in the chapter on microscopy.

One of the most important parts of the work is that relating to the bacteriological examination of water, milk, and canned foods. The author has had considerable experience in this field of work, and it is a pity that this section of the subject has not been extended. The notes on the diagnosis of certain diseases (two and

a half pages) and those on vaccines (five pages) are too condensed to be of guidance.

Other parts of the book describe methods for the testing of disinfectants and for animal inoculation.

There are numerous references in the text to current literature; a full list of papers cited would have added to the practical value of the work.

The book is thoroughly sound in advocating methods whereby a high standard may be attained. For the reference shelf in the laboratory this volume should prove its value to all those whose professional study leads them from time to time to bacteriological problems.

XXI. *Proceedings of Learned Societies.*

GEOLOGICAL SOCIETY.

March 9th, 1932.—Mr. J. F. N. Green, B.A., Vice-President, in the Chair.

THE following communications were read :—

1. 'The Permian Lavas of Devon.' By Wilfred George Tidmarsh, Ph.D. D.I.C. F.G.S.

The Permian lavas of Devon lie on or near the boundary between the Culm and Permian rocks. With the exception of certain members in the south of the area, they are intermediate rocks ranging from types resembling basalts to normal and olivine minettes.

Some members of the series contain, as xenocrysts, quartz, felspars, biotite, pyroxene, iddingsite, olivine, and apatite. From the occurrence of these minerals as xenocrysts and from the character of their alteration, it is concluded that the rocks in which they are found result from the hybridization of a late acid fluid residuum with the basic 'depth-residuum' of the Dartmoor igneous mass, both fractions containing solid as well as liquid phases at the time of admixture.

The Exeter lavas are divided into two series according to the nature of the contained xenocrysts; each series contains sodic, sodipotassic, and potassic types—a fact which implies differentiation subsequent to hybridization. The various types resulting from these processes are described.

The Withnoe and Cawsand lavas are believed to be of earlier date than the other members of the suite; they are rhyolites traversed by elvan dykes, and both types show evidence of contamination in the abundant development of pinite after cordierite.

Analyses of fourteen rocks and three minerals (iddingsite and two micas) are presented. The inability to construct

linear variation diagrams for the series as a whole is in accordance with the suggested hybrid origin of these rocks. From the mineral analyses, the relationship of iddingsite to the chlorites has been established and the micas are shown to be specifically phlogopitic.

As many lamprophyric rocks exhibit phenomena similar to those developed in the Exeter lavas and there attributed to hybridization, the suggestion that similar processes play an important part in the genesis of some lamprophyres is put forward and discussed.

2. 'The Geology of the Fairbourne–Llwyngwril District, Merioneth.' By Brynmor Jones, M.Sc. (communicated and read by Prof. A. H. Cox, D.Sc. Ph.D. F.G.S.).

The area described is situated on the shores of Cardigan Bay between the towns of Barmouth on the north and Towyn on the south. It is occupied by a westward extension of the Upper Cambrian and of the Ordovician rocks of the Arthog–Dolgelley and Cader Idris districts, and the sequence is, in general, similar to that in those districts, with, however, certain noteworthy differences.

A small outcrop of Menevian and uppermost Harlech Beds was found on the coast south of Fairbourne, this being the most southerly occurrence of these beds in North Wales. An important fault—the Llanegryn Fault— with an apparent downthrow to the west of 7000 feet, cuts across the district in a north-north-west direction. The discovery of this fault necessitates an important modification of the geological map of the area; some five square miles of country formerly regarded as Cambrian must now be assigned to the Ordovician.

The sequence and lithology of the Ordovician rocks south of this fault show considerable differences from those of the corresponding strata on the north side. South of the fault the Ordovician sequence appears remarkably condensed as compared with that of Cader Idris, partly owing to strike-faulting, and partly to the effects of a probable overlap, believed to be at the horizon of the Cader Idris oolitic iron-ore.

An unexpected discovery was that of a wide expanse of Bala Beds extending along the Dysnni Valley and north of the Talyllyn (Bala) Fault.

The topography is briefly described. Much of the area is heavily drift-covered; the hills are for the most part greatly rounded, and the steep craggy ridges and narrow deep valleys characteristic of the Cader Idris and Dolgelley areas are absent; most of the streams show little rejuvenation.

[*The Editors do not hold themselves responsible for the views expressed by their correspondents.*]

Fig. 1.

(a)

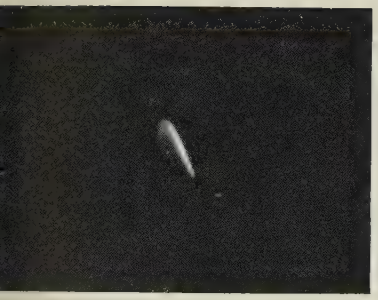

(b)

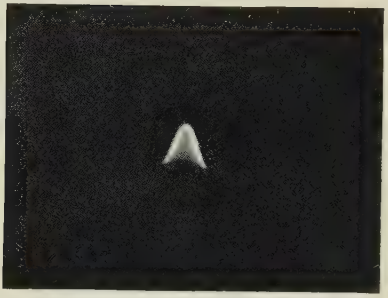

(c)

(d)

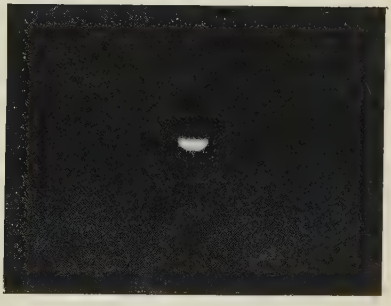

(e)

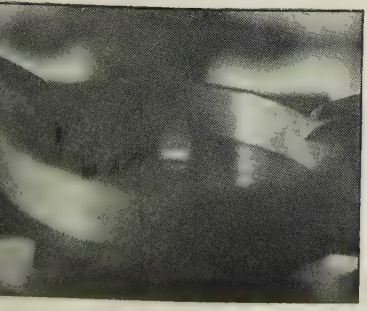

(f)

Fig. 2.

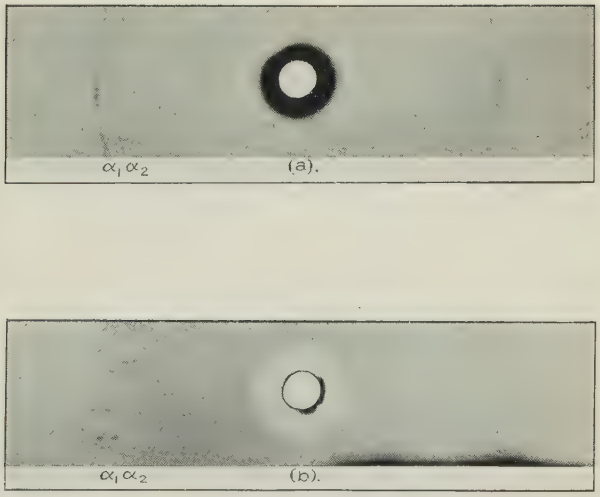

Powder photographs of silver-rich alloys containing 3·69 atoms per cent. of copper, showing the CuK reflexions from 511.

(*a*) Quenched from 728° C.

(*b*) Annealed to room temperature.

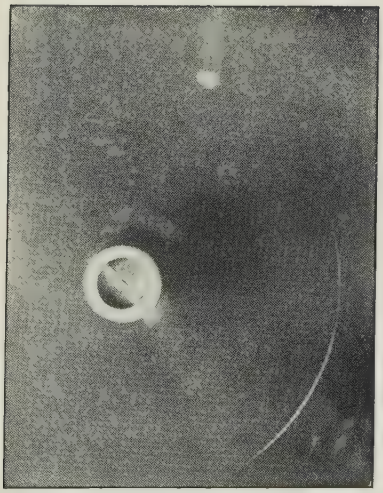

(a)

(b)

(c)

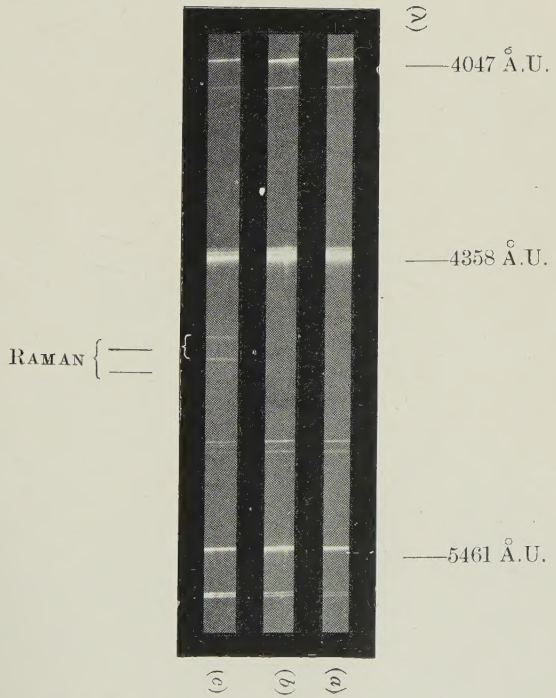
(4)
4047 Å.U.
4358 Å.U.
Raman
5461 Å.U.
(3)
(2)
(1)

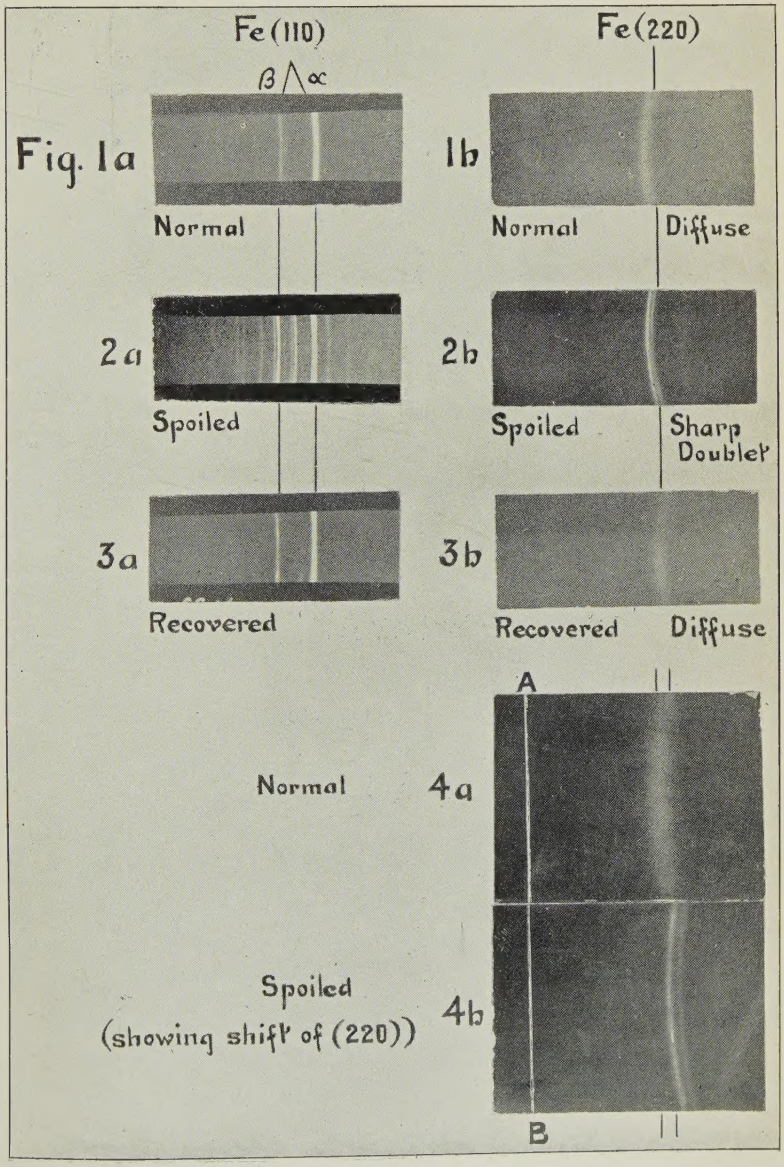
Fe(110)
β ∧ α
Fe(220)
Fig. 1a
1b
Normal
Normal
Diffuse
2a
2b
Spoiled
Spoiled
Sharp Doublet
3a
3b
Recovered
Recovered
Diffuse
A
Normal
4a
Spoiled
(showing shift of (220))
4b
B